

TC171
.M41-24
.1799
no. 326

THE ANALYSIS OF RIVER BASINS AND CHANNEL NETWORKS USING DIGITAL TERRAIN DATA



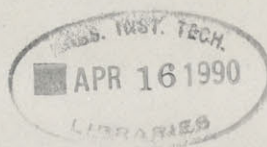
by
DAVID G. TARBOTON
RAFAEL L. BRAS
IGNACIO RODRIGUEZ-ITURBE

RALPH M. PARSONS LABORATORY
HYDROLOGY AND WATER RESOURCE SYSTEMS

Report Number 326

Prepared under the support of the
National Science Foundation Grant No. ECE-8513556
and
National Research Council of Italy through a
Cooperative Agreement with the University of Florence

September, 1989



BARKER ENGINEERING LIBRARY

MIT

DEPARTMENT
OF
CIVIL
ENGINEERING

SCHOOL OF ENGINEERING
MASSACHUSETTS INSTITUTE OF TECHNOLOGY
Cambridge, Massachusetts 02139

R89-24

THE ANALYSIS OF RIVER BASINS AND CHANNEL NETWORKS
USING DIGITAL TERRAIN DATA

by

David G. Tarboton
Rafael L. Bras
Ignacio Rodriguez-Iturbe

RALPH M. PARSONS LABORATORY
HYDROLOGY AND WATER RESOURCE SYSTEMS

Report Number 326

Prepared under the support of the
National Science Foundation Grant No. ECE-8513556
and
National Research Council of Italy through a cooperative
Agreement with the University of Florence

SEPTEMBER 1989

THE ANALYSIS OF RIVER BASINS AND CHANNEL NETWORKS USING DIGITAL TERRAIN DATA

ABSTRACT

This work examines patterns of regularity and scale in landform and channel networks. Digital elevation model data sets from throughout the United States are used as a data source.

First we consider the two-dimensional planform properties of channel networks. We find that networks as a whole may be regarded as space filling fractals, i.e., with fractal dimension 2. The scaling may be described by Horton's laws and provides a link between Horton length and bifurcation ratios.

Second we focus on elevation where the mean slope of rivers is characterized by a power law scaling with area. Investigations have recently used this to suggest that channel slopes are self-similar with magnitude or area as a scaling index. Our data indicates otherwise; in particular the variance of channel slope is larger than that predicted by simple self-similarity. The coefficient of variation of link slopes increases with area contributing to the link. This suggests multi-scaling. The scaling exponent for the standard deviation is approximately half the corresponding exponent in the relationship of the slope mean to magnitude or area. A model for channel slopes based on a point process of elevation drops along the channel is suggested. This model reproduces the observed multi-scaling properties when the density of elevation increments is related to area (or magnitude) as $A^{-\theta}$.

This scaling cannot hold in the limit of small area and must break at some point. We suggest that this break defines the lower bound scale for which channels exist and can therefore be used to determine the drainage density, the basic horizontal length scale associated with the dissection of the landscape by the channel network. This break in scale can also be detected as a break in the constant drop property, namely the empirical fact that the elevation drop along Strahler streams is on average constant. That the break in scale gives drainage density is justified using a stability analysis of landform development processes and empirical comparison of drainage densities from many DEM data sets. This work provides a rational way to extract channel networks with physically justifiable drainage density from digital elevation models.

Acknowledgements

This report essentially constitutes the Doctor of Science thesis of David G. Tarboton.

This work was supported by the National Science Foundation (Grant No. ECE-8513556) and National Research Council of Italy through a cooperative agreement between the University of Florence and M.I.T. This support is gratefully acknowledged.

Thanks to Elaine Healy and Carole Solomon for efficiently typing this work.

Table of Contents

	<u>Page</u>
Abstract	2
Acknowledgement	3
Table of Contents	4
List of Figures	6
List of Tables	10
Chapter 1. Introduction	11
1.1 Scope	11
1.2 Outline	13
Chapter 2. Literature Review	15
2.1 Motivation	15
2.2 Terminology and Ordering Systems	16
2.3 Drainage Density, Dissection and Hillslope Scale	21
2.4 The Random Topology Model	23
2.5 Scaling in River Networks	26
2.6 Fractals and Scaling	35
2.7 Channel Network Evolution and Processes	44
Chapter 3. Data Analysis, Procedures and Techniques	54
3.1 Review	54
3.2 Data Sources and Accuracy	57
3.3 Procedures and Storage Conventions	59
3.4 Data	64
Chapter 4. Planar Space Filling Properties of River Networks	74
4.1 Introduction	74
4.2 Empirical Evidence	74

4.3 Fractal Dimension and Horton's Laws	81
4.4 Fractal Dimension and Tokunaga cyclicity	87
4.5 Planar Scaling Summary	91
Chapter 5. Slope Scaling	93
5.1 Introduction	93
5.2 Self-Similar Drop Model	94
5.3 Empirical Evidence of Scaling in Elevation	97
5.4 Link Slope Scaling Model	110
5.5 Conclusions	127
Chapter 6. Basic Scales in the Landform	128
6.1 Introduction	128
6.2 Slope-Area Scaling	129
6.3 The Constant Stream Drop Property	161
6.4 Localized DEM Procedures	188
6.5 Detailed Results	193
Chapter 7. Conclusions	203
7.1 Introduction	203
7.2 Planar Scaling	203
7.3 Slope Scaling	204
7.4 Basic Scale	204
7.5 Concluding Remarks	205
7.6 Future Research	206
References	210
Appendix: Computer Codes	221

List of Figures

<u>Figure</u>	<u>Title</u>	<u>Page</u>
2.1	Horton/Strahler ordering and link magnitude	18
2.2	Big Creek (CALD) Horton Analysis	19
2.3	Structurally Hortonian network with bifurcation ratio 4	27
2.4	Sections of (A) a regular square-wave form and (B) a randomized square-wave form	37
2.5	Graph of number of divider steps against step length for the randomized square-wave form	37
2.6	Graph of measured length against scale of measurement for the randomized square-wave form	37
2.7	Burwash TQ62 Richardson plots for 300' and 400' contours	41
2.8	Variograms for the Aughwick, Pennsylvania (A) and Shadow Mountain, Colorado (B) digital elevation models	42
2.9	Characteristic form slope profiles	48
3.1	(a) Location map for 7.5 min Data sets	68
	(b) Location map for 1 ⁰ DMA Quadrangles	69
3.2	Channel networks from DEM with varying support area compared to blue lines for the W15 data set	73
4.1	Ruler method results for typical river networks	76
4.2	Functional box counting results from W15 data set	77
4.3	Geometric stream length exceedance probability	79
4.4	Stream length (along stream) exceedance probability	80

5.1	St. Joe River and Big Creek location map	98
5.2	Link slopes for the St. Joe River, Idaho	100
5.3	Link slopes for Big Creek, Idaho	101
5.4	Link slope variances, St. Joe River, Idaho	102
5.5	Link slope variances, Big Creek, Idaho	103
5.6	St. Joe River link slopes normalized with $n^{-0.6}$	104
5.7	Big Creek link slopes normalized with $n^{-0.6}$	105
5.8	Model slope distributions by simulation	123
5.9	Normalized slope distributions from model by simulation	124
5.10	Big Creek link slopes (not normalized)	125
6.1	CALD (Big Creek, Idaho) link slopes with support area of 50 pixels used to extract network	130
6.2	Equilibrium slope profiles for superposed transport functions	134
6.3	CALD (Big Creek, Idaho) residual sum of squares from two phase regression as a function of switch point	138
6.4	Slope versus area and two phase regression plot for	
	(a) W15	140
	(b) W15A2S	141
	(c) W7	142
	(d) CALD	143
	(e) SPOKBC	144
	(f) NELK	145
	(g) STJOE	146
	(h) STJOEUP	147

(i)	STREGIS	148
(j)	STREGISDMA	149
(k)	HAK	150
(l)	HAKA2S	151
(m)	SCHO	152
(n)	EDEL	153
(o)	RACOON	154
(p)	RACOONDMA	155
(q)	BEAVER	156
(r)	BUCK	157
(s)	BRUSHY	158
(t)	MOSHANNON	159
(u)	TVA	160
6.5	(a) Stream drops in W15 network extracted using a support area of 50 pixels	162
6.5	(b) Stream drops in W15 network extracted using a support area of 20 pixels	163
6.6	Stream drop distributions for the W15 network	165
6.7	Stream drops variation with order and support area for	
	(a) W15	167
	(b) W15A2S	168
	(c) W7	169
	(d) CALD	170
	(e) SPOKBC	171
	(f) NELK	172
	(g) STJOE	173
	(h) STJOEUP	174

(i)	STREGIS	175
(j)	STREGISDMA	176
(k)	HAK	177
(l)	HAKA2S	178
(m)	SCHO	179
(n)	EDEL	180
(o)	RACOON	181
(p)	RACOONDMA	182
(q)	BEAVER	183
(r)	BUCK	184
(s)	BRUSHY	185
(t)	MOSHANNON	186
(u)	TVA	187
6.8	Pixels identified by the Peucker and Douglas Algorithm applied to the CALD data set	190
6.9	Pixels identified as one way local minima in the CALD data set	191
6.10	Pixels that exceed accumulation area threshold of 200 pixels in the CALD data set	192
6.11	Comparison of drainage density from different techniques	195
6.12	Schematic diagram of simulated slope profiles	199
6.13	Slope–area plots for simulated hillslopes profile A	200
6.14	Slope–area plots for simulated hillslope profile B	201

List of Tables

<u>Table</u>	<u>Title</u>	<u>Page</u>
2.1	Typical values of Exponents m and n in the empirical relationships $F \propto a^m S^n$ (Equation 2.44)	47
3.1	Binary Matrix Format	60
3.2	Network Storage Structure	61
3.3	Digital Elevation Model Data Sets	65
3.4	River Basins	70
3.5	Statistics of Adjustments Required to Fill Pits	72
4.1	Network Geometry Data for Several River Networks	86
5.1	Big Creek Link Statistics	107
5.2	St. Joe River Link Statistics	108
5.3	Significance Tests for the Difference between Normalized Slopes of Different Order	109
6.1	W15 Data set Link Lengths	139
6.2	Summary of Landform Scale Results	194

Chapter 1

INTRODUCTION

1.1 Scope

Scientific and engineering work should always be based on the best available data that can be utilized effectively. This is also the case in hydrology where an important component of data is the channel network. The channel network defines the paths on the land surface along which water flows, and is a common component of flood routing or more general runoff routing models. Traditionally channel networks have been obtained from topographic maps. This requires that high resolution maps be available and for large basins is a tedious and time consuming task. Also channel networks on maps are scale-dependent and somewhat dependent on subjective judgment by the map maker. More recently the advent of computers has led to the development of digital elevation models (DEM's) as an alternative source of topographic information. These are gaining increasing use in the earth sciences, including hydrology, but especially in Geographic Information Systems. It is important that hydrologists keep abreast of the development of geographic information systems to ensure the availability of hydrologically relevant data and information. It is our opinion that DEM's are presently underutilized in hydrology. One objective of this work is to further develop the use of DEM's for the analysis of channel networks and more generally hydrologic aspects of the whole landscape surface.

Another more scientific objective is research into the basic scales and scaling properties in river networks and the landscape. The composition, regularity, symmetries and scaling in natural river basins has interested scientists for a long time. Attempts to quantify and understand these have been motivated by the idea that landscapes are shaped and sculpted by rivers and the flow of water in them, so the shape of the landscape may hold information about runoff and river flow. We

attempt to answer the following questions. Are there fundamental length scales perhaps related to the processes or mechanisms involved in landform development? Are there landform properties that are scaling, i.e., invariant under transformations of scale, and if so over what range of scales does the scaling hold? The notions of drainage density (Horton, 1945), texture (Smith, 1950), and representative elementary area (Wood, et al., 1988) are measures of fundamental length scales. On the other hand, Horton's laws are really geometric scaling laws, implying that channel networks are self-similar over a range of channel orders or scales. Does this scaling have a physical lower limit at the drainage density, or is the lower limit just a matter of map resolution?

Through the use of digital elevation data we clarify and extend some of the older notions of scaling and symmetry of river networks, introducing modern concepts such as fractal dimension and multi-scaling. We also relate some of the scaling found to sediment transport and landscape forming processes, showing how the fundamental or basic scale associated with river networks, drainage density, can be interpreted as a scale where the dominating sediment transport process changes. Stable diffusive sediment transport processes dominate at the small scale leading to smooth hillslopes, while at large scale the instability caused by the convergence of surface flow and sediment transport results in channelization. This transition is detected in the data as a break in scaling. Below a certain scale the traditional scaling laws that characterize river networks no longer hold. The use of digital elevation data to detect this break in scaling lets us extract channel networks with a physically justifiable drainage density that is related to the basic scales present in the landscape and independent of subjective judgment by the map maker.

1.2 Outline

This work is divided into five main chapters, followed by a concluding chapter that summarizes the important results and an appendix giving details of the computer codes used.

Chapter 2 is a literature review and analysis of previous work. After reviewing the ideas that have motivated this study, we describe the terminology and ordering systems used. We then define drainage density, which is interpreted as the basic length scale associated with the dissection of the landscape by the river network. The random topology model is then described and scaling in river networks reviewed. The notion of fractal dimension used to characterize scaling is then presented, together with techniques to measure fractal dimension. We conclude the review with discussion of channel network and landscape evolution processes.

Chapter 3 goes into the technical details of the computer procedures used for processing DEM's and extracting channel networks. It gives the data structures and conventions used. It also gives the sources of digital elevation data reviewing the procedures used in preparation of the data and discussing data accuracy. Tables at the end of Chapter 3 list the data sets used in this study.

Chapter 4 focuses on the planar properties of river networks. We show that in planform river networks can be regarded as space filling fractals and that this provides a relationship between the scaling of stream lengths and numbers given by Horton's Laws.

Chapter 5 discusses the scaling of channel slope with area as a scaling index. Here DEM data shows that link slopes are not self-similar, but are characterized by a scaling that has coefficient of variation increasing with area. This scaling is such that the density of independent elevation increments has a negative power law scaling with area.

Chapter 6 focuses on the basic scale or drainage density. It first shows how the slope scaling of Chapter 5 breaks at a certain basic scale and then provides an interpretation of this in terms of sediment transport processes and a stability criterion. The fact that slope scaling is practically equivalent to a constant stream drop property then allows us to use the drop property as an alternative test for the break in scaling and measure of drainage density. A third measure of drainage density is obtained from localized DEM procedures and then the three measures of drainage density are compared for 21 DEM data sets.

Chapter 2

LITERATURE REVIEW

2.1 Motivation

There has been increasing interest during the last decade in the geomorphology of river networks and its relation to hydrology. The effort has been stimulated by the work of Rodriguez–Iturbe and Valdes (1979) relating the instantaneous unit hydrograph to network morphology, and further work on this theme, Gupta et al. (1980), Rodriguez–Iturbe, et al. (1982), Troutman and Karlinger (1984; 1985). As a result investigators like Mesa (1986), Gupta and Mesa (1988), Abrahams (1984) have re–examined the structure of river networks and models describing that structure.

New sources of data, namely digital elevation models and powerful computers allow us to quickly test more alternatives and examine larger data sets than has ever been possible. O'Callaghan and Mark (1984) and Band (1986) have pioneered the extraction of channel networks from digital elevation models. The importance of scale issues and hydrologic similarity has received considerable interest recently [Conference proceedings, Gupta et al., (eds.), (1986); Rodriguez–Iturbe and Gupta (eds.) (1983)], with a realization that a basin scale approach is needed to understand the structure and similarity of river basins. It is hoped that this will ultimately lead to hydrologic predictions from ungauged basins.

The flow of water over long time scales has shaped river basins. Also the shape of river basins is a controlling factor in the generation of runoff and hydrologic response. This reciprocity is the fundamental reason for efforts to link hydrology and geomorphology and needs to be better understood. Through the analysis of a lot of digital terrain data, this work takes steps towards this understanding. The focus is on the scaling properties of river networks and landscapes, as well as the fundamental scales at which certain processes dominate or

where there may be changes from control by one process to another.

2.2 Terminology and Ordering Systems

The terminology used is basically that of Horton (1945), Shreve (1966), and in common use in hydrogeomorphology. A river network is idealized as a trivalent planted tree, the root of which is the outlet or point furthest downstream. Sources are points furthest upstream, and a point at which two upstream channels join to form one downstream channel is called a junction or node. Exterior links are the segments of channel between a source and the first junction downstream and interior links are the segments of channel between two successive nodes or a node and the outlet. Each link has certain properties: length along the stream; geometric length, the distance between end points; height, the elevation difference between upstream and downstream nodes; average slope, height divided by length; contributing area, the total area draining through the link measured at the downstream end and local area, the area draining directly into a link, i.e., not through any other links.

Ordering systems are used to group or categorize links or segments of channels. Ordering systems can work through the network from the root, or outlet, upstream, or from each source, downstream or inwards. The upstream ordering schemes have been unsuccessful so will not be discussed here.

A major contribution of Horton (1932, 1945) was the introduction of a downstream ordering system. Strahler (1952, 1957) revised Horton's scheme to avoid some ambiguities. The revised Horton/Strahler ordering system is as follows. All exterior links have order 1. When 2 upstream links of the same order join the downstream link has order increased by 1. When 2 upstream links of different order join the downstream link takes the higher order of the two incoming upstream links. Strahler streams are segments of channel consisting of links of the same order.

Another ordering system is the concept of link magnitude due to Shreve (1966). Here source streams or links have magnitude 1. At a bifurcation the downstream link takes magnitude the sum of the two incoming magnitudes. Thus the magnitude of each link represents the number of sources in the network draining into that link. Figure 2.1 shows the Horton/Strahler ordering system and concept of link magnitude.

Horton/Strahler ordering is usually used in characterizing a river network according to the Horton ratios.

$$R_b = \frac{N_{w-1}}{N_w} \quad (2.1)$$

$$R_\ell = \frac{L_w}{L_{w-1}} \quad (2.2)$$

$$R_a = \frac{A_w}{A_{w-1}} \quad (2.3)$$

$$R_s = \frac{S_{w-1}}{S_w} \quad (2.4)$$

where N_w is the number of streams of order w , L_w is the mean length of streams of order w , A_w is the mean area contributing to streams of order w , and S_w is the mean slope of streams of order w . R_b , R_ℓ , R_a , and R_s are bifurcation, length, area, and slope ratios, respectively. Horton discovered that these ratios were approximately constant through semi-log plots of N_w , L_w , A_w , and S_w against order. The ratio or "Horton number" is obtained from the slope of the straight line fit to such plots, the procedure is called a "Horton analysis" (see Figure 2.2). Since the ratios are approximately constant, the above geometric descriptors are called

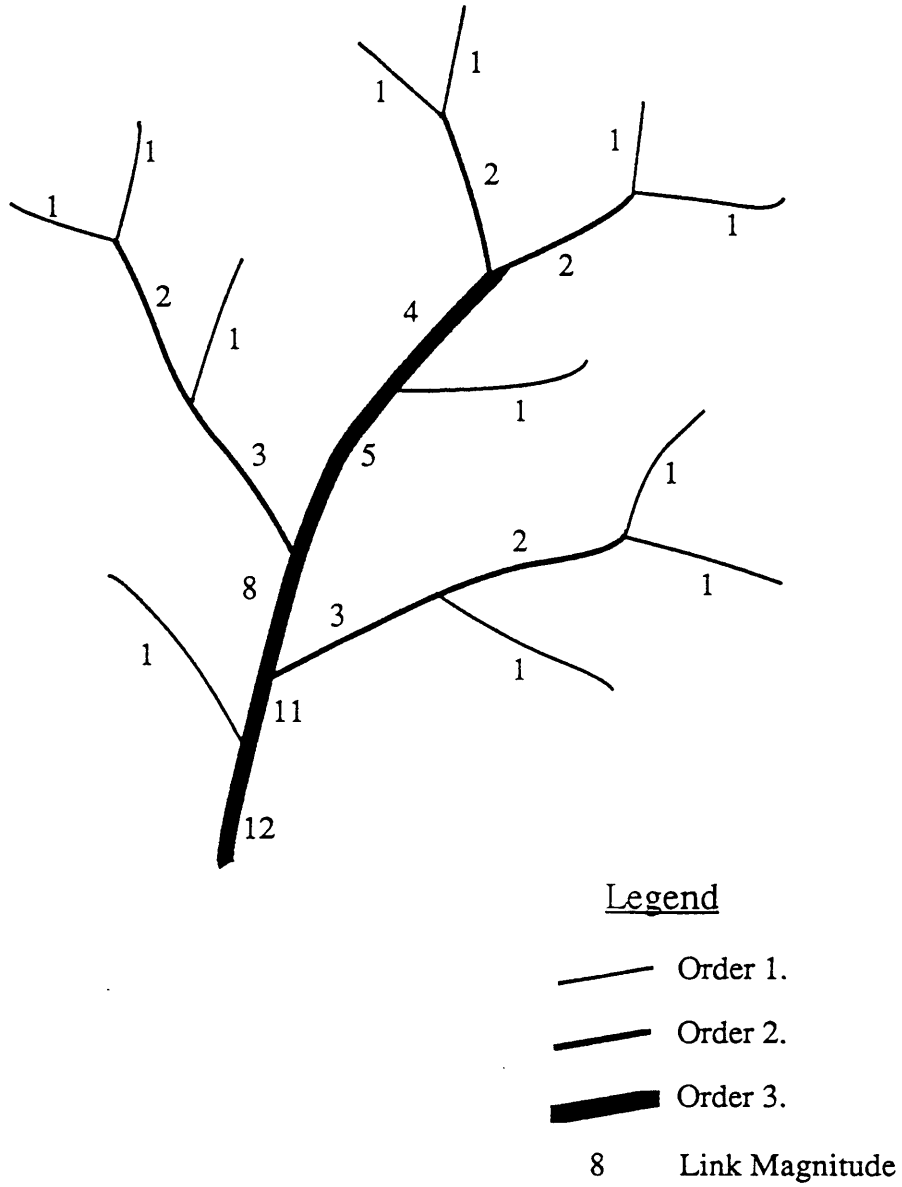


Figure 2.1. Horton/Strahler ordering and Link Magnitude

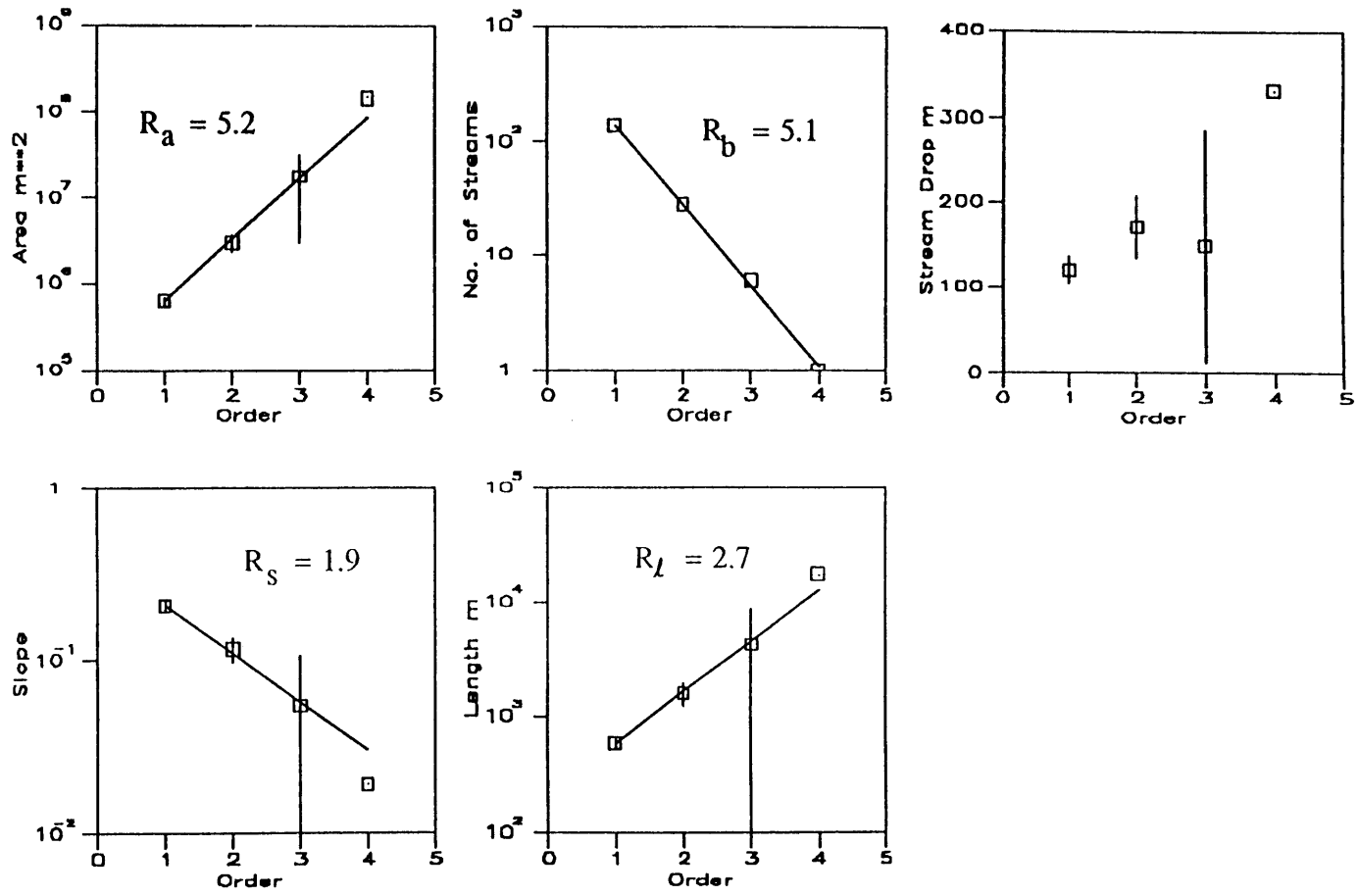


Figure 2.2. Big Creek (CALD) Horton Analysis

"Horton's laws." The area law above was not explicitly stated by Horton, and is due to Schumm (1956). Smart (1978, p. 131) notes that the Horton analysis has proved unsuccessful in the two major applications that Horton envisaged for it, namely the characterization of basins in different environments and the estimation of complete network properties by extrapolation of measurements from small-scale maps. Smart (1981) found this latter procedure to be highly inaccurate and badly biased. As far as characterizing basins in different environments the following are some of the studies that have found no significant differences in Horton ratios for different regions (Strahler 1952, 1957; Chorley, 1957; Woodruff, 1964; Eyles, 1968; Shreve, 1969). Abrahams (1972) found a significant correlation of R_b with relief. These deviations are more significant in terms of the link based analysis and random model to be discussed later.

Leopold and Miller (1956) extended Horton's ideas by showing that the log of many hydraulic variables are approximate linear functions of basin order. This behavior is due to the fact that most quantities depend strongly on the size of the drainage basin. A common measure of size or scale is basin area and the dependence of a general variable on area is often expressed, by a power law

$$X \propto A^b \tag{2.5}$$

with b a constant.

This implies

$$\log X \propto \log A \tag{2.6}$$

and since order is proportional to $\log A$ (area law) the linear relationships with order follow.

Smart (1978) concludes that after 30 years of use the benefits from Horton analysis have been few and limited. Order just provides a simple objective (though not always consistent) measure of size or scale. It is not clear that order has any advantage for such purposes over other size related properties such as area and magnitude. Smart (1978) suggests, following Shreve (1966) that the link rather than Strahler stream segment should be regarded as the basic unit of network composition.

2.3 Drainage Density, Dissection and Hillslope Scale

The previous section presented the Horton/Strahler ordering system and concept of link magnitude as measures of size or scale of the network. These are topological, dimensionless, measures of size. They need to be related to the physical size, area, of the basin. This relationship will be through the drainage density which is a measure of the degree to which the basin is dissected by channels. It is also closely related to stream and link frequency (to be defined later), mean link length, and mean hillslope length. These are measures of a fundamental length scale associated with the dissection of the landscape by the river network. Horton (1932, 1945) defines the drainage density

$$D_d = \frac{L_T}{A} \quad (2.7)$$

where L_T is the total length of streams and A is area. Horton suggested that the average length of overland flow or hillslope length could be approximated by $1/2 D_d$. Smith (1950) measured the fundamental scale of topography in terms of a texture ratio, the number of contour crenulations divided by contour length. He essentially showed that texture was correlated with D_d so the notion of a well or poorly drained

basin corresponds to the notion of fine or coarse texture.

Horton defines stream frequency as

$$F_s = \frac{N}{A} \quad (2.8)$$

where N is the number of Strahler streams. Link frequency F is similarly defined using the number of links. Melton (1958) showed that F_s was strongly correlated with drainage density. Smart (1978) states that mean link length and link frequency are also closely related to drainage density. If the mean area draining to a link is $\kappa \ell^2$ (suggested by Shreve, 1967), where ℓ is mean link length, the relationship is

$$D_d = F\ell = \frac{1}{\kappa \ell} \quad (2.9)$$

We see that drainage density, stream or link frequency, mean link or hillslope length and texture are all essentially measures of the same thing, the fundamental horizontal length scale associated with how the channel network dissects the landscape. The determination of this scale is generally dependent on the resolution of the map used. Historically workers have called for the highest resolution maps and/or field work to measure these quantities.

Mark (1983) discusses the differences between drainage networks obtained from maps and field surveys, and the merits of various procedures such as use of contour crenulations to "extend" the network. He concludes that first order basins defined from contour crenulations on 1:24,000 maps do exist as topographic features in the field. However, the form has often been simplified by cartographic generalization. Most first order basins defined on the map contain more than one fluvial channel in the field. Accordingly the exterior links drawn by contour crenulations do not represent unbranched channels. The question arises in the

context of scaling and fractals (Mandelbrot, 1983) as to whether this notion of scale is well founded or whether the river networks dissect the landscape infinitely, requiring characterization as a scaling phenomena. This is one of the main questions addressed by this work and was recognized early by Davis (1899, p. 495), who wrote

"Although the river and hillside waste do not resemble each other at first sight, they are only the extreme members of a continuous series and when this generalization is appreciated one may fairly extend the 'river' all over its basin and up to its very divide. Ordinarily treated the river is like the veins of a leaf; broadly viewed it is the entire leaf."

2.4 The Random Topology Model

The notions of topologically distinct and topologically random channel networks due to Shreve (1966) have been fundamental to the assessment of network composition laws, such as Horton's laws. Topologically distinct networks as defined by Shreve (1966) are networks whose schematic map projections cannot be continuously deformed and rotated in the plane so as to become congruent. Shreve (1966) quantified the notion of "randomly merging channels" by proposing that all topologically distinct networks with a given number of links (i.e., fixed magnitude or scale) are equally likely. This is referred to as the first hypothesis of the random model. Using this idea Shreve (1966) showed that the most likely set of stream numbers were those that obeyed Horton's bifurcation law and furthermore that given a number of first order streams and basin order, the variability of number of streams of each order was topologically constrained to a narrow window around the straight line representing Horton's law. Shreve (1967) generalizes this result to infinite networks and shows that if mean link lengths, and areas draining to each link, are constant then Horton's length and area laws also follow. In infinite

networks Shreve (1967) obtains $R_b = 4$, $R_\ell = 2$, $R_a = 4$. Smart (1968) first articulates the second hypothesis of the random model, namely that interior and exterior link lengths and the associated areas are independent random variables. The results of Shreve (1967) for R_b , R_ℓ and R_a given above become expected values under this model. Shreve (1969) gives details of these results.

The fact that Horton ratios are approximately constant and that these constant values are reproduced by the random model is the main basis for Smart's (1978) conclusion above regarding the lack of utility of Horton analyses. The Horton ratios R_b , R_ℓ and R_a may be seen as the effect of randomly merging channels and do not characterize different environments or networks. The same cannot be said about the slope ratio R_s since the random model says nothing about slope or elevation effects.

Shreve (1967) noted the connection between random networks and random walks. This connection is made concrete in terms of his representation of network topology symbolically as a string of Es and Is. The EI string is constructed as follows:

Start at the outlet and traverse the network always turning left at bifurcations and reversing direction at sources, until the outlet is again reached. During the traverse record an I, the first time a given interior link is traversed and an E the first time a given exterior link is traversed. Each link will be traversed twice but recorded only the first time.

A random network is equivalent to a random walk in which I's count +1 and E's count -1 and occur with equal probability. Gupta and Waymire (1983) point out that the equal probability of bifurcation and termination does not follow from the equal likelihood of topologically distinct random networks assumption and emphasize that the equal probability of termination and bifurcation should be added to the first random postulate. The IE string representation of network topology

coded as a binary string of 0's and 1's is also useful for computer storage of network topology information.

Random networks are also analogous to branching processes, which have been widely studied. Troutman and Karlinger (1984), Gupta et al. (1986), Mesa (1986), and Gupta and Mesa (1988) have used this fact to derive statistical properties of hydrologically important geomorphological functions, in particular the width function, for topologically random networks. The width function $L(x)$ is defined as the number of links, or points on the channel network at a distance x , measured along the channels, from the outlet, and was defined by Kirkby (1976). It is important because under the assumption of constant flow velocity in channels, it represents a time area diagram or unit response function for the channel network. The width function can be generalized by letting x be a more general measure of distance from the outlet. One such generalization is the link concentration function $\check{L}(h)$ defined by Gupta, et al. (1986). Here the generalized distance is height or elevation above the outlet, denoted h .

The random model was very successful at "explaining" Horton's laws. However, using link based analyses Abrahams (1984) records many significant deviations from topologic randomness. In particular the random model predicts that cis and trans links occur with equal frequency. A cis link is where the upstream lower magnitude link and downstream lower magnitude link both enter on the same side of the link in consideration. A trans link is where they enter from opposite sides. James and Krumbein (1969) reported significantly more trans links than cis links and an abundance of short trans links in real basins.

These deviations may be a useful way of characterizing the difference between networks in different environments. Alternatively, they may be due to the geometric space filling constraints imposed when basins must be packed together on a surface (Goodchild, 1988) in which case they will be present in all networks,

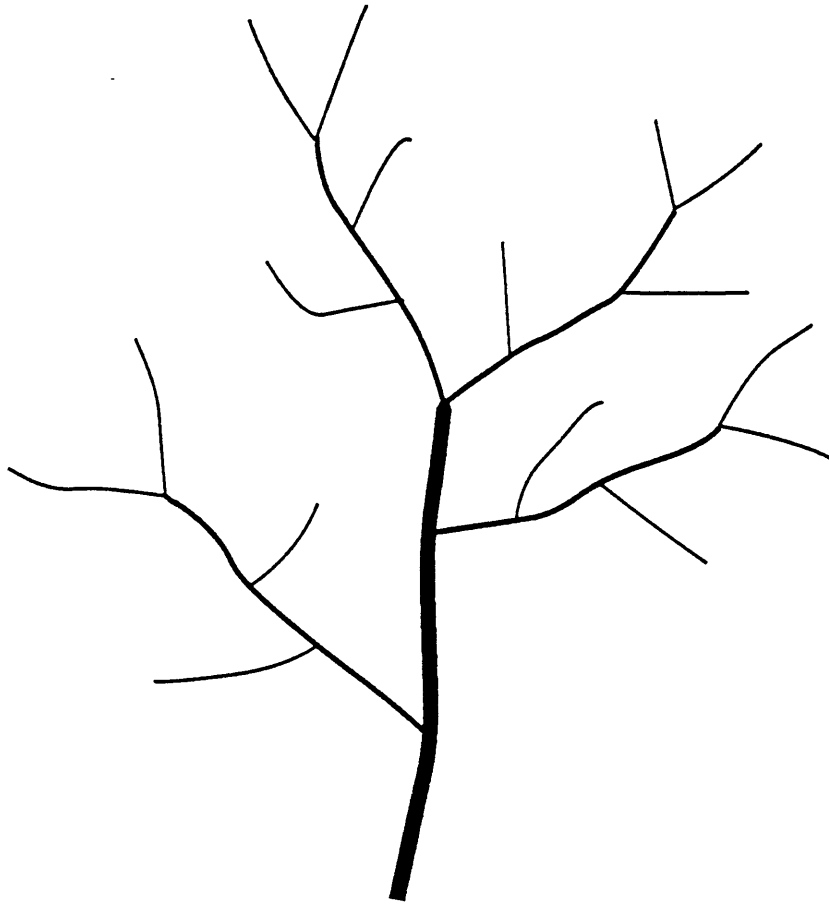
irrelevant of the environment.

2.5 Scaling in River Networks

An important feature of the link based analysis and the topologically random network model is that the link provides a fundamental scale. Link length is a fundamental length scale related to drainage density by Equation (2.9). A basic length scale may not be desirable if it is dependent on the scale of map used, and is inconsistent with the notion of Davis (1899) of rivers extending over the whole land surface.

On the other hand, Horton's laws are scaling laws that relate properties at small scale (low stream order) to properties at large scale (high stream order). They characterize scaling at scales larger than the basic scale and may apply down to infinitesimally small scale if the notion of a lower bound basic scale is rejected. When analyzing scaling, the notion of self-similarity (defined formally in Section 2.6) is important. The use of Horton's laws as exact descriptors of scaling is not consistent with self-similarity. A network constructed to have Horton's bifurcation law hold exactly cannot be self-similar and have low order streams flow directly into streams more than one order higher. To see this consider the third order network shown in Figure 2.3 with bifurcation ratio 4. There must be 4 second order and 16 first order streams. To maintain self-similarity and the same bifurcation ratio, 4 first-order streams must flow into each second order stream. There are no first-order streams remaining to flow directly into the third-order stream. This property is not borne out in practice.

Furthermore it seems reasonable to assume at least as a first approximation that the area draining directly into each link is approximately constant. This constant is the average area draining first-order streams A_1 (since they are single



Legend




-  Order 1.
-  Order 2.
-  Order 3.

Figure 2.3. Structurally Hortonian network with bifurcation ratio 4.

links). Now the number of links in any network is $2n-1$ so the total area draining a basin order ω is

$$A_{\omega} = A_1(2n - 1) \quad (2.10)$$

Now Horton's bifurcation law [Equation (2.1)] implies

$$n = R_b^{\omega-1} \quad (2.11)$$

so we get

$$A_{\omega} = A_1(2R_b^{\omega-1} - 1) \quad (2.12)$$

from which

$$R_a = (2R_b^{\omega-1} - 1)^{\frac{1}{\omega-1}} \quad (2.13)$$

Thus for R_b constant, R_a is dependent on order, i.e., not constant. The bifurcation and area laws together with constant average area per link are mutually inconsistent.

This inconsistency is also manifested if instead of assuming the area draining directly into each link constant, we assume the area draining directly into each link is proportional to link length (with mean link length constant, these amount to the same thing). The average length of streams of order ω is $L_1 R_{\ell}^{\omega-1}$ so the average area draining directly into a stream of order ω is $A_1 R_{\ell}^{\omega-1}$. Hack (1957) sums these areas to get

$$A_\omega = A_1 R_b^{\omega-1} [(R_\ell/R_b)^\omega - 1] / [R_\ell/R_b - 1] \quad (2.14)$$

which implies

$$R_a = R_b \{ [(R_\ell/R_b)^\omega - 1] / [R_\ell/R_b - 1] \}^{1/\omega-1} \quad (2.15)$$

Again for R_ℓ and R_b constant, R_a is not constant. Perhaps these are the reasons why Horton never stated an area law (leaving it to Schumm, 1956). Horton (1945) believed in the constancy of the length of overland flow ($1/2 D_d$) which amounts to area draining directly into a stream being proportional to length and leads to the inconsistency of the area law with other laws.

This discrepancy is not resolved by assuming differences between external and internal links. If we denote the average area draining internal links a_1 (with $a_1 < A_1$), we get analogously to Equation (2.15)

$$A_\omega = (A_1 - a_1) R_b^{\omega-1} + a_1 R_b^{\omega-1} [(R_\ell/R_b)^\omega - 1] / [R_\ell/R_b - 1] \quad (2.16)$$

which cannot be expressed as an exponential function of ω , as would be required for an area law.

These inconsistencies are resolved in the cyclic scaling model suggested by Tokunga (1978). Horton/Strahler ordering is still used, with the interpretation of the lowest order streams being the smallest resolvable at the scale of resolution being used. Order is used as a relative, rather than absolute measure, with Ω the highest order stream and $\Omega-1, \Omega-2, \dots$, lower order streams, extending to infinitely small order. The absolute order Ω is never actually known, but the differences

between orders of different streams gives an idea of their relative sizes. Denote the number of streams of order i flowing laterally into a higher order stream of order j by ${}_j\epsilon_i$. Tokunaga (1978) suggests that ${}_j\epsilon_{j-k}$ ($k > 0$) are on average independent of j , denoted

$$\epsilon_k = {}_j\epsilon_{j-k}$$

and that furthermore

$$K = \frac{\epsilon_k}{\epsilon_{k-1}}$$

is on average constant. The two parameters ϵ_1 and K are analogous to R_b in that they completely describe the number of streams of each order. In practice K and ϵ_1 suffer from some of the same drawbacks as R_b . They show scatter within particular networks, do not distinguish between qualitatively different networks from different environments and cluster around approximately constant values. Tokunaga (1978) gives

$$N(\Omega, w) = \frac{Q^{\Omega-w-1} - P^{\Omega-w-1}}{Q - P} Q(2 + \epsilon_1 - P) + P^{\Omega-w-1}(2 + \epsilon_1) \quad (2.17)$$

for the number of streams of order w within a basin of order Ω . Here P and Q are parameters given by

$$P = \frac{2 + \epsilon_1 + K - \sqrt{(2 + \epsilon_1 + K)^2 - 8K}}{2} \quad (2.18)$$

$$Q = \frac{2 + \epsilon_1 + K + \sqrt{(2 + \epsilon_1 + K)^2 - 8K}}{2}$$

Equation (2.17) gives a law of stream numbers such that the log of stream numbers plots against order as a slightly concave shape, agreeing qualitatively with this tendency reported by Shreve (1966). This is a slight deviation from Horton's bifurcation law, Equation (2.1) that makes the Horton ratio and Tokunaga formulations mathematically different, but practically indistinguishable given the scatter of real data.

Tokunaga (1978) shows that in infinite topologically random channel networks the expected values of K and ϵ_1 are $\epsilon_1 = 1$ and $K = 2$. In practice stream number data clusters around these values. With the assumption that the inter basin areas, i.e., areas draining directly into internal links, are less than the lowest order stream areas on average and $K < 2 + \epsilon_1$ as is usually borne out in practice, Tokunaga derives

$$A_w = Q^{w-\lambda} A_\lambda \quad (2.19)$$

where A_w is the area draining a basin of order w . This is equivalent to Horton's area law with $R_a = Q$. With $\epsilon_1 = 1$ and $K = 2$, Equation (2.18) gives $Q = 4$, corresponding to the random model result. With the additional assumption (analogous to Shreve, 1967),

$$A_\lambda = \kappa L_\lambda^2 \quad (2.20)$$

where L_λ is the length of stream of order λ Tokunaga gets

$$L_w = Q^{(w-\lambda)/2} L_\lambda \quad (2.21)$$

equivalent to Horton's length law with $R_\ell = \sqrt[Q]{Q}$.

The appeal of Tokunaga's formulation is its self-similarity. Subnetworks within a network are statistically equivalent, except for a scaling factor.

Except for Horton's slope law the discussion so far has been devoid of any consideration of elevation in channel networks. It is widely recognized that elevation, related to potential energy is an important part of the network and we need to understand the structure and scaling of river networks with the third dimension elevation included. Qualitatively streams are steep near their sources and flatter downstream. This is quantified by Horton's slope law which implies an exponential decrease of slope with order.

$$S_w = (R_s S_1) R_s^{-w} = R_s S_1 e^{-w \ln R_s} \quad (2.22)$$

Broscoe (1959) noted that the average drop H_w along Strahler streams of order w was approximately constant, i.e., independent of order. This "constant drop law" is sometimes added to Horton's laws and Yang (1971b) claims that it is due to a variational principle, equal distribution of stream power. Recognize that on average $H_w = S_w L_w$, so H_w constant implies

$$\frac{S_w}{S_{w-1}} = \frac{L_w}{L_{w-1}} \quad (2.23)$$

i.e., $R_s = R_\ell$

Typically R_s is close to R_ℓ but it is not evident whether this coincidence is responsible for the constant drop law or is due to the constant drop law.

Flint (1974), building on the power law relationships of Wolman (1955), Leopold and Maddock (1953), Leopold and Miller (1956) and Leopold, et al. (1964) finds slope empirically related to area by

$$S = C A^{-\theta} \quad (2.24)$$

with θ ranging from 0.37 to 0.83 with a mean of 0.6. Substituting in Horton's area and slope laws Flint (1974) gets

$$\theta = \frac{\ln R_s}{\ln R_a} \quad (2.25)$$

again showing the connections between power law scaling with area (as a size or scale measure) and exponential scaling with order.

Recognizing that link magnitude is often a good surrogate measure for area, Equation (2.24) can be written

$$S = C n^{-\theta} \quad (2.26)$$

Horton's slope law, the constant drop law and power law scaling of slope with area are all equivalent empirical descriptions of the concavity of stream profiles.

Gupta, et al. (1986) and Mesa (1986) tried to extend the topologically random network model to elevations by assuming that link heights were independent random variables. They had little success due to the inhomogeneity of the link height distributions, something that in retrospect should have been obvious from the

slope scaling described above.

Gupta and Waymire (1989) point out the close connection between power law scaling and notions of statistical self-similarity. This is as follows. A random variable S is called self-similar with respect to scaling index A if

$$S(\lambda A) \stackrel{d}{=} \mu(\lambda) S(A) \quad (2.27)$$

where $\mu(\lambda)$ is a scaling function and λ a scale factor. $\stackrel{d}{=}$ denotes equality in probability distribution. Gupta and Waymire (1989) show quite generally that $\mu(\lambda)$ must be of the form

$$\mu(\lambda) = \lambda^{-\theta} \quad (2.28)$$

Gupta and Waymire (1989) suggest that the hypotheses that link slopes (or link drops) are self-similar with respect to area (or magnitude as a surrogate) as a scaling index seems reasonable and would "explain" the observed slope scaling. In Chapter 5 we focus on this issue and show that the slope scaling is not simple self-similarity, but a more general multiscaling. Multiscaling is required to fit the mean slope trends described above as well as the scaling of higher order moments obtained from data.

The importance of notions of similarity in hydraulic geometry had been recognized earlier by Smith (1974) who used a simple model of sediment movement in stream channels and Manning's equation to derive a set of differential equations governing channel bed forms. He notes that the equations are of the diffusion type that permit similarity solutions and hypothesizes similarity solutions of the form

$$S = k x^\mu \tag{2.29}$$

$$d = x^\nu f(y/x^\tau)$$

Here d is depth, x the along stream coordinate, y the transverse coordinate, S slope, k a constant and μ , ν and τ scaling exponents. Solutions of the form (2.29) are then used in the governing equations to solve for the scaling exponents. The power law scaling of hydraulic parameters (width, depth, velocity, and slope) as functions of discharge Q are then obtained in terms of these exponents. The exponents obtained compare well with the empirical observed values of Leopold and Maddock (1953).

2.6 Fractals and Scaling

The study of scaling has been considerably advanced by the notions of fractals and fractal dimension (Mandelbrot, 1977, 1983). Fractals provide a mathematical framework for treatment of irregular seemingly complex shapes that display similar patterns over a range of scales. Many objects in nature are statistically self-similar.

Voss (1986) defines statistical self-similarity:

"The set S is statistically self-similar if it is composed of N distinct subsets each of which is scaled down by the ratio r from the original and is identical in all statistical respects to rS ."

The fractal or similarity dimension of S is given by

$$D = \frac{\log N}{\log 1/r} \tag{2.30}$$

Statistical self-similarity implies invariance of the full probability distribution describing the random object under simple geometric transformations or changes of

scale. In practice though claims of statistical self-similarity are usually based on measurement of a few moments.

Direct methods of measuring fractal dimensions are the ruler method (Mandelbrot, 1977) and Box counting (Hentschel and Procaccia, 1983; Voss, 1986; Lovejoy et al., 1987). These methods are based on the fact that the measure or size, M , of a fractal object or set is

$$M = N r^D \tag{2.31}$$

where N is the number of objects of linear size or scale r required to measure the object. A decrease in r results in an increase in N . The fractal dimension D is the value of the scaling exponent on r for which M is constant. This may occur over a limited range of scales r for which self-similarity holds and where the opposing tendencies of decreasing r and increasing N are exactly balanced in the product Nr^D . The ruler method counts the number, N , of rulers of length r needed to measure the apparent "length" of a curve, for several different ruler lengths r . On a plot of $\log N$ vs. $\log r$, the slope is $-D$ according to Equation (2.30). Andrie and Abrahams (1989) show that this technique is not foolproof. They simulated a curve with a fixed scale (i.e., not fractal) by perturbing a square wave (see Figure 2.4). Figure 2.5 gives the $\log N$ vs. $\log r$ plot for this wave. The approximate straight line is suggestive of scaling with $D = 1.11$, which is clearly wrong by construction of the curve. Andrie and Abrahams (1989) then plot apparent length $L = Nr$ versus r (reproduced in Figure 2.6) which for a fractal should satisfy

$$L \propto r^{1-D} \tag{2.32}$$

It is evident from Figure 2.6 that Equation (2.32) does not hold for the simulated

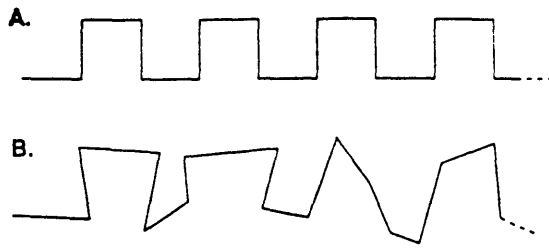


Figure 2.4. Sections of (A) a regular square-wave form and (B) a randomized square-wave form. (from Andrie and Abrahams, 1989)

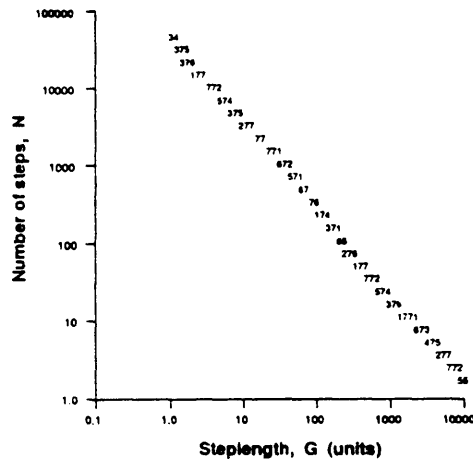


Figure 2.5. Graph of number of divider steps against steplength for the randomized square-wave form. Numerals on the graph indicate the number of superimposed points. (from Andrie and Abrahams, 1989)

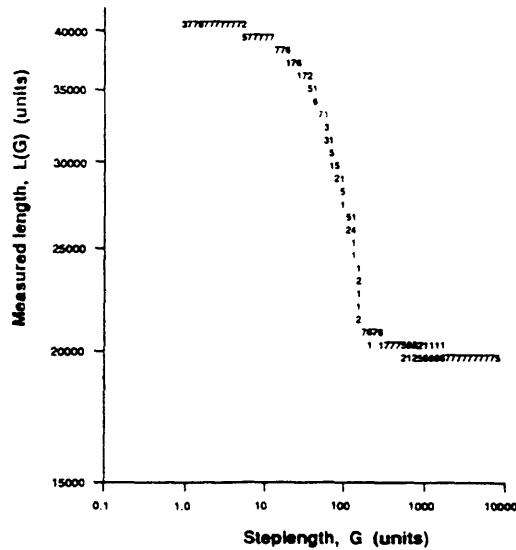


Figure 2.6. Graph of measured length against scale of measurement for the randomized square-wave form. Numerals on the graph indicate the number of superimposed points. (from Andrie and Abrahams, 1989)

curve of Andrieu and Abrahams (1989). The principle of plotting apparent measure $L = Nr^D$ versus r with D obtained from the N vs. r plot appears to be a good one, as a check for breaks in scaling. The apparent measure should be a constant function of r .

Box counting uses the fact that the number of boxes of side r , needed to cover a fractal set S is theoretically

$$N_{\text{box}}(r) \propto r^{-D} \quad (2.33)$$

Therefore, the slope of $\log N$ vs. $\log r$ plots give estimates of D .

Indirect methods of measuring D include use of variograms and spectral densities. Voss (1986) gives ways to relate variogram (difference) scaling exponents and spectral scaling exponents to fractal dimension D .

Goodchild and Mark (1987) review the application of fractal models in geography. Here we will just focus on two aspects, the land surface and the channel network.

Mandelbrot (1977) found that many natural lines, such as coastlines, contours, political boundaries (sometimes consisting of rivers or coastlines), etc., seemed to have fractal dimensions near 1.2 – 1.3. He also noted that simulations of fractional brownian surfaces with $D \simeq 2.3$ looked remarkably like the real landscape. He took this as evidence that landscapes were fractal characterized by $D \simeq 2.3$. The relationship between the fractal dimensions of a surface and a line projected from the surface (e.g., contour or profile) is

$$D_{\ell} = D_s - 1 \quad (2.34)$$

so these results are consistent.

Mark and Aronson (1984) used variogram techniques to estimate the fractal dimension of the land surface of 17 USGS 7.5 min quadrangles from digital elevation data. Sixteen of these showed some evidence of characteristic scales at which fractal dimension changed, often sharply. Over short scales (below 0.6 km) they found that many surfaces do indeed resemble fractional brownian surfaces with dimensions of around 2.3. At larger scales however many areas were characterized by much higher dimensions, around 2.75. Ahnert (1984) notes the relationship

$$R \sim L^H \tag{2.35}$$

with exponent $H \simeq 0.8$. Here R is local relief (difference in elevation) in an area with diameter L . Ahnert (1984) attributes the log slope of 0.8 to a morphological expression of the dynamic equilibrium between the maximum geophysically possible rate of long-term uplift and the denudational response. Culling (1986) notes that this is analogous to a Hurst phenomenon (i.e. the persistence in long term hydrologic time series, noted by Hurst (1951)) in the landscape, and as such characterizes the landscape as scaling with fractal dimension

$$D = 3 - H \tag{2.36}$$

For further information on the Hurst phenomenon, a feature of long-term hydrologic time series, see Bras and Rodriguez-Iturbe (1985). Culling and Datko (1987) also look at scaling in the landscape. They claim to predict theoretically, although the basis for the predictions is not clear from their paper, that:

- The Hausdorff dimension of soil slopes governed by a diffusion degradation regime will take values between 2 and 2.3 tending towards the lower value as diffusion proceeds.

- The landscape will show evidence of a second fractal structure associated with the drainage network with fractal dimension between 2.4 and 2.6.
- The dimension of a level set (intersection with horizontal plane, i.e., a contour) or vertical set (intersection with vertical plane, i.e., a profile) is one less than that of the parent surface [i.e., consistent with Equation 2.34)].

Culling and Datko present results from 17 1:25,000 ordinance survey maps in southern England. The intersection of mapped contours with lines traversing the sheets diagonally was used to produce profiles. The fractal dimension of the profiles were estimated using the ruler method and variogram techniques. For many of these data sets two different fractal dimensions are quoted, presumably from two distinct slopes at different scales. Although Culling and Datko (1987) do not discuss it, their Figure 6 [reproduced here, Figure 2.7] has similar sharp breaks in scaling to those discussed by Mark and Aronson (1984) [Figure 2.8], with different fractal dimension above and below the characteristic scale determined by the break in scaling.

The above studies suggest that the domains with different fractal dimensions could be interpreted in terms of different geomorphological processes operating or dominating at different scales. Goodchild and Mark (1987) point out that most real geomorphological entities are not pure fractals in the sense of having a constant D , but in a lesser sense of exhibiting the behavior associated with a fractional dimension over some range of scales. D thus provides a characteristic parameter whose variation can be usefully interpreted in terms of the important processes over the range of scales for which D holds constant.

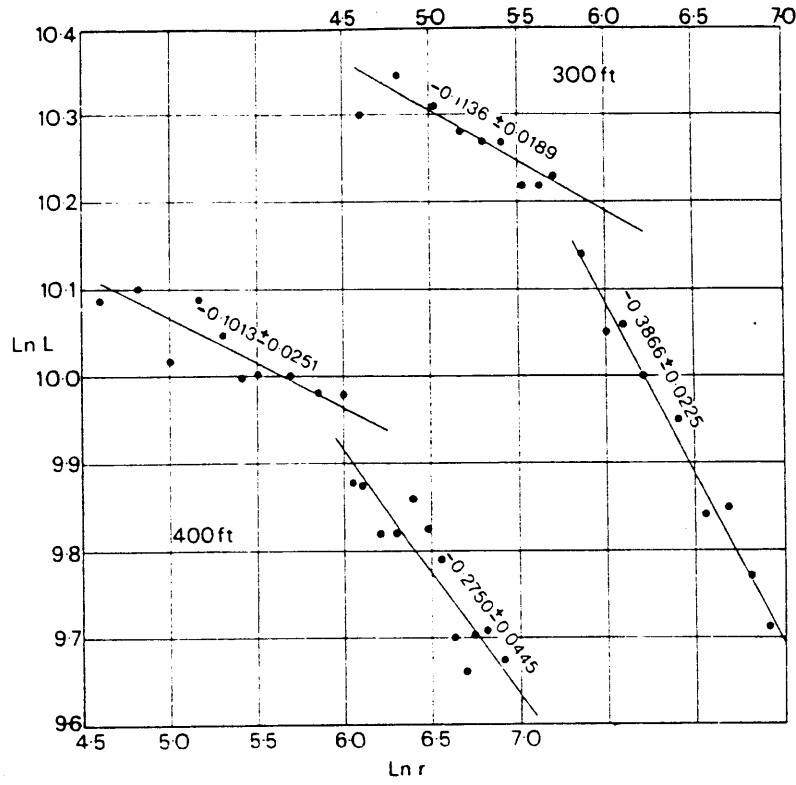


Figure 2.7. Burwash TQ 62. Richardson plots for 300' and 400' contours. (from Culling and Datko, 1987)

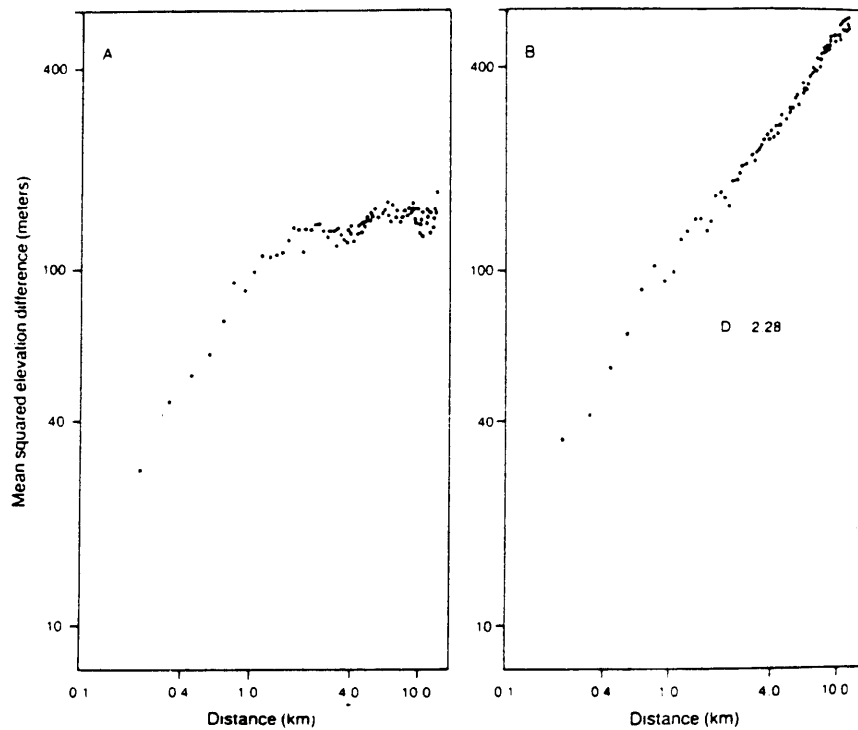


Figure 2.8. Variograms for the Aughwick, Pennsylvania (A) and Shadow mountain, Colorado (B) digital elevation models. Each point represents the mean squared elevation difference for points within a certain distance class. Total sample size was 32,000 pairs of points: distance classes with fewer than 64 pairs have been omitted from the diagram. (from Mark and Aronson, 1984)

Eagleson (1970, p. 379) presents data from several studies that support the relationship first suggested by Hack (1957)

$$L = k A^\alpha \quad (2.37)$$

where L is mainstream length and A basin area. k and α are coefficients, typically $k = 1.4$ and $\alpha = 0.57$. Dimensional consistency and geometric similarity would suggest that α should be 0.5. Mandelbrot (1977; 1983) uses this result to suggest that rivers are fractals with dimension $2\alpha \simeq 1.1$ or 1.2. Mandelbrot (1983) also describes some fractal geometric patterns that resemble river networks where the fractal dimensions of individual lines is 1.1 but the complete network is space filling with $D = 2$. He suggests that these patterns are models of river networks. Hjelmfelt (1988) uses the ruler method in eight individual streams in Missouri and estimates fractal dimension near 1.1.

La Barbera and Rosso (1989) and Tarboton, et al. (1988) show that for river networks that obey Horton's laws, the fractal dimension is given by

$$D = \begin{cases} \frac{\log R_b}{\log R_\ell} & R_b > R_\ell \\ 1 & R_b < R_\ell \end{cases} \quad (2.38)$$

In practice $R_b > R_\ell$ always holds. They use measurements of R_b and R_ℓ to estimate D and find D for the whole network ranging from 1.5 to 2.

This fractal dimension of river networks clearly can only apply at scales where we have a network. This may be all scales if we use the generalization of Davis (1899) given above or more likely it may be above a threshold scale related to the drainage density. Church and Mark (1980) discuss the relationship between

total length of channels and area. They note that below a certain threshold, a finite drainage area may have no channels. Above this threshold they use data from Wood and Snell (1957) to show that total length (L_T) is proportional to area (A), supporting the idea that drainage density (defined in equation (2.7)) is independent of area. Above the threshold, L_T could be used as a surrogate measure for A , suggesting that the total length behaves or scales the same as area, and therefore should have the same fractal dimension, i.e., be space filling with $D = 2$.

A series of papers (Goodchild, et al., 1985; Goodchild and Mark, 1987; Goodchild, 1988) investigates drainage networks on fractional brownian (fbm) surfaces. They note that networks on fbm surfaces show similar deviations from topologic randomness to those noted by Abrahams (1984). This supports the notion that these deviations are due to the geometric constraints imposed when basins must pack together on a surface, a space filling constraint. The abundance of pits (areas that do not drain) on fbm surfaces casts doubt on the generality of these results and the suitability of fbm as a model for terrain. However Goodchild (1988) suggests that if pits are assumed to fill as lakes, fbm may be a useful model for lake-rich landscapes.

2.7 Channel Network Evolution and Processes

It is important when considering channel network and landscape geometry to have an appreciation of the processes that have and are continuing to sculpt the landscape. Ultimately we want to understand the relationship between form and processes and be able to make quantitative statements about the processes from detailed analysis of the form. Hydrologists are particularly interested in the runoff processes and movement of water and their excursion into geomorphology is from a need to address the problem of prediction from ungauged basins and an attempt to deduce processes from land form and channel network morphology. This section

will review the literature in geomorphological processes restricting ourselves to work that we feel is relevant. There is no attempt at completeness.

There is general agreement that elevation in channel networks and hillslopes may be thought of as an "open dissipative system" (Leopold and Langbein, 1962; Scheidegger, 1970; Thornes, 1983; Huggett, 1988). Carson and Kirkby (1972) provide a good review of the early work on evolution of hillslopes, relating form to processes. The formalism of differential equations describing the landscape surface is useful. Kirkby (1971) and Smith and Bretherton (1972) give the equation describing conservation of sediment as

$$\frac{\partial z}{\partial t} = -\nabla \cdot \underline{F} \quad (2.39)$$

where z is elevation and \underline{F} is the sediment or debris flux vector. With the reasonable assumption that this flux is in the direction of steepest gradient, Smith and Bretherton (1972) write

$$\underline{F} = F \underline{n}$$

where

$$\underline{n} = -\frac{\nabla z}{|\nabla z|}$$

is a unit downslope vector, and F is the magnitude of the sediment transport flux, per unit contour width, a scalar field, With this

$$\frac{\partial z}{\partial t} = \nabla \cdot \underline{n} F \quad (2.40)$$

Smith and Bretherton (1972) further assume $F(S,q)$, i.e., F is a function of the slope $S = |\nabla z|$ and flow of water q . The water flow is assumed to be a function of the area draining through unit contour width a with drainage in the steepest direction. Thus we can write $F(S,q(a)) = F(S,a)$, with a , a field which by continuity obeys

$$\nabla \cdot \underline{n} a = -1 \quad (2.41)$$

Note that in the context of hillslopes lower case a is used to denote area per unit contour width, a two-dimensional scalar field, while in the context of channel networks A denotes total contributing area. A is thought of as concentrated, i.e., flowing through a point with width neglected. When using digital elevation data, unit width is taken as the pixel size so the two notions of area are numerically equivalent. Smith and Bretherton (1972) carry out a linear stability analysis of Equation (2.40) and (2.41) and show that the pair of equations is unstable in the sense that small perturbations grow when

$$F - a \frac{\partial F}{\partial a} < 0 \quad (2.42)$$

Smith and Bretherton (1972) also show that a one-dimensional equilibrium or constant form solution is concave when Equation (2.42) is satisfied and convex otherwise. There is therefore an equivalence between concavity of a one-dimensional profile and instability in the two-dimensional landscape. Instability as characterized above would lead to rilling and channel growth. Otherwise, smooth hillslopes would prevail.

Luke (1972, 1974) generalizes the Smith and Bretherton (1972) formulation. Instead of assuming $F(S,q)$, which assumes the sediment load is always in equilibrium with slope, he suggests an additional equation

$$\frac{\partial z}{\partial t} = -f(S, q, F) \quad (2.43)$$

The function $f(\cdot)$ will be such that when the sediment load F is small, $f(\cdot)$ is positive, i.e., erosion, whereas when F is large, $f(\cdot)$ will be negative, i.e., deposition. Luke (1974) shows how the basic equations (2.40), (2.41), and (2.43) can be solved using the method of characteristics. He also shows how under conditions of instability troughs develop into shock discontinuities, interpreted as channels.

The behavior of Equation (2.42) is clearly dependent on the form of the sediment transport flux function $F(S, a)$. A common form is (Kirkby, 1971)

$$F \propto a^m S^n \quad (2.44)$$

Table 2.1 excerpted from Kirkby (1971) gives typical m and n for various processes.

Table 2.1
Typical Values of Exponents m and n in the empirical relationship
 $F \propto a^m S^n$ (Equation (2.44))

Process	m	n	Sources
Soil creep	0	1.0	C. Davison, 1889; Culling, 1963
Rainsplash	0	1-2	Schumm, 1964
Soil wash	1.3-1.7	1.3-2	Musgrave, 1947; U.S. Agric. Res. Serv., 1961; Zingg, 1940; Kirkby, 1969
Rivers	2-3	3	Derived from Leopold and Maddock, 1953

(from Kirkby, 1971)

Kirkby (1971) studied the solution to Equations (2.40) and (2.41) in one dimension and identified characteristic profiles under different assumptions for the sediment transport F (Equation 2.44). These are reproduced in Figure 2.9 and show

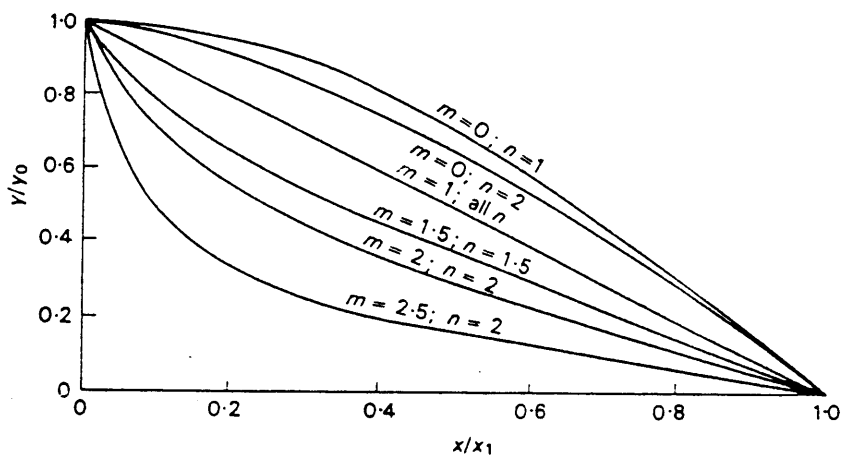


Figure 2.9. Characteristic form slope profiles. (from Carson and Kirkby, 1976)

convex profiles for soil creep progressing to concave profiles for rivers.

Kirkby (1980) focuses on the instability criterion of Smith and Bretherton (1972) and notions of dominant domains and transition thresholds. The instability threshold is analyzed explicitly as a predictor of drainage density. Kirkby (1980) shows that where a combination of creep and wash sediment transport processes are present, there is a critical area a_c where instability [according to Equation (2.42)] occurs. He suggests that for a landscape with fully developed drainage, the area drained per unit length of channel bank must be less than a_c , which results in

$$D_d \geq \frac{1}{2a_c} \quad (2.45)$$

He suggests that for efficient networks, this approaches equality and provides a way to estimate D_d . The notion of a critical area or critical hillslope length is also recognized by Dunne (1980). Dunne (1980) points out that sheet flow can still occur in the stable domain and rilling and channelization occur some way beyond the point (down a hillslope) where sheet flow occurs. This, Dunne (1980) suggests, may be because of the diffusive, leveling influence of rainsplash. The instability occurs where the unstable sheet flow transport dominates. Thornes (1983) also emphasizes the importance of defining domains where different processes dominate, and transitions between domains.

Kirkby (1986) makes slightly different assumptions for the form of the sediment transport equation, F . He uses a conceptualization of runoff production, q , suggested by Beven and Kirkby (1979) (TOPMODEL) and a transport mechanism of the form,

$$F = KS + \alpha q^m S^n \quad (2.46)$$

This is a sum of creep and wash processes.

Andrews and Bucknam (1987), in the context of scarp degradation have suggested

$$F = K_0 \frac{S}{1 - (S/f)^2} \quad (2.47)$$

where f is a friction or sliding slope. This form is derived from consideration of the distance a particle travels before sliding to a stop after being given an initial velocity (perhaps from a raindrop or animal hoof).

It should be pointed out that sediment transport functions of the form $F(S,q)$ or $F(S,a)$ are most appropriate when the sediment transport is transport limited, i.e., F is really the sediment transport capacity of the processes involved. Where the removal is weathering limited hillslope development depends on variations in weathering rate, which is controlled by other factors. Carson and Kirkby (1972) discuss many of these factors. The more general formulation of Luke (1974), Equation (2.43) may be more appropriate with the weathering rate $f(\cdot)$ also dependent on these external factors.

Culling (1960, 1963, 1965) used the diffusion equation to model slope development. In the context of the above discussion any process (raindrops or creep) for which

$$\underline{F} = bS\underline{n} = -b\underline{\nabla}z \quad (2.48)$$

when substituted in Equation (2.39) gives the widely studied linear diffusion equation

$$\frac{\partial z}{\partial t} = b \nabla^2 z \quad (2.49)$$

Here b is a constant, the diffusion coefficient. If F is dependent on S nonlinearly, we get nonlinear diffusion. In fact if the main contribution to variation of F is S , then the process will be predominantly diffusive, whereas if the main contribution to variation of F is a , a measure of concentration of flow, the process is concentration controlled and results in channelization.

Culling (1986) argued that diffusion-type (Davisian downwasting) models of slope development, as widely suggested by many, must lead to landforms of Hausdorff dimension slightly above 2. Furthermore the surface should be a fractional Brownian function and Gaussian in the limit.

The notion of profiles in dynamic equilibrium has been important and was recognized early (Davis, 1899). In the present context Hirano (1975) considers a landscape subject to a constant rate of uplift U . Thus Equation (2.39) becomes

$$\frac{\partial z}{\partial t} = -\nabla \cdot \underline{F} + U \quad (2.50)$$

The dynamic equilibrium, graded form, or constant form solution, is defined by $\frac{\partial z}{\partial t} = 0$, i.e., the steady state solution to Equation (2.50). This is usually fairly easily obtained. More generally U may be thought of as the rate of erosional degradation, or lowering, which for dynamic equilibrium is spatially constant, or at least varies spatially at scales large relative to the scale of the phenomenon considered.

Band (1985) uses the continuity Equation (2.39) with diffusive and surface wash sediment transport components [effectively Equation (2.46)] to model the development of slope profiles in an abandoned gold mine. He notes that the relative magnitudes of the diffusive and surface wash rates are crucial to the resulting slope shapes. Ahnert (1987) describes a model (SLOP3D), developed over the past three

decades, that models slope denudation. This is based on the continuity equation with the added feature that sediment removal is a function of regolith (i.e., soil cover) thickness. This allows the modeling of weathering limited, as well as transport limited situations. The effect of weathering limited denudation is only explored in a limited way. Ahnert (1987) also notes that the surface wash form of sediment transport results in concave slope profiles and diffusive sediment transport results in convex profiles. He suggests that the concave (wash dominated) part of a profile represents the longitudinal profile of streams and the convex part (shaped by diffusive mass movements) represents the valley side slopes.

Recently Willgoose (1989) has developed a catchment and channel network evolution model. The model is based on sediment transport continuity (Equation 2.50) but postulates an explicit difference between sediment transport on a hillslope and in a channel. This is implemented numerically by using a sediment transport function F dependent on an index of channelization Y . Y is an indicator variable taking the value 1 in channels and 0 on hillslopes and Willgoose (1989) uses (analogous to Equation 2.44)

$$F(S, a, Y) = \begin{cases} \beta O_t a^m S^n & Y = 0 \\ \beta a^m S^n & Y = 1 \end{cases} \quad (2.51)$$

The factor O_t gives the relative differences between sediment transport on hillslopes and in channels. Willgoose (1989) suggests that channelization occurs (the switch from $Y = 0$ to $Y = 1$) when an activator function exceeds a certain threshold. He uses sediment transport arguments to suggest an activator function of the form

$$AF(S,a) = \beta_1 a^{m_1} S^{n_1} \quad (2.52)$$

The switch to channelization is implemented through the equation

$$\frac{dY}{dt} = d_t \left[0.0026 \text{ AF}(S,a)/T_a + \left[\frac{Y^2}{1 + 9Y^2} - 0.1 Y \right] \right] \quad (2.53)$$

This equation has the property that for $\text{AF}(S,a)$ less than T_a , Y remains practically 0, but when $\text{AF}(S,a)$ exceeds T_a , Y switches to 1. The rate of switching is controlled by d_t . The form of Equation (2.53) is very similar to the cusp catastrophe model used by Thornes (1980, 1983) to model the instability in sediment transport.

Willgoose (1989) shows that simulations based on this model result in realistic looking channel networks that have many properties of channel networks found in nature. The notion of sediment transport rate being different on hillslopes and channels is intuitively appealing although it has not been observed in the field or experimentally justified. The data of Priest (1975) used by Willgoose (1989) to suggest $O_t = 0.4$ do not indicate that this is significantly different from $O_t = 1$. The channels in this model are different from the shock discontinuities that Luke (1974) shows will develop under conditions of nonlinear instability and suggests should be interpreted as channels. Clearly more work is needed to clarify and understand the nature of channel forming mechanisms.

Chapter 3

DATA ANALYSIS, PROCEDURES AND TECHNIQUES

3.1 Review

There has over the last decade been a growing interest in the use of digital elevation data in geomorphology and hydrology, specifically the analysis of channel networks. This has resulted in the development of procedures for processing digital elevation data and extracting channel networks. O'Callaghan and Mark (1984) provide a good review of the early development in this field, as well as suggesting the algorithms on which much of this work is based.

O'Callaghan and Mark (1984) define a digital elevation model (DEM) as any numeric or digital representation of the elevations of all or part of a planetary surface. They restrict themselves to the most commonly used data structure for DEM's: the regular square grid. In such a grid elevations are available as a matrix of points equally spaced in two orthogonal directions. Here we will restrict ourselves to grid based DEM's but generalize them so that the spacing in each direction is not necessarily the same, i.e., rectangular grids.

Other data structures have been used for DEM's in hydrologic analysis. O'Callaghan and Mark (1984) suggest that triangular irregular networks (TIN) which include channels directly as triangle edges may have substantial advantages. Palacois-Velez and Cuevas-Renaud (1986) develop procedures using TIN networks. Problems arise however because flows along the steepest gradient are not constrained to follow triangle edges. Contour based DEM's have been used with some success by O'Loughlin (1986) and Moore, et al., (1988). These have the advantage of dividing the catchment into natural units related to water flow, i.e., polygons formed by equipotential lines and their orthogonals, streamlines. By comparison grid based models match flow trajectories crudely by transition from one grid cell to another. Moore, et al. (1988) state disadvantages of the contour

based approach: "...one needs at least an order of magnitude more points in contour line form than in regular grid form to adequately describe an elevation surface. Also it is computationally slower than the grid cell approach." It is not clear whether with equal computational effort, i.e., correspondingly finer grid, the grid based or contour based approach is better. Carrara (1988) discusses schemes for interpolation of a grid based DEM from contour data. These schemes range from general (moving average, splines, etc.) to morphology dependent algorithms that endeavor to interpolate the way a skillful reader would interpolate contour maps.

This work uses grid based DEM data structures because the majority of U.S.G.S. DEM data sets are grid based and grid based procedures are simple and unambiguous. Many of the important concepts in grid based DEM work are defined by O'Callaghan and Mark (1984) and Mark (1988). Elevations are stored in an elevation matrix arranged in a grid with each entry giving the elevation of a point. The location within the matrix implies the spatial location of the point, so only elevation values need to be stored (as opposed to TIN networks that have to store x and y location and elevation data for each point and contour-based structures that store strings of x and y locations along a contour).

A pit is defined as a point or set of adjacent points surrounded by neighbors that have higher elevations. A drainage direction matrix contains a set of pointers from each grid cell or pixel to one of its neighbors. Usually pointers are in the direction of steepest slope. The drainage direction matrix defines a drainage direction network as a forest of rooted sub trees.

A drainage accumulation function is defined as an operator which given the drainage direction matrix and a weight matrix determines an accumulated area matrix such that each element in the area matrix represents the sum of the weight of all elements in the matrix which drain to that element. If the weights are all set at one, then the area matrix gives the total contributing area in number of elements

or pixels.

O'Callaghan and Mark (1984) suggest defining channels on a DEM as all points with accumulated area above some threshold. Mark (1988) notes that at horizontal scales of 10m or greater, true pits or closed depressions are rare in natural earth topography, being restricted to a few special geomorphic environments (e.g., glaciated or karst). Pits occur frequently in DEM's due to data errors and sampling effects (e.g., a narrow channel may pass between grid points). Mark (1988) suggests pit removal based on actual drainage patterns (in the form of digitized stream channels) or by a local "flooding" procedure where pits are made to drain towards the point at which water would overflow from the pit.

The procedure for identifying channels suggested by O'Callaghan and Mark (1984) and Mark (1988) is basically:

1. Pit removal and calculation of drainage direction matrix.
2. Calculation of the accumulated area matrix.
3. Define channels as pixels exceeding an accumulated area threshold.

This is the procedure used here. Details of the algorithms are given in a later section.

Band (1986) following Peuker and Douglas (1975) has suggested the use of local operators to flag upward concave pixels as potential stream points. The Peuker and Douglas (1975) algorithm flags the pixel of highest elevation from each possible square of four adjacent pixels. After one sweep of the matrix the unmarked pixels represent drainage courses. The set of points obtained is not necessarily connected so Band (1986) describes several thinning and connection procedures. An advantage of this approach is that no arbitrarily chosen support area has to be specified and networks should have the "correct" drainage density corresponding to the basic scale of dissection of the landscape. Chapter 5 will compare drainage densities obtained from this approach with drainage density estimated using other

techniques.

The drainage direction/area matrix procedures (O'Callaghan and Mark, 1984) of extracting channel networks seem to be becoming popular and more widely used (manifest Carrara, 1988; Morris and Heerdegen, 1988).

3.2 Data Sources and Accuracy

The data used in this work was obtained largely from the National Digital Cartographic data based collected and made available by the U.S. Geological survey. Digital elevation model (DEM) data is supplied at two resolutions:

- 7.5 minute quadrangle coverage in a 30m grid
- 1⁰ quadrangle coverage on a 3 arc sec grid.

U.S.G.S. (1987) describes the DEM data available, from where the following information is excerpted. The 7.5 min DEM's are produced using one of the following four processes:

a. The Gestalt photo Mapper II (GPMII):

Aerial photographs are scanned at a pixel size of 182 μ m at the scale of the photographs (equivalent to a ground distance of approximately 47 ft). Electronic image correlation is used to match features and calculate elevations from the parallax within a stereo model.

b. Manual profiling from photogrammetric stereo models:

High altitude aerial photographs are used as source material. Stereo plotters interfaced with 3 axis electronic digital profile recording modules are used to scan successive terrain profiles in these photographs. The most common profile separation used is 90m with elevations recorded every 30m along the profile. The profiled data are reformatted and regridded to a regular 30m UTM grid.

c. Stereo model digitizing of contours:

Digital contour data are acquired on stereo plotters equipped with three-axis digital recording modules, as the contours are stereo compiled for 1:24,000 scale quadrangle maps. The contour data are processed into profile lines and the elevation matrix found using bilinear interpolation.

d. Derivation from digital line graph hypsography and hydrography:

Hypsography (contours) and Hydrography (rivers and lakes) in digital line graph form are required as input. Contour to grid software (details not specified) is used to interpolate gridded elevations.

The 1⁰ DEM's are produced by the defense mapping agency, but distributed by the U.S.G.S. Cartographic (maps scale 1:24,000 through to 1:250,000) and photographic sources are used. The accuracy together with data spacing are claimed to adequately support computer applications which analyze features to a level of detail similar to manual interpolations of printed maps at scales not larger than 1:250,000.

The vertical accuracy of DEM data is dependent on the spatial resolution, quality of source material and processing procedures. The 7.5 min DEM accuracy is quoted in terms of a root mean square error (RMSE). The error is the difference between "true" elevations (of bench marks, etc.) and linearly interpolated elevations in the DEM. Test points (at least 20) are well distributed in the area. Typical RMSE is 7m, for 7.5 min DEM's. The 1⁰ DEM data does not have accuracy quoted, but is constructed to have an absolute vertical accuracy of $\pm 30\text{m}$ (relative to mean sea level). When discussing accuracy of DEM data, it is necessary to distinguish between absolute error, the difference between true and quoted elevation above a fixed datum, and relative error, the error in the elevation difference between nearby pixels. For our purposes absolute accuracy is less important than relative accuracy since it is the difference in elevation between adjacent pixels that is used to

determine slopes and drainage directions. U.S.G.S (1987) claims, for the 1⁰ DEM's, that the relative vertical accuracy of adjacent points, although not specified, will in many cases conform to the actual hypsographic features, i.e., errors much less than the absolute accuracy. This comment probably also applies to relative errors of the 7.5 min data given the distribution of the test points and the fact that topographic features (such as valleys) can be recognized in the data.

3.3 Procedures and Storage Conventions

To consistently work with data sets from different sources, the data is first converted to our binary matrix format, given in Table 3.1. A set of input/output routines listed with the computer codes in the Appendix was used to read and write data in this format. The procedure followed in processing DEM data is basically:

1. Convert elevation data from supplied format to binary matrix format.
2. Run pointer algorithm. This produces a drainage direction matrix and adjusted elevation matrix that has pits removed. Drainage directions are assigned in the direction of steepest descent. Where the slope in two or more directions is the same, as is typically the case in a flat area, the directions are assigned arbitrarily, but such that no loops are formed. The pointer algorithm also resolves pits by filling them, i.e., increasing the elevation until they overflow.
3. Run accumulation area algorithm. This produces an accumulation area matrix, by counting the number of pixels draining through each pixel.
4. Plot pixels with accumulation area above a convenient threshold and identify the location of the outlet of the basin to be studied.
5. Zero the accumulation area of pixels that do not drain to the identified outlet to isolate the basin of interest.

6. Specify an accumulation area threshold and run network extraction algorithm. Outputs are two files that list link properties and co-ordinates of pixels along each link in the river network.

Table 3.2 gives the structure of the files defining the channel network. The Appendix gives listings of codes required for this procedure as well as example input files to control them. These procedures form the basic routine processing package used to process each data set.

Table 3.1: Binary Matrix Format

Record 1: NX NY DX DY
 Records 2 to NY+1: Matrix of values (elevation, direction, or accumulation area) as follows

(1,1)	(1,2)	...	(1,NX)
(2,1)			
.			
.			
(NY,1)	(NY,NX)

NX is the number of columns
 NY is the number of rows
 DX is the column spacing in m
 DY is the row spacing in m

Elevations and drainage direction matrices are stored as 16 bit integers (integer*2). Accumulation area matrices are stored as 32 bit integers (integer*4). The convention for drainage directions is the same as Band (1986) namely, a direction towards one of the eight neighbors as follows.

4	3	2
5		1
6	7	8

A drainage direction of -1 is used to mark pixels outside or on the edge of the range of the data.

Table 3.2: Network Storage Structure

a. Link File

An ASCII file in free format consisting of a record for each link. Each record consists of, in the following order:

link number:	Link number 0 (the first listed) is the outlet or root link.
link start:	Pointer to first pixel of link in co-ordinate file.
link end:	Pointer to last pixel of link in co-ordinate file.
next link:	Link number of downstream link (-1 indicates no links downstream, i.e., root link).
previous link 1:	Link numbers of two upstream links. These are either both non-zero or both 0, indicating no links upstream of the link.
previous link 2:	
order:	Horton/Strahler order of the link

b. Co-ordinate File

An ASCII file in free format consisting of a record for each point (pixel) on the channel network. The records are associated with links in the link file, numbered from 0, and in order from the upstream to downstream end of each link. Each record consists of, in the following order:

x co-ordinate:	The origin of co-ordinates is the bottom left, i.e., SW corner of the DEM matrix (m).
y co-ordinate:	
Distance:	Distance measured along channels from the point to the basin outlet (m).
Elevation:	Elevation of the point (m).
Area:	Total area contributing to that point. i.e., number of pixels from contributing area x pixel area (m ²).

Many other ad hoc procedures were developed to examine particular issues and test particular hypotheses. These are not described here as they are mostly trivial and their functioning can be deduced from the various results presented in forthcoming chapters. Examples of procedures in this category are procedures to do functional box counting, tabulate link or stream property values, compute mean link or stream properties for classes of links or streams, etc.

Descriptions of the important algorithms in the basic package are given next.

Pointer Algorithm

1. *Initialize all directions to zero.*
2. *Set directions of all pixels towards the neighbor for which the positive downwards slope is maximum.*

At this point pixels with 0 direction are unresolved flat areas or pits.

3. *Repeatedly test unresolved pixels to see if they have a neighbor of equal elevation that has drainage direction assigned. Assign drainage direction towards this pixel.*

This has the intent of making flat areas drain as directly as possible towards the point where they “overflow” while ensuring that no loops are formed. Pixels unresolved after this step are pits.

4. *If there are still unresolved pixels*
Increase the elevation of unresolved pixels by Max (1, elevation difference to lowest neighbor). Go to Step 1 and repeat procedure
else
end.

This algorithm is time consuming due to all the looping while elevations are increased to resolve pits, so it is applied first to subsets of the data set and then to

the whole data set. More efficient procedures may be possible, based on searching the boundary of the area draining into a pit and then immediately raising the level to the lowest boundary elevation. We have not tried procedures along these lines.

Accumulation Area Algorithm

The accumulation area algorithm used is a slight modification of a recursive procedure suggested by Mark (1988). $DAREA(loc)$ is a recursive procedure (i.e. it can call itself) that returns the accumulation area for a pixel identified by loc , its location in the matrix. $AREA(loc)$ is the accumulation area matrix.

```

procedure DAREA(loc):
    if  $AREA(loc)$  is known
    then
        return  $[AREA(loc)]$ 
    else
         $AREA(loc) = \text{unit cell area}$ 
        for each neighbor
            if  $(\text{the neighbor drains into the current cell})$ 
            then
                 $AREA(loc) = AREA(loc) + DAREA(neighbor)$ 
        return  $[AREA(loc)]$ 
end.

```

This is called for each pixel in the data set. Notice that the procedure just keeps calling itself until it reaches a pixel with no drainage inputs. The areas of each pixel upstream of a called pixel are stored so that when that pixel is reached the procedure does not have to repeat itself. The running time is a linear function of the number of pixels in the data set or a square function of the size of a square

matrix data set (n^2). In earlier work we used a procedure that assigned a catchment area of 1 to each pixel and then for each pixel in turn followed flow lines to the edge of the data incrementing by 1 the catchment area of all points en route. This procedure is used by Carrara (1988) and Morris and Heerdegen (1988) and has running time proportional to n^3 . We were able to process 1000 x 1000 data sets that had previously taken 8 hours of CPU time on a Microvax II in a few minutes with the recursive algorithm so it is strongly recommended it over other procedures.

Zero Area Algorithm

To isolate the basin of interest, the drainage area procedure is called for the outlet pixel only. This recursively computes the area of each pixel in the drainage basin, but leaves pixels outside the basin untouched, i.e., with accumulation area 0.

3.4 Data

Table 3.3 gives a list of all the digital elevation model data sets used in this work and their exact location. Figure 3.1 shows their location in the United States. Table 3.4 gives the location of river basins within these data sets, identified by their outlet pixel. The adjustments to the elevation data required to fill in pits are relatively minor. Table 3.5 gives statistics of these adjustments for some typical data sets.

The subsequent chapters will go into detailed analysis of river networks extracted from DEM'S with various support areas. Traditionally geomorphologists have worked with river networks obtained from topographic maps. We given Figure 3.2 as a comparison of networks from DEM's with these from a map. The "blue lines" were digitized by hand from 1:24,000 U.S.G.S. maps with additional detail inferred using operator judgment and contour crenulations. The comparison with the DEM network with support area 200 is reasonably good.

Table 3.3 Digital Elevation Model Data Sets

Acronym	Pixel Size	Map Quad-ranges Used	N. W. Corner Coordinates		Array Size	
			Easting/Longitude	Northing/Latitude	Rows	Cols.
W7	30m	Hay Mtn. (AZ)	584040m	3511710m	201	201
W15	30m	Hay Mtn., Tombstone (AZ)	586740m	3512220m	402	402
W15A2S ¹	60m	Hay Mtn., Tombstone (AZ)	586755m	3512205m	202	202
CONN	30m	Tolland, West Granville (CN/MA)	661530m	4665630m	420	431
HAK	30m	Hunter, Kaaterskill (NY)	561870m	4677810m	471	694
HAKA2S ¹	60m	Hunter, Kaaterskill (NY)	561885m	4677795m	235	347
BING	3"(68.3x92.67m)	Binghamton (NY)	75 ^o W	43 ^o N	1201	1201
CALD	30m	Calder NW,NE,SW and SE (ID)	556470m	5261010m	935	642
STJOEUP	30m	Simmons Peak SE and SW, Pole Mtn., Bacon Peak Chamberlain Mtn, Illinois Peak SE and SW (ID,MO)	613770m	5220780m	956	1278

Table 3.3 Digital Elevation Model Data Sets Continued.

Acronym	Pixel Size	Map Quad— rangles Used	N. W. Corner Easting/ Longitude	Coordinates Northing/ Latitude	Array Size Rows	Cols.
STJOE	3"(62.6x 92.67m)	Spokane E, Hamilton W, Wallace W (MT,ID)	116 ⁰ 22'33"	4737'33"	951	1652
SPOKBC	3"(62.6x 92.67m)	Spokane E (ID)	116 ⁰ 15'	47 ⁰ 30'	301	301
SPOK	3"(62.6x 92.67m)	Spokane E (ID)	117 ⁰	48 ⁰	1201	1201
CANTON	3"(70.47x 92.67)	Canton E (OH,PA,MN)	81 ⁰	41 ⁰	1201	1201
RACOON	30m	Hookstown, Midway, Burgettstown, Clinton, Alquippa, Avella (PA)	542280m	4497210m	1395	718
TVA ²	100 ft	—	2490100 ³ ft	734000 ³ ft	300	441
STREGIS	30m	Wallace NE, Saltese NE, NW and SE, Haugan NE, NW, SE and SW, Simmons Peak NE, Illinois peak NW (MO)	590700m	5262240m	1169	1719
BUCK	30m	Gasquet SW and SE, Ship Mtn. NW, NE, SW and SE, Dillon Mtn. NW and SW, Preston Peak SW (CA)	416520m	4636170m	1399	1055

Table 3.3 Digital Elevation Model Data Sets Continued.

Acronym	Pixel Size	Map Quad— rangles Used	N. W. Corner Easting/ Longitude	Coordinates Northing/ Latitude	Array Size Rows	Size Cols.
BRUSHY	30m	Upshaw, Houston, Grayson, Massey, Moulton, Addison (AL)	465390m	3806100m	850	1011
MOSHANNON	30m	Ramey, Blandburg, Wallaceton, Houtzdale, Tipton, Philipsburg, Sandy Ridge (PA)	710640m	4542540m	1071	1422

Notes:

A data set here is a rectangular matrix of elevation data chosen to as to completely cover one or more river basins. The location of the matrix is identified by the coordinates of the NW corner, array element (1,1), given in UTM Coordinates for USGS 7.5min series data and latitude and longitude for 1⁰ DMA series data. The matrix rows are numbered from North to South and columns from East to West. The pixel size gives the grid spacing, as well as identifying the type of DEM. Pixels size 30m are USGS 7.5 min series data and 3 arc sec (3") pixels are 1⁰ DMA series data.

1. Formed by averaging together groups of 4 adjacent pixels to obtain a course resolution dataset.
2. Obtained courtesy of the Tennessee Valley Authority, Maps and Surveys Department.
3. Tennessee State plane coordinates in ft.

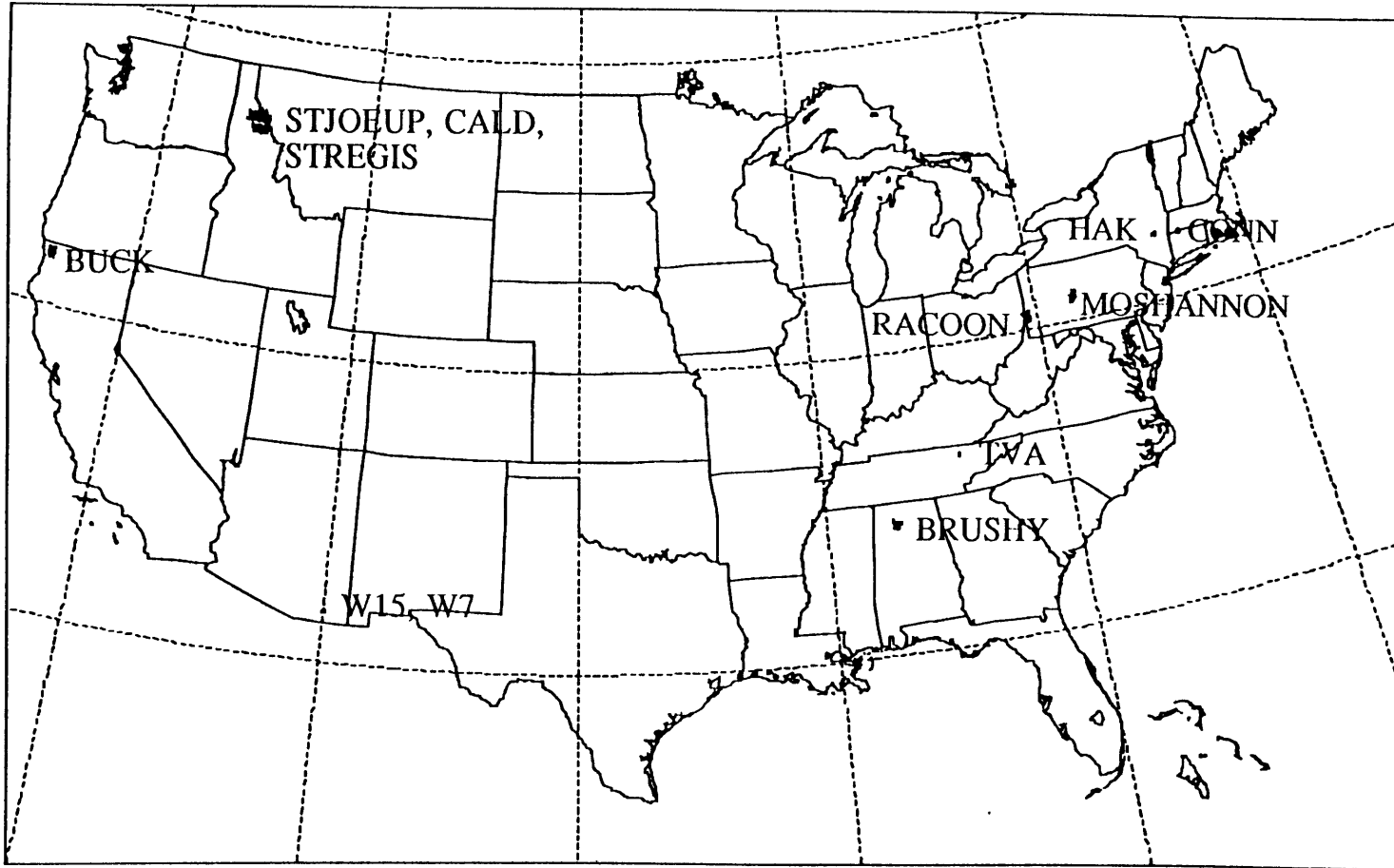


Figure 3.1(a). Location map for 7.5 min Datasets.

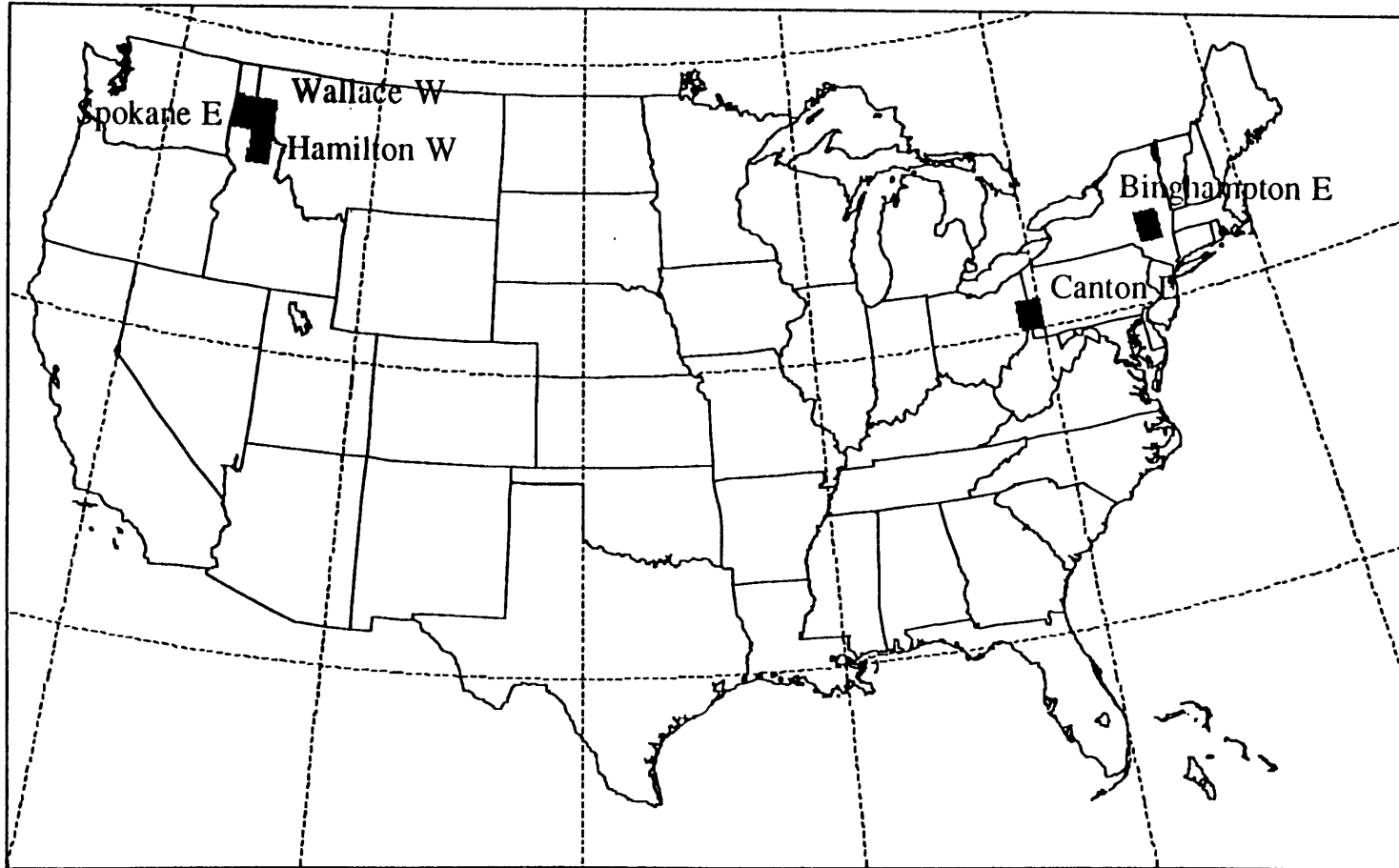


Figure 3.1(b). Location Map for 1⁰ DMA Quadrangles.

Table 3.4 River Basins

Acronym	Name	Digital Elevation Model Data Set	Outlet Location Easting/ Longitude	Northing/ Latitude	Within DEM Rows	Columns
W7	Subbasin no. 7 in Walnut Gulch experimental watershed	W7	585360m	3511140m	20	45
W15	Subbasin no. 15 in Walnut Gulch experimental watershed	W15	590940m	3509040m	107	141
W15A2S	Subbasin no 15 in Walnut Gulch experimental watershed	W15A2S	590895m	3508965m	55	70
CALD	Big Creek	CALD	567330m	5235300m	858	363
SPOKBC	Big Creek	SPOKBC	116 ⁰ 06'39"	47 ⁰ 16'18"	275	168
NELK	N. Fork Cour d'Alene River	SPOK	116 ⁰ 14'27"	47 ⁰ 35'51"	484	912
STJOE	St. Joe River	STJOE	116 ⁰ 16'15"	47 ⁰ 18'36"	380	127
STJOEUP	St. Joe River	STJOEUP	623040m	5217360m	115	310
STREGIS	St. Regis River	STREGIS	611670m	5239860m	747	700
STREGISDMA	St. Regis River	STREGISDMA	115 ⁰ 08'06"	47 ⁰ 17'51"	395	1490

Table 3.4 River Basins Continued.

Acronym	Name	Digital Elevation Model Data Set	Outlet Location Easting/ Longitude	Northing/ Latitude	Within DEM Rows	Columns
HAK	Schoharie Creek headwaters	HAK	564390m	4673430m	147	85
HAKA2S	Schoharie Creek Headwaters	HAKA2S	564465m	4673415m	74	44
SCHO	Schoharie Creek	BING	74 ⁰ 17'06"	42 ⁰ 55'48"	85	859
EDEL	East Delaware River	BING	74 ⁰ 57'24"	42 ⁰ 04'30"	1111	53
RACoon	Racoon Creek	RACoon	558270m	4495650m	53	534
RACoonDMA	Racoon Creek	CANTON	80 ⁰ 21'24"	40 ⁰ 39'27"	412	773
BEAVER	Beaver Creek	CANTON	80 ⁰ 30'54"	40 ⁰ 38'42"	427	583
BUCK	Buck Creek	BUCK	418350m	4620660m	518	62
BRUSHY	Brushy Creek	BRUSHY	433230m	4591290m	980	497
MOSHANNON	Moshannon Creek	MOSHANNON	735420m	4532580m	333	827
TVA	Montgomery Fork	TVA	2492200ft	707200ft	269	22
CONN	Hubbard and Valley Brook at confluence	CONN	670980m	4655040m	354	316

Table 3.5 Statistics of Adjustments Required to Fill Pits

Data Set	Number of pixels	Mean adjustment (m)	% of pixels adjusted	Number and Percentage of Pixels Adjusted by Amount				
				1-5 (m)	6-10 (m)	11-20 (m)	20+ (m)	Max. (m)
CALD	600270	4.8	1.6%	6656 (1.1%)	1839 (0.31%)	896 (0.15%)	136 (0.02%)	35
STREGIS	2009511	4.9	0.9%	12382 (0.6%)	3424 (0.17%)	1768 (0.08%)	315 (0.02%)	44
MOSHANNON	1522962	2.6	4.7%	64535 (4.2%)	5554 (0.4%)	786 (0.05%)	109 (0.007%)	89
SPOK	1442401	11.2	3.7%	20769 (1.4%)	6731 (0.47%)	6732 (0.47%)	19013 (1.3%)	61

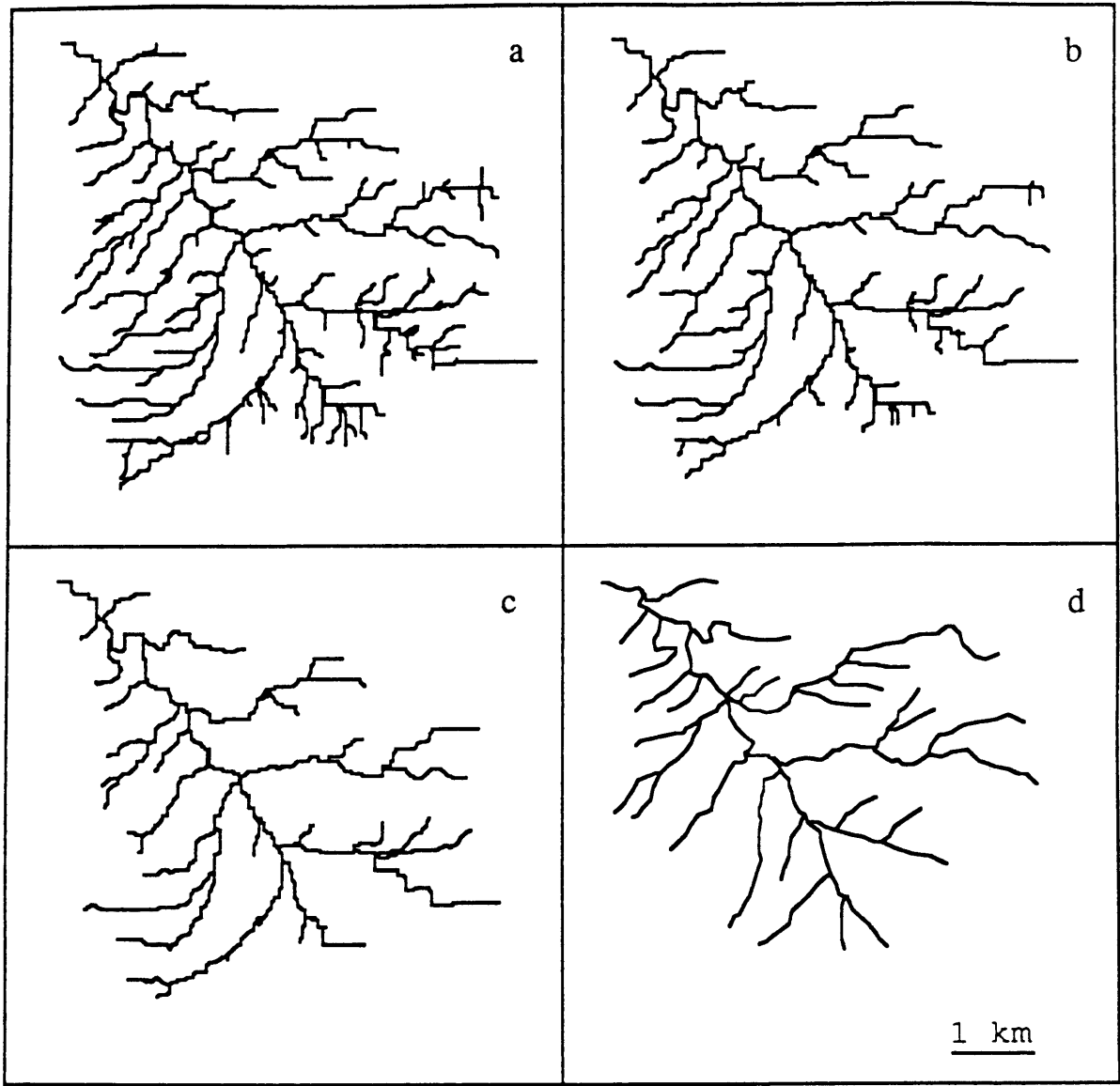


Figure 3.2. Channel Networks from DEM with varying support area compared to Blue Lines for the W15 dataset: a) 50 pixels, b) 100 pixels, c) 200 pixels, d) "Blue Lines".

Chapter 4

PLANAR SPACE FILLING PROPERTIES OF RIVER NETWORKS

4.1 Introduction

The main tenet of this chapter is that at large scale, in plan, river networks fill space, that is they drain the whole river basin. This places constraints on their planar scaling properties, namely that their fractal dimension must be 2. This is still consistent with the notion of their being fractals since networks are idealized as line graphs with topologic dimension 1. This notion of plane filling is clearly only valid at scales where we have a network, i.e., scales larger than the basic scale of dissection of the landscape (i.e., hillslope scale or drainage density).

The fact that river networks fill space may be self-evident to some; however, some workers have suggested that river networks have fractal dimension different from 2 (La Barbera and Rosso, 1989) so we feel it is necessary to provide empirical evidence that $D = 2$. This will be done in the next section. Networks estimated from digital elevation models with a constant support area threshold are constrained to drain any area larger than the support area, so at scales larger than the support area must be space filling and have $D = 2$. The question is whether this is the case for networks not necessarily extracted from DEM's with this technique. The empirical analysis for networks from DEM's as well as for networks digitized from the "blue lines" of topographic maps supports space filling.

4.2 Empirical Evidence

The "ruler" method (Chapter 2) was used to investigate the scaling properties of river networks. When measuring apparent length of a network by stepping along it with rulers, the question arises as to which branch to follow at a bifurcation. We resolved it by measuring the apparent length of individual Strahler

streams separately and adding the results.

At the end of streams there is, generally, a leftover piece of stream shorter than the ruler length r . If the distance from the last stepping point to the end was greater than $r/2$, it was counted in the number of steps N ; otherwise it was not included in the length. Figure 4.1 gives results for several different networks. The Souhegan is a 440 km^2 basin in southern New Hampshire that was digitized by hand from 1:24,000 U.S.G.S. maps. A neighboring river basin, the Squannacook (area 163 km^2) also hand digitized was included in the sum of which consisted of the two hand digitized networks (Souhegan and Squannacook) and six networks obtained from three DEM basins with support area's of 50 and 20 pixels. The DEM basins used were CONN, W15 and W7 (see Tables 3.3 and 3.4). The pattern for all of these is the same, a gently sloping line with slope about 0.05 for small ruler lengths, followed by an abrupt change to slope of about 1 for large ruler lengths. This clearly indicates two distinct regions of scaling. The fractal dimension characterizing these regions of scaling is obtained from Equation (2.32). The first with $D \simeq 1.05$ is due to the sinuosity of individual rivers, and corresponds to the scaling implied by Equation (2.37). The second, with D near 2, is due to the branching characteristic of networks. More precisely it is due to streams shorter than $r/2$ not being counted at all, reflecting the fact that at coarse resolution we see fewer streams. In Figure 4.1 the break point corresponds to the basic scale or drainage density of the respective networks which in the case of networks from DEM's is a function of the support area used to extract the network.

The fractal dimension of channel networks was also estimated using functional box counting (Chapter 2 and Lovejoy, et al., 1987). Here it was applied to pixels with accumulation area exceeding a specified support area threshold. Figure 4.2 gives plots of the number of boxes required to cover all selected pixels, versus box size. The negative slope gives fractal dimension. We see that there are

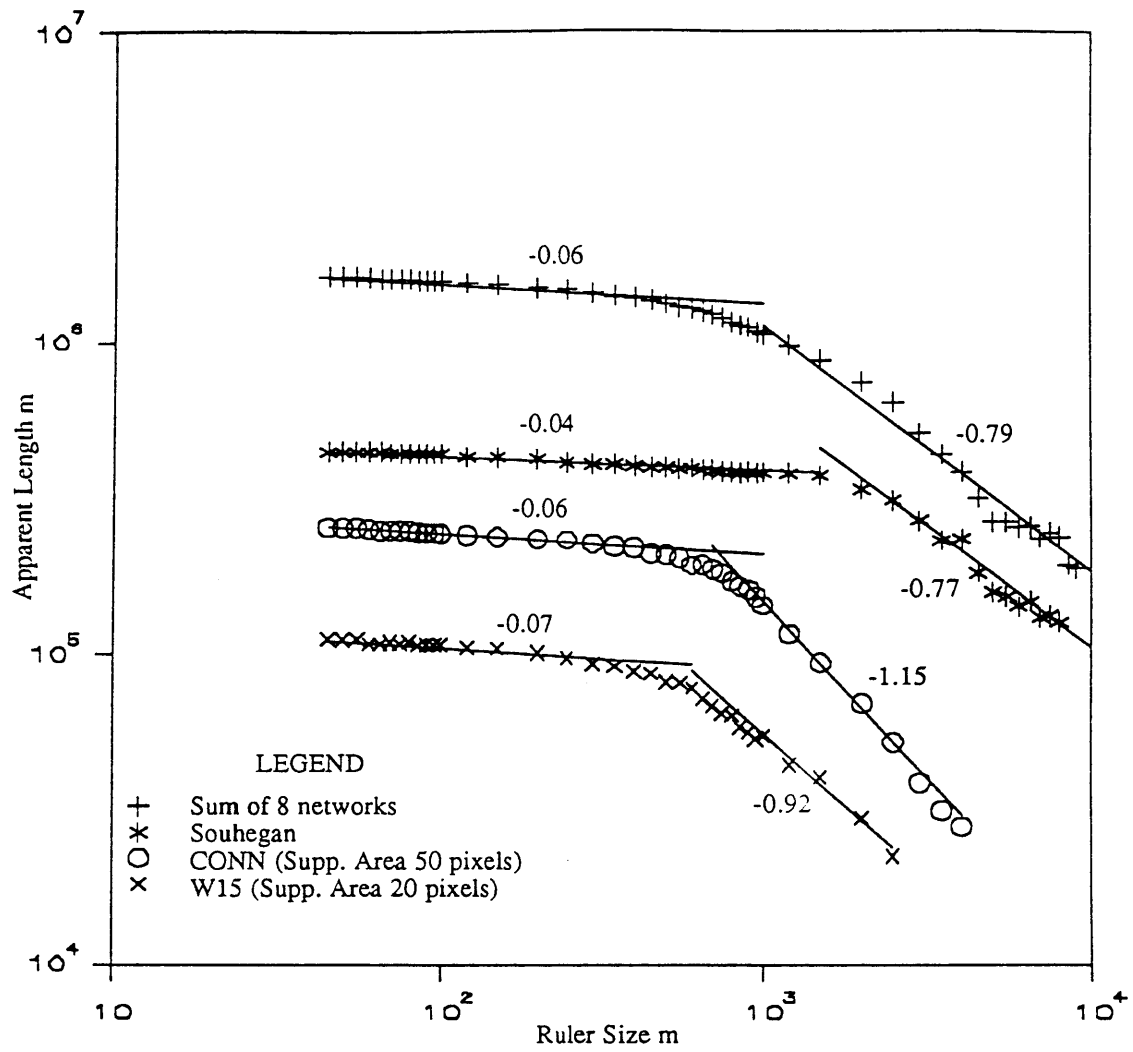


Figure 4.1. Ruler method results for typical river networks.

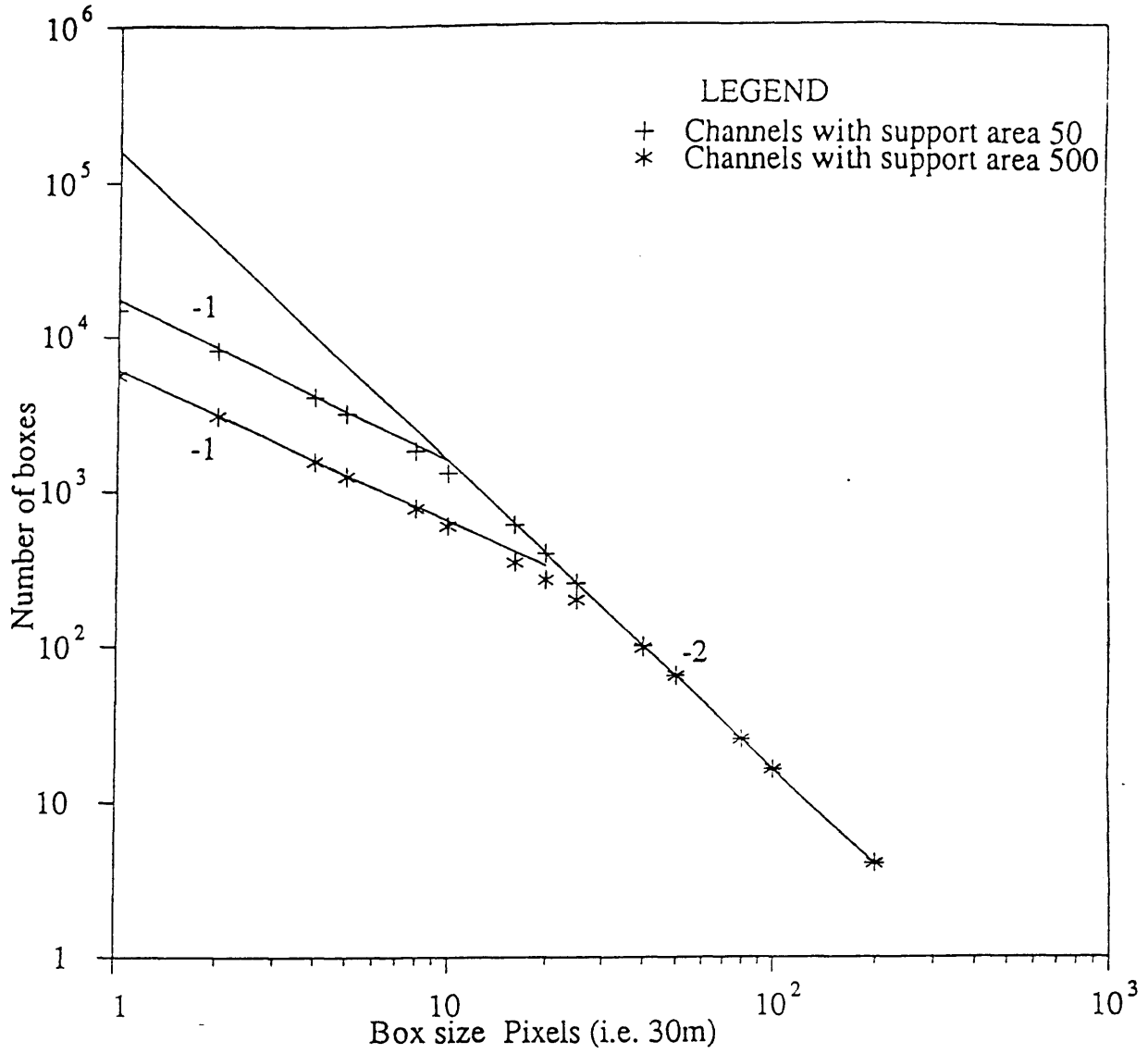


Figure 4.2. Functional box counting results from W15 dataset.

basically two asymptotic slopes, a slope close to -1 for small box size, implying that at scales small relative to the scale of dissection, channels have dimensions close to that of a line. At the large box size end of the scale, the slope is -2 indicating that practically all boxes are intersected by a channel. At this scale the network is space filling with $D = 2$. Note that the more detailed the network (lower support area) the smaller the scale above which the network is space filling.

As previously mentioned, the region with slopes near -1 in Figure 4.1 is due to short streams being excluded as ruler size r increases. The region with slope of -1 can be interpreted as giving the number of streams with length greater than r proportional to r^{-D} . Mandelbrot (1983) notes that the probabilistic counterpart to this is a hyperbolic distribution:

$$\text{Prob}[\text{length} > \ell] \propto \ell^{-D} \quad (4.1)$$

where D is again the fractal dimension and ℓ refers to stream length. Hyperbolic distributions have the desired property that they are self-similar.

Figures 4.3 and 4.4 give the exceedance probability of stream length aggregated from several river basins. Points were plotted using the plotting position

$$P = \frac{m}{n + 1} \quad (4.2)$$

where m is the ranking from longest to shortest stream length and n is the number of streams in the sample. The figures indicate a hyperbolic tail with $D \simeq 2$. Figure 4.3 uses geometric length, defined as the straight line distance between end points of a stream. Figure 4.4 uses length measured along the stream, naturally limited by the resolution of the map or DEM from which the network is obtained. In Figure 4.4 the slope is slightly less than 2. We believe this is due to length along the

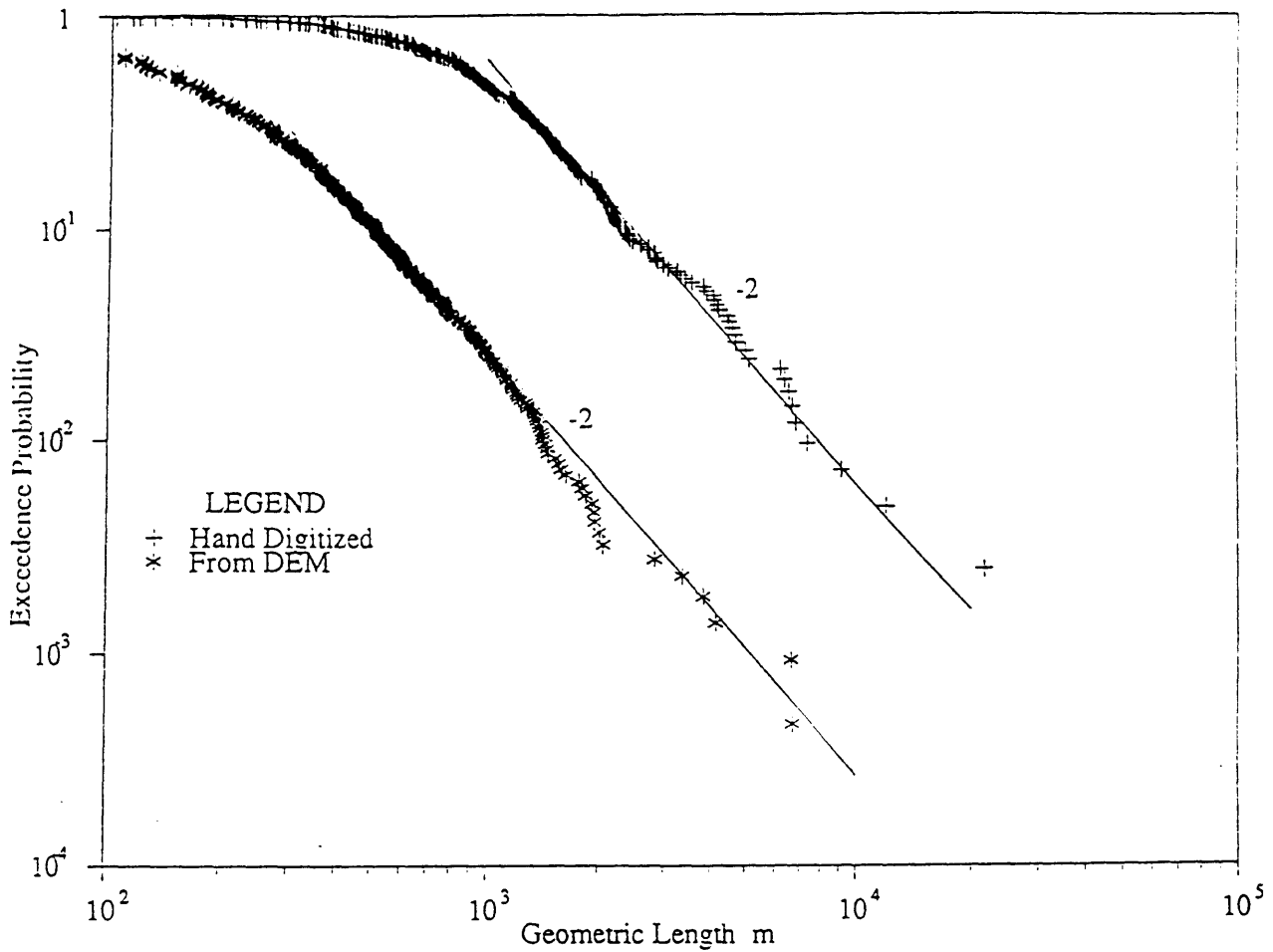


Figure 4.3. Geometric Stream length Exceedence probability. The DEM data is based on 2178 streams from the W15, W7 and CONN networks with support area of 20 pixels. The hand digitized data is based on the Souhegan and Squannacook networks with 409 streams digitized by hand from 1:24,000 maps.

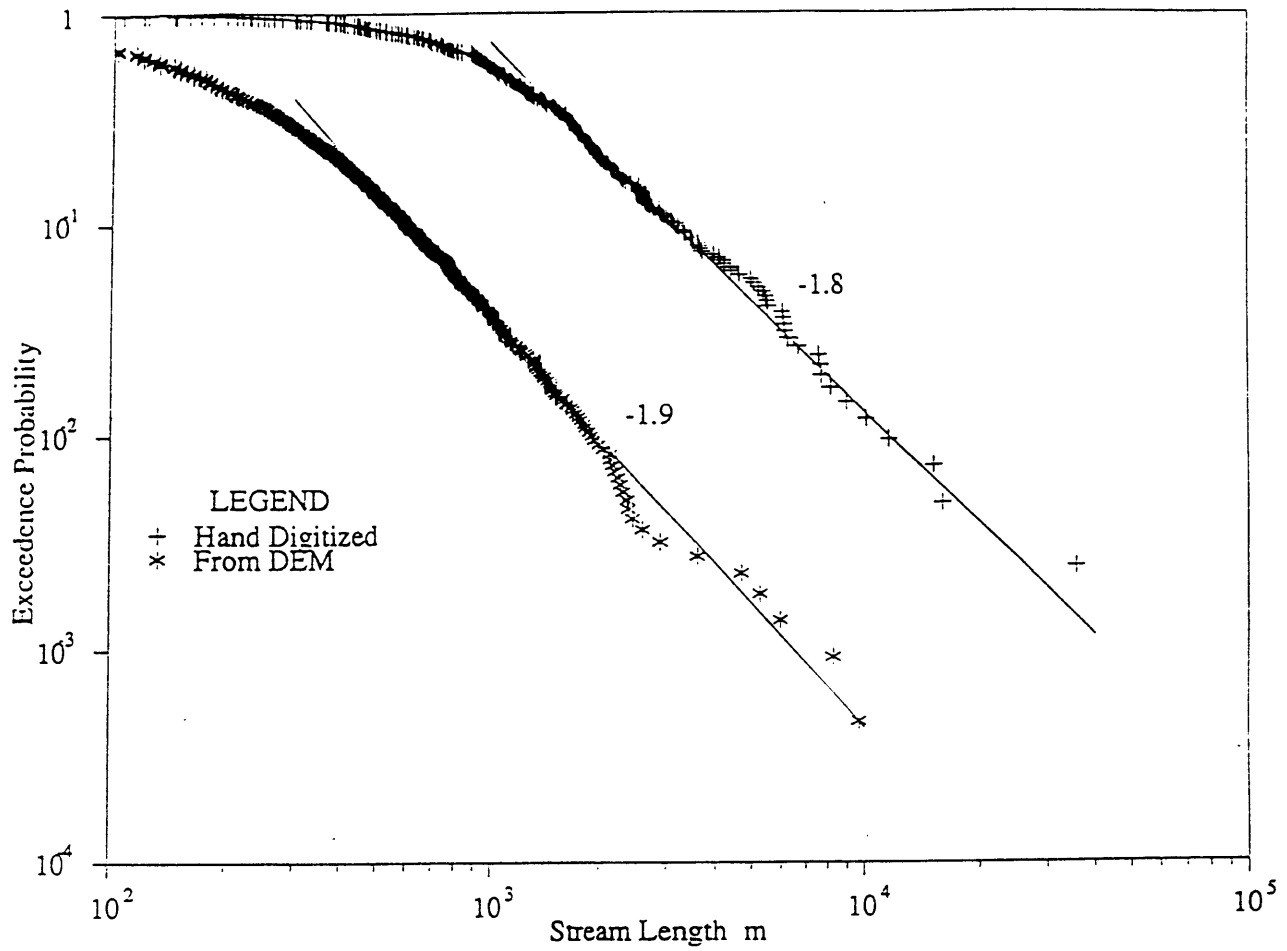


Figure 4.4. Stream length along stream Exceedence probability. The DEM data is based on 2178 streams from the W15, W7 and CONN networks with support area of 20 pixels. The hand digitized data is based on the Souhegan and Squannacook networks with 409 streams digitized by hand from 1:24,000 maps.

stream itself being a fractal measure with dimension D slightly in excess of 1. Suppose we have from Equation (4.1) fitted to Figure 4.4

$$\text{Prob}[\text{length} > \ell] \propto \ell^{-\lambda} \quad (4.3)$$

Now if ℓ is itself a fractal with dimension D_ℓ we get

$$\ell \propto r^{D_\ell} \quad (4.4)$$

where r is a linear ($D=1$) measure or length scale. Combining we get

$$\text{Prob}[\text{length} > \ell] \propto r^{-\lambda D_\ell} \quad (4.5)$$

Thus the fractal dimension of the whole network is $D = \lambda D_\ell$. The result $D = 2$ is therefore consistent with slope $\lambda = 1.8$ seen in Figure 4.4 and $D_\ell = 1.1$ as suggested by Equation (2.37) and the flatter slopes of Figure 4.1. We interpret these figures as strong evidence that the network is space filling with $D = 2$.

4.3 Fractal Dimension and Horton's Laws

In this section we show how fractal dimension is related to Horton's empirical laws, and hence relate the fractal scaling of river networks to concepts from classical fluvial geomorphology. Horton's laws are basically geometric scaling relationships that hold for all orders or resolutions above the basic scale.

La Barbera and Rosso (1987; 1989) suggest that the fractal dimension of river networks is

$$D = \text{Max} \left[\frac{\log R_b}{\log R_\ell}, 1 \right] \quad (4.6)$$

The derivation of this assumes that Horton's bifurcation and length ratios are constant at all scales in the network.

Let a network of order Ω have main stream length L_Ω . Then, using the Horton's length ratio the mean length of a stream of order ω ($\omega < \Omega$) is $L_\Omega / (R_\ell)^{\Omega-\omega}$. By Horton's bifurcation law, there are $R_b^{\Omega-\omega}$ of these streams, so the total length of streams of order ω is $L_\Omega \left[\frac{R_b}{R_\ell} \right]^{\Omega-\omega}$. Adding over all ω to get the total length of the streams in the network, L_T , we get the geometric series

$$\begin{aligned} L_T &= \sum_{\omega=1}^{\Omega} L_\Omega \left[\frac{R_b}{R_\ell} \right]^{\Omega-\omega} \\ &= L_\Omega \frac{1 - \left[\frac{R_b}{R_\ell} \right]^\Omega}{1 - \frac{R_b}{R_\ell}} \end{aligned} \quad (4.7)$$

Strahler (1964) gives this result.

If $\frac{R_b}{R_\ell} < 1$, the series converges to a finite L as Ω approaches infinity and we have $D = 1$. This is a limit process where L_Ω is held constant and Ω increases by the resolution being refined. However, if $\frac{R_b}{R_\ell} \geq 1$, as is most often the case in river channel networks, the series diverges and for large Ω we get

$$L_T \propto \left[\frac{R_b}{R_\ell} \right]^{\Omega-1} \quad (4.8)$$

Now the first order streams have average length

$$s = L_{\Omega} \left[\frac{1}{R_{\ell}} \right]^{\Omega-1} \quad (4.9)$$

This is interpreted as the resolution used to measure the length of the network.

From Equation (4.9) write

$$\Omega-1 = - \frac{\log (s/L_{\Omega})}{\log R_{\ell}} \quad (4.10)$$

which in Equation (4.8) gives

$$L_T \propto s^{1 - \frac{\log R_b}{\log R_{\ell}}} \quad (4.11)$$

By comparison to Equation (2.32), we get fractal dimension

$$D = \frac{\log R_b}{\log R_{\ell}} \quad (4.12)$$

Implicit in this derivation is the assumption that individual streams are linear measures and that the sum in Equation (4.7) is a counting of linear lengths. This counting can be represented

$$L_T = N s \quad (4.13)$$

If the individual streams are themselves fractal with dimension D_{ℓ} then Equation

(4.11) is not analogous to Equation (2.32). Instead we have from (4.11) the equivalent count of number of fractal measures

$$N \propto \frac{L_T}{s} = s^{-\frac{\log R_b}{\log R_\ell}} \quad (4.14)$$

Analogous to Equation (4.4)

$$s \propto r^{D_\ell} \quad (4.15)$$

where r is a linear (fractal dimension 1) resolution measure. With this we get

$$N \propto r^{-D_\ell \frac{\log R_b}{\log R_\ell}} \quad (4.16)$$

and fractal dimension of the whole network is

$$D = D_\ell \frac{\log R_b}{\log R_\ell} \quad (4.17)$$

or

$$\frac{\log R_b}{\log R_\ell} = \frac{D}{D_\ell} \quad (4.18)$$

Now the constraint $D = 2$ implies

$$\frac{\log R_b}{\log R_\ell} = \frac{2}{D_\ell} \quad (4.19)$$

or

$$R_b = R_\ell^{\frac{2}{D_\ell}} \quad (4.20)$$

The result [Equation (4.20)] provides a fundamental relationship between Horton's length and bifurcation ratios, showing that they both describe the same scaling property evident in channel networks. We believe that the fact that D_ℓ is greater than 1 is responsible for La Barbera and Rosso's (1989) findings that $\frac{\log R_b}{\log R_\ell}$ is usually less than 2. Table 4.1 gives $\frac{\log R_b}{\log R_\ell}$ for some of the networks analyzed. We do not believe it is possible for D of the planform of river networks to be different from 2 as La Barbera and Rosso (1989) suggest. Estimation of Horton ratios are in any case very imprecise and strong evidence for $D = 2$ was given in the previous section.

In a river network with Horton's bifurcation and length ratio laws holding exactly, we have seen that there are $R_b^{\Omega-\omega}$ order ω streams of length $L_\Omega/R_\ell^{\Omega-\omega}$. So the total number of streams exceeding a length $\ell = L_\Omega/R_\ell^k$ is

$$\sum_{i=0}^k R_b^i = \frac{R_b^{k+1} - 1}{R_b - 1} \quad (4.21)$$

where $k = \frac{\log(L_\Omega/\ell)}{\log R_\ell}$. This sum counts all the Strahler streams between orders ω and Ω , with $k = \Omega - \omega$.

Table 4.1 Network Geometry data for Several River Networks

Basin	Magnitude	R_b	R_ℓ	$\frac{\log R_b}{\log R_\ell}$
Souhegan, NH	177	3.5	2.0	1.8
Squanacook, NH	133	3.5	1.7	2.5
W15 Supp. A 20	329	4.2	2.1	1.9
W15 Supp. A 50	107	3.3	1.6	2.4
CONN Supp. A 20	1217	4.1	2.1	1.9
CONN Supp. A 50	486	4.7	2.3	1.8
Youghiogheny, MD*	1798	4.6	2.2	1.9
Daddys Creek, TN*	1181	4.1	2.2	1.8
Allegheny River, PA*	5966	4.5	2.4	1.7

* Based on data from Morisawa (1962).

If the total number of streams is N_T , we can write

$$\text{Prob}[\text{length} \geq \ell] = \frac{R_b^{k+1} - 1}{R_b - 1} / N_T \quad (4.22)$$

For k large so that R_b^{k+1} dominates 1 this becomes

$$\text{Prob}[\text{length} \geq \ell] \propto \ell^{-\frac{\log R_b}{\log R}} \quad (4.23)$$

This explains the hyperbolic tail of the stream length distributions, Figures 4.3 and 4.4, in terms of Horton's laws and gives the connection between Equation (4.5) and

the result, Equation (4.17) as $\lambda = \frac{\log R_b}{\log R}$.

4.4 Fractal Dimension and Tokunaga Cyclicity

The Tokunaga (1978) parameterization of scaling in river networks is appealing because of its intrinsic self-similarity. This section will show how the fractal dimension of channel networks is related to the Tokunaga (1978) parameters K and ϵ_1 and functions of them, P and Q , defined in Chapter 2. The Tokunaga system does not suffer from the same inconsistencies as described above for Horton's laws, another reason why it may be more appealing.

Tokunaga (1978) assumed $L_\lambda = \sqrt{\lambda A}$ to derive a length scaling law. This has the implied assumption that the basin is space filling and has linear channel elements. We do not necessarily want to restrict ourselves to these assumptions, so we rather assume that at the smallest resolution resolvable link lengths are on average constant.

It is fairly easy to show that under the Tokunaga system with lowest resolvable order λ , the number of links in a stream of order ω is

$$M(\omega, \lambda) = 1 + \epsilon_1 \left[\frac{K^{\omega-\lambda} - 1}{K - 1} \right] \quad (4.24)$$

so with the constant link length assumption

$$L_\omega = M(\omega, \lambda) L_\lambda = \left\{ 1 + \epsilon_1 \left[\frac{K^{\omega-\lambda} - 1}{K - 1} \right] \right\} L_\lambda \quad (4.25)$$

This is a stream length scaling, which for $\omega - \lambda$ large and $K > 1$ (which it practically always is) gives

$$\frac{L_\omega}{L_{\omega-1}} \simeq K \quad (4.26)$$

which is Horton's length law with $R_\ell = K$.

The total length of channels can be computed

$$L_T = \sum_{\omega=\lambda}^{\Omega} N(\Omega, \omega) \frac{L_\Omega}{M(\Omega, \omega)} \quad (4.27)$$

which with Equation (2.17) gives

$$\begin{aligned}
L_T &= \frac{L_\Omega Q(2 + \epsilon_1 - P)}{Q - P} \sum_{\omega=\lambda}^{\Omega} \frac{Q^{\Omega-\omega-1} - P^{\Omega-\omega-1}}{1 + \epsilon_1 \left[\frac{K^{\Omega-\omega-1}}{K-1} \right]} \\
&+ (2 + \epsilon_1) L_\Omega \sum_{\omega=\lambda}^{\Omega} \frac{P^{\Omega-\omega-1}}{1 + \epsilon_1 \left[\frac{K^{\Omega-\omega-1}}{K-1} \right]}
\end{aligned} \tag{4.28}$$

This consists of series of the form

$$\sum_{\ell=0}^{\Omega-\lambda} \frac{A^\ell}{K^\ell - B} \tag{4.29}$$

with B a constant and A either P or Q. We are interested in the limit of small resolution, i.e., $\lambda \rightarrow -\infty$ or $\ell \rightarrow \infty$. In the limit K^ℓ dominates B and the series are dominated by $\left(\frac{Q}{K}\right)^\ell$ [Q is larger than P, Equation (2.18)]. We therefore get

$$L_T \propto \left(\frac{Q}{K}\right)^{-\lambda} \tag{4.30}$$

Now with the approximation, Equation (4.26), the first order streams have length measure

$$s = L_\Omega K^{\lambda-\Omega} \tag{4.31}$$

analogous to Equation (4.9). Interpreting this as the resolution we get similarly to Equation (4.11)

$$L_T \propto s^{1 - \frac{\log Q}{\log K}} \tag{4.32}$$

Now allowing the individual streams to be fractal (dimension D_ℓ), we get, analogous to Equation (4.17)

$$D = D_\ell \frac{\log Q}{\log K} \quad (4.33)$$

or

$$\frac{\log Q}{\log K} = \frac{D}{D_\ell} \quad (4.34)$$

With the space filling constraint $D = 2$, this implies

$$\frac{\log Q}{\log K} = \frac{2}{D_\ell} \quad (4.35)$$

and

$$Q = K^{\frac{2}{D_\ell}} \quad (4.36)$$

This shows how the parameters K and ϵ_1 must be related for networks to be space filling. Also in the special case with linear individual streams, $D_\ell = 1$, we get $Q = K^2$ which relates Equation (4.26) with Equation (2.21) given by Tokunaga.

Tokunaga (1978) derived the area scaling law (Equation 2.19) as an asymptotic result under the assumption that inter basin areas are less than source areas. This result can also be obtained under the assumption of constant average area per link, or equivalently link area proportional to link length with link lengths on average constant. To see this recognize that

$$\begin{aligned}
A_{\Omega} &= A_{\lambda} \sum_{\omega=\lambda}^{\Omega} N(\Omega, \omega) M(\omega, \lambda) \\
&= A_{\lambda} \sum_{\omega=\lambda}^{\Omega} \left\{ \frac{Q^{\Omega-\omega-1} - P^{\Omega-\omega-1}}{Q - P} Q(2 + \epsilon_1 - P) + P^{\Omega-\omega-1}(2 + \epsilon_1) \right\} \\
&\quad \left\{ 1 + \epsilon_1 \left[\frac{K^{\omega-\lambda} - 1}{K - 1} \right] \right\} \tag{4.37}
\end{aligned}$$

This is a sum of geometric series with factor Q , Q/K , P , P/K . Since $Q > P$ and $K > 1$ in the limit $\lambda \rightarrow -\infty$, the series with factor Q dominates and we get Equation (2.19).

4.5 Planar Scaling Summary

This chapter has emphasized the fact that river networks in plan fill space, and therefore have a fractal dimension $D = 2$. The first section showed that three different techniques all indicate empirically that D is 2. The next section showed that in terms of Horton's scaling the space filling implies a relationship between R_b and R_ℓ . The following section showed how fractal dimension is related to Tokunaga's scaling, and that space filling implies a relationship between K and ϵ_1 . Thus it is clear that space filling networks are in principle possible under both the Horton and Tokunaga parameterizations of scaling. Furthermore the topologically random model, which presumably has linear stream elements, results in $R_\ell = 2$, $R_b = 4$ (Shreve, 1967) satisfying Equation (4.20) with $D_\ell = 1$. Also $\epsilon_1 = 1$, $K = 2$ (Tokunaga, 1978) implies $Q = 4$ and satisfies Equation (4.36) with $D_\ell = 1$. It is therefore plausible that random networks can be space filling and satisfy the observed scaling laws. It is not clear whether this is a property of the particular

form of the random model assumed by Shreve (1967), with networks of equal magnitude being equally likely, or a property of more general random models. Karlinger and Troutman (1989) have suggested a random model based on equal likelihood of all geometric trees spanning a grid. This is constrained to be space filling. Further work is required on this model to investigate its scaling properties.

Chapter 5

SLOPE SCALING

5.1. Introduction

A necessary step in understanding the link between erosive energy balance and network form is the description of the variation of slopes and elevation drops within a river network. This chapter focuses on the slopes of individual links within channel networks and their variability. Link slope is regarded as a random variable. The issue is how the probability distribution of link slope scales with link magnitude, or area.

The recent paper by Gupta and Waymire (1989) suggested a model of link drops with self-similar probability distribution functions (pdf), with area or magnitude taking the role of scaling parameter. In this chapter we present results based on large digital elevation model (DEM) data sets that show that while correct for the mean their model does not fit the data for higher moments. A more general multi-scaling model is needed to characterize the scaling of the full probability distribution of link slope.

The next section describes the self-similar link drop model suggested by Gupta and Waymire. Section 5.3 then gives the data we have on the scaling of link slopes and drops. In Section 5.4 we present a model for link slopes that focuses on the interplay between size and density of individual elevation increments, idealized as steps. This model fits the observation when the density of elevation increments changes with area as $A^{-\theta}$. This idea provides a mathematical characterization of the multi-scaling variability of link slopes. The physical causes and mechanisms resulting in this variability are still an open question. Section 5.5 summarizes our findings and conclusions.

5.2. Self-Similar Drop Model

Gupta and Waymire (1989) suggest a model for link drops given by

$$\frac{H(\alpha n)}{\mu(\alpha)} \stackrel{d}{=} H(n) \quad (5.1)$$

where $H(n)$ is the random link drop for a link of magnitude n , α is a scaling factor, $\mu(\alpha)$ is a normalization function, and $\stackrel{d}{=}$ denotes equality of probability distribution. Equation (5.1) is the definition of self-similarity, or scaling invariance of a random variable $H(n)$, dependent on and therefore indexed by scale parameter n . Gupta and Waymire (1989) show that quite generally $\mu(\cdot)$ is of the form

$$\mu(n) = n^{-\theta} \quad (5.2)$$

Note that here magnitude n is used as a surrogate for area, as discussed in Chapter 2. Gupta and Waymire (1989) also suggest that link slopes are independent of link lengths. Our data, as will be shown below, indicates lack of correlation between link slopes and lengths, which justifies the independence assumption. The implication is that link drop is dependent on link length, which is also verified in the data. Therefore, we prefer to start with a self-similar assumption, analogous to Equation (5.1), for slopes:

$$S(\alpha n) \stackrel{d}{=} \mu(\alpha) S(n) \quad (5.3)$$

where $S(n)$ is link slope dependent on magnitude, with $\mu(\cdot)$ given by Equation (5.2).

The justification for this assumption is the notion of self-similarity, and the empirical observations of Flint (1974), and others, described in Chapter 2, with magnitude used as a surrogate for area. Denote the random link length, assumed independent of magnitude, by L . In our data we have not been able to detect significant trends of L with magnitude. Then link drop is

$$H(n) = S(n)L \quad (5.4)$$

so

$$H(\alpha n) = S(\alpha n)L \stackrel{d}{=} \mu(\alpha) S(n)L = \mu(\alpha) H(n) \quad (5.5)$$

equivalent to Equation (5.1).

Gupta and Waymire (1989) started with (5.1) and used the inverse argument to derive (5.3). Equation (5.3) can alternatively be stated as:

$$Z = \frac{S(n)}{\mu(n)} \stackrel{d}{=} S(1) \quad (5.6)$$

i.e., the variable $S(n)/\mu(n)$ is an iid random variable [equal in distribution to $S(1)$] which we call Z . The self-similar model is simply

$$\begin{aligned} S(n) &= \mu(n) Z \\ &= n^{-\theta} Z \end{aligned} \quad (5.7)$$

This clearly shows the nature of the self-similar model which is characterized by power law scaling, the scale parameter n is raised to the power $-\theta$.

Moments of the self-similar model scale proportionally to $(n^{-\theta})^k$, i.e.,

$$\begin{aligned} E[S(n)] &= n^{-\theta} E(Z) \\ \text{Var}[(S(n))] &= n^{-2\theta} \text{Var}(Z) \\ M_k[S(n)] &= n^{-k\theta} M_k(Z) \end{aligned} \quad (5.8)$$

where $M_k(\cdot)$ denotes the k th moment.

The quantiles of the self-similar model all scale proportional to $n^{-\theta}$, i.e.,

$$QS_{\gamma}(n) = QZ_{\gamma} n^{-\theta} \quad (5.9)$$

where $QS_{\gamma}(n)$ is a quantile (non-random value) of the slope corresponding to a probability of exceedance γ , i.e.,

$$\text{Prob}[S(n) > QS_{\gamma}(n)] = \gamma \quad (5.10)$$

and similarly QZ_{γ} is a quantile of Z

$$\text{Prob}(Z > QZ_{\gamma}) = \gamma \quad (5.11)$$

Gupta and Waymire (1989) incorporated this scaling in terms of link drops, Equation (5.5), into the random topology model. They computed the expected value of link concentration function (lcf), conditional on magnitude from this model, and showed that it compared well with empirically observed lcf's. This had been a problem in earlier efforts [Gupta and Mesa (1988); Gupta, et al. (1986); Mesa (1986)].

The good fit to mean lcf's were the only results used by Gupta and Waymire (1989) to justify the model [Equation (5.1)]. We feel that comparisons to the mean lcf such as those of Gupta and Waymire (1989) are limited because only the mean trend of drop variation with magnitude is tested. Higher moment or quantile properties are not tested. Also using the mean lcf introduces unnecessary mathematical complications to test notions that can be tested directly. Gupta and Waymire (1989) emphasize the importance of the scaling invariance or self-similarity of the link drop probability distribution as providing a fundamental theoretical basis for empirical power law relationships. Although they also suggest that multi-scaling corrections may be necessary, based on the fact that the empirical scaling exponents reported by Wolman (1955) vary with quantile value, they did not explore nor attempt to explain the inconsistency of this observation with their self-similar model. In the next section we show that direct analysis of data does not support scaling invariance as a model for link slopes.

5. 3. Empirical Evidence of Scaling in Elevation

The data presented in this chapter is from Big Creek, a tributary of the St. Joe River near Calder, Idaho, and the St. Joe River itself (CALD and STJOE in Table 3.4). Big Creek is a $147 \times 10^6 \text{ m}^2$ basin covered by a combination of four U. S. Geological Survey 7.5 minute DEM's that give elevations on a 30m grid. The St. Joe River is a $2834 \times 10^6 \text{ m}^2$ basin with DEM data from a combination of three 1⁰ Defense mapping agency series DEM's that give elevations on a 3 arc second grid (60m x 90m approximately). Figure 5.1 gives a map of the St. Joe River and Big Creek.

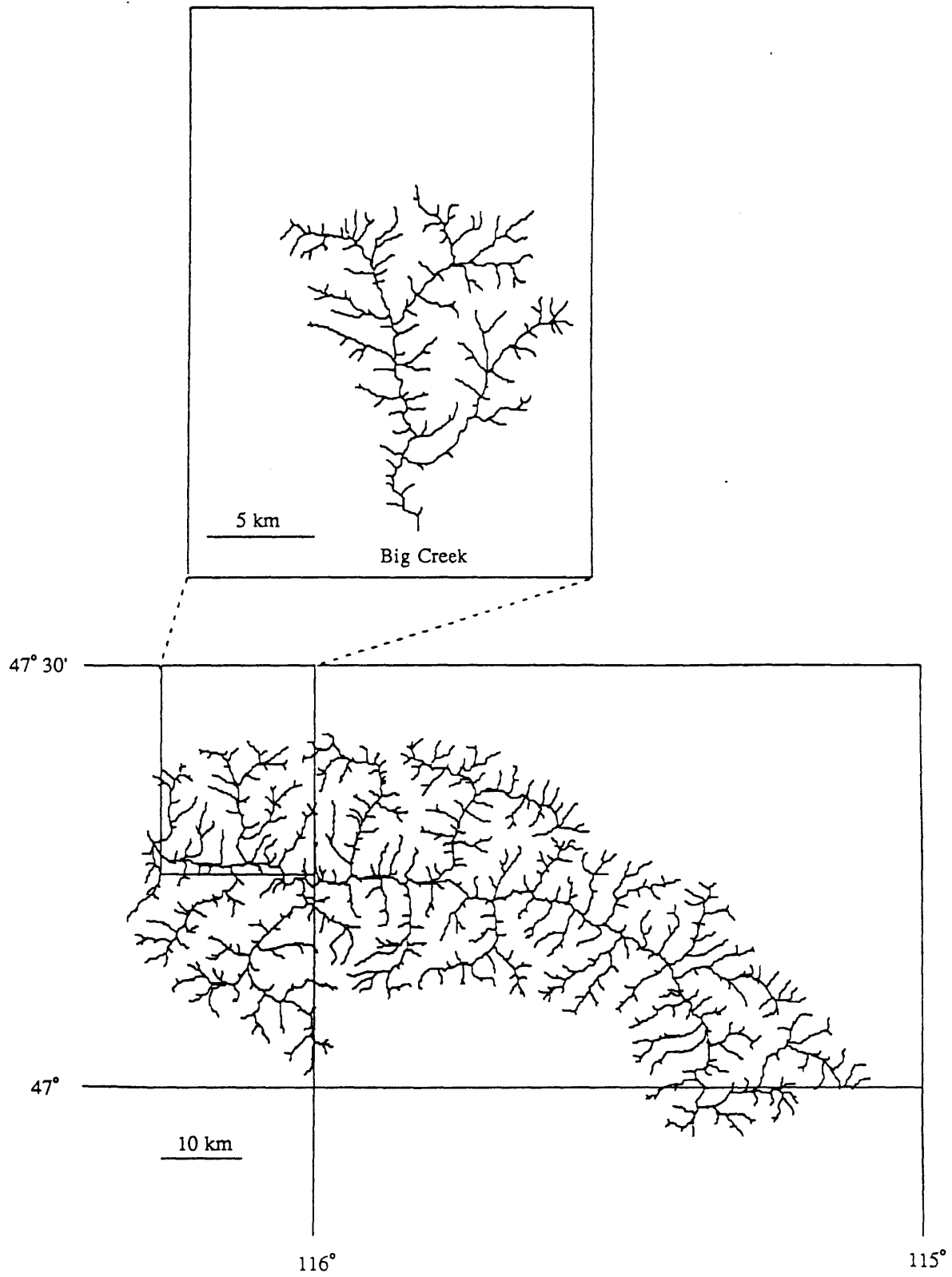


Figure 5.1. St Joe River and Big Creek Location Map

Figures 5.2 and 5.3 show link slopes plotted against magnitude, $2n-1$ and area for these two data sets. To obtain these figures a support area of 300 pixels was used for the Big Creek (CALD) basin and 200 pixels for the St. Joe River (STJOE). These are the physically justifiable support areas for these basins identified by the procedures of the next chapter. In these figures n , $2n-1$, and area are for practical purposes interchangeable scaling indices. We interpret area as being the fundamental scaling index, with n and $2n-1$ good surrogate measures. In the remainder of this chapter we use A as our scaling index. We could have obtained the same results using $2n-1$ or n as surrogates for A .

In Figures 5.2 and 5.3 there is considerable scatter in the individual link slopes; however, by ranking the links according to scale index (A , n or $2n-1$), the links are grouped into bins containing at least 20 links that cover a narrow range of scale index. The group sample means are plotted as circles in Figures 5.2 and 5.3 and show power law scaling approximately proportional to $A^{-0.5}$. This by itself is in agreement with the self-similar model. The group sample variances are plotted in Figures 5.4 and 5.5 and show power law scaling proportional to $A^{-0.5}$. If the exponent θ is estimated from the mean (Figures 5.2 and 5.3) as 0.5, the self-similar model [Equation (5.8)] would predict that slope variances should scale proportional to A^{-1} . This is not the case in Figures 5.4 and 5.5 and is the first indication of failure of the self-similar model.

Further evidence of the failure can be obtained by looking at the distribution of the normalized variable $Z = S(A)/\mu(A)$ [Equation (5.6)]. With $\theta = 0.5$ from Figures 5.2 and 5.3, we can compute Z for each link. This gives $N = 2n-1$ realizations of Z , so for n large (which it is) we can get an idea of the probability distribution of Z by ranking and plotting according to the plotting position $P = \frac{i}{N+1}$, where i is the rank from largest (1) to smallest (N) of the N realizations of Z . This is done in Figures 5.6 and 5.7 for the Big Creek and St. Joe Rivers.

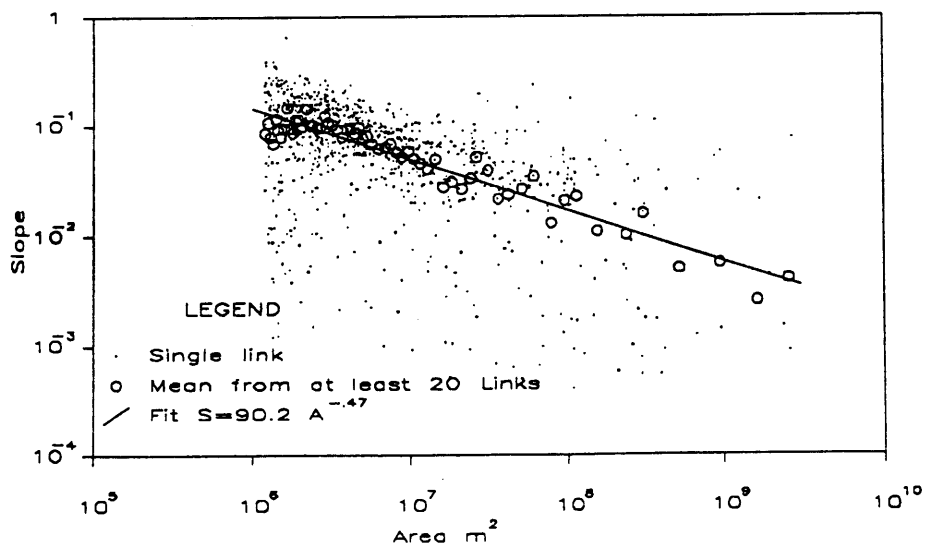
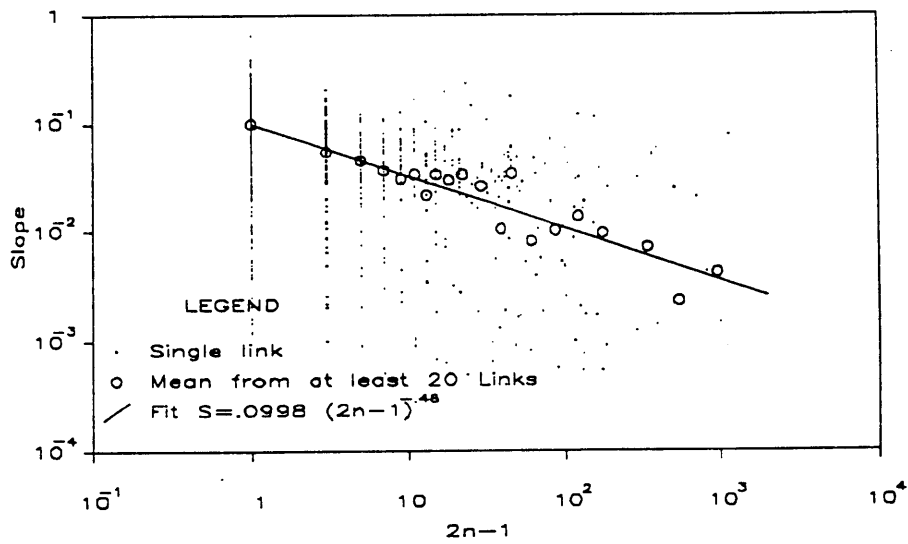
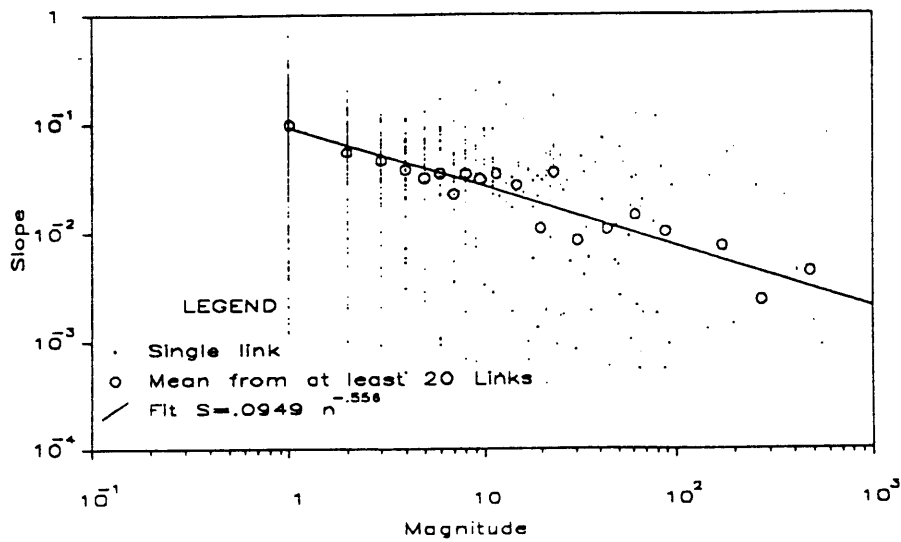


Figure 5.2. Link Slopes for the St. Joe River, Idaho.

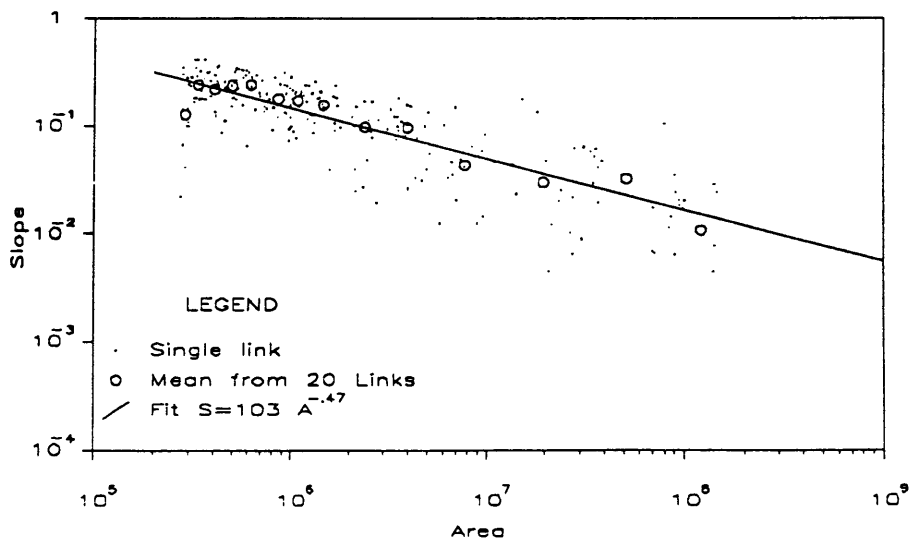
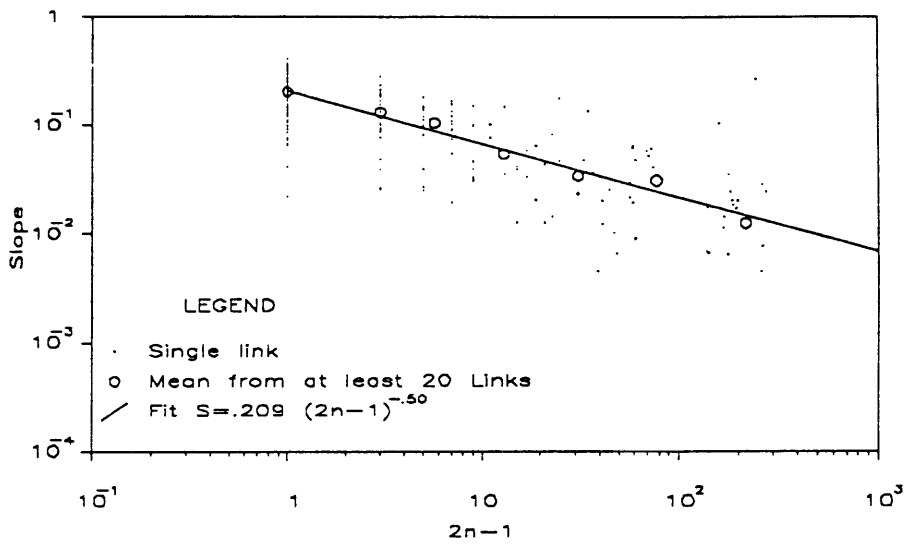
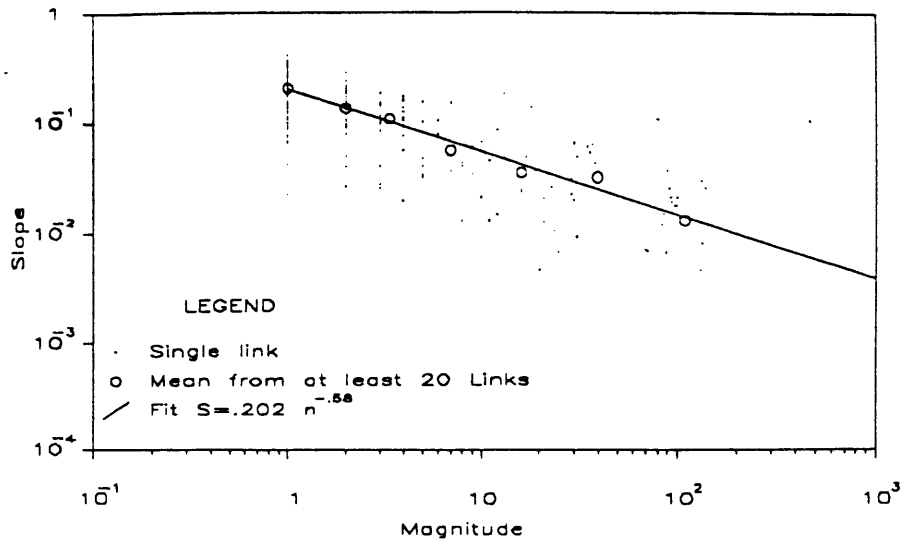


Figure 5.3. Link Slopes for Big Creek, Idaho.

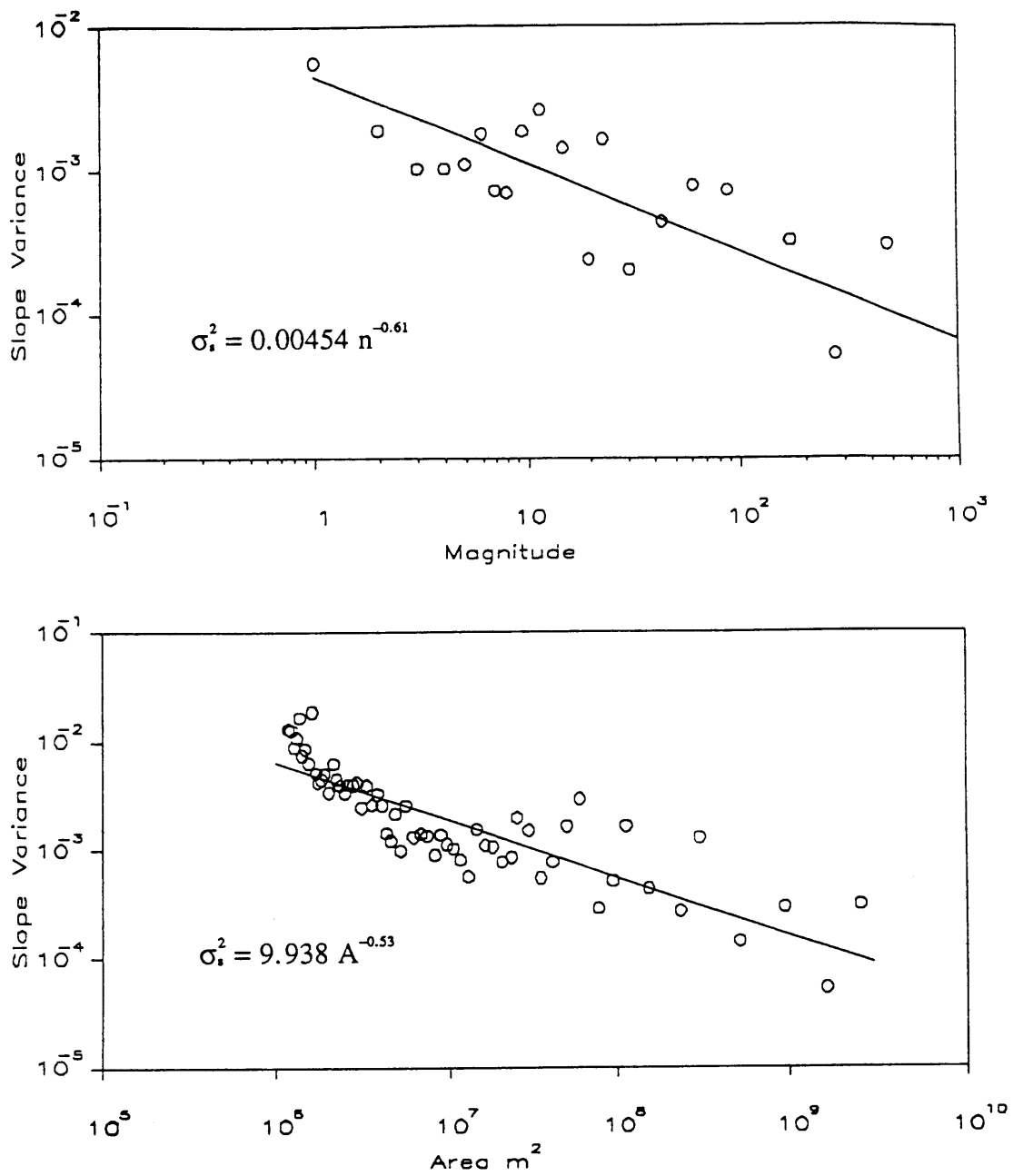


Figure 5.4. Link Slope Variances, St. Joe River, Idaho.

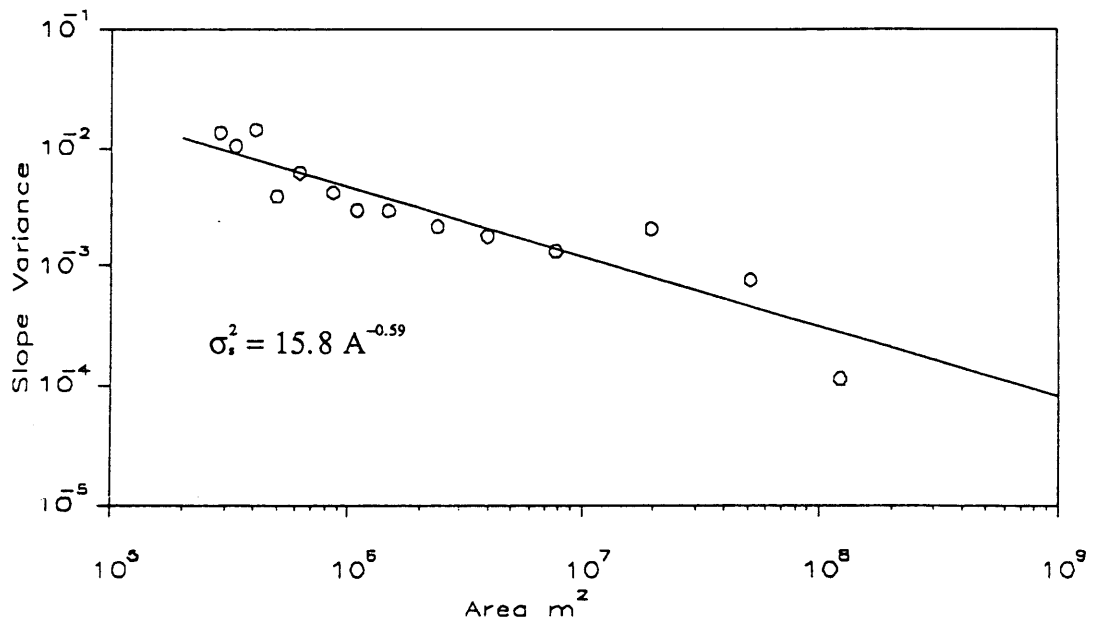
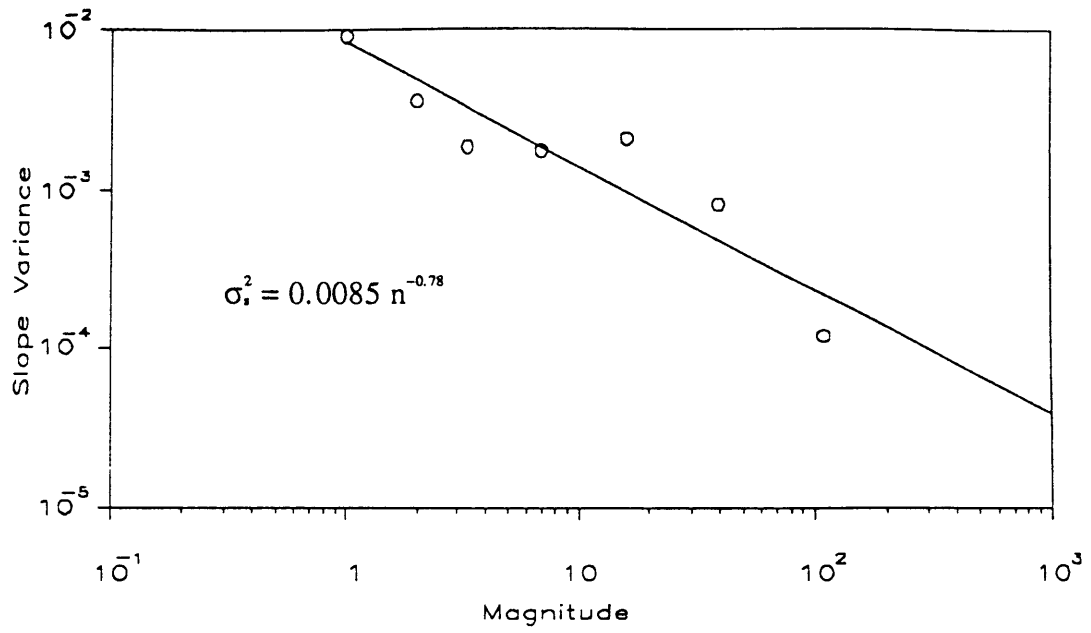


Figure 5.5. Link Slope Variances, Big Creek, Idaho.

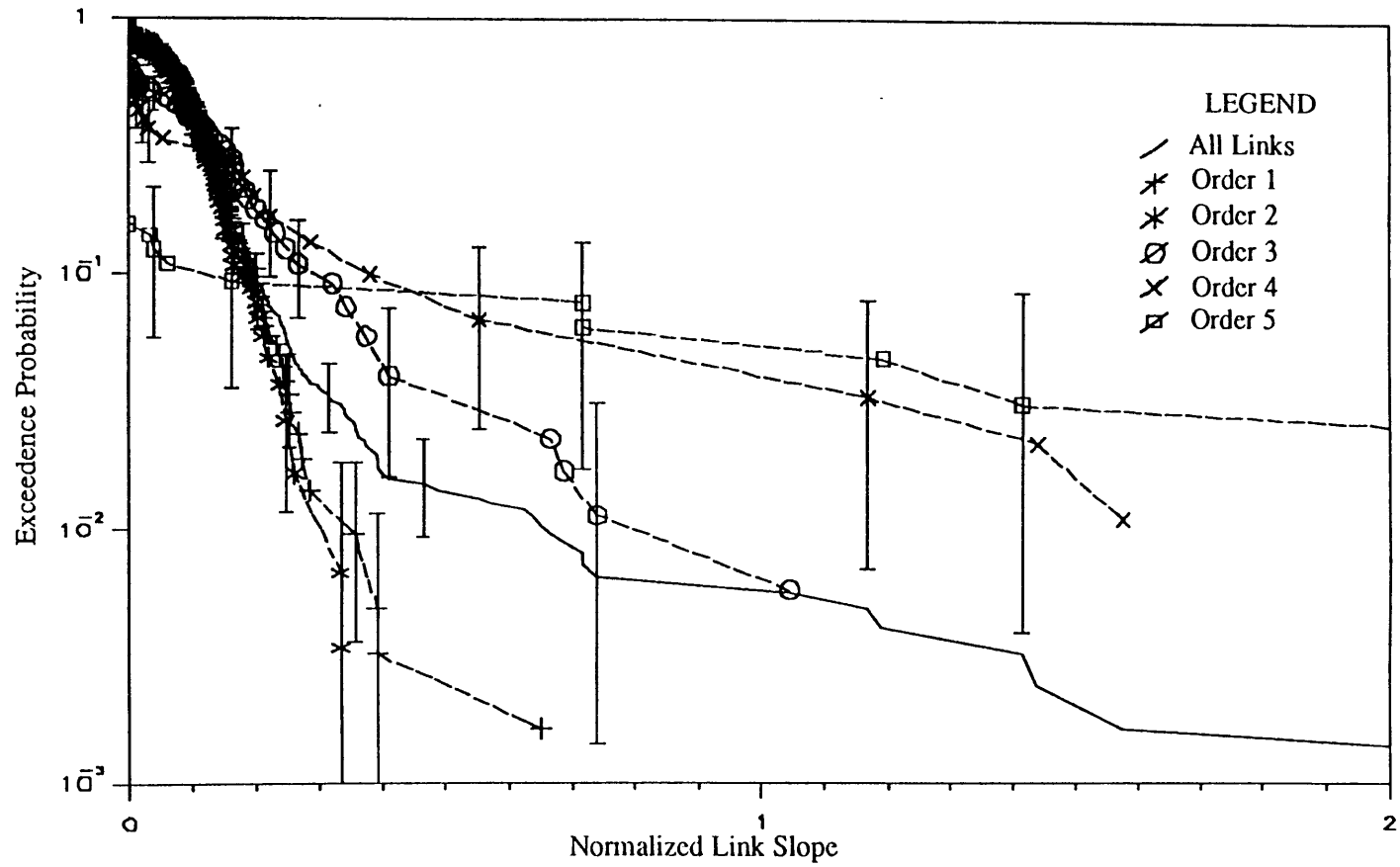


Figure 5.6. St. Joe River Link Slopes
Normalized with $n^{-0.6}$

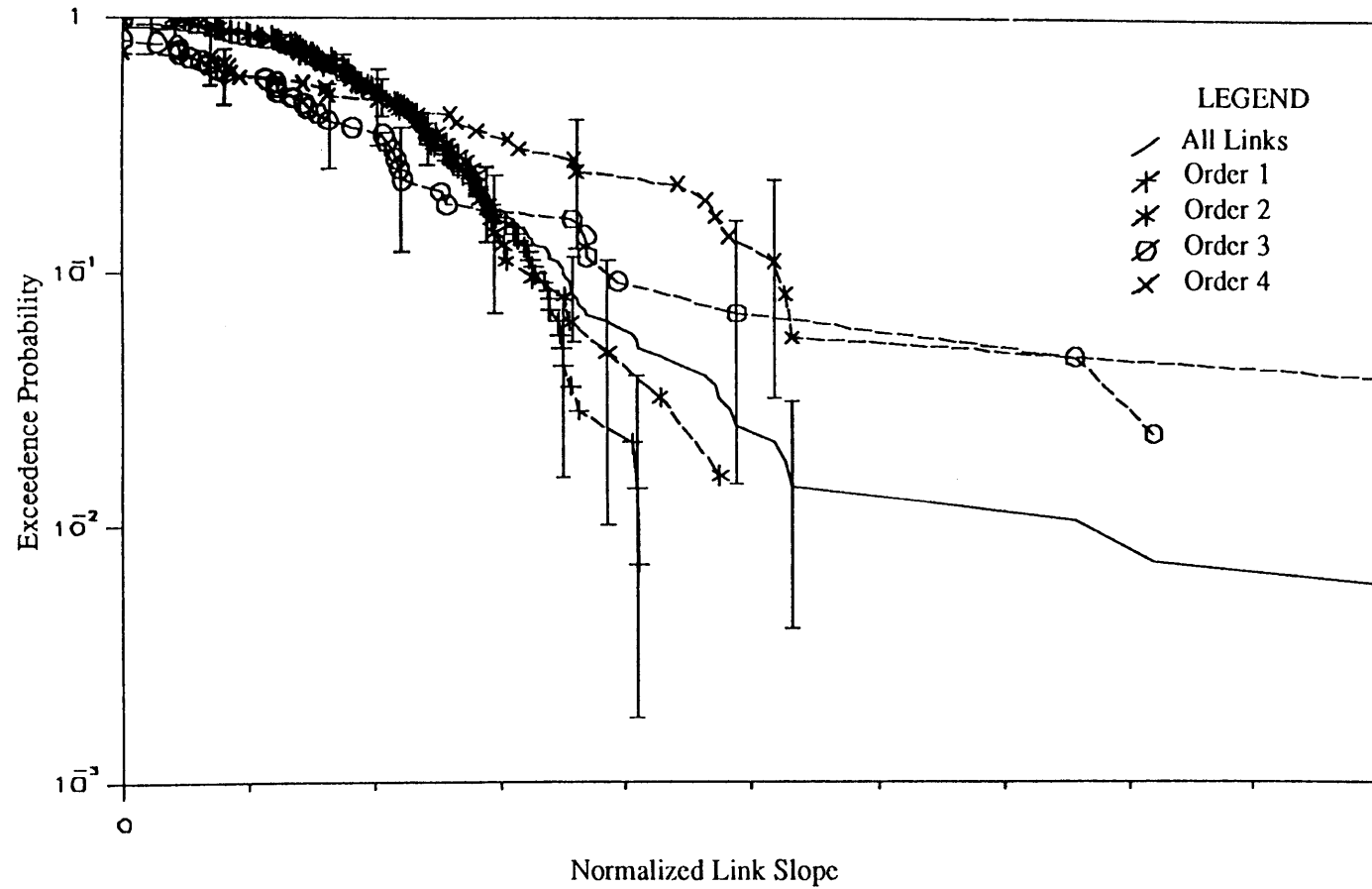


Figure 5.7. Big Creek Link Slopes
Normalized with $n^{-0.6}$

Also shown are the probability distributions estimated from subsets consisting of all links with a given Strahler order. 95% confidence limit error bars in the plotting position probability computed from the incomplete beta distribution are shown. [The incomplete beta distribution is the theoretical distribution of non-parametric estimates of probability. For further information on this, see for example Zhang (1982) and references therein.] The Z are supposed to be iid, i.e., independent of Strahler order, so sets of links from different Strahler orders should have the same probability distribution. This is not the case and is another indication of the failure of the self-similar model of slopes.

Tables 5.1 and 5.2 give statistics of link properties for the Big Creek and St. Joe Rivers. The tables show how the mean and variance of slope and drop both decrease with order. The normalization accounts for the trends in the mean, but makes the normalized variance and hence coefficient of variation increase with order, counter to what the self-similar model for full distribution would predict. Also note that correlation coefficients between slope and length are negligible, whereas the correlation between drop and length is not. This gives some credence to the assumption of independence between slopes and lengths, and is the basis for our regarding slope as the more fundamental variable than link drop in Equation (5.3). Significance tests on the difference between the mean (t test) and variance (F test) of the normalized slopes given in Tables 5.1 and 5.2 are given in Table 5.3. These indicate very little significant differences between the mean normalized slope of links of different orders, indicating that the normalization works for the mean. However, for the variances the hypothesis that the different order links are from the same population is rejected at the 0.05 level for the great majority of cases. This is a clear failure of the self-similar model to characterize the link slope distribution.

Table 5.1. Big Creek Link Statistics.

Magnitude 139, Order 4 basin

		All	Strahler Order			
			1	2	3	4
Number of Links		277	139	61	42	35
Mean	H (m)	82	121	79	21	9.4
	S	0.136	0.203	0.114	0.039	0.020
	L (m)	614	591	735	612	497
Variance	H (10^3m^2)	7.36	9.0	3.6	0.54	0.12
	S (10^{-3})	11.1	9.2	2.9	1.9	0.55
	L (10^3m^2)	240	221	228	384	141
Coefficient of Variation	H	1.04	0.79	0.77	1.10	1.16
	S	0.78	0.47	0.48	1.12	1.20
	L	0.80	0.79	0.65	1.01	0.76
Normalised Mean	H/ $\mu(n)$ (m)	123	121	145	102	117
	S/ $\mu(n)$	0.204	0.203	0.208	0.173	0.238
Normalised Variance	H/ $\mu(n)$ (10^3m^2)	11.9	9.0	12.6	16.2	16.7
	S/ $\mu(n)$ (10^{-3})	22	9.2	9.0	34.7	78.1
Coeff. of Var. for Norm.	H/ $\mu(n)$	0.89	0.79	0.77	1.24	1.10
	S/ $\mu(n)$	0.72	0.47	0.46	1.07	1.17
Correlation Coefficient Between	H & L	0.61	0.84	0.66	0.77	0.55
	S & L	-0.02	0.009	-0.20	-0.09	-0.02
	Norm. H & L	0.77	0.84	0.67	0.85	0.59
	Norm. S & L	-0.04	0.009	-0.17	-0.03	-0.01

H = Link Drop

L = Link Length

S = Link Slope defined as H/L

The function $\mu(n) = n^{-0.6}$ is divided into H or S to get the normalised statistics.

Table 5.2. St. Joe River Link Statistics.

Magnitude 621, Order 5 Basin

		Strahler Order					
		All	1	2	3	4	5
Number of Links		1241	621	295	173	89	63
Mean	H (m)	90.6	135	72.8	30.5	14.9	4.8
	S	0.066	0.100	0.047	0.026	0.013	0.0038
	L (m)	1356	1383	1465	1233	1180	1176
Variance	H (10^3m^2)	11.2	14.7	5.1	1.27	0.53	0.26
	S (10^{-3})	4.7	5.6	1.4	1.3	0.78	0.20
	L (10^3m^2)	1209	1527	1054	785	616	675
Coefficient of Variation	H	1.17	0.90	0.98	1.17	1.55	3.33
	S	1.04	0.75	0.82	1.41	2.08	3.66
	L	0.81	0.89	0.70	0.72	0.66	0.70
Normalised Mean	H/ $\mu(n)$ (m)	136	135	135	131	145	149
	S/ $\mu(n)$	0.102	0.100	0.088	0.109	0.13	0.126
Normalised Variance	H/ $\mu(n)$ (10^3m^2)	32.6	14.8	16.9	24.8	65.1	262
	S/ $\mu(n)$ (10^{-3})	26.3	5.6	5.1	24.8	78.5	264
Coeff. of Var. for Norm.	H/ $\mu(n)$	1.33	0.90	0.96	1.20	1.75	3.43
	S/ $\mu(n)$	1.59	0.74	0.81	1.44	2.16	4.08
Correlation Coefficient	H & L	0.67	0.79	0.73	0.61	0.32	0.16
Between	S & L	0.01	-0.03	0.09	-0.03	-0.04	0.02
	Norm. H & L	0.51	0.78	0.74	0.57	0.28	0.14
	Norm. S & L	-0.01	-0.03	0.09	-0.03	-0.04	0.004

H = Link Drop

L = Link Length

S = Link Slope defined as H/L

The function $\mu(n) = n^{-0.6}$ is divided into H or S to get the normalised statistics.

Table 5.3
Significance Tests for the Difference Between Normalized Slopes of
 Different Order

Difference of means t test

$$\frac{\bar{x} - \bar{y}}{\sqrt{\frac{(n_x - 1) S_x^2 + (n_y - 1) S_y^2}{n_x + n_y - 2} \left(\frac{1}{n_x} + \frac{1}{n_y} \right)}} \sim t_{\alpha/2, n_x + n_y - 2}$$

Difference of Variances F test

$$\frac{S_x^2}{S_y^2} \sim F_{\alpha/2, n_x - 1, n_y - 1}$$

Comparisons by order for Big Creek

	All	1	2	3	4	
All		0.07	0.2	1.22	1.13	t
1	2.39*		0.34	1.39	1.23	
2	2.44*	1.02		1.25	0.77	
3	1.58*	3.77*	3.86*		1.22	
4	3.55*	8.5*	8.68*	2.25*		
			F			

Comparisons by Order for St. Joe River

	All	1	2	3	4	5	
All		0.29	1.4	0.53	1.48	0.96	t
1	4.7*		2.3*	1.1	2.19*	1.15	
2	5.1*	1.1		1.97*	2.34*	1.22	
3	1.1	4.4*	4.9*		0.78	0.39	
4	3.0*	14.0*	15.4*	3.2*		0.06	
5	10.0*	47.0*	51.8*	10.7*	3.4*		
			F				

* = Significant at $\alpha = 0.05$ level

5.4. Link Slope Scaling Model

Let us view the fall in elevation along a stream as composed of distinct discrete steps. This is consistent with the notion of pools and riffles due to Yang (1971a) and has possible justification in terms of energy expenditure arguments. The location of steps will be taken as random according to a general stationary point process along the length of channel. Thus the number of steps in a fixed length of channel will be a random variable. The size of individual steps will be taken as iid random variables, which implies that the accumulation of elevation changes is a marked point process. The scaling will be introduced through the intensity or rate of the point process λ , which will be taken proportional to $\mu(A) = A^{-\theta}$.

Let a link have a random length L . Then the number of steps in the link is a random variable J with distribution, conditional on L , denoted $P_{J|L}(j|\ell)$ for j a non-negative integer (0,1,2,...). From properties of general orderly point processes (Cox and Isham, 1980), we get

$$E[J|L] = \lambda L \quad (5.12)$$

and we characterize the point process by its index of dispersion defined

$$I(L) = \frac{\text{Var}[J|L]}{E[J|L]} \quad (5.13)$$

Note that for a Poisson process $I(L) = 1$, and for a process with uniform step spacing (i.e., no randomness or variance), $I(L) = 0$. The index of dispersion indicates over dispersion or under dispersion of the points with respect to the Poisson process, and in general may be scale dependent, i.e., dependent on L .

The steps are iid random variables denoted by Y_i , so the link drop is

$$H = \sum_{i=1}^J Y_i \quad (5.14)$$

Define the random link slope

$$S = \frac{H}{L}. \quad (5.15)$$

The objective is to derive the moments of S and H , since these describe the random structure of the network in elevation. This is done in terms of the joint distribution of H and L . H is a function of J which is conditional on L , so H and L are not independent.

Let the Y_i have probability density function (pdf) $f_Y(y)$. Then for J given the pdf of H is the J fold convolution of $f_Y(y)$, Feller (1971), denoted $f_Y^{J*}(h)$. Summing this over the distribution of J we get, conditional on L

$$f_{H|L}(h|\ell) = \sum_{j=0}^{\infty} P_{J|L}(j|\ell) f_Y^{j*}(h) \quad (5.16)$$

From the definition of conditional probability, the joint pdf of H and L is

$$\begin{aligned} f_{H,L}(h,\ell) &= f_{H|L}(h|\ell) f_L(\ell) \\ &= f_L(\ell) \sum_{j=0}^{\infty} P_{J|L}(j|\ell) f_Y^{j*}(h) \end{aligned} \quad (5.17)$$

where $f_L(\ell)$ is the pdf of link lengths L . With this

$$\begin{aligned}
E[S] &= E\left[\frac{H}{L}\right] \\
&= \int_{h=0}^{\infty} \int_{\ell=0}^{\infty} \frac{h}{\ell} f_{H,L}(h,\ell) \, dh \, d\ell \\
&= \int_{\ell=0}^{\infty} \frac{1}{\ell} f_L(\ell) \sum_{j=0}^{\infty} P_{J|L}(j|\ell) \int_{h=0}^{\infty} h f_Y^{j*}(h) \, dh \, d\ell \\
&= \int_{\ell=0}^{\infty} \frac{1}{\ell} f_L(\ell) \sum_{j=0}^{\infty} P_{J|L}(j|\ell) j \bar{Y} \, d\ell \\
&= \int_{\ell=0}^{\infty} \frac{1}{\ell} f_L(\ell) \lambda \ell \bar{Y} \, d\ell \\
&= \lambda \bar{Y}
\end{aligned} \tag{5.18}$$

Similarly

$$\begin{aligned}
E[S^2] &= \int_{\ell=0}^{\infty} \int_{h=0}^{\infty} \frac{h^2}{\ell^2} f_{H,L}(h,\ell) \, dh \, d\ell \\
&= \lambda \left[\sigma_Y^2 E\left[\frac{1}{Y}\right] + \bar{Y}^2 E\left[\frac{I(L)}{L}\right] \right] + \lambda^2 \bar{Y}^2
\end{aligned} \tag{5.19}$$

where σ_Y is the standard deviation of the step height Y and the expectation is now over the distribution of link length. Then

$$\begin{aligned}
\text{Var}[S] &= E[S^2] - [E[S]]^2 \\
&= \lambda \left[\sigma_Y^2 E\left[\frac{1}{L}\right] + \bar{Y}^2 E\left[\frac{I(L)}{L}\right] \right]
\end{aligned} \tag{5.20}$$

Similarly, we obtain

$$E[H] = \lambda \bar{L} \bar{Y} \tag{5.21}$$

$$\text{Var}[H] = \sigma_L^2 \lambda^2 \bar{Y}^2 + \lambda \left[\sigma_Y^2 \bar{L}^2 E[LI(L)] \right] \quad (5.22)$$

$$\text{Cov}(S,L) = \text{Corr}(S,L) = 0 \quad (5.23)$$

$$\text{Corr}(H,L) = \frac{1}{\sqrt{1 + \frac{E[LI(L)]/\bar{L} + \sigma_Y^2/\bar{Y}^2}{\lambda \bar{L} (\sigma_L^2/\bar{L}^2)}}} \quad (5.24)$$

where Cov denotes covariance and Corr denotes correlation. Note that the correlation between S and L is 0 as observed in Tables 5.1 and 5.2, whereas the correlation between H and L is not. Implicit in these results is the assumption that expectations $E[\frac{I(L)}{L}]$, $E[LI(L)]$, and $E[\frac{1}{L}]$ exist. This places minor restrictions on the distribution that can be used for L and the point process that can be used. Now the scaling can be introduced by letting

$$\lambda = k\mu(A) = k A^{-\theta} \quad (5.25)$$

From (5.18) we then get

$$E[S] = k \bar{Y} A^{-\theta} \quad (5.26)$$

and from (5.20)

$$\text{Var}[S] = k \{ \sigma_Y^2 E[\frac{1}{L}] + \bar{Y}^2 E[\frac{I(L)}{L}] \} A^{-\theta} \quad (5.27)$$

This is of the form observed in Figures 5.2, 5.3, 5.4, and 5.5 and is different from the

scaling predicted by the self-similar slope model of Gupta and Waymire (1989). From Equations (5.26) and (5.27), we get the coefficient of variation of slope

$$C_s = \frac{\sqrt{\text{Var}[S]}}{E[S]} = \left[\frac{\frac{\sigma_Y^2}{\bar{Y}^2} E[L] + E\left[\frac{I(L)}{L}\right]}{k} \right]^{1/2} A^{1/2} \quad (5.28)$$

which is an increasing function of A or order, as observed in Tables 5.1 and 5.2.

The elements of this model essential to explain the multi-scaling of link slopes are the Y_i being iid and the mean density of steps (or rate of the point process) being proportional to $A^{-\theta}$. For a fixed length of channel, x , and letting λ be proportional to $A^{-\theta}$ in Equations (5.18) and (5.20), we get

$$E[S] \sim A^{-\theta} \bar{Y} \quad (5.29)$$

$$\text{Var}[S] \sim \frac{A^{-\theta}}{x} \{ \sigma_Y^2 + \bar{Y}^2 I(x) \} \quad (5.30)$$

In constructing models of link drops or slopes, there are two possibilities. The normalization $A^{-\theta}$ can be applied to the step height Y or step density λ . We see that the choice results in fundamentally different scaling behavior. Applying the normalization to step height Y leads to moments scaling proportional to $(A^{-\theta})^k$ and the self-similar model. Applying the normalization to the density λ leads to moments scaling proportional to $A^{-\theta}$ as observed. An important finding is therefore that the scaling of slopes is consistent with self-similarity in the density of steps or rate of elevation changes and not with simple self-similarity of the slopes or drops of individual links. This clarifies the nature of the multi-scaling of channel slopes. A physical explanation of why the density of steps or elevation increments

scale the way suggested here is an open question.

The discreteness of the steps in this model can be removed by considering a limit process with $k \rightarrow \infty$ and $\bar{Y} \rightarrow 0$, that maintains the desired properties. In particular we must have $E[S]$ given by Equation (5.26) remain bounded, i.e., not diverge to ∞ or 0. This suggests a limit in which

$$\lim_{\substack{k \rightarrow \infty \\ \bar{Y} \rightarrow 0}} (k \bar{Y}) = \text{constant} \quad (5.31)$$

i.e., $k \sim \frac{1}{\bar{Y}}$. Also, $\text{Var}[S]$ as given by Equation (5.27) must remain bounded. The variance can be written as

$$\text{Var}[S] = k \bar{Y}^2 \left[E\left[\frac{1}{L}\right] C_Y^2 + E\left[\frac{1}{L}\right] \right] A^{-\theta} \quad (5.32)$$

where $C_Y = \frac{\sigma_Y}{\bar{Y}}$. From Equation (5.31) $\lim_{\substack{k \rightarrow \infty \\ \bar{Y} \rightarrow 0}} (k \bar{Y}^2) = 0$, so we must have

$$\lim_{\substack{k \rightarrow \infty \\ \bar{Y} \rightarrow 0}} (k \bar{Y}^2 C_Y^2) = \text{constant} \quad (5.33)$$

With Equation (5.31) this implies

$$\lim_{\substack{k \rightarrow \infty \\ \bar{Y} \rightarrow 0}} (\bar{Y} C_Y^2) = \lim_{\substack{k \rightarrow \infty \\ \bar{Y} \rightarrow 0}} \left(\frac{\sigma_Y^2}{\bar{Y}} \right) = \text{constant} \quad (5.34)$$

The question is whether distributions exist that have $\bar{Y} \rightarrow 0$, $\sigma_Y^2 \rightarrow 0$, but $C_Y \rightarrow \infty$ as is needed by (5.34). One possibility is the Gamma distribution, which also has the desirable property that $Y > 0$ as is sensible for link drops. The Gamma pdf is (Feller, 1971)

$$f_Y(y) = \frac{\beta(\beta y)^{\nu-1} e^{-\beta y}}{\Gamma(\nu)} \quad (5.35)$$

where β is the scale parameter and ν the shape parameter. This has moments

$$\bar{Y} = \frac{\nu}{\beta} \quad (5.36)$$

$$\sigma_Y^2 = \frac{\nu}{\beta^2}$$

which give

$$C_Y = \frac{1}{\nu} \quad (5.37)$$

Therefore,

$$C_Y^2 \bar{Y} = \frac{1}{\beta} \quad (5.38)$$

and

$$k \bar{Y} = \frac{k \nu}{\beta} \quad (5.39)$$

so a Gamma distribution with β held constant and $\nu \sim \frac{1}{k}$ will satisfy our conditions (5.34) and (5.31) in the limit as $k \rightarrow \infty$.

This limit process is analogous, but not equivalent to the limit of a random walk resulting in Brownian motion. In Brownian motion the central limit theorem gives the Gaussian distribution as the limit distribution. The central limit theorem (Feller, 1971, p. 259) applies to the limit sum of mutually independent random variables with common distribution. Here the limit involves changing the shape of the distribution as the limit is approached. Clearly the central limit theorem does not apply. In fact when Y is Gamma distributed [Equation (5.35)] and we consider a fixed length of channel L with uniform step distribution [I(L) = 0], the number of steps is $kn^{-\theta}L$ so H and S are Gamma distributed. For S

$$f_{S|L}(s|\ell) = \frac{\beta \ell (\beta s \ell)^{kC\nu-1} e^{-\beta s \ell}}{\Gamma(kC\nu)} \quad (5.40)$$

where $C = A^{-\theta} \ell$.

In the limit $\nu \rightarrow 0$, $k \rightarrow \infty$, but $\nu \sim \frac{1}{k}$, i.e., take $\nu k = C_2$ a constant. Therefore the pdf of slope for a fixed length of channel is by construction, for all k including the limit $k \rightarrow \infty$, the Gamma distribution

$$f_{S|L}(s|\ell) = \frac{\beta \ell (\beta s \ell)^{CC_2-1} e^{-\beta s \ell}}{\Gamma(CC_2)} \quad (5.41)$$

In fact, a result from statistical mechanics, the saddle point approximation or method of steepest descent, can be used to show that when a Gamma distribution is assumed for increment heights, the limit slope distribution conditional on length is also the gamma distribution given in Equation (5.41), for all point processes that are asymptotically normal. This is a wide class of point processes including the Poisson

process, renewal processes and Neyman Scott processes (Cox and Isham, 1980); we do not believe that the asymptotic normal assumption is particularly restrictive.

Equation (5.35) in (5.16) gives for fixed L with $\nu = C_2/k$ and the change of variables $H = SL$

$$f_{S|L}(s|\ell) = \sum_{j=0}^{\infty} P_{J|L}(j|\ell) \frac{\beta \ell (\beta s \ell)^{\frac{C_2 j}{k} - 1}}{\Gamma(\frac{j C_2}{k})} e^{-\beta s \ell} \quad (5.42)$$

Now substituting the normal density function for $P_{J|L}(j|\ell)$ we get

$$\begin{aligned} f_{S|L}(s|\ell) &= \int_{-\infty}^{\infty} \frac{1}{\sqrt{2\pi k C}} e^{-(j-kC)^2/2kC} \left[\frac{\beta \ell (\beta s \ell)^{\frac{C_2 j}{k} - 1}}{\Gamma(\frac{j C_2}{k})} \right] e^{-\beta s \ell} dj \\ &= \int_{-\infty}^{\infty} e^{k\varphi(j)} dj \end{aligned} \quad (5.43)$$

where

$$\begin{aligned} \varphi(j) &= -\frac{(j-kC)^2}{2k^2 C} + \frac{\ln \beta \ell}{k} + \left(\frac{C_2 j - k}{k^2}\right) \ln \beta s \ell - \frac{\beta s \ell}{k} - \frac{1}{k} \ln \sqrt{2\pi k C} \\ &\quad - \frac{1}{k} \ln \Gamma\left(\frac{j C_2}{k}\right) \end{aligned} \quad (5.44)$$

Theorem:

$$\lim_{k \rightarrow \infty} \int_{-\infty}^{\infty} e^{k\varphi(x)} dx = e^{k\varphi(x_m)} \quad (5.45)$$

where this limit exists. Here x_m is the value of x that corresponds to the global maximum of $\varphi(x)$. Clearly for the limit to exist, $\varphi(x)$ must have highest order k terms proportional to k^{-1} except for isolated x . An integral analogous to Equation (5.45) occurs in statistical mechanics.

Proof:

This proof repeated here for convenience can also be deduced from Negele and Orland (1987, p. 121) or Huang (1963, p. 210).

Expand $\varphi(x)$ about x_m in a Taylor series

$$\begin{aligned} \varphi(x) &= \varphi(x_m) + (x-x_m) \varphi'(x_m) + \frac{(x-x_m)^2}{2!} \varphi''(x_m) \\ &+ \sum_{n=3}^{\infty} \frac{(x-x_m)^n}{n!} \varphi^{(n)}(x_m) \end{aligned} \quad (5.46)$$

Since $\varphi(x_m)$ is a maximum $\varphi'(x_m) = 0$ and $\varphi''(x_m) < 0$, we can write

$$\begin{aligned} I &= \int_{-\infty}^{\infty} e^{k\varphi(x)} dx \quad (5.47) \\ &= \int_{-\infty}^{\infty} e^{k\varphi(x_m) - \frac{k}{2}(x-x_m)^2 |\varphi''(x_m)| + \sum_{n=3}^{\infty} k \frac{(x-x_m)^n}{n!} \varphi^{(n)}(x_m)} dx \end{aligned}$$

With the change of variables $\tau = \sqrt{k |\varphi''(x_m)|} (x-x_m)$ this becomes

$$I = \frac{e^{k\varphi(x_m)}}{\sqrt{k|\varphi''(x_m)|}} \int_{-\infty}^{\infty} e^{-\tau^2/2 + \sum_{n=3}^{\infty} \left[\frac{\tau}{\sqrt{\varphi''}} \right]^n \frac{1}{k^{n/2-1}} \varphi^{(n)}(x)} d\tau \quad (5.48)$$

For $k \rightarrow \infty$ the terms with $n \geq 3$ go to zero and the integral is Gaussian so we get:

$$I = e^{k\varphi(x_m)} \sqrt{\frac{2\pi}{|\varphi''(x_m)|k}} \quad (5.49)$$

So

$$\frac{\ln I}{k} = \varphi(x_m) + \frac{1}{2k} \ln \left[\frac{2\pi}{k|\varphi''(x_m)|} \right] \quad (5.50)$$

and

$$\lim_{k \rightarrow \infty} \frac{\ln I}{k} = \varphi(x_m) \quad (5.51)$$

so

$$\lim_{k \rightarrow \infty} I = e^{k\varphi(x_m)} \quad (5.52)$$

$\varphi(j)$, Equation (5.44), has a maximum for k large at $j_{\max} = kC$, so (using the above theorem) we get for $k \rightarrow \infty$,

$$f_{S|L}(s|\ell) = \frac{\beta \ell (\beta s \ell)^{CC_2 - 1} e^{-\beta s \ell}}{\Gamma(CC_2)} \quad (5.53)$$

which is identical to Equation (5.41).

Empirical support for the link slope scaling model suggested in this section is obtained by looking at the probability distribution of link slopes. The unconditional or marginal distribution for link slope is

$$f_S(s) = \int_{\ell=0}^{\infty} f_L(\ell) f_{S|L}(s|\ell) d\ell \quad (5.54)$$

A common although perhaps not the best distribution for link lengths is the Gamma distribution, written here (analogous to Equation 5.35)

$$f_L(\ell) = \frac{1}{\mu} \frac{(\ell/\mu)^{\alpha-1} e^{-\ell/\mu}}{\Gamma(\alpha)} \quad (5.55)$$

See van der Tak and Bras (1989), Abrahams (1984), or Abrahams and Miller (1982) for discussion of the merits of various link length distributions.

We were not able to evaluate the integral in Equation (5.54). This at first glance appears simply the product of Gamma functions; however, the realization that $C = A^{-\theta} \ell$ in (5.53) complicates the integration over ℓ . Hence, we estimated $f_S(s)$ by simulation. First we sample from the distribution of L [Equation (5.55)], and then with L known from the distribution of $S|L$ [Equation (5.53)].

Figures 5.8 and 5.9 give estimates for the exceedance probability distribution of link slopes. The parameters used were $\alpha = 1.96$, $\mu = 313.7$, $\beta = 0.04225$, $C_2 = \nu k = 0.0086$, $\theta = 0.6$, and λ given by Equation (5.25). These parameters were chosen

to match the following moments of the Big Creek data set: $E[L]$, $E[\frac{1}{L}]$, $E[S]$, $\text{Var}[S]$. One thousand variates were simulated and the exceedance probability obtained from the plotting position $P = \frac{i}{N+1}$. The magnitudes of 1, 4, 16, and 64 were chosen as surrogates for area because according to the random topology model in infinite networks they are equivalent to Strahler orders 1, 2, 3, and 4. In Figure 5.8 note the decrease in mean slope with order as well as change in shape emphasizing the non-self-similarity of the slope distributions. Figure 5.9 gives the same data but here the slopes have been normalized by $\mu(n) = n^{-\theta}$. The mean is preserved but the distributions differ in shape. The similarity between simulated (Figure 5.9) and empirical (Figure 5.6) distributions is evident. In Figure 5.10 the link slope data for Big Creek are plotted without normalization (contrary to Figure 5.7). The comparison of the simulated link slope distributions (Figure 5.8) and the empirical distributions for Big Creek (Figure 5.10) is very good.

Chapter 2 mentioned the empirical finding of Broscoc (1959) that the average drop in elevation along Strahler streams was approximately constant, basically due to the fact that $R_s \simeq R_\ell$ for many networks. Here we investigate the effect of this in the context of the discrete step model. The change in elevation along a length of channel L is composed of a random number J of discrete jumps distributed conditionally on length, $P_{J|L}(j|\ell)$. This probability distribution is dependent on the rate λ . Many point processes, including all those for which $I(L)$ is constant, are scale independent and will have a dimensionless form of the probability distribution written $P_{J|\lambda L}(j|\lambda\ell)$, i.e., conditioned on the dimensionless parameter λL . Now consider the length L to be a Strahler stream. Then assuming Horton's length law, the mean length is

$$L_\omega = L_1 R_\ell^{\omega-1} \tag{5.56}$$

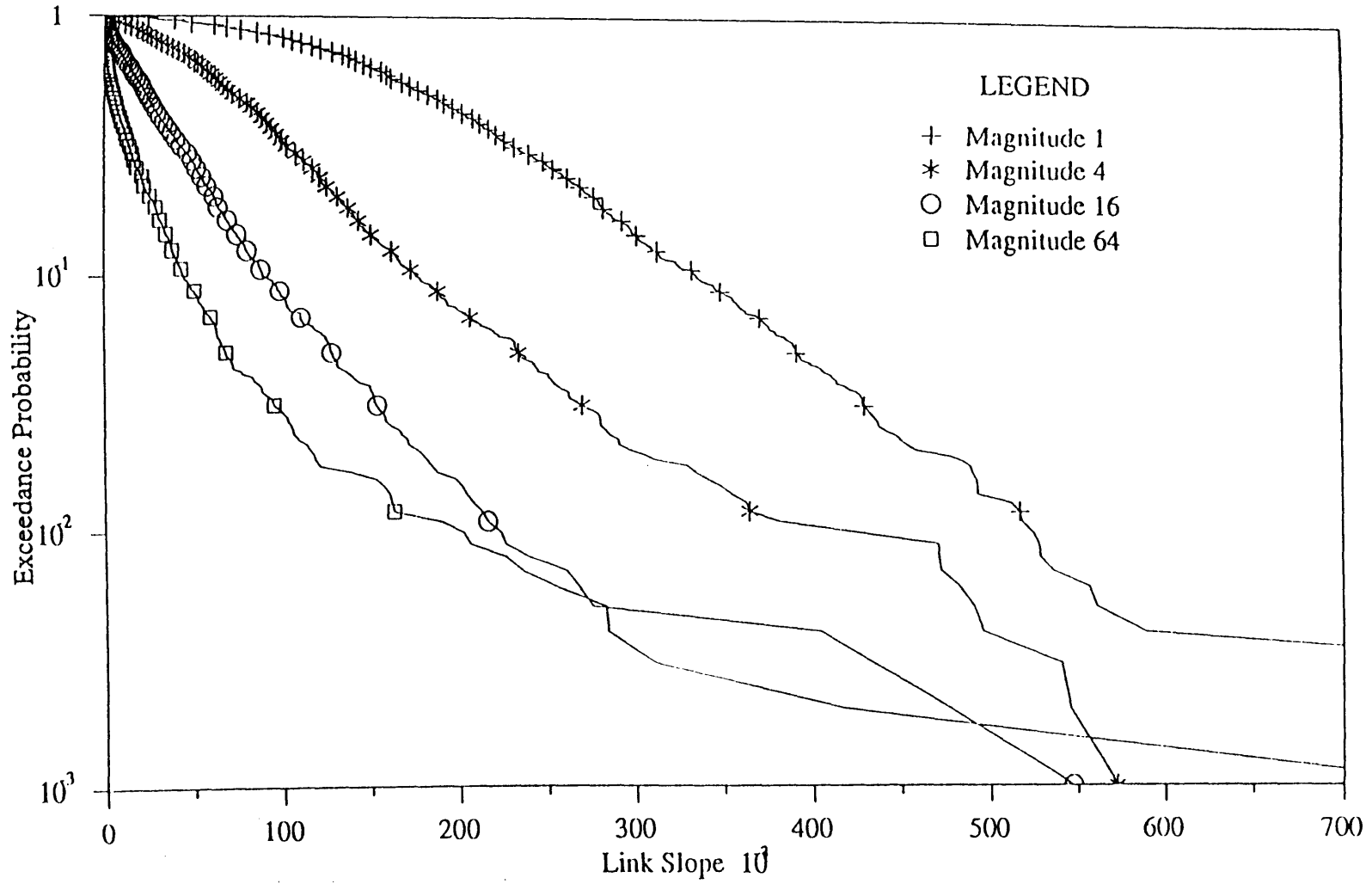


Figure 5.8. Model Slope Distributions by Simulation.

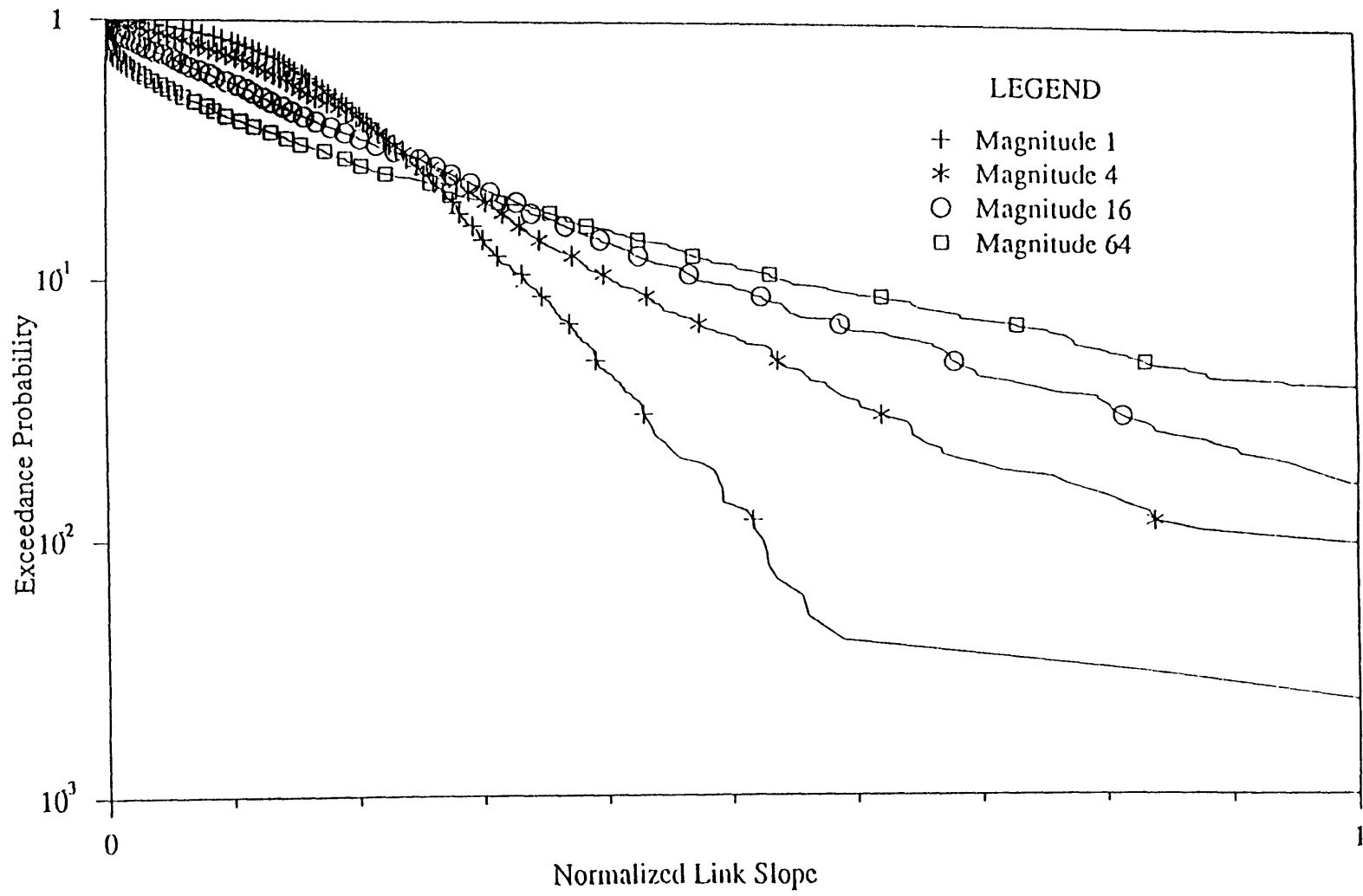


Figure 5.9. Normalized Slope Distributions from model by Simulation.

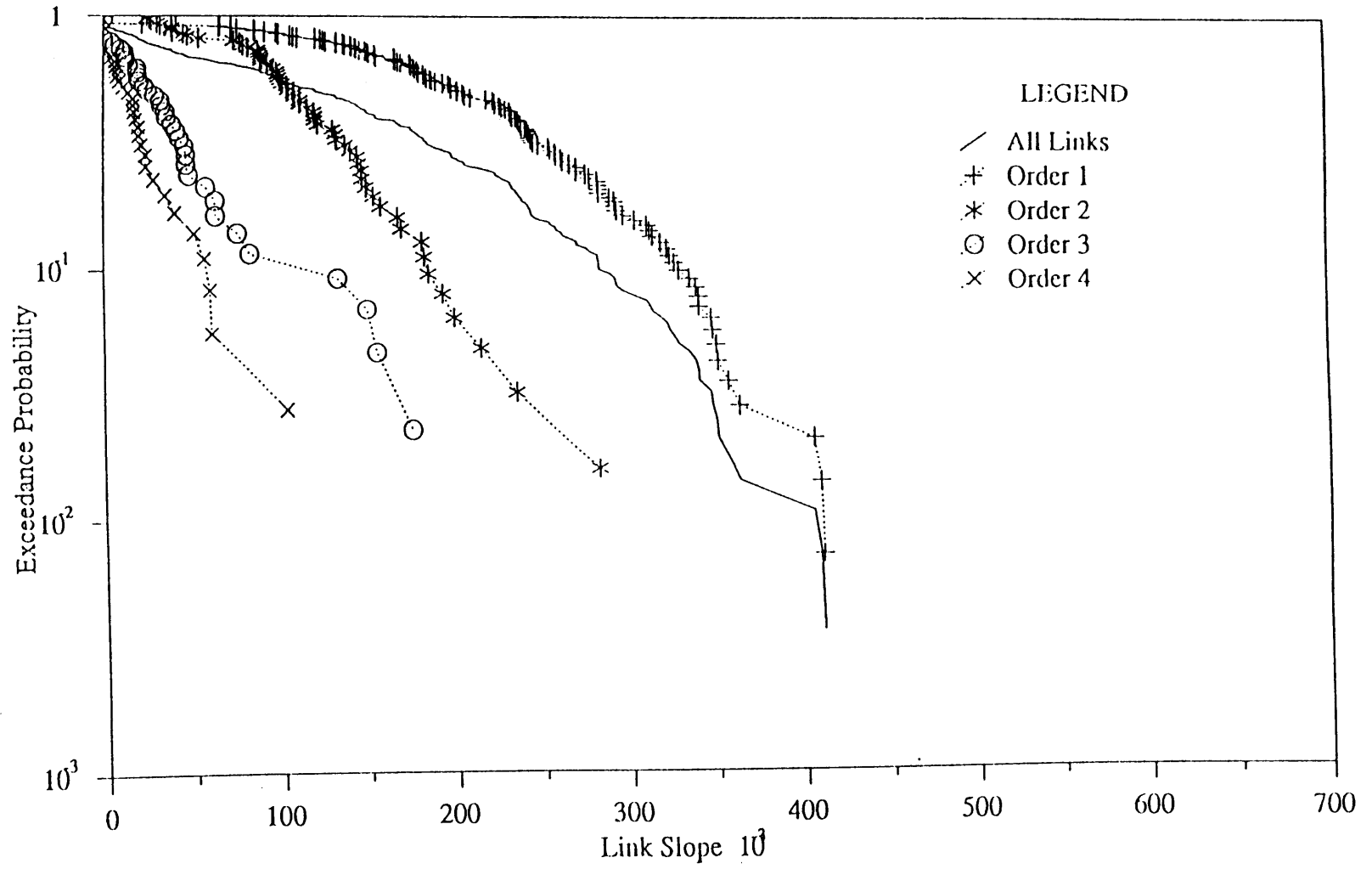


Figure 5.10. Big Creek Link Slopes (Not Normalized).

Thus the dimensionless parameter for stream drop distributions is $\lambda L_1 R_L^{\omega-1}$. Now step heights are taken to be iid, so for the constant drop property to hold the number of jumps on average in each stream should be the same. This implies that the distribution of stream drops should be the same for all streams. Some data presented in chapter 6 (figure 6.6) supports this.

This implies, with λ given by Equation (5.25)

$$\lambda L_1 R_\ell^{\omega-1} = k A^{-\theta} L_1 R_\ell^{\omega-1} = \text{constant} \quad (5.57)$$

or since k and L_1 are constants

$$A_\omega^{-\theta} R_\ell^{\omega-1} = \text{constant} \quad (5.58)$$

Here the dependence of A on order ω has been shown. Equation (5.58) gives

$$R_\ell = \left[\frac{A_{\omega-1}}{A_\omega} \right]^\theta = R_a^\theta \quad (5.59)$$

with $\theta \approx 0.5$ to 0.6 as found for a lot of our data this is within the typical values found for R_ℓ ($1.5 - 2.5$) and R_a ($3 - 5$), at least within the scatter of estimation of R_ℓ and R_a . This result, achieved by assuming Horton's laws, the constant drop property and the slope scaling model has intriguing connotations. It links length and area aspects of river basin geometry. Empirically lengths and areas have been linked by a power law, Equation (2.37), [Eagleson (1970); Hack (1957)], as

$$L \propto A^{-\alpha} \quad (5.60)$$

where L is mainstream length and A basin area. The exponent $\alpha \approx 0.56$. If we assume that mainstream length can be scaled to length of the highest order stream by a constant coefficient, a self-similarity assumption, Equation (5.60) can give

$$R_\ell = R_a^\alpha \quad (5.61)$$

identical to Equation (5.59). This is an unexpected connection between the length area scaling and slope scaling exponents.

5.5. Conclusions

The important conclusions from this chapter are:

- link slopes are not self-similar with respect to area as a scale index. Rather they are multi-scaling, manifested by the fact that the coefficient of variation of slope increases with scale (i.e., area or magnitude).
- The nature of this multi-scaling has been identified. It is such that the density of elevation increments within a channel scales proportional to $A^{-\theta}$ (or $n^{-\theta}$) while the increments themselves show no apparent trend.
- The data has confirmed that link slope and link length are uncorrelated, although not necessarily independent. This implies that link drop is correlated with link length and that therefore slope is a more fundamental variable than drop.

Although the data presented is for only two river basins, the conclusions are believed to be generally valid for the majority of rivers in a state of balance or equilibrium. Further work is required to discover the physical mechanisms that result in these observations.

Chapter 6

BASIC SCALES IN THE LANDFORM

6.1 Introduction

Clearly the scaling discussed in the previous chapter, represented as

$$S \propto A^{-\theta} \tag{6.1}$$

cannot hold over all ranges of scales in the landscape. In particular as $A \rightarrow 0$ towards hilltops, Equation (6.1) would predict infinite slopes, a nonsensical result. The main point of this chapter is that the scaling breaks at the scale of dissection of the landscape, or drainage density scale. We will show how a break in slope scaling manifests itself in digital elevation data and use an analysis of sediment transport processes to justify that this break in scaling is the basic scale or drainage density. The break in slope scaling is due to a switch in the dominating sediment transport mechanism from fluvial at large scale to diffusive hillslope mechanisms like soil creep and landsliding at small scale.

The break in scaling can also be detected by a failure of the constant stream drop property. The third section focuses on this, providing the connection between stream drops and link drops discussed in Chapter 5.

The last section presents a table of results comparing the drainage density for all the DEM's analyzed, determined by both techniques for detecting the break in scaling, as well as estimated directly from the DEM based on local procedures to identify concave pixels.

6.2 Slope–Area Scaling

Figure 6.1 gives a plot of slope versus area, where a small support area was used to extract the network. Area is total contributing area measured at the downstream end of each link and slope is mean link slope defined as elevation drop divided by link length. It is a link average slope at the scale the network is extracted. Here the scale or support area of extraction of the network serves to define the length of averaging for computation of slopes. Figure 6.1 has significant scatter indicating that link slope is highly variable. However, when many links with similar area are grouped together and averaged (circles in Figure 6.1) the mean slope is seen to follow a fairly smooth trend. The straight lines are fitted to the circles using two phase regression. The line to the right of the switch point, with negative slope, corresponds to the scaling described in Chapter 5. The switch point gives the scale at which this scaling breaks and is the support area that should be used to extract channel networks from DEM's. Then the drainage density obtained will correspond to the basic scale in the landscape.

To understand the nature of the break, we need to look in more detail at the sediment transport processes present on the hillslopes and in the channels. The literature (see Chapter 2) has suggested that sediment transport can be written $F(S,a)$ where a is contributing area per unit contour width and S slope. Chapter 2 gave the conditions for dynamic equilibrium, or a constant form solution in terms of continuity equations of water and sediment. Solution to these equations must result in the sediment transport past every point being equal to the amount of material added upstream of that point due to the uplift U . This is expressed mathematically

$$F(S,a) = Ua \tag{6.2a}$$

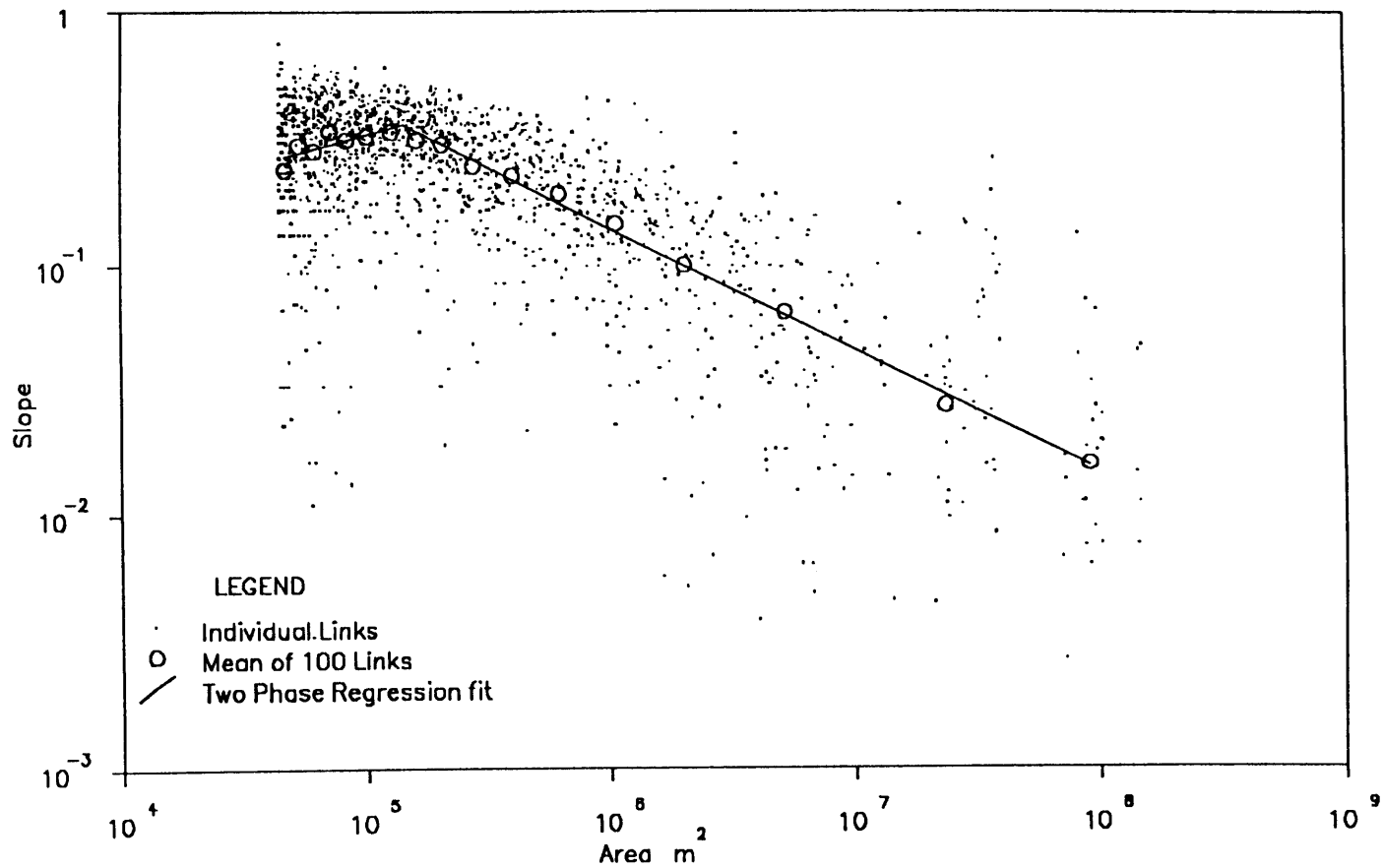


Figure 6.1. CALD (Big Creek, Idaho) Link Slopes with Support area of 50 pixels used to extract network.

which for U given and the functional form $F(\cdot)$ known, is an implicit relationship between slope S and area a . In this expression U does not have to be restricted to uplift but can be thought of as average degradation rate over a fairly large area. A common form of $F(\cdot)$ given in Chapter 2 is

$$F(S,a) = \beta a^m S^n \quad (6.3a)$$

with exponents from Table 2.1. Together with Equation (6.2a) this implies

$$S \propto a^{-\frac{m-1}{n}} \quad (6.4a)$$

The same argument can be used in the context of channels and concentrated flow contributing area A to get analogous to Equations (6.2a), (6.3a), and (6.4a)

$$F[S, Q(A)] = F(S,A) = UA \quad (6.2b)$$

$$F(S,A) = \beta A^m S^n \quad (6.3b)$$

[perhaps with different coefficients β , m , n from Equation (6.34a)]

$$S \propto A^{-\frac{m-1}{n}} \quad (6.4b)$$

which is analogous to Equation (6.1) with $\theta = \frac{m-1}{n}$. Typical values for river sediment transport $m = 2.5$, $n = 3$ (Table 2.1 or Leopold and Maddock, 1953), give $\theta = 0.5$, possibly an explanation of the mean scaling of slope with area (Willgoose, 1989).

The numerical equivalence of a and A in digital elevation data allows us to apply notions developed for a to the concentrated area A . This will be done here for the Smith and Bretherton (1972) stability criteria [see Chapter 2, Equation (2.42)].

Recognizing that Equation (6.2b) defines a function $S(A)$ implicitly, we can write

$$F[S(A), A] = U A \quad (6.5)$$

which upon differentiation and multiplication by A gives

$$A \frac{\partial F}{\partial S} \frac{dS}{dA} + A \frac{\partial F}{\partial A} = U A = F \quad (6.6)$$

This can be rewritten

$$A \frac{\partial F}{\partial S} \frac{dS}{dA} = F - A \frac{\partial F}{\partial A} \quad (6.7)$$

Here the right-hand side is equivalent to the stability criterion of Smith and Bretherton (1972) which Kirkby (1980) suggests can be used to determine drainage density. For $F - A \frac{\partial F}{\partial A} < 0$, small perturbations grow into rills and ultimately channels.

For $F - A \frac{\partial F}{\partial A} > 0$, small perturbations do not grow so the landform remains smooth, i.e., hillslopes. Now on the left-hand side of Equation (6.7), A is always positive and $\frac{\partial F}{\partial S}$ we expect to be positive so stability depends on the sign of $\frac{dS}{dA}$. $\frac{dS}{dA} < 0$ results when there is instability and channelization, otherwise $\frac{dS}{dA} > 0$. This suggests that a break, or change in gradient of the $S(A)$ function is a dividing scale separating the distinctly different regimes of channels and hillslopes, and

justifies our assumption that the break in Figure (6.1) gives the basic scale in the landscape.

Equation (6.3) considered only one sediment transport function under dynamic equilibrium. In principle many sediment transport processes may operate at the same scale. Here we consider what happens when two mechanisms are operating and we assume the total sediment flux is the sum of the two mechanisms.

$$F(S,A) = F_1(S,A) + F_2(S,A) \quad (6.8)$$

Putting this equal to UA as in Equation (6.5) and solving for $S(A)$, the slope–area profile under dynamic equilibrium for combined sediment transport is obtained. This is given in Figure 6.2 for three different plausible hillslope sediment transport functions combined with a river sediment transport function. These figures show that in all three cases a slope–area profile that changes from positive, or near zero gradient, to negative gradient is obtained. This change over is accompanied by a switch in the process that dominates the sediment transport. At small contributing areas, or small scale, the sediment transport is dominated by the hillslope process whereas for large contributing areas or scale river erosion dominates.

Thus the break in slope–area scaling is accompanied by a switch in process dominating sediment transport, consistent with the notion of change from a channelized to a hillslope regime. This analysis points out the importance of slope–area curves in analyzing landforms. They give information about the fundamental scales and suggest how the scaling in between these scales can be interpreted in terms of sediment transport processes.

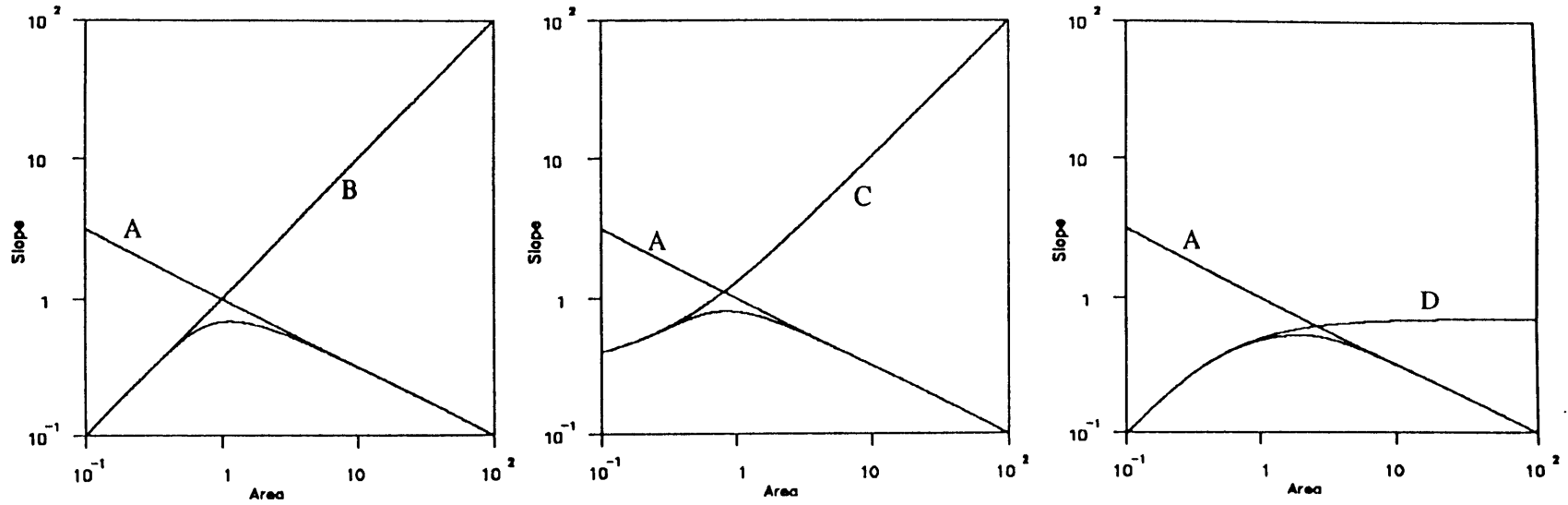


Figure 6.2. Equilibrium slope profiles for superposed transport functions.

Sediment Transport Functions:

- A. $F = A^{2.5} S^3$ Rivers Leopold and Maddock, 1953; Kirkby 1971.
 B. $F = S$ Soil Creep Davison, 1889; Kirkby, 1971.
 C. $F = S - 0.3$ Landsliding Kirkby, 1971.
 D. $F = \frac{S}{1-(S/0.7)^2}$ Sliding Andrews and Bucknam, 1987.

(Upper lines are solutions to $F(S, A) = A$

Lower lines are solutions to Eqn. (6.8), i.e. superposed sediment transport.)

To objectively test for the break in scaling we use two-phase regression (Solow, 1987; Hinkley, 1969). The technique is applied to a set of ordered pairs (x_i, y_i) , $i=1, \dots, n$, that are assumed to be related by

$$y_i = a_0 + b_0 x_i + b(x_i - c)I(x_i - c) + e_i \quad (6.9)$$

where a_0 , b_0 , b and c are parameters in the regression. $I(\cdot)$ is the indicator function defined

$$I(x) = \begin{cases} 0 & \text{for } x \leq 0 \\ 1 & \text{for } x > 0 \end{cases} \quad (6.10)$$

and e_i are the errors, assumed iid. The parameter c gives the switch point. The slope for $x < c$ is b and for $x > c$ is $b_0 + b$. The parameters are estimated by minimizing the sum of squares

$$SS = \sum_{i=1}^n \left[y_i - \left[a_0 + b_0 x_i + b(x_i - c)I(x_i - c) \right] \right]^2 \quad (6.11)$$

For c fixed SS is a quadratic function of a_0 , b_0 , and b so by differentiating Equation (6.11) with respect to a_0 , b_0 , and b and setting the derivatives equal to 0, the normal equations are

$$n a_0 + \sum_1 x_i b_0 + (\sum_2 x_i - c n_2) b = \sum_1 y_i$$

$$\sum_1 x_i a_0 + \sum_1 x_i^2 b_0 + (\sum_2 x_i^2 - c \sum_2 x_i) b = \sum_1 x_i y_i \quad (6.12)$$

$$\begin{aligned} & (\sum_2 x_i - c n_2) a_0 + (\sum_2 x_i^2 - c \sum_2 x_i) b_0 + (\sum_2 x_i^2 + c^2 n_2 - 2c \sum_2 x_i) b \\ & = \sum_2 x_i y_i - c \sum_2 y_i \end{aligned}$$

where \sum_1 is the sum over all data, \sum_2 is the sum over points with $x_i > c$, and n_2 is the number of points with $x_i > c$. These can be solved to give values a_0 , b_0 , and b that minimize SS. A grid search over possible values of c is then used to obtain the set a_0 , b_0 , b , c that minimizes SS. According to the model (6.9), these are maximum likelihood estimates of the parameters (Solow, 1987).

This regression should be tested against the null model, normal linear regression without a switch point.

$$y_i = a_n + b_n x_i \quad (6.13)$$

with residual sum of squares SS_0 . Solow (1987) gives the likelihood ratio statistic

$$R = \frac{(SS_0 - SS)/3}{SS/(n-4)} \quad (6.14)$$

The test is to reject the null hypothesis, that the two phase regression is not different from linear regression, at the $1 - \alpha$ level if

$$R \geq F_{3, n-4} (1 - \alpha)$$

where $F_{3,n-4}(1 - \alpha)$ is the $1 - \alpha$ quantile of the F distribution with 3 and $n - 4$ degrees of freedom.

Confidence intervals can be placed on the estimate of the switch point c . Following Solow (1987), the two-sided test of null hypothesis $H_0: c = c_0$ with significance level $1 - \alpha$ is to accept H_0 if

$$(SS' - SS)/[SS/(n-4)] \leq F_{1,n-4}(1 - \alpha) \quad (6.15)$$

where SS' is the sum of squares from fitting model (6.9) conditional on $c = c_0$. Then the $(1 - \alpha)$ confidence interval for c is the set of c_0 satisfying (6.15). For the data in Figure 6.1, the regression was done using the natural logs of the mean data (circles). Parameters were $a_0 = -4.18$, $b_0 = 0.266$, $b = -0.75$, $c = 11.87$, and the regression was significant [Equation (6.14)] up to the level $1 - \alpha$ with $\alpha = 5 \times 10^{-6}$, i.e., with 99.9994% confidence. Figure 6.3 gives a plot of the sum of squares, SS , versus c for this data. The minimum SS at $e^c = 143 \times 10^3 \text{m}^2$ is clearly seen. 95% confidence limits for the switch point obtained from this data using (6.15) are $107 \times 10^3 < e^c < 221 \times 10^3$.

It is possible to apply this technique to slopes and areas of individual pixels, as well as slopes and areas of "links" from a channel network with small support area. In principle the individual pixel data is like using a support area of 1 pixel to extract a network. The use of higher support areas just means slopes are averaged over longer distances thus reducing the effect of DEM data error. Table 6.1 gives an idea of the averaging length associated with different support areas for the W15 data set. It is similar for other data sets.

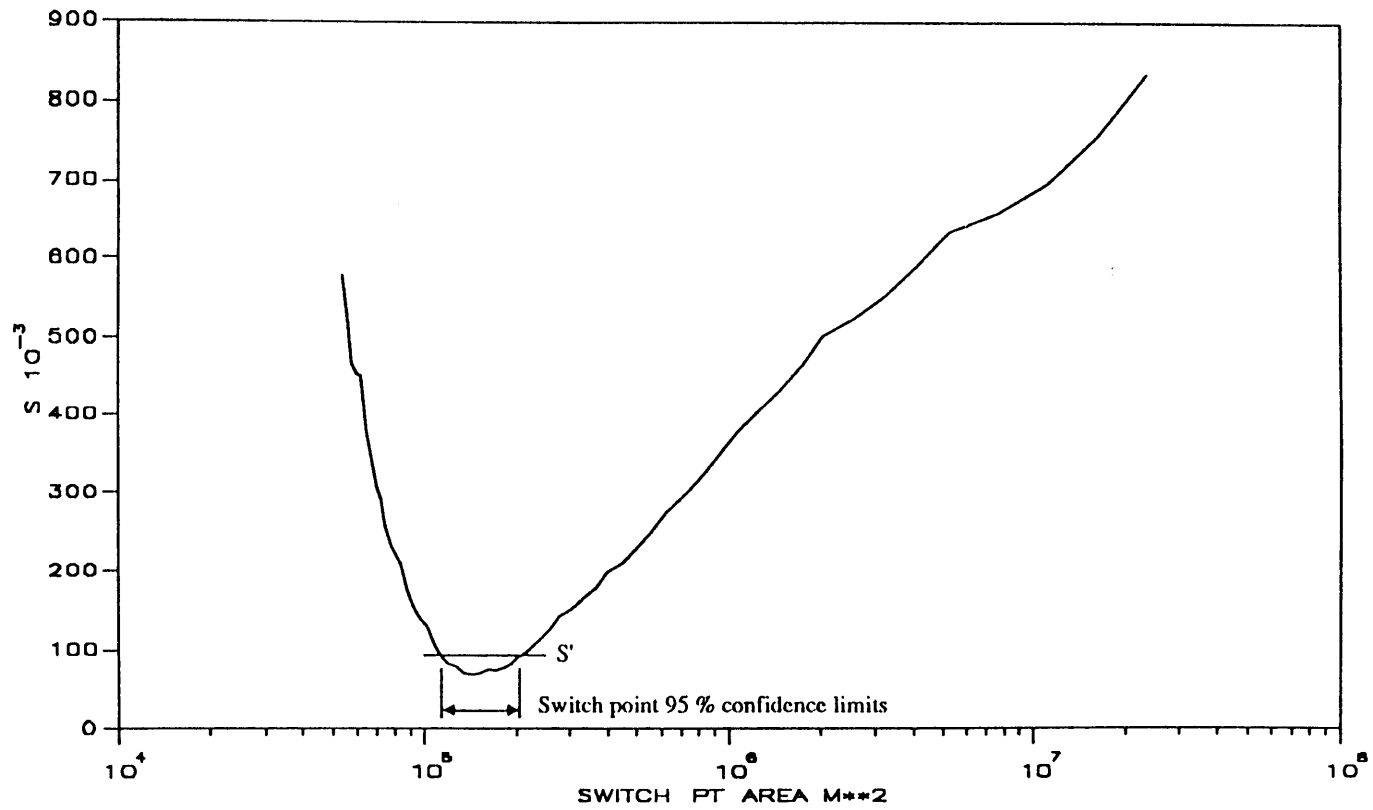


Figure 6.3. CALD (Big Creek, Idaho) Residual sum of squares from two phase regression as a function of switch point.

Table 6.1: W15 Data set Link Lengths

Support Area (no. of pixels)	Mean Link Length (m)
1	30 (grid spacing)
5	84
10	116
20	177
50	365

We have applied both techniques to our data sets to obtain the series of plots, Figure 6.4(a)–(u). In these the minimum number of points (pixels or links) averaged together was chosen large enough to minimize the scatter. This number is indicated in parentheses in the legend of each plot. Two phase regression was applied to all the points plotted. The drainage densities determined from using the break point in these figures as a support area to extract channel networks are given in Table 6.2 where they are compared to drainage density estimated from other techniques.

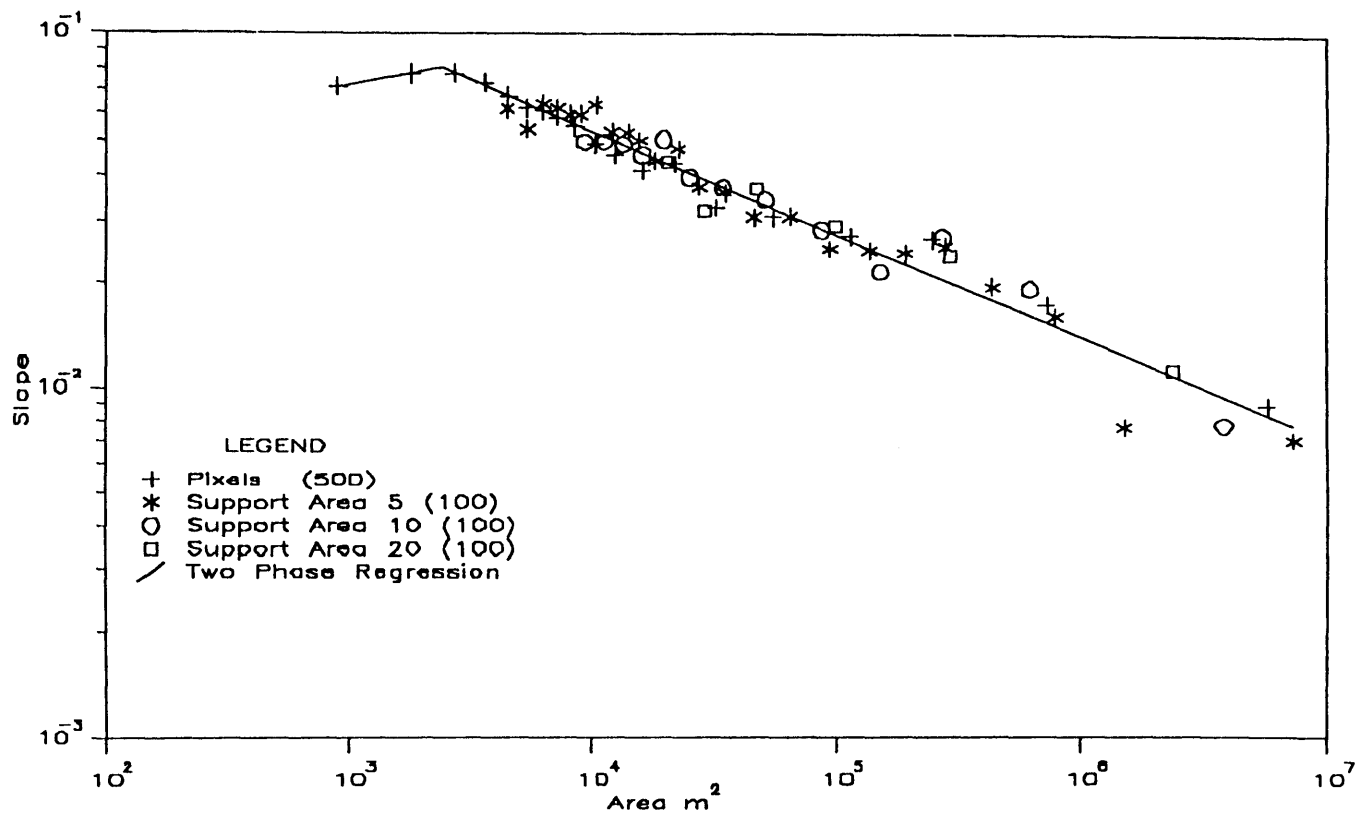


Figure 6.4(a). W15 Slope versus Area and Two Phase Regression Plot.

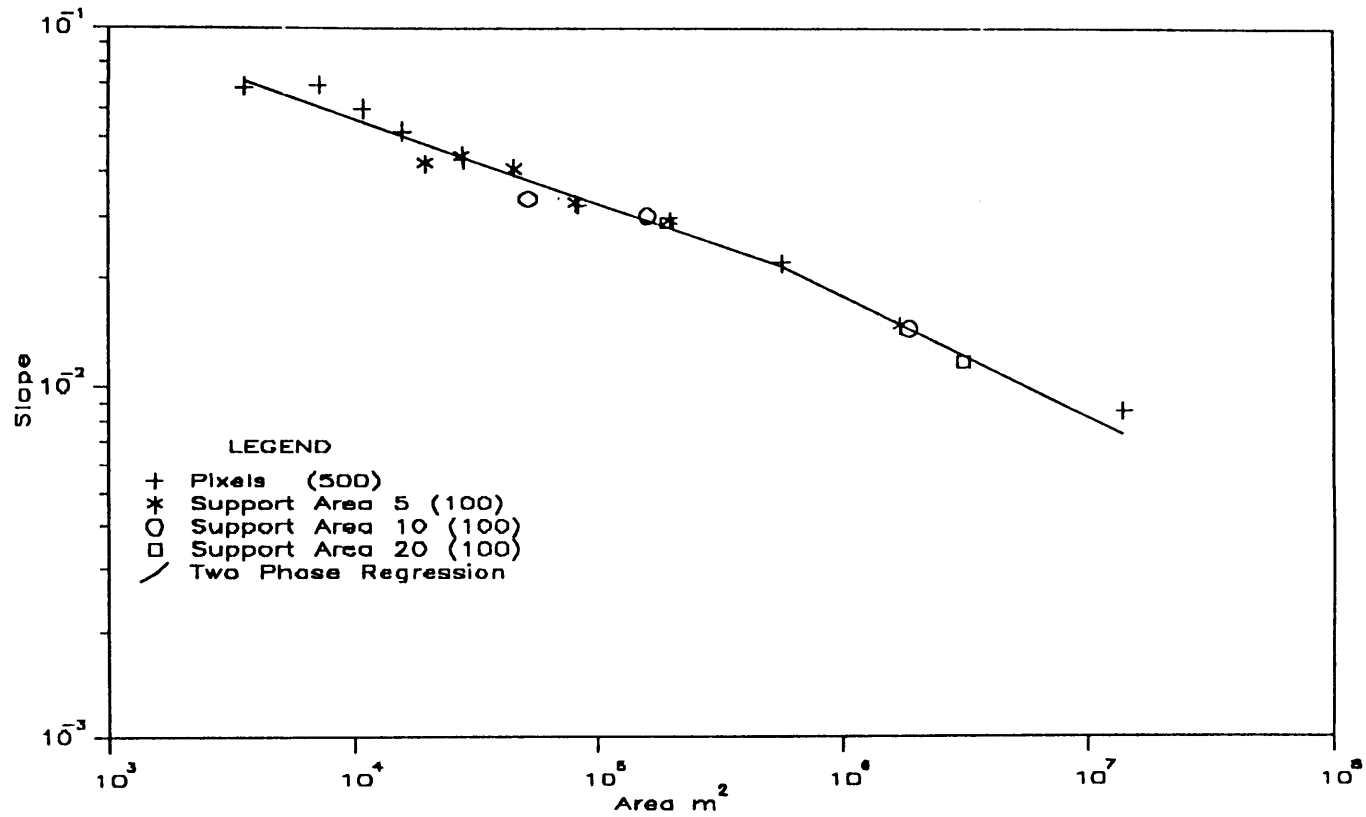


Figure 6.4(b). W15A2S Slope versus Area and Two Phase Regression Plot.

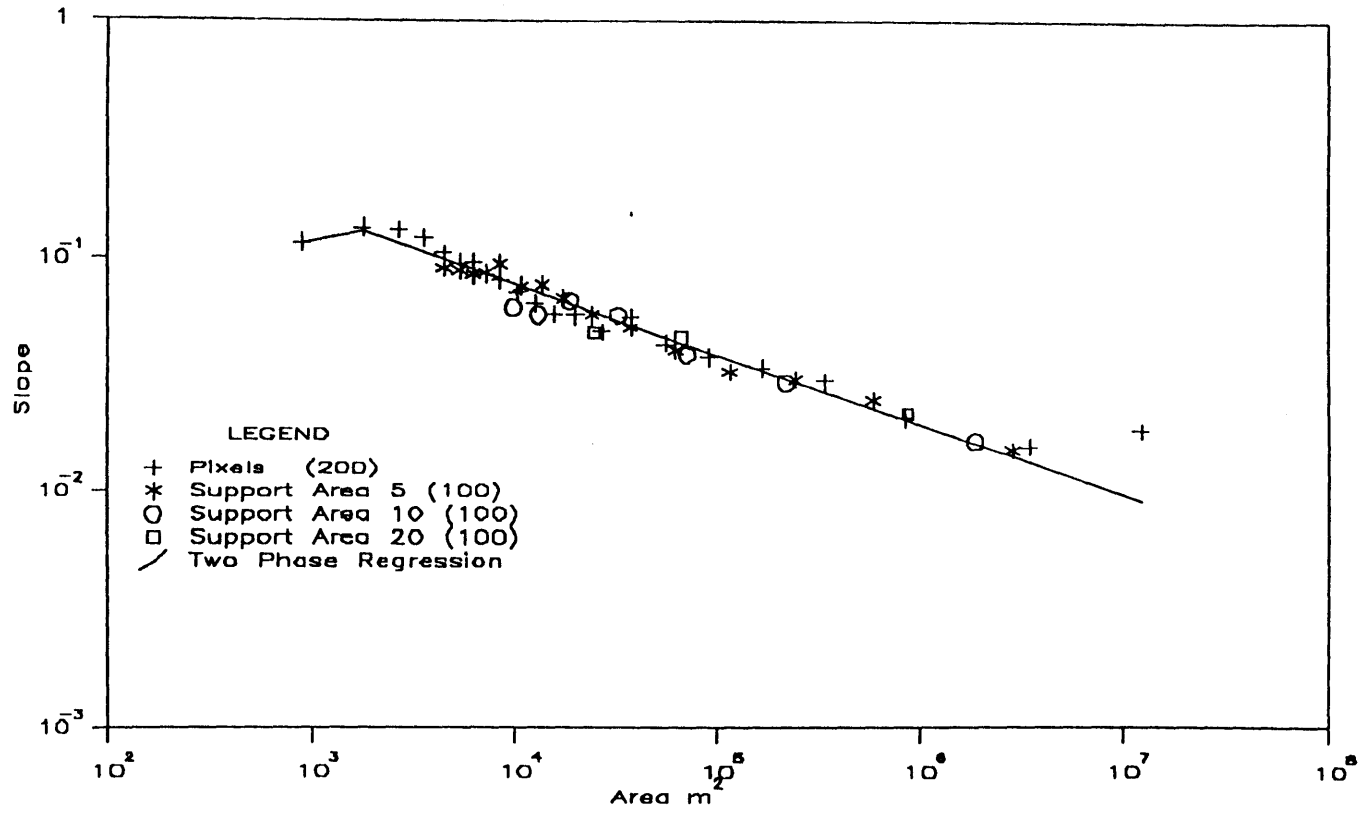


Figure 6.4(c). W7 Slope versus Area and Two Phase Regression Plot.

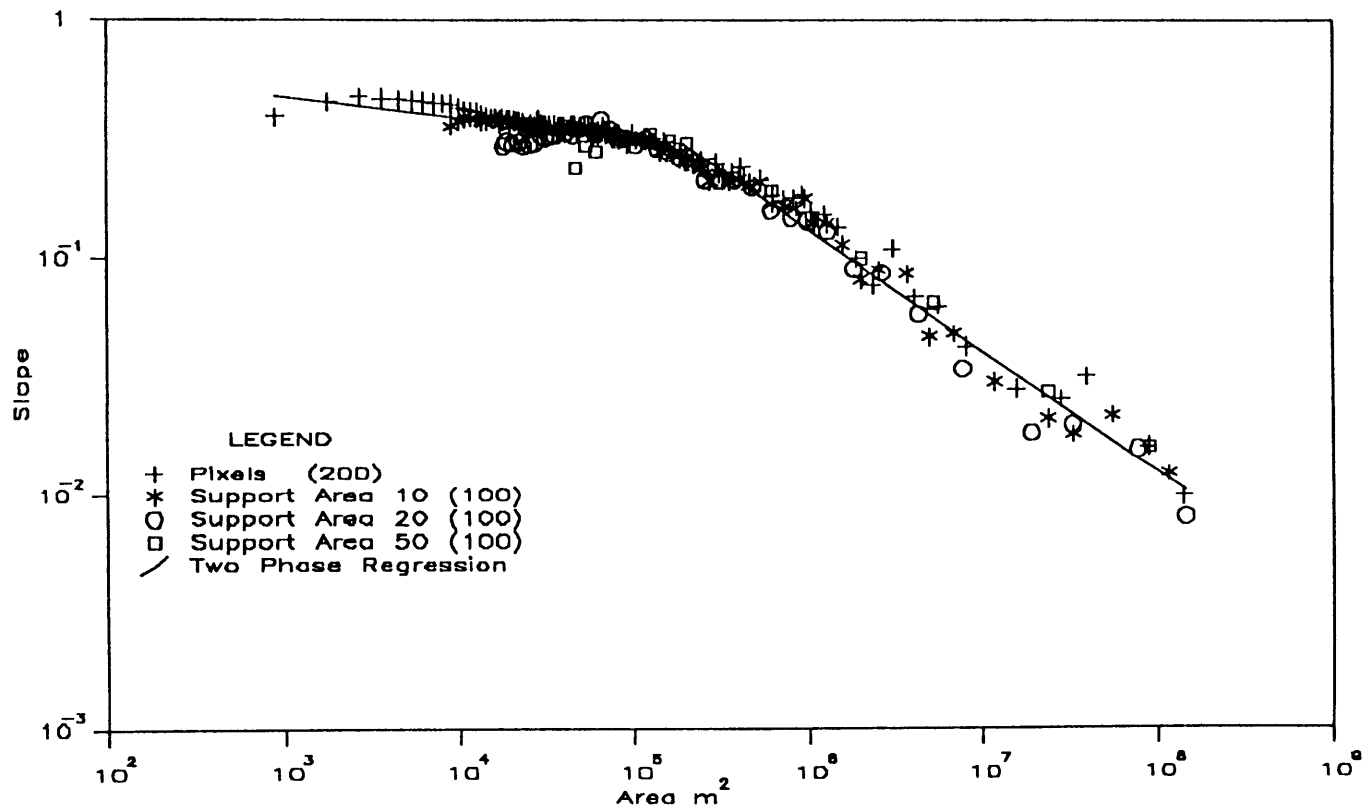


Figure 6.4(d). CALD Slope versus Area and Two Phase Regression Plot.

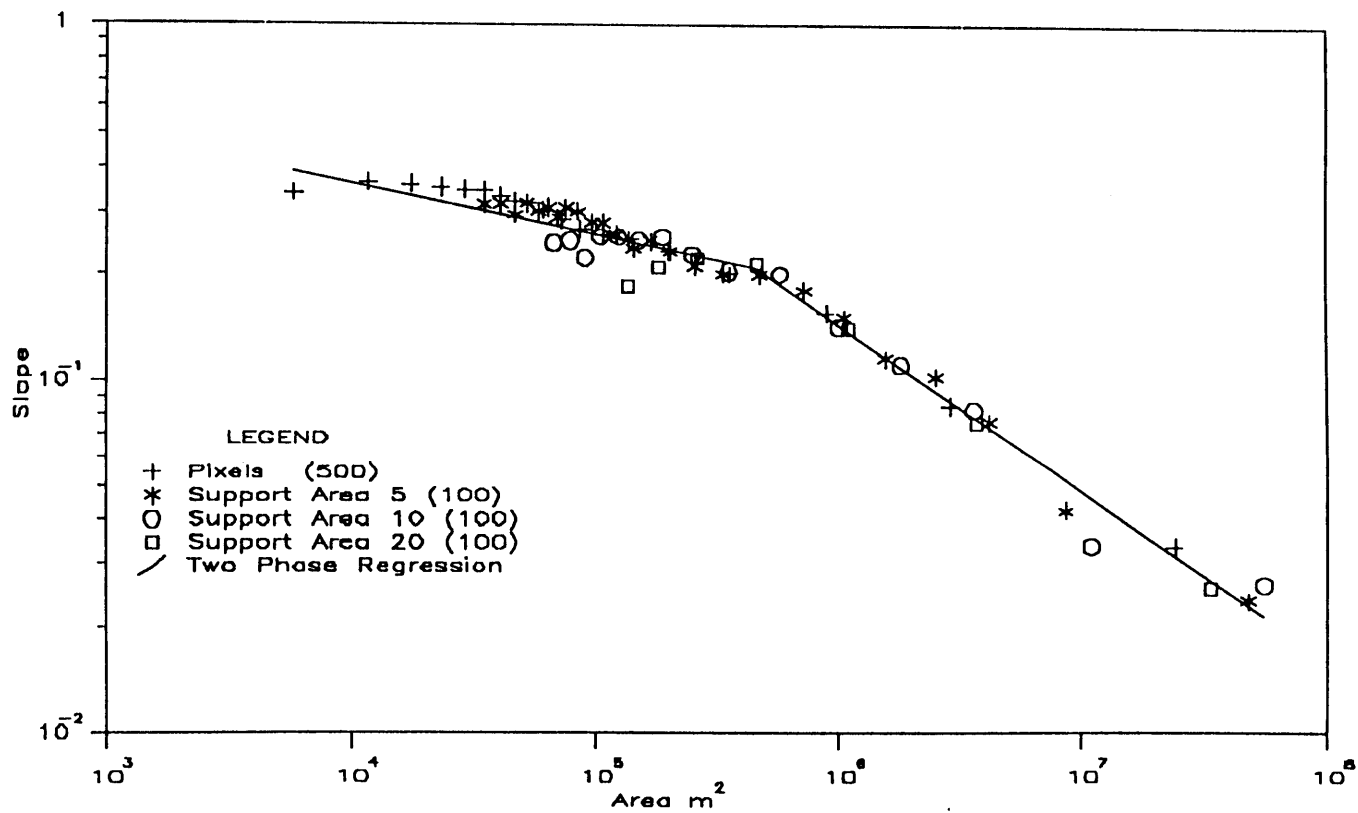


Figure 6.4(e). SPOKBC Slope versus Area and Two Phase Regression Plot.

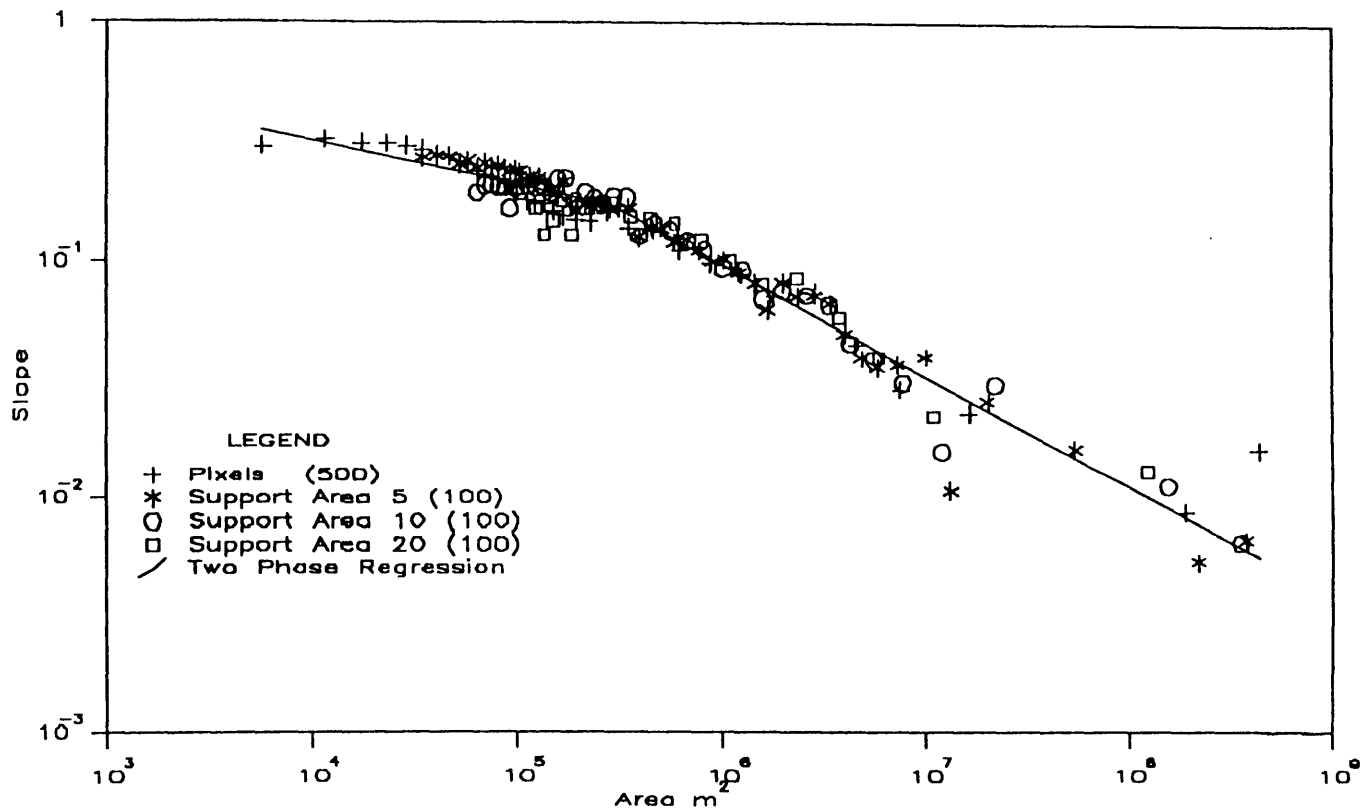


Figure 6.4(f). NELK Slope versus Area and Two Phase Regression Plot.

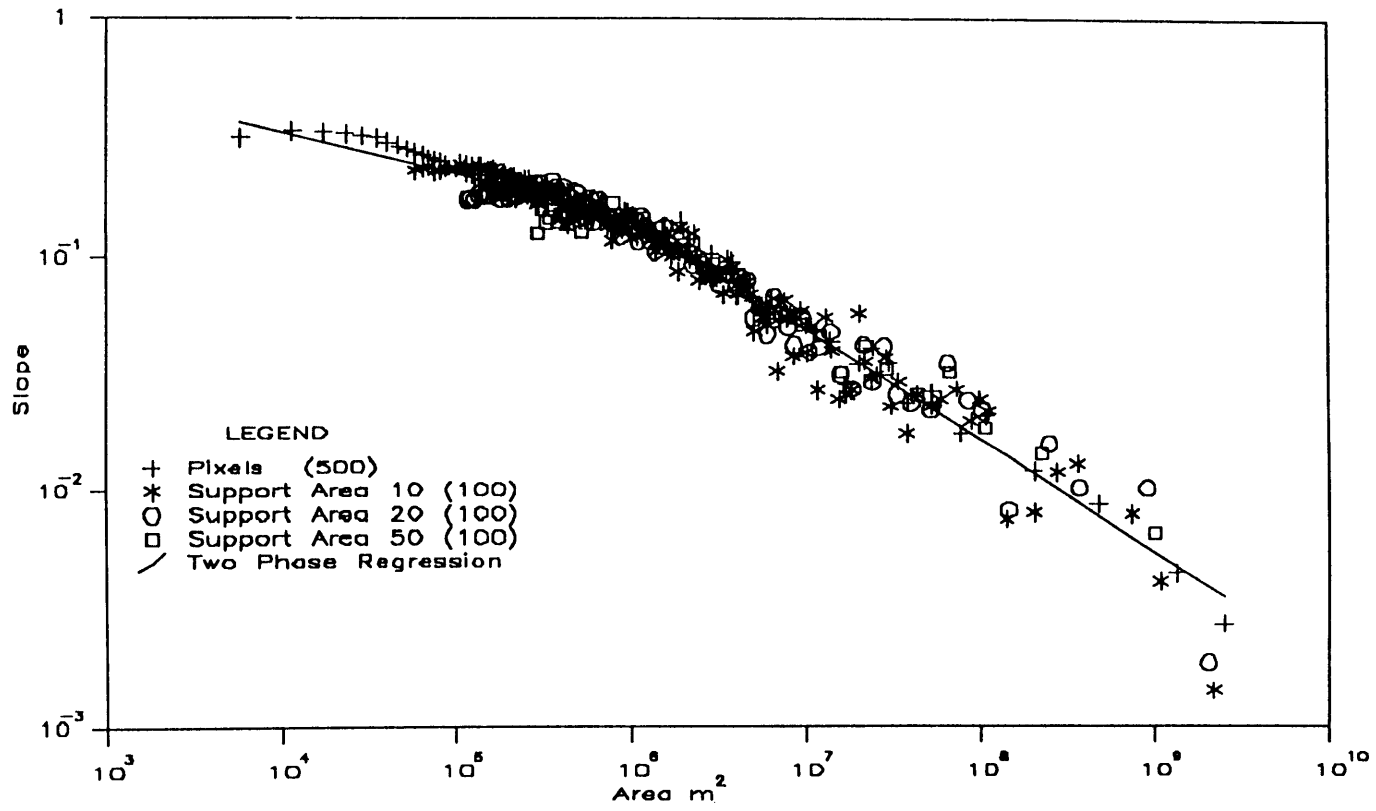


Figure 6.4(g). STJOE Slope versus Area and Two Phase Regression Plot.

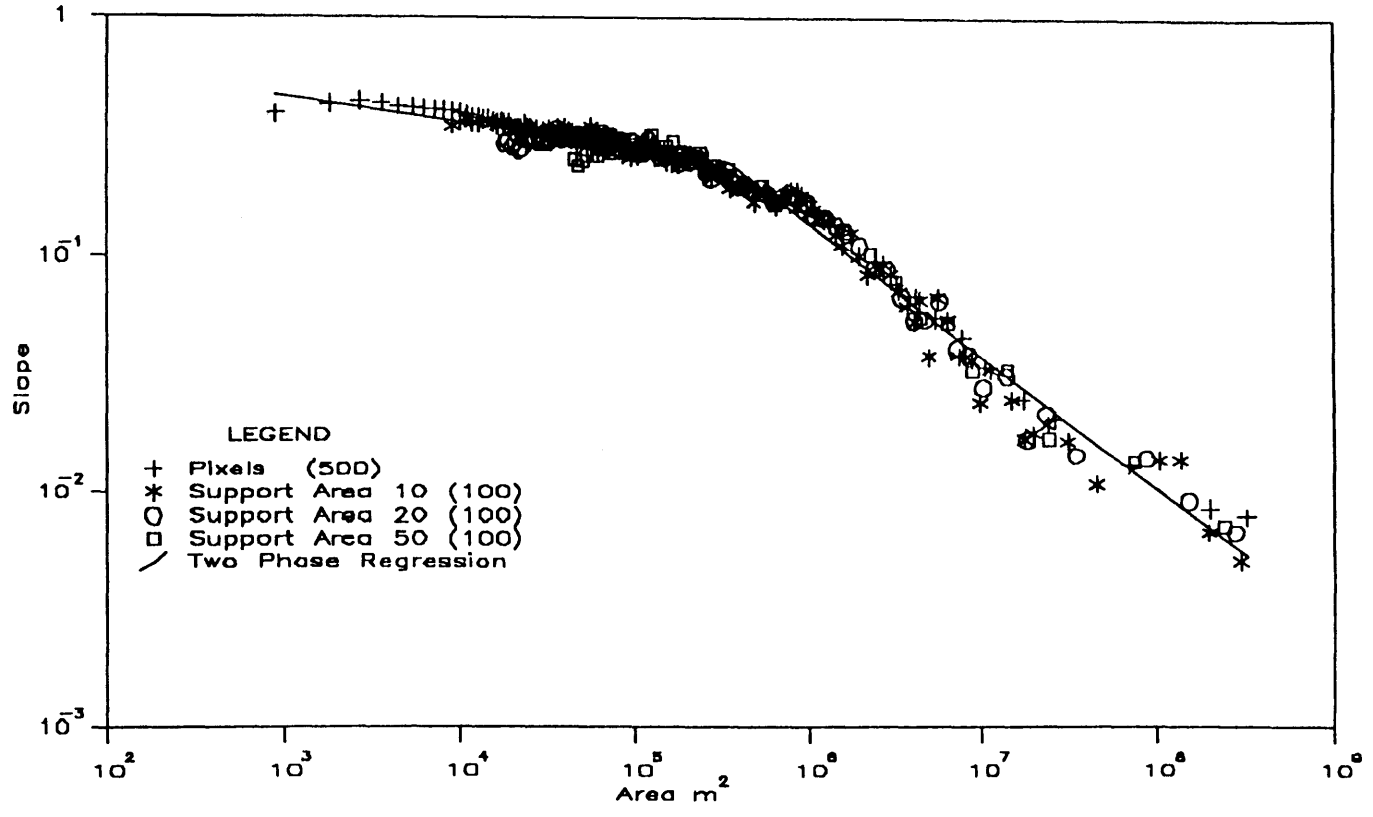


Figure 6.4(h). STJOEUP Slope versus Area and Two Phase Regression Plot.

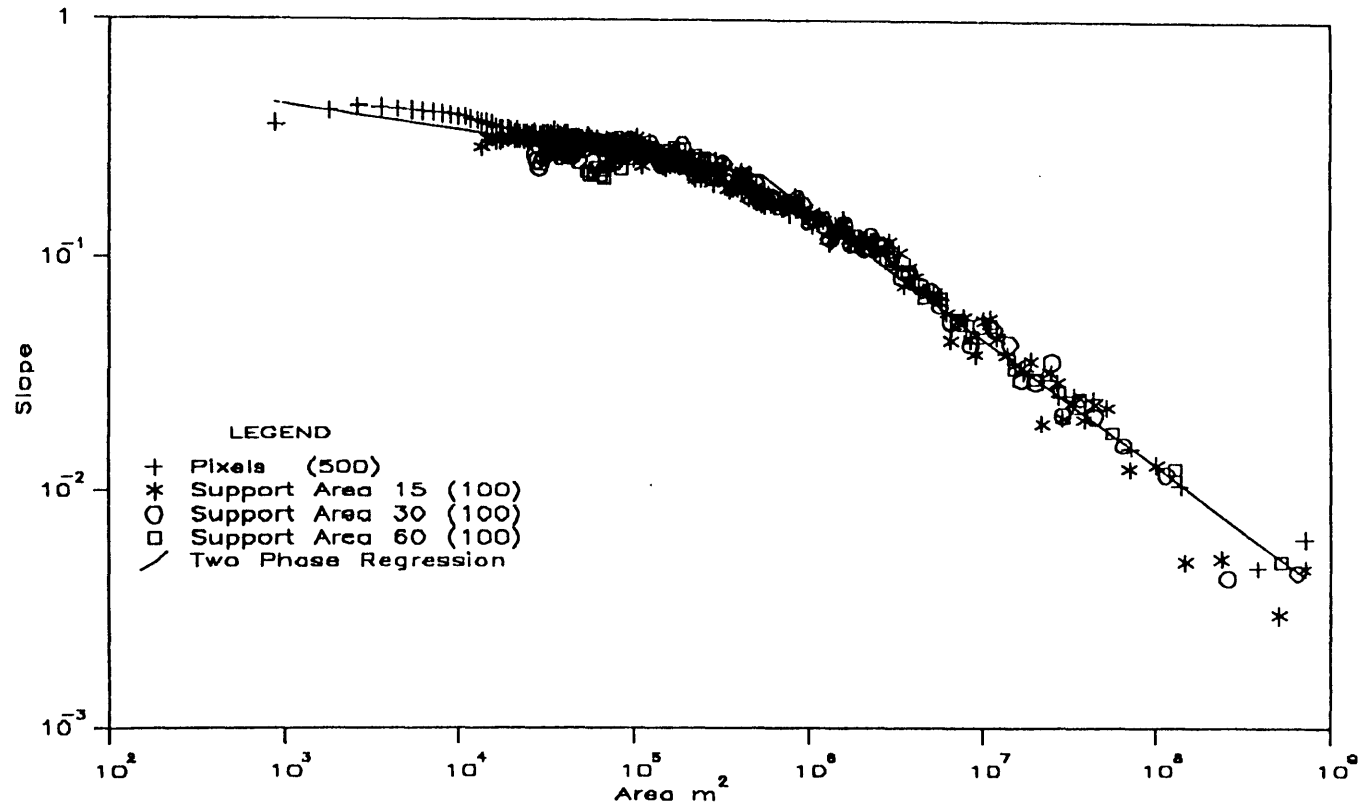


Figure 6.4(i). STREGIS Slope versus Area and Two Phase Regression Plot.

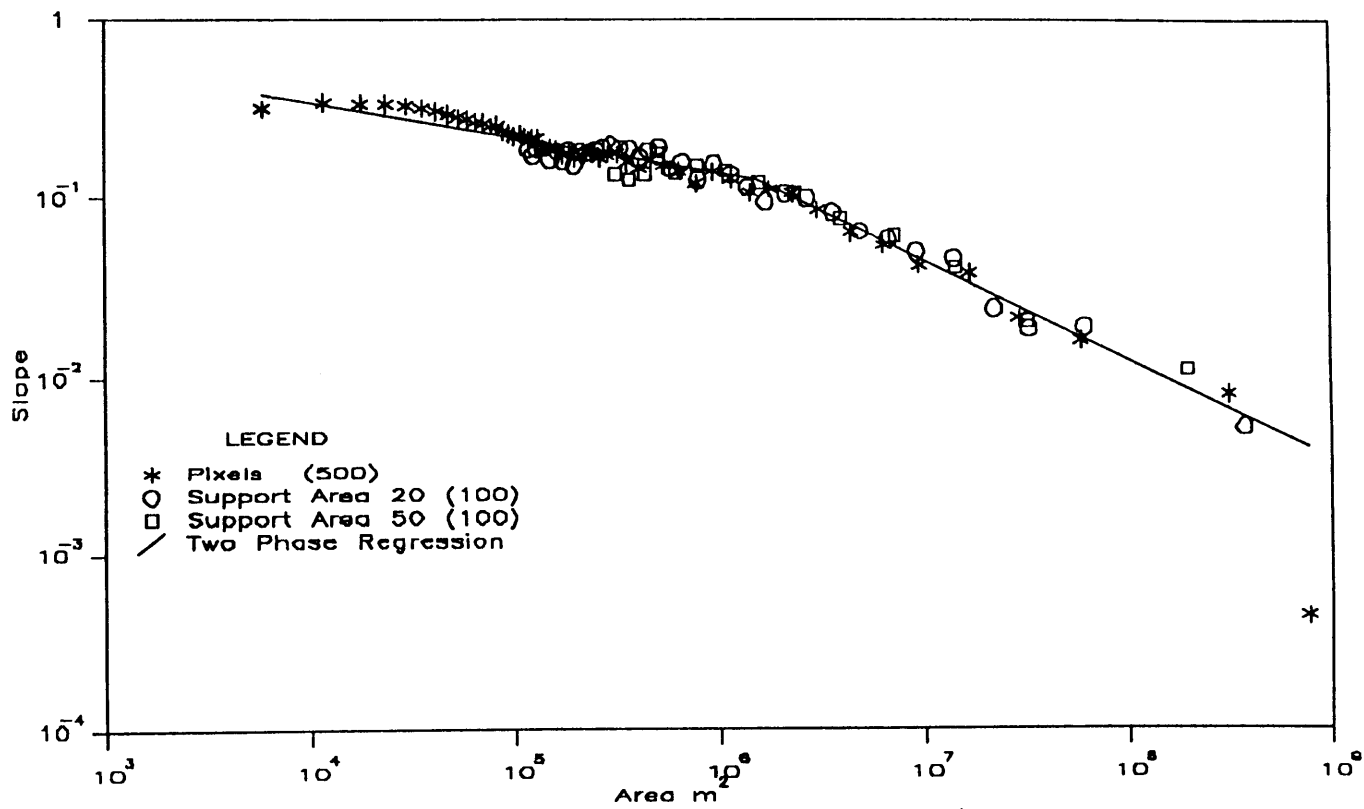


Figure 6.4(j). STREGISDMA Slope versus Area and Two Phase Regression Plot.

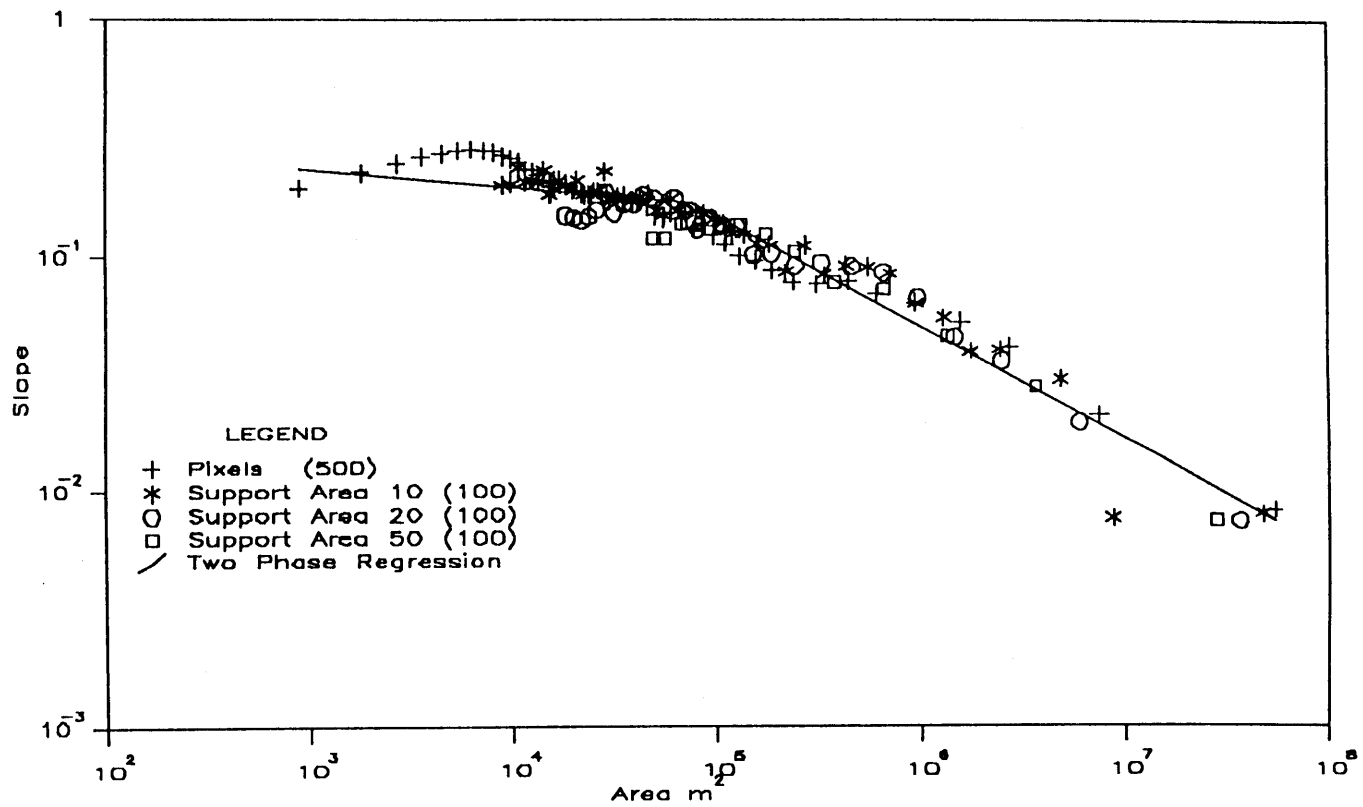


Figure 6.4(k). HAK Slope versus Area and Two Phase Regression Plot.

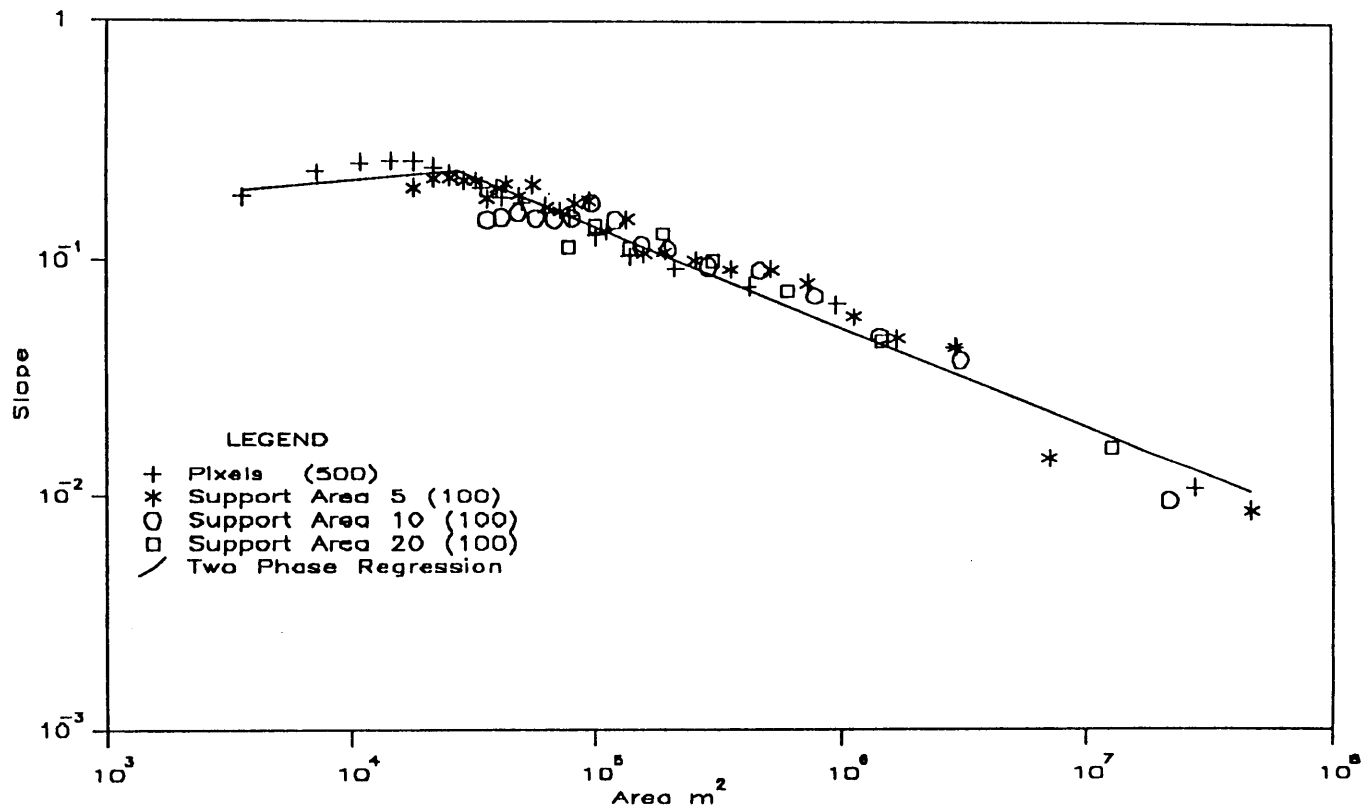


Figure 6.4(l). HAKA2S Slope versus Area and Two Phase Regression Plot.

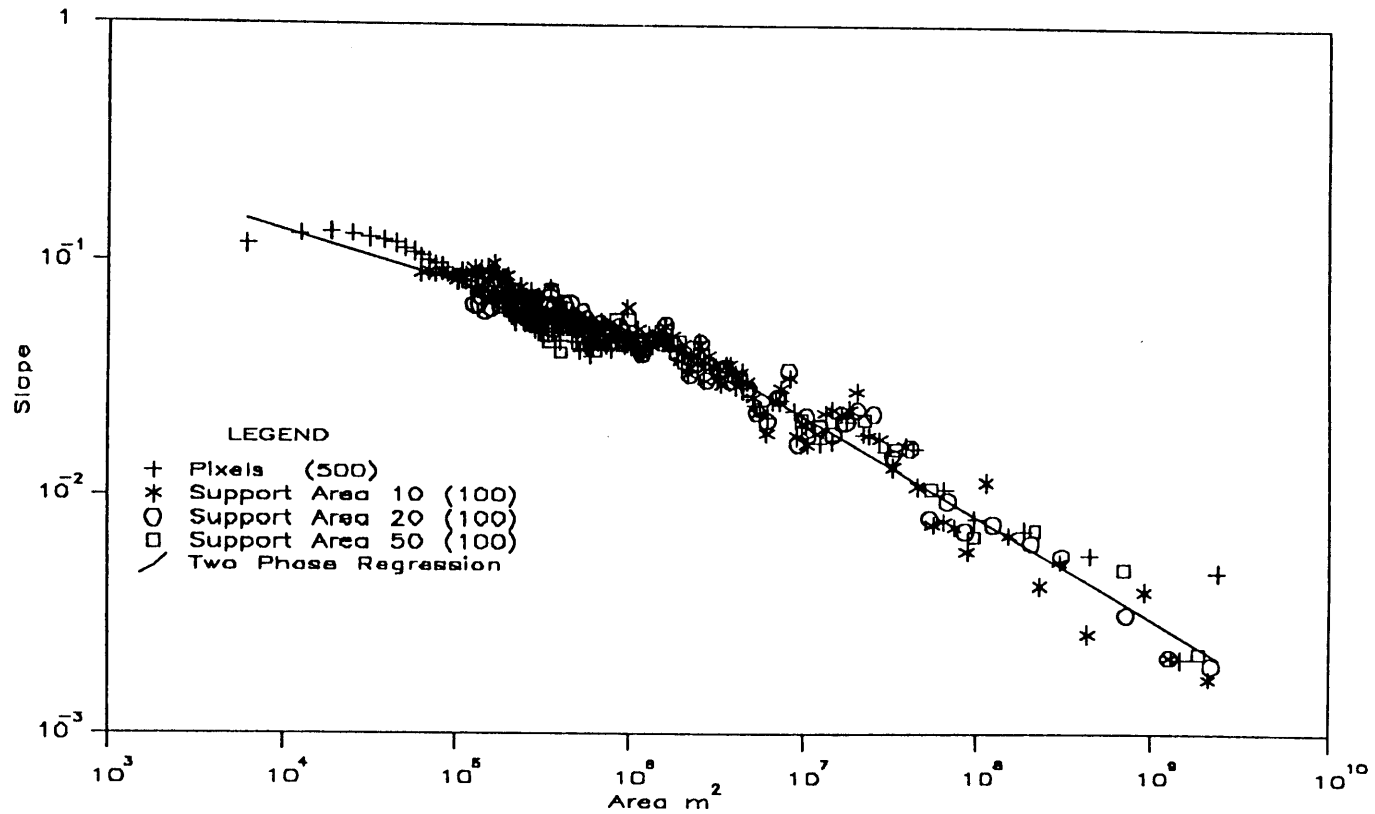


Figure 6.4(m). SCHO Slope versus Area and Two Phase Regression Plot.

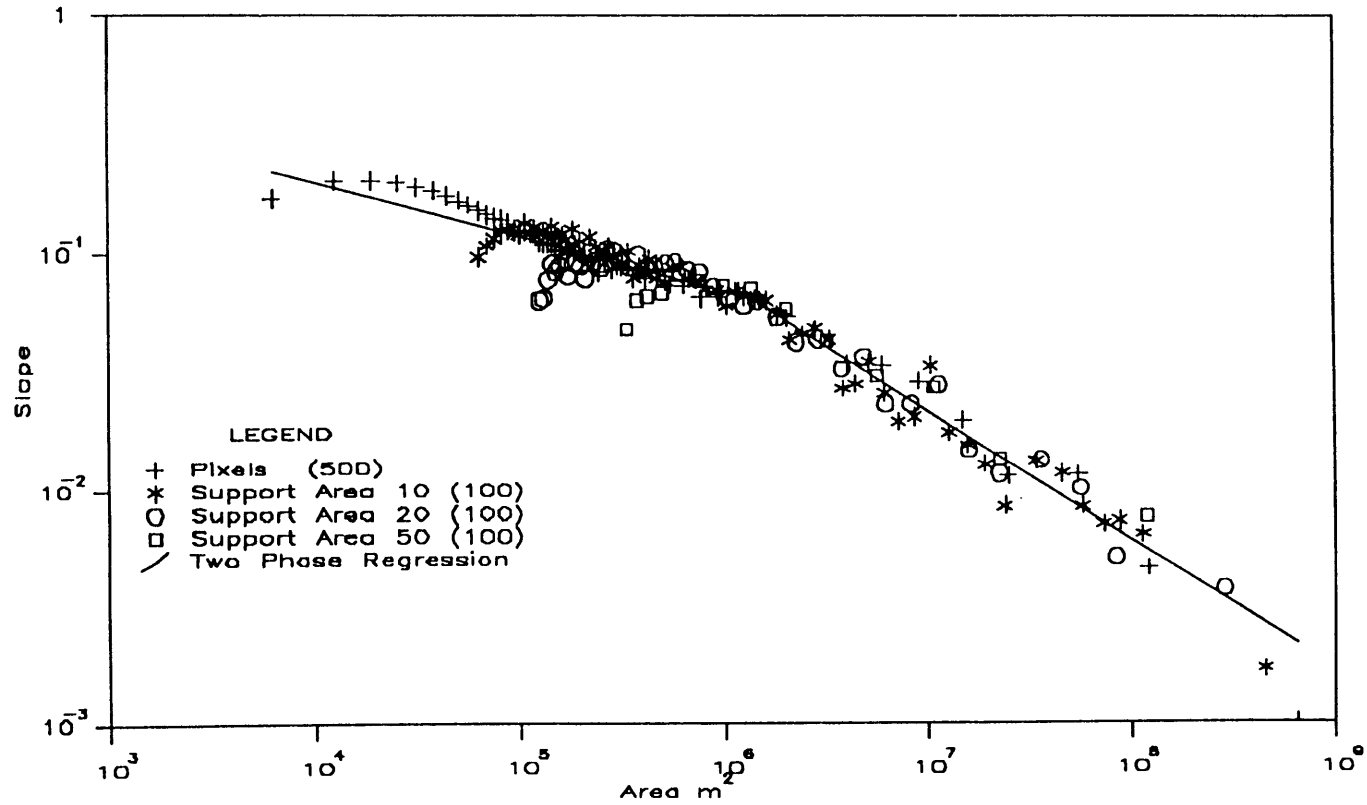


Figure 6.4(n). EDEL Slope versus Area and Two Phase Regression Plot.

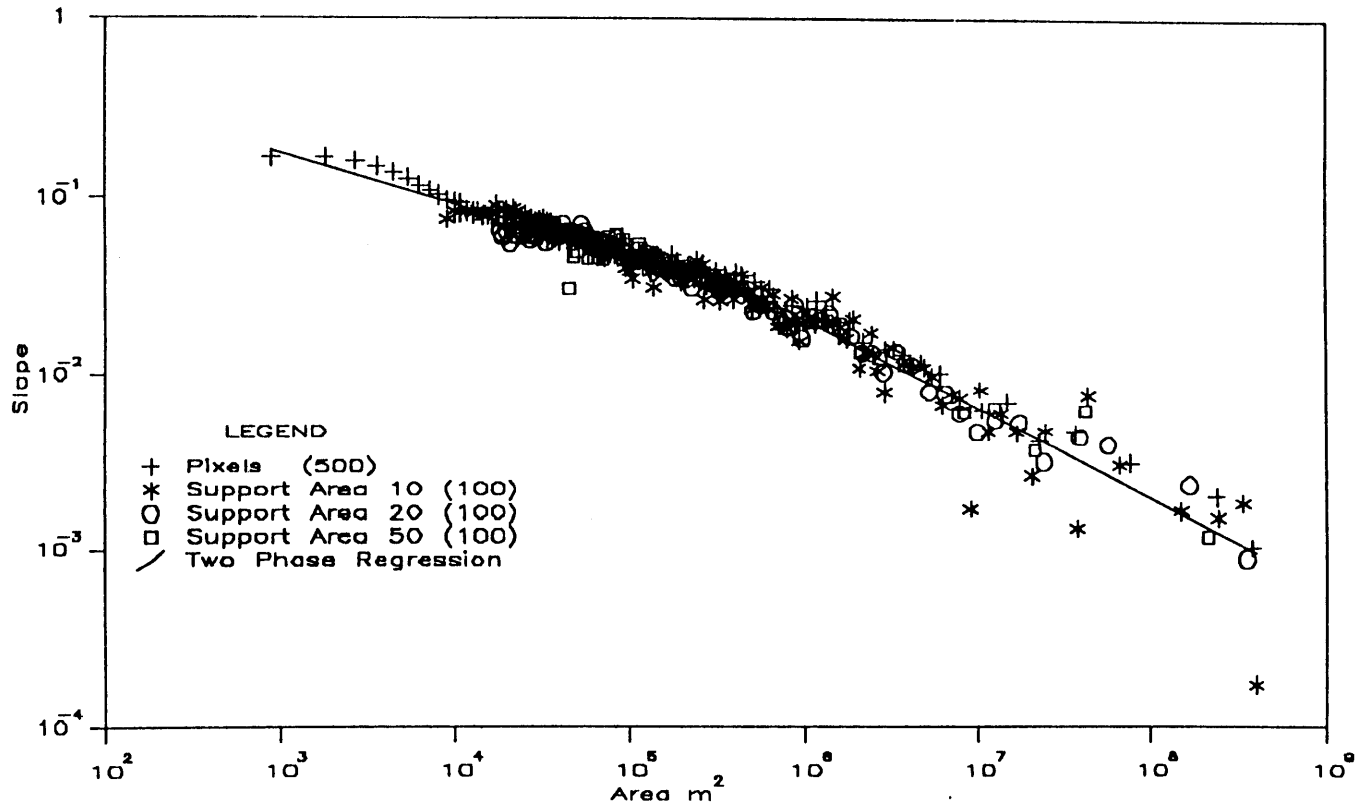


Figure 6.4(o). RACOON Slope versus Area and Two Phase Regression Plot.

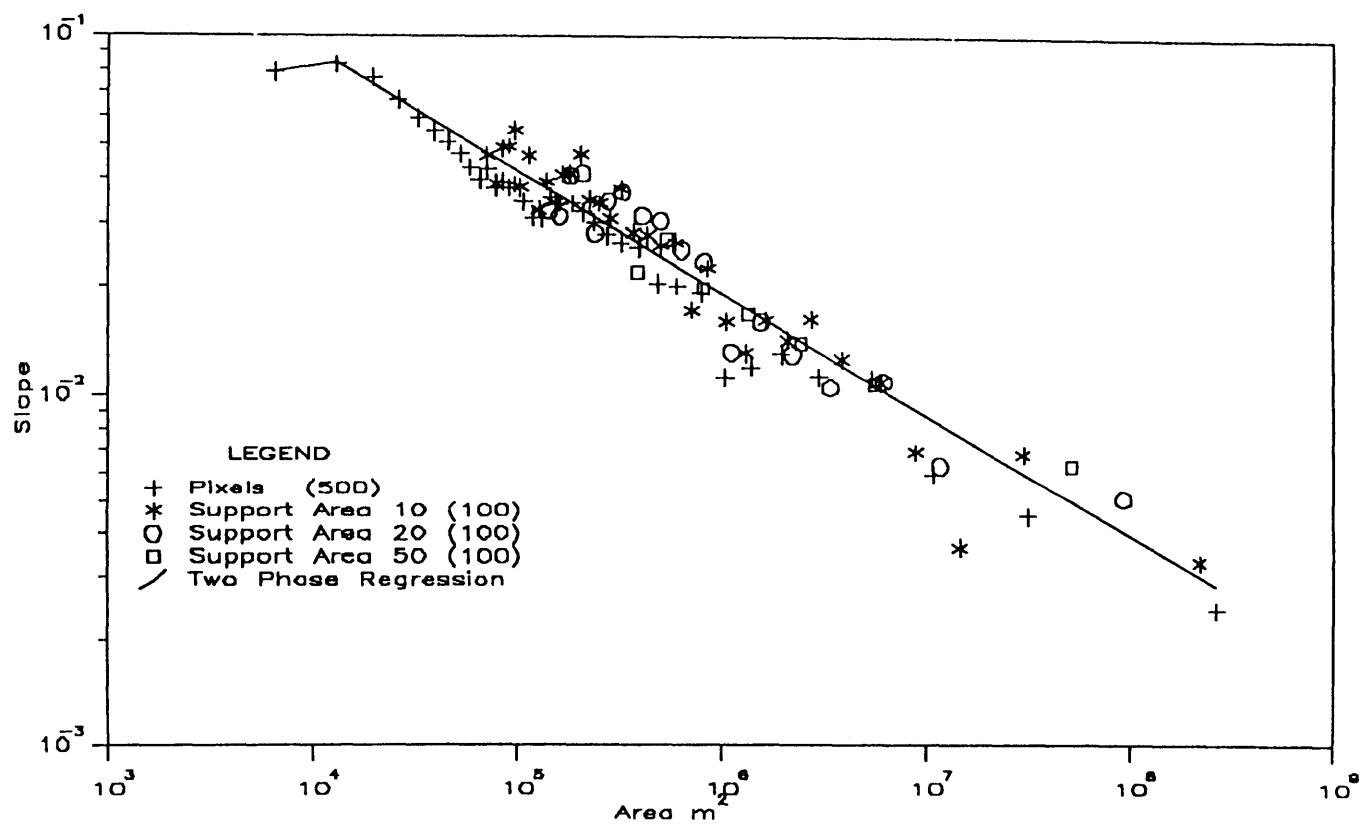


Figure 6.4(p). RACOONDMA Slope versus Area and Two Phase Regression Plot.

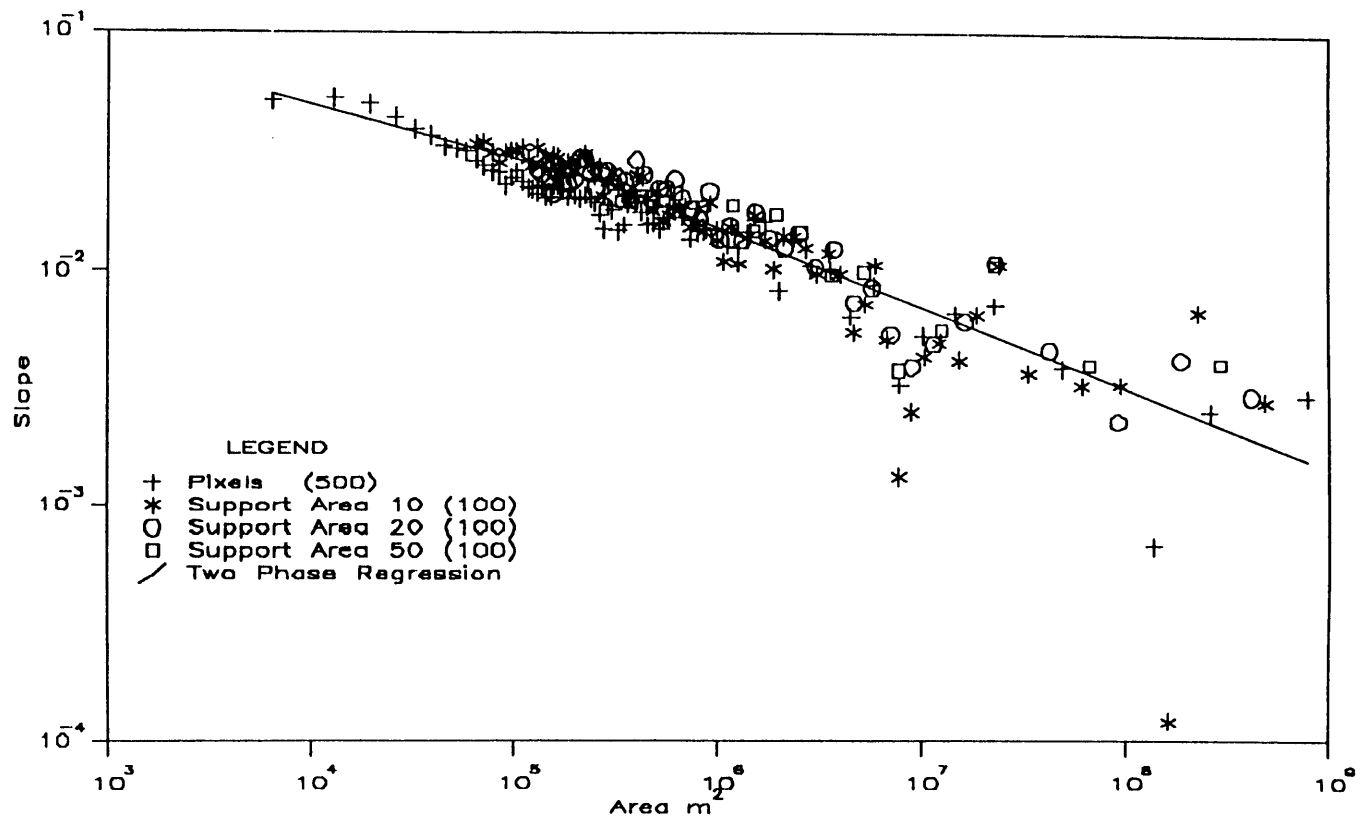


Figure 6.4(q). BEAVER Slope versus Area and Two Phase Regression Plot.

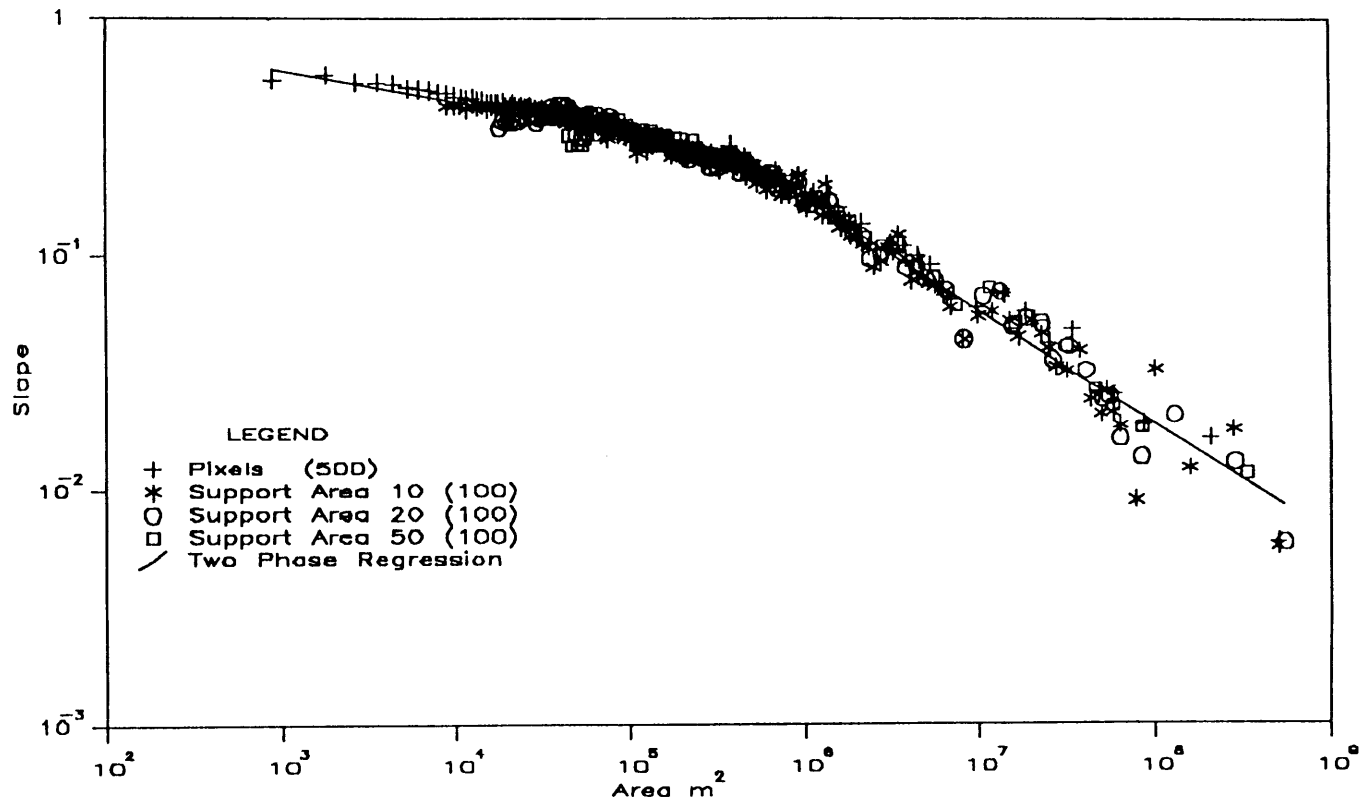


Figure 6.4(r). BUCK Slope versus Area and Two Phase Regression Plot.

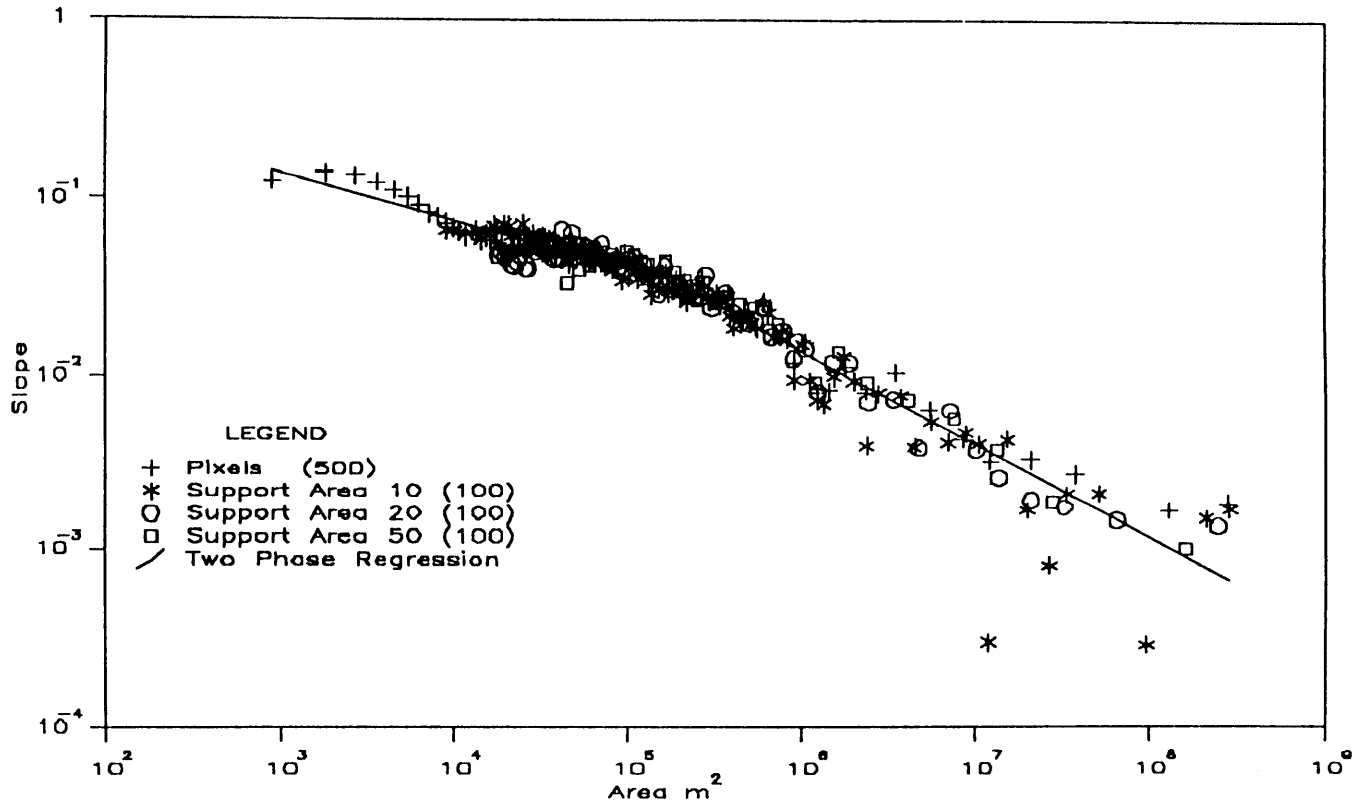


Figure 6.4(s). BRUSHY Slope versus Area and Two Phase Regression Plot.

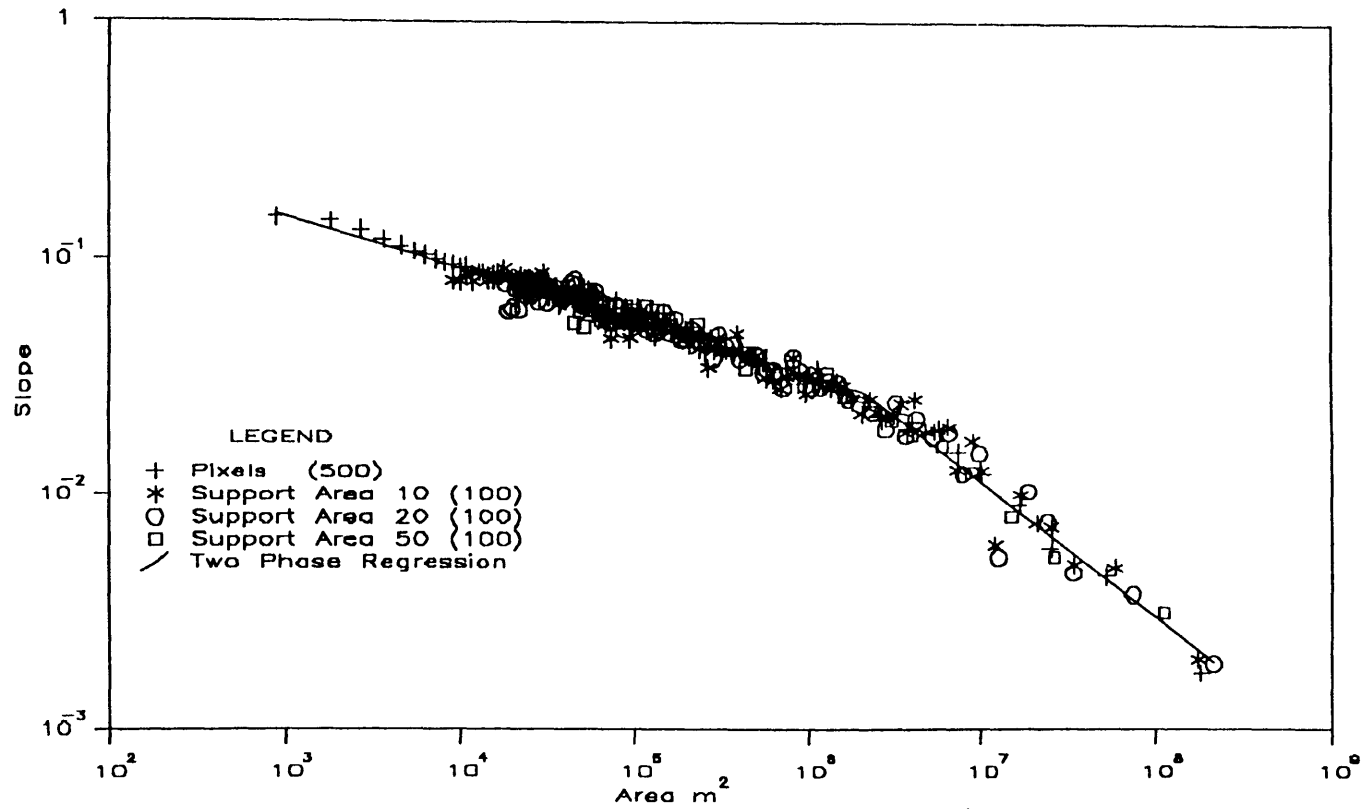


Figure 6.4(t). MOSHANNON Slope versus Area and Two Phase Regression Plot.

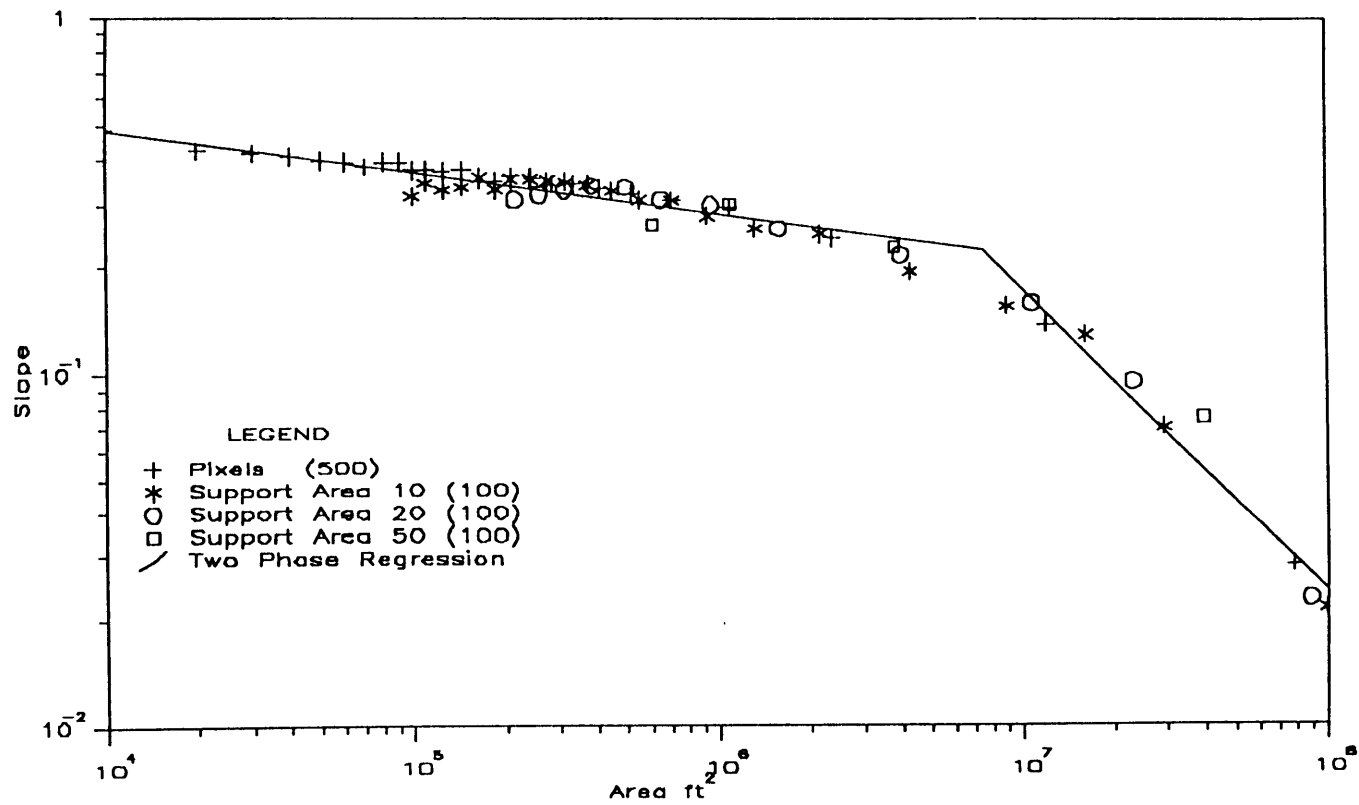


Figure 6.4(u). TVA Slope versus Area and Two Phase Regression Plot.

6.3 The Constant Stream Drop Property

Broscoe (1959) reported that on average the drop in elevation along Strahler streams was approximately constant. Chapter 2 showed how this is basically due to the fact that $R_s \approx R_\ell$ for many networks. Here we use the constant drop property as a test for the break in scaling. This is based on the assumption that the constant drop property, Horton's slope law and the slope area scaling are really manifestations of the same thing and should break at the same scale. The results will show how well this is borne out.

Figure 6.5(a) shows the drops of all 142 streams in the magnitude 107, order 5 network extracted from the W15 data set with support area threshold of 50 pixels. Stream drops are highly variable and we need to test whether the constant drop property is valid in the sense that the mean drop is independent of stream order. The t statistic for the comparison of means of different populations (Beyer, 1984) is used to compare the mean drop for streams of different order.

$$t = \frac{\bar{x} - \bar{y}}{\sqrt{\frac{(n_x - 1) S_x^2 + (n_y - 1) S_y^2}{n_x + n_y - 2} \left(\frac{1}{n_x} + \frac{1}{n_y} \right)}} \quad (6.9)$$

where \bar{x} and \bar{y} are the sample means, S_x^2 and S_y^2 the sample variance, and n_x and n_y the sample sizes of the two populations x and y . The t for the difference between successive orders is given in Figure 6.5(a). The fact that $|t|$ is not larger than 2 indicates that the null hypothesis of no difference the means cannot be rejected at the 95% confidence level. This is also seen graphically in terms of 95% confidence limits on the sample mean assuming it is t distributed. A horizontal line that passes through all the error bars could be drawn, indicating constant mean drop that is not significantly different from the sample mean drops at any

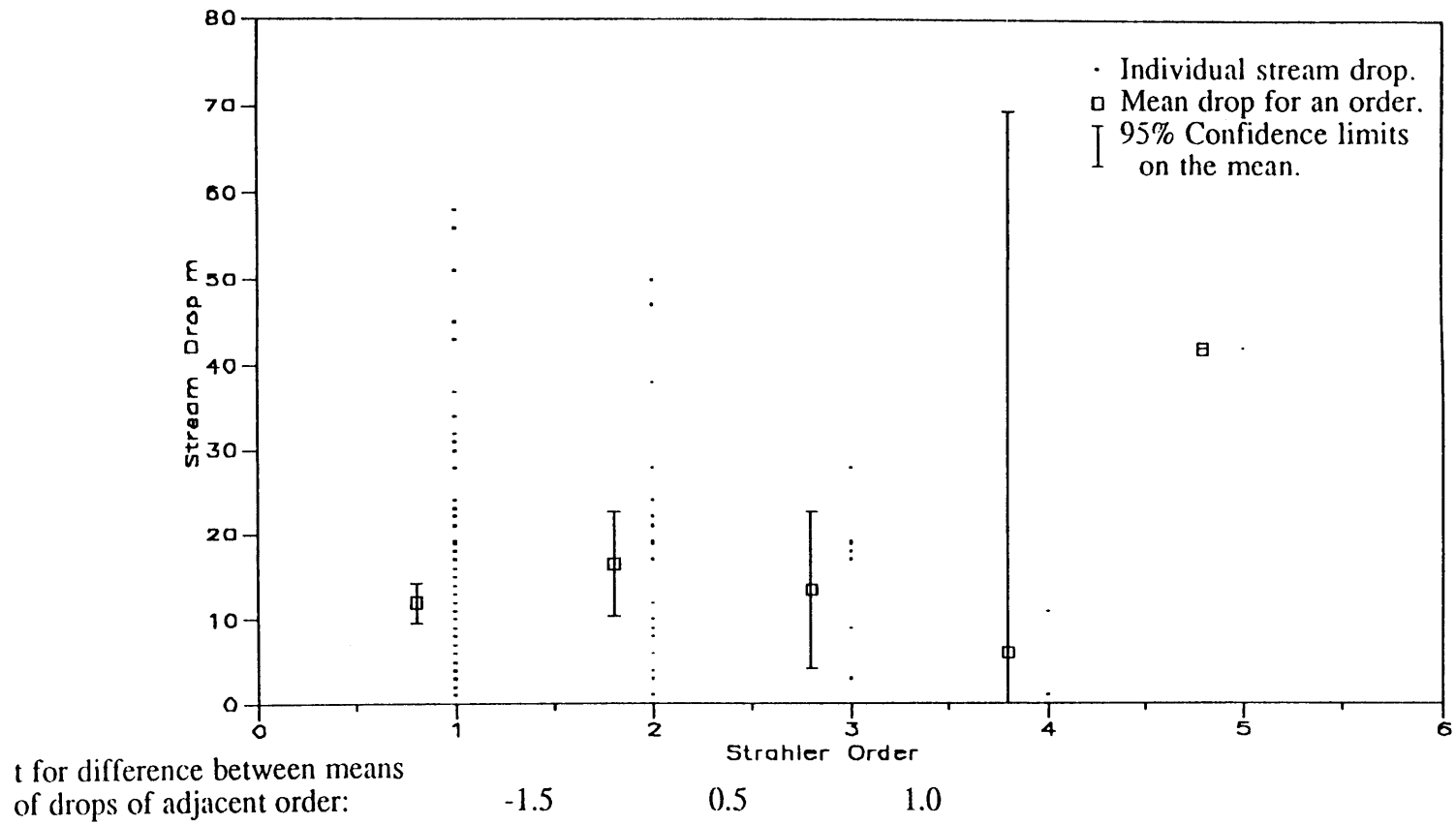


Figure 6.5(a). Stream drops in W15 network extracted using a support area of 50 pixels.

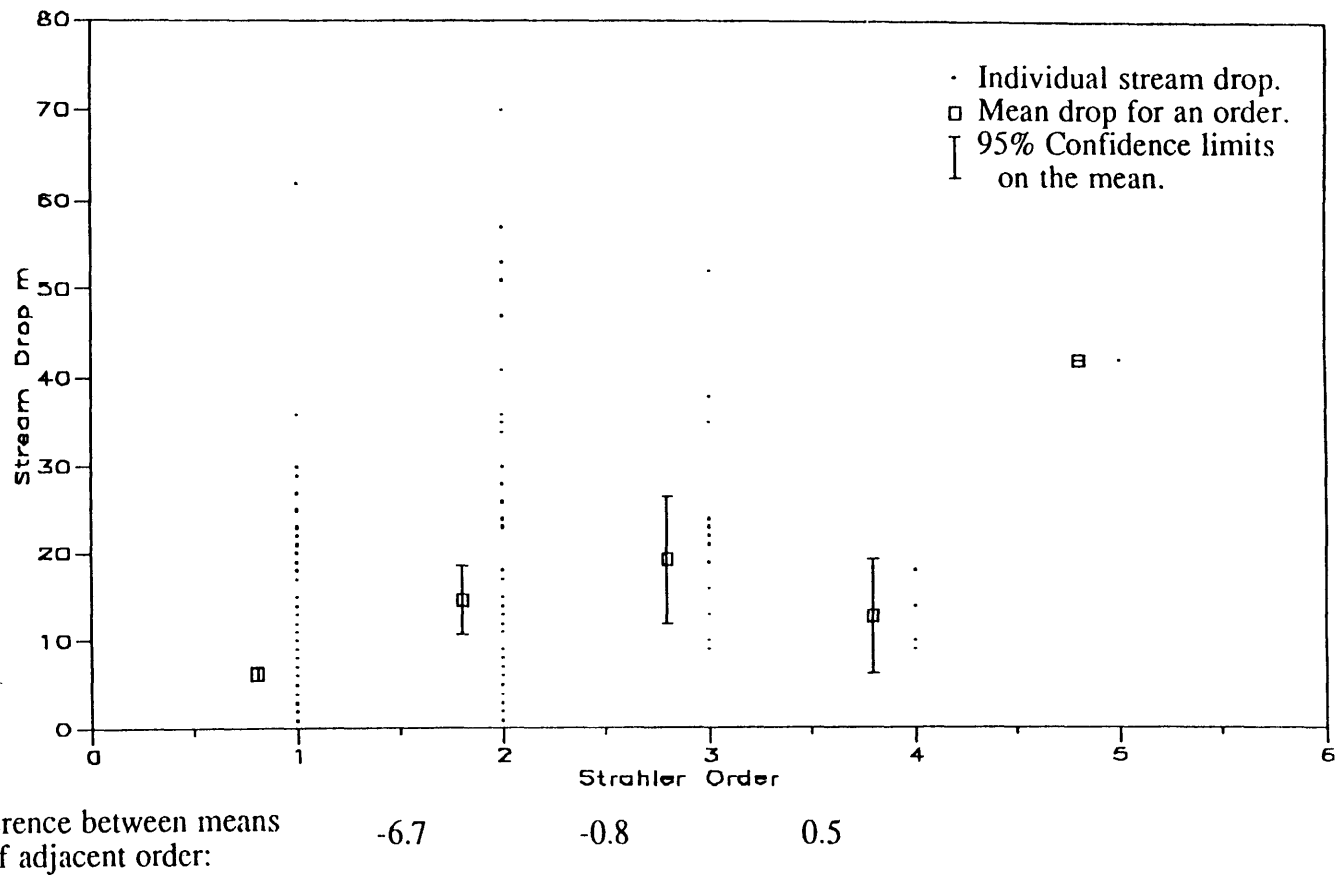


Figure 6.5(b). Stream drops in W15 network extracted using a support area of 20 pixels.

order. This is not always the case. Figure 6.5(b) gives the case where a support area of 20 pixels has been used to define channel networks in the W15 catchment. Notice that the mean drop of first order streams is significantly less than the other mean drops. According to the t statistics, the break in scaling occurs between support areas of 20 and 50 pixels.

Dramatic evidence of the break in scaling is given by considering the stream drop probability distribution. This is done in Figure 6.6 for the W15 basin. Exceedance probabilities are calculated using the Weibull plotting position

$$P = \frac{i}{N + 1} \quad (6.10)$$

where i is the ranking from smallest to largest and N is the number of streams in the sample, are plotted. 95% confidence limits computed from the beta distribution are shown. We see that the distribution of first order drops in the support area 20 network stands out from the other distributions which are all intermingled. This corroborates the difference between first order drops at support area 20, and other stream drops. Straight line fits on this semi log plot suggest the exponential distribution as a good model for stream drops, and that Strahler streams of different order have practically the same probability distribution above the point where scaling behavior breaks. This data justifies the assertion in Chapter 5 that the distribution of stream drops is the same for all Strahler streams.

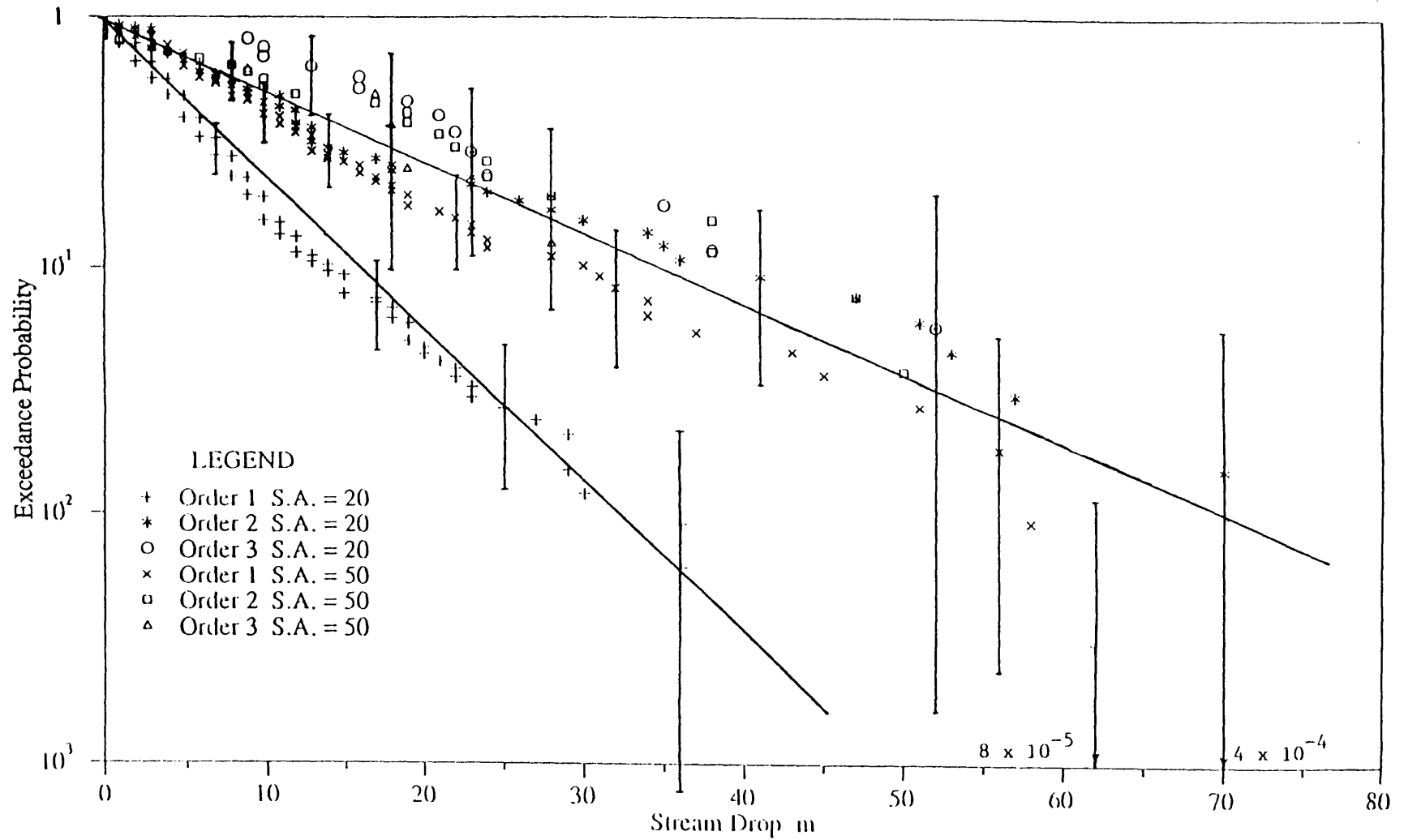
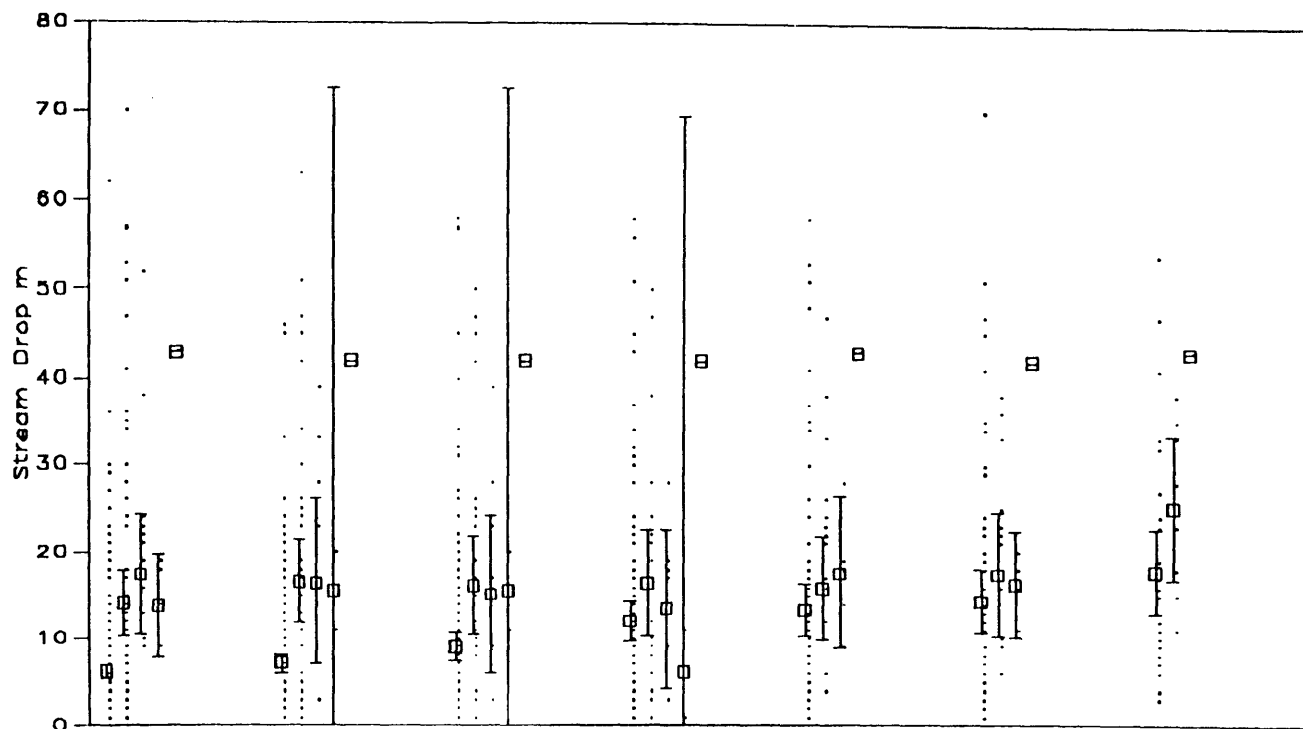


Figure 6.6. Stream Drop distributions for the W15 network. S.A. in the legend denotes Support area. Error bars are 95% confidence limits using the Beta Distribution.

Tests for the break in scaling using the constant drop property can be done graphically with several plots like Figure 6.5(a) and (b) compressed into one plot. Figures 6.7(a)–(u) give these for all the basins analyzed. For each support area the stream drops, mean drop and 95% confidence limits of the mean are plotted against order. Within each grouping order increases from left to right. Statistics, including the t statistic for the difference between mean first order stream drop and higher order stream drops are printed below the figures. There is a common pattern apparent in most of these figures. To the left (small support area) of a limit or threshold support area, the constant drop property fails whereas to the right (large support area), the constant drop property holds. This limit, the smallest support area for which the constant drop property is not rejected, gives another measure of the basic horizontal length scale in the landscape, measured in terms of support area or drainage density. The basic scale obtained from these figures is listed in Table 6.2 for comparison with data from other procedures.

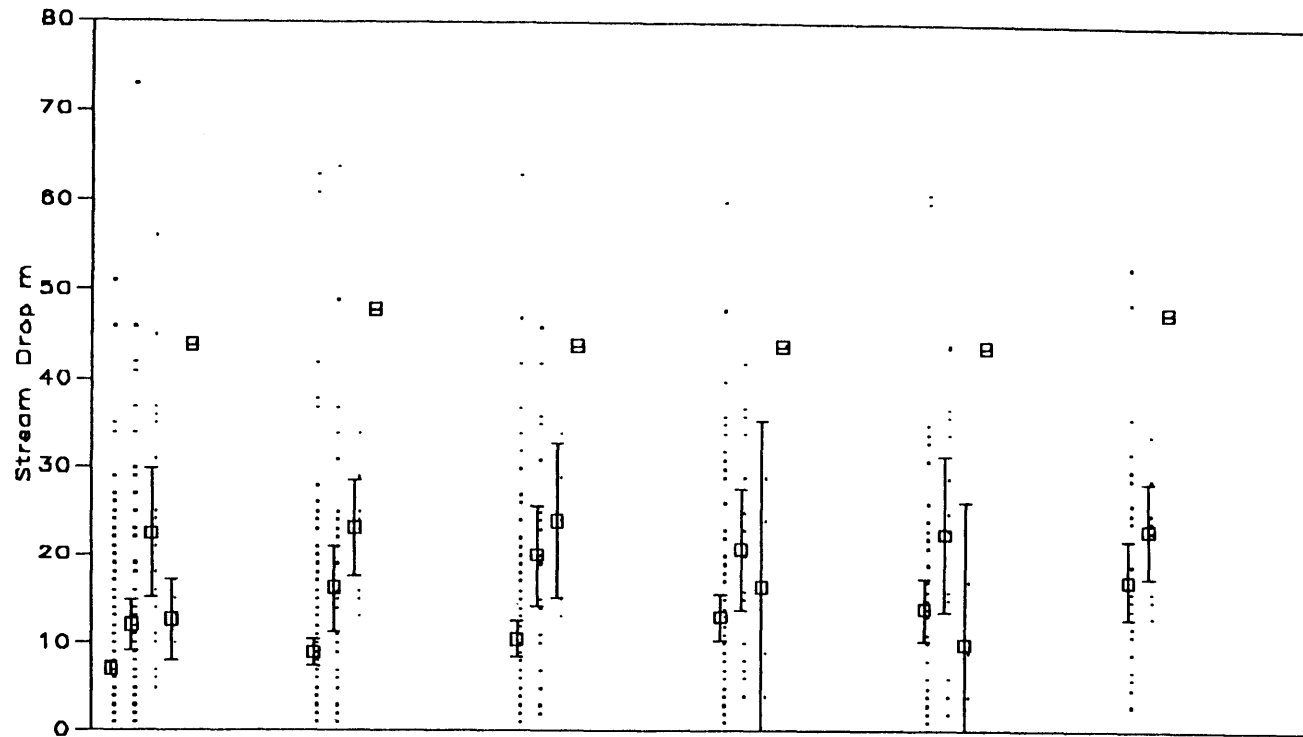
Since the constant drop property is basically equivalent to $R_s \approx R_\ell \approx 2$, it corresponds to slope–area scaling with $\theta = 0.5$. The test for the break in the constant drop property is really a test for deviation from $\theta = 0.5$ and is therefore slightly different from the two–phase regression which tests for any break in the slope versus area functions. Nevertheless, as will be discussed in Section 6.5, results from the two procedures agree fairly well.

The outcome of the constant drop analysis is basically two length scales. The horizontal length scale ($1/D_d$) and vertical length scale, mean stream drop H . The ratio of these HD_d gives a form of ruggedness number (see Strahler, 1964), which is a dimensionless number that characterizes the steepness of the channel network. We could speculate that it is related to climate, tectonic uplift, etc. Table 6.2 includes HD_d data for the basins we analyzed.



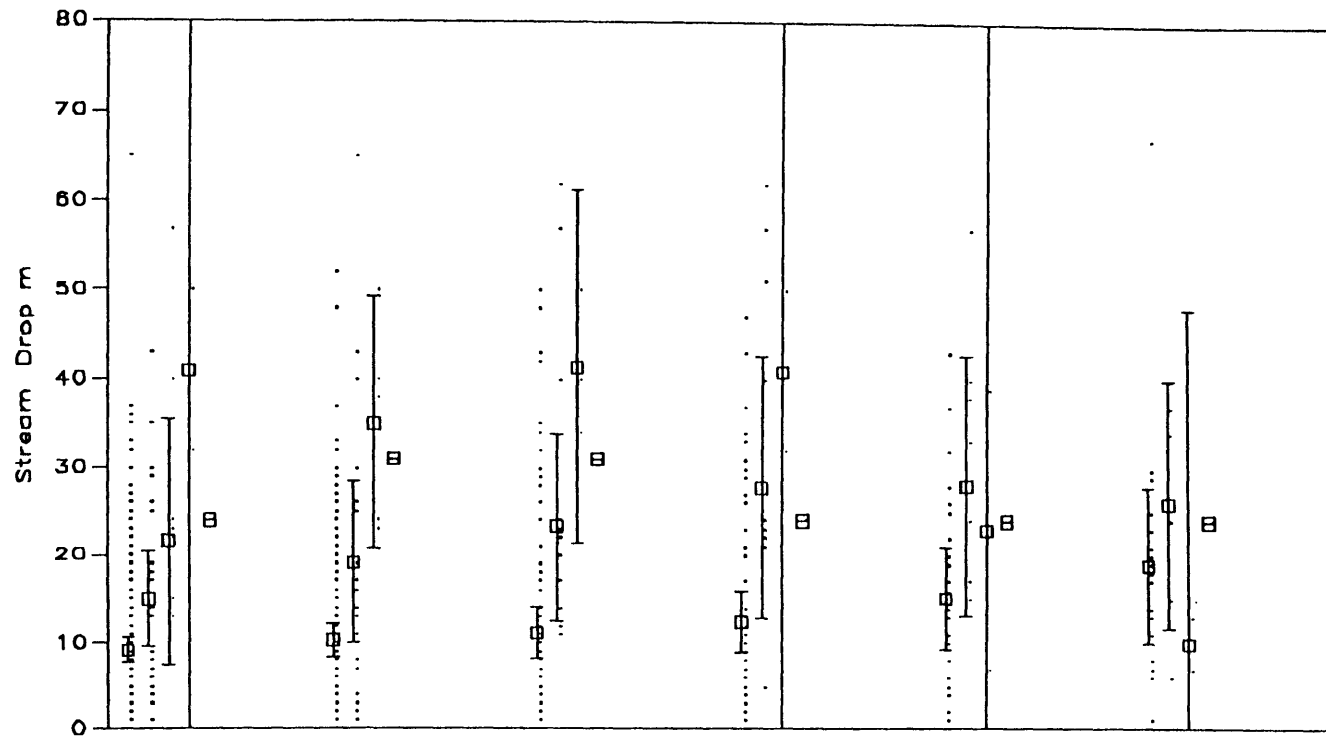
Support Area	20	30	40	50	70	100	200
Drainage Density (km^{-1})	5.2	4.2	3.7	3.4	3.0	2.7	2.0
Magnitude	331	203	147	107	80	64	34
t	8.2	6.7	3.8	1.6	1.3	1.1	1.8

Figure 6.7(a) W15 Stream drops variation with order and support area



Support Area	5	10	15	20	30	50
Drainage Density (km^{-1})	5.5	3.7	3.1	2.7	2.2	1.8
Magnitude	394	163	115	81	57	33
t	6.8	5.1	4.8	2.7	2.0	1.9

Figure 6.7(b) W15A2S (i.e. 2 x 2 pixel average DEM dataset) Stream drops variation with order and support area.



Support Area	20	30	50	70	100	150
Drainage Density (km^{-1})	4.8	4.1	3.2	2.9	2.5	2.1
Magnitude	174	119	71	52	36	23
t	4.4	4.5	4.3	3.9	1.9	0.5

Figure 6.7(c) W7 Stream drops variation with order and support area.

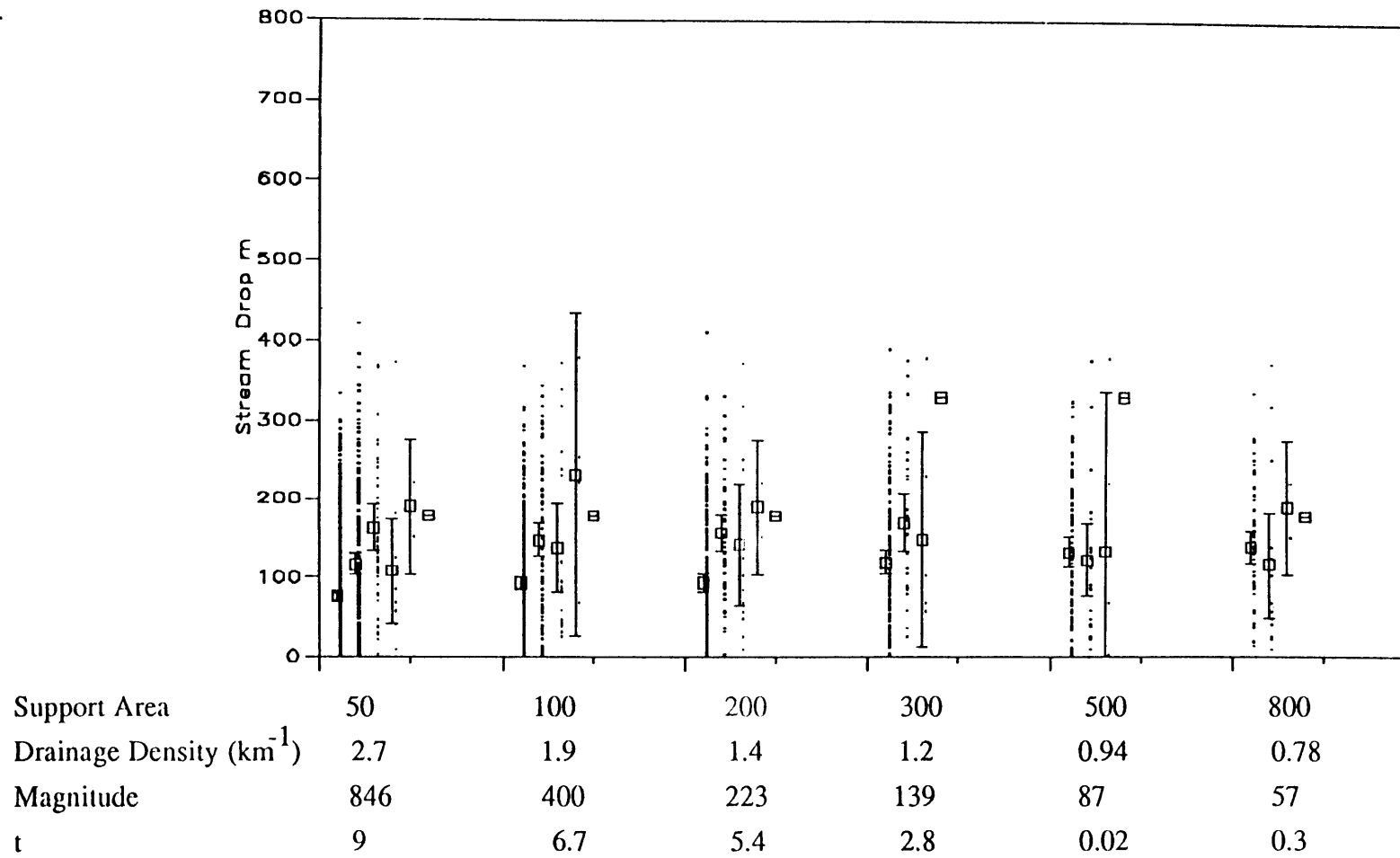


Figure 6.7(d) Big Creek (CALD) from 7.5 min series. Stream drops variation with Order and support area.

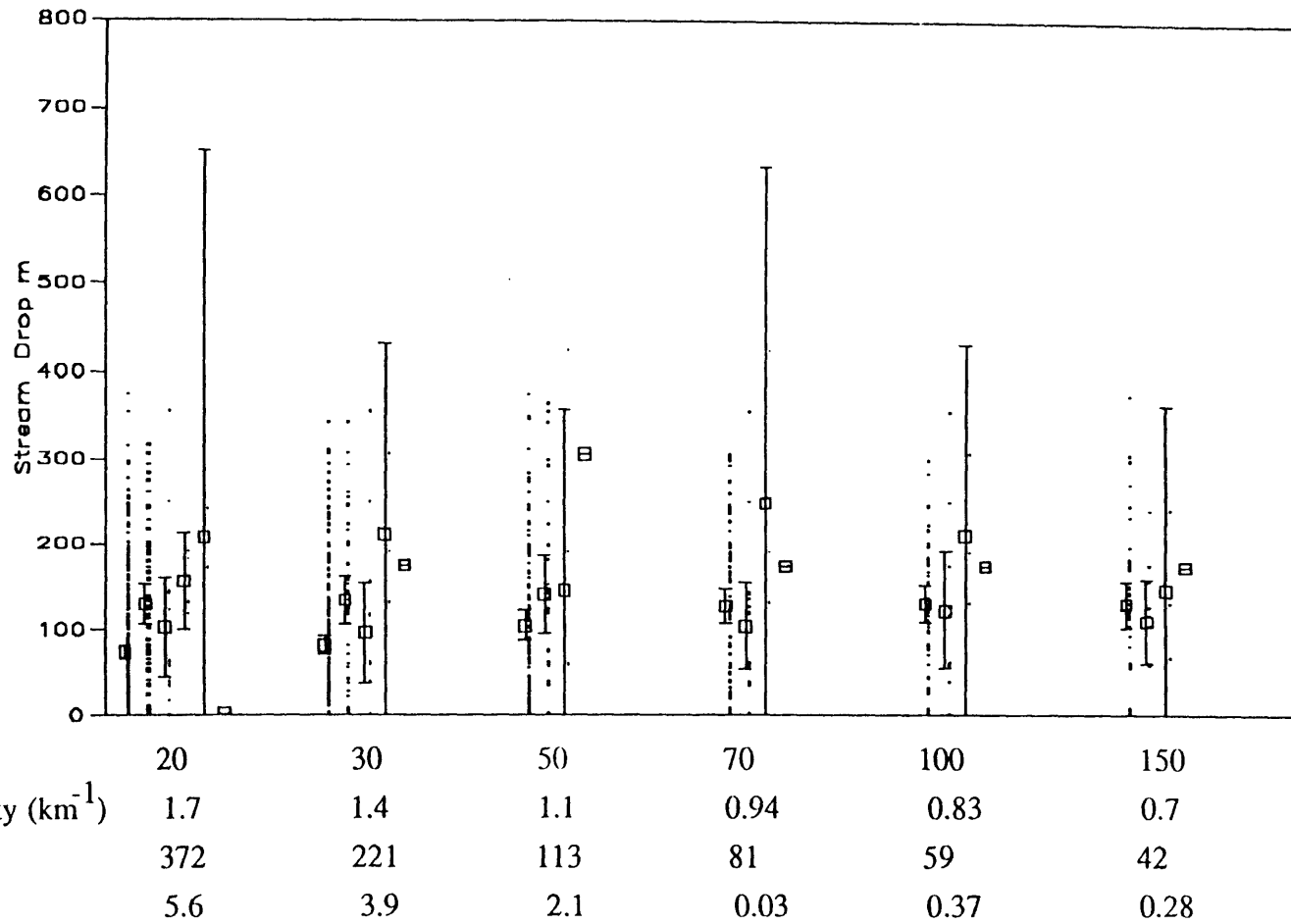


Figure 6.7(e) SPOKBC Big Creek (from 1 deg. series) Stream drops variation with Order and support area.

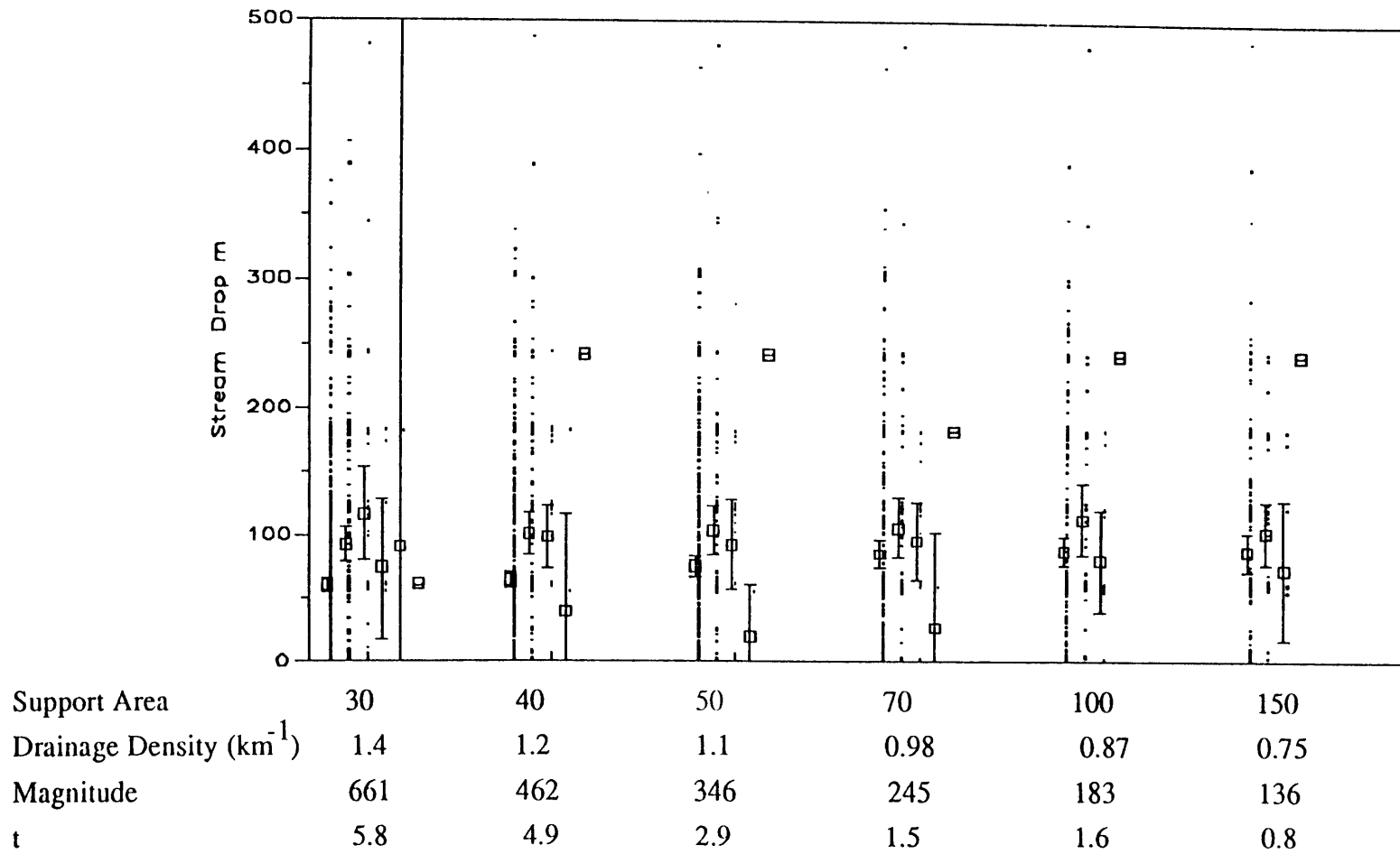


Figure 6.7(f) NELK Stream drops variation with Order and support area.

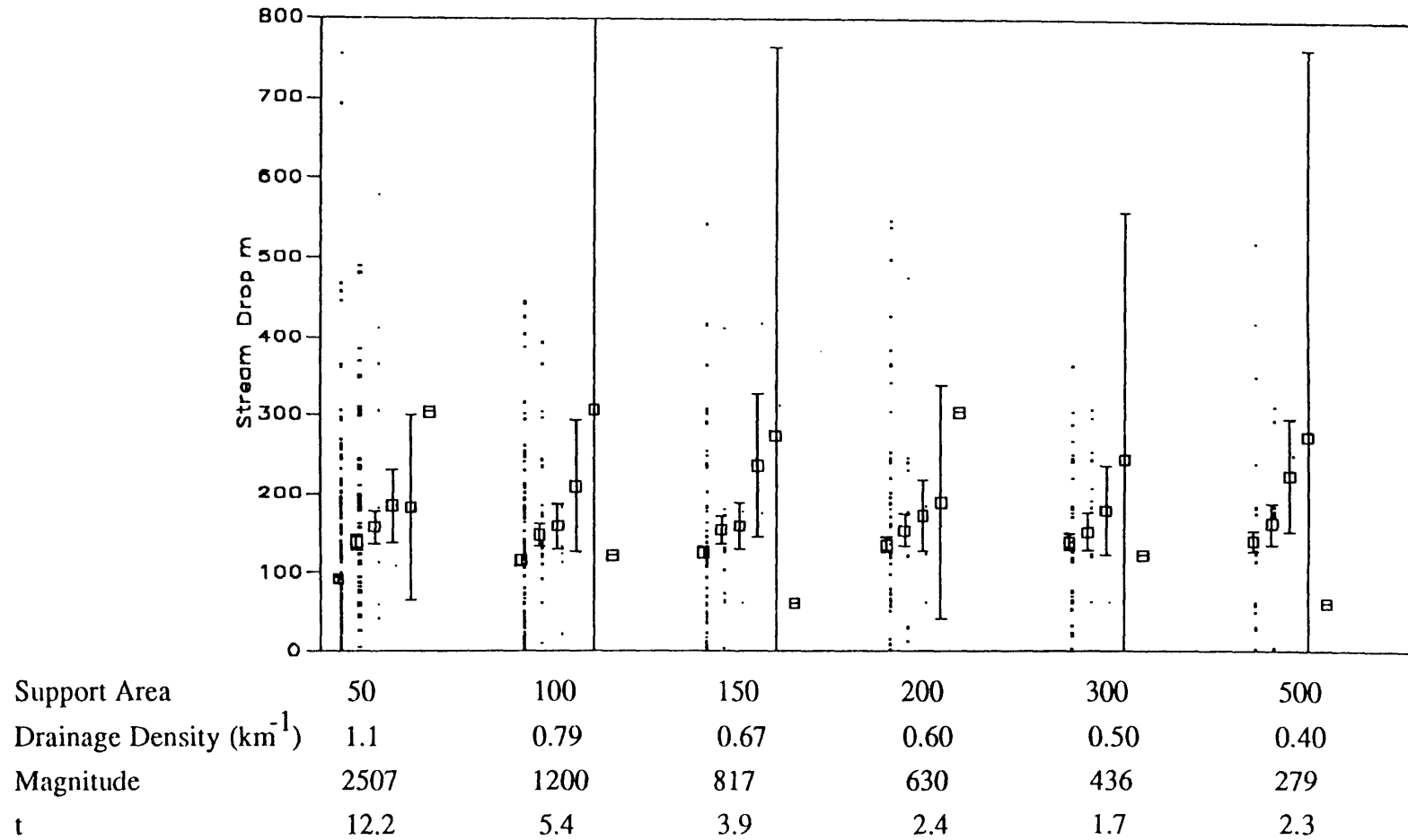
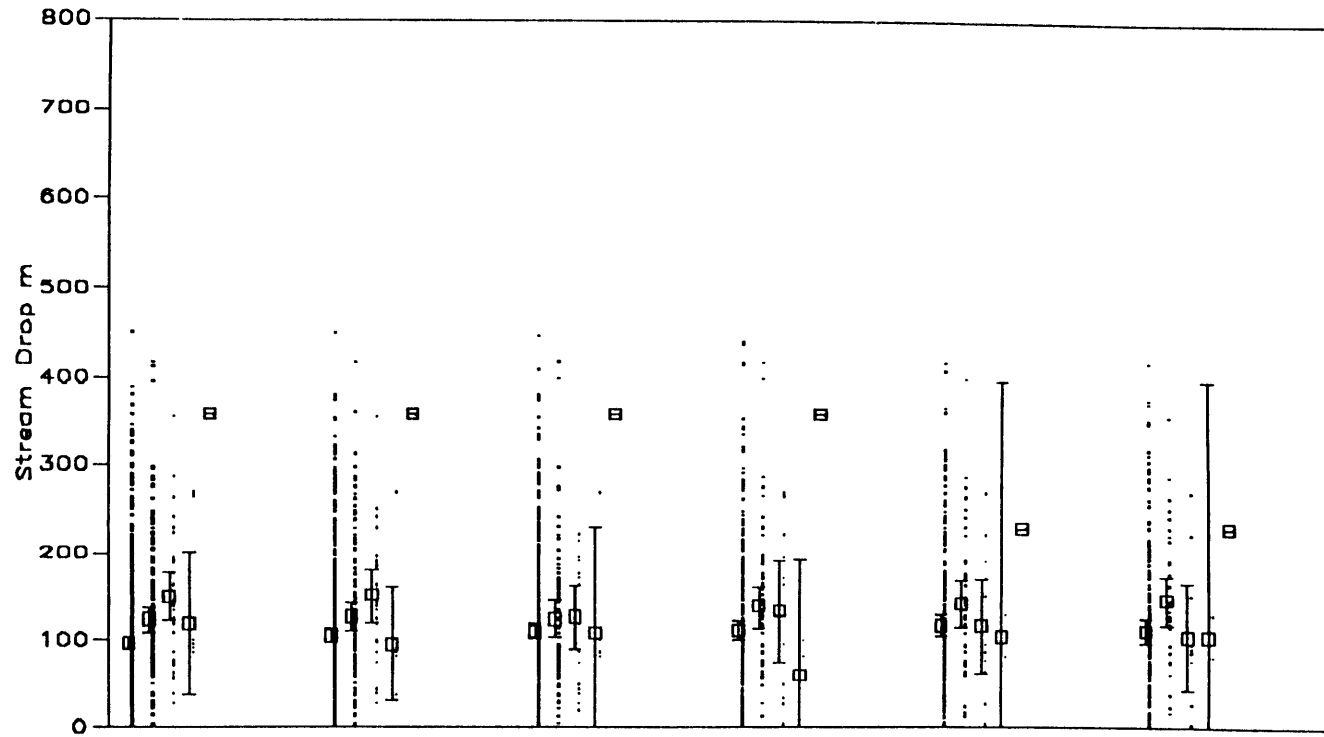


Figure 6.7(g) STJOE Stream drops variation with Order and support area.
(Points have been omitted for clarity of plot)



Support Area	150	200	300	400	500	700
Drainage Density (km^{-1})	1.5	1.3	1.1	1.0	0.9	0.8
Magnitude	696	523	371	287	226	174
t	4.6	3.1	1.5	2.1	1.5	1.8

Figure 6.7(h) STJOEUP Stream drops variation with Order and support area.

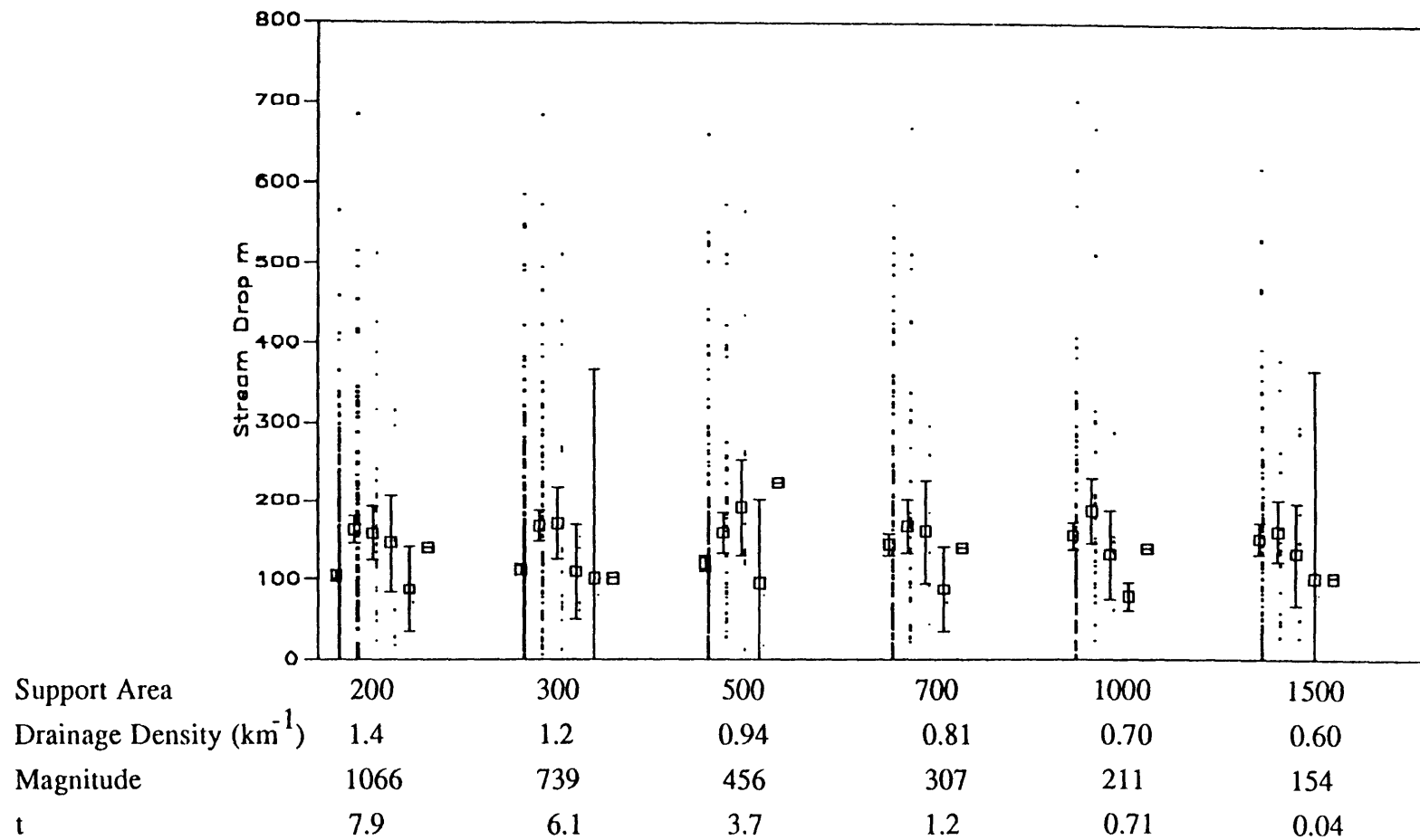


Figure 6.7(i) STREGIS Stream drops variation with Order and support area.
(Points have been omitted for clarity of plot)

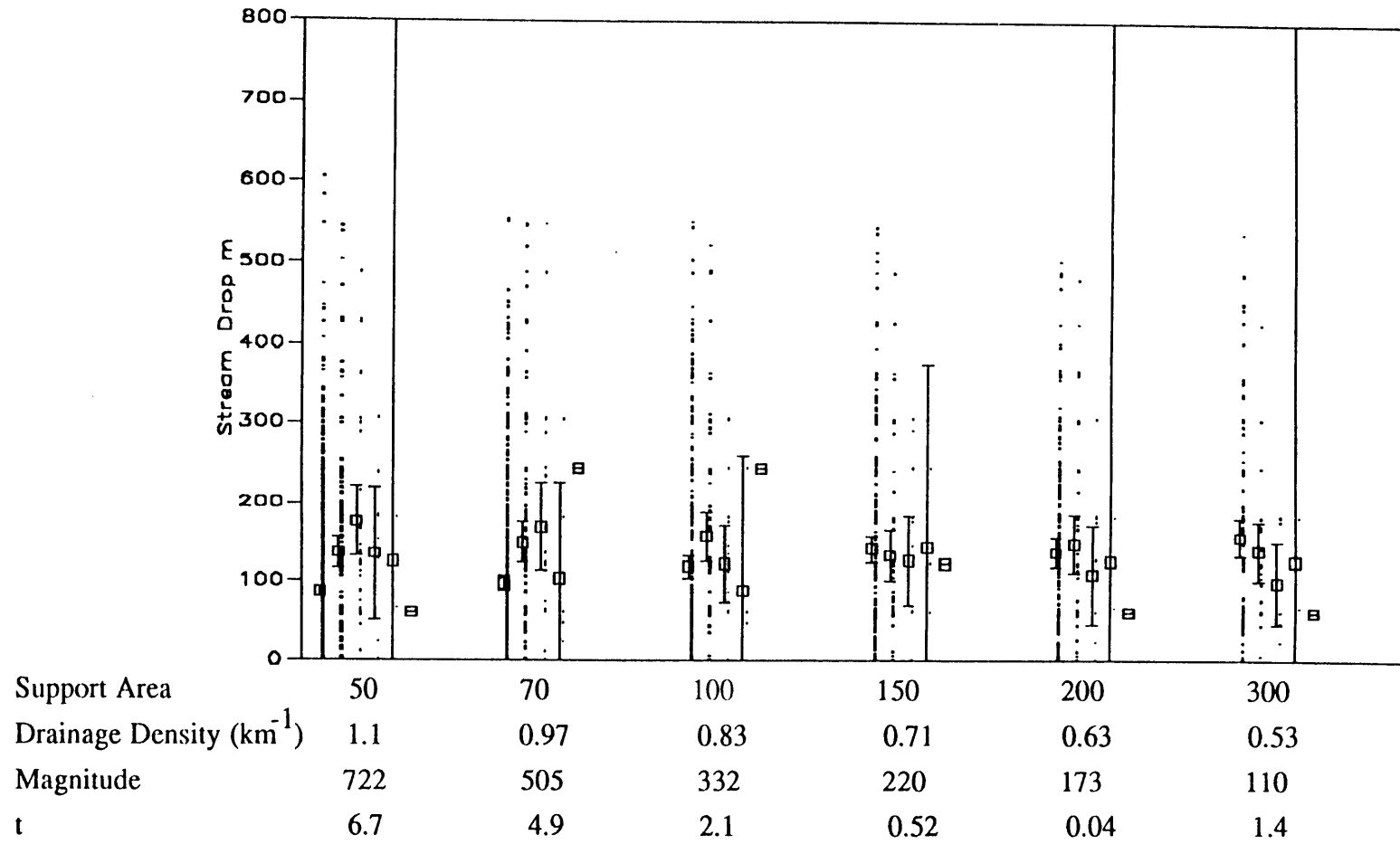


Figure 6.7(j) STREGISDMA Stream drops variation with Order and support area.

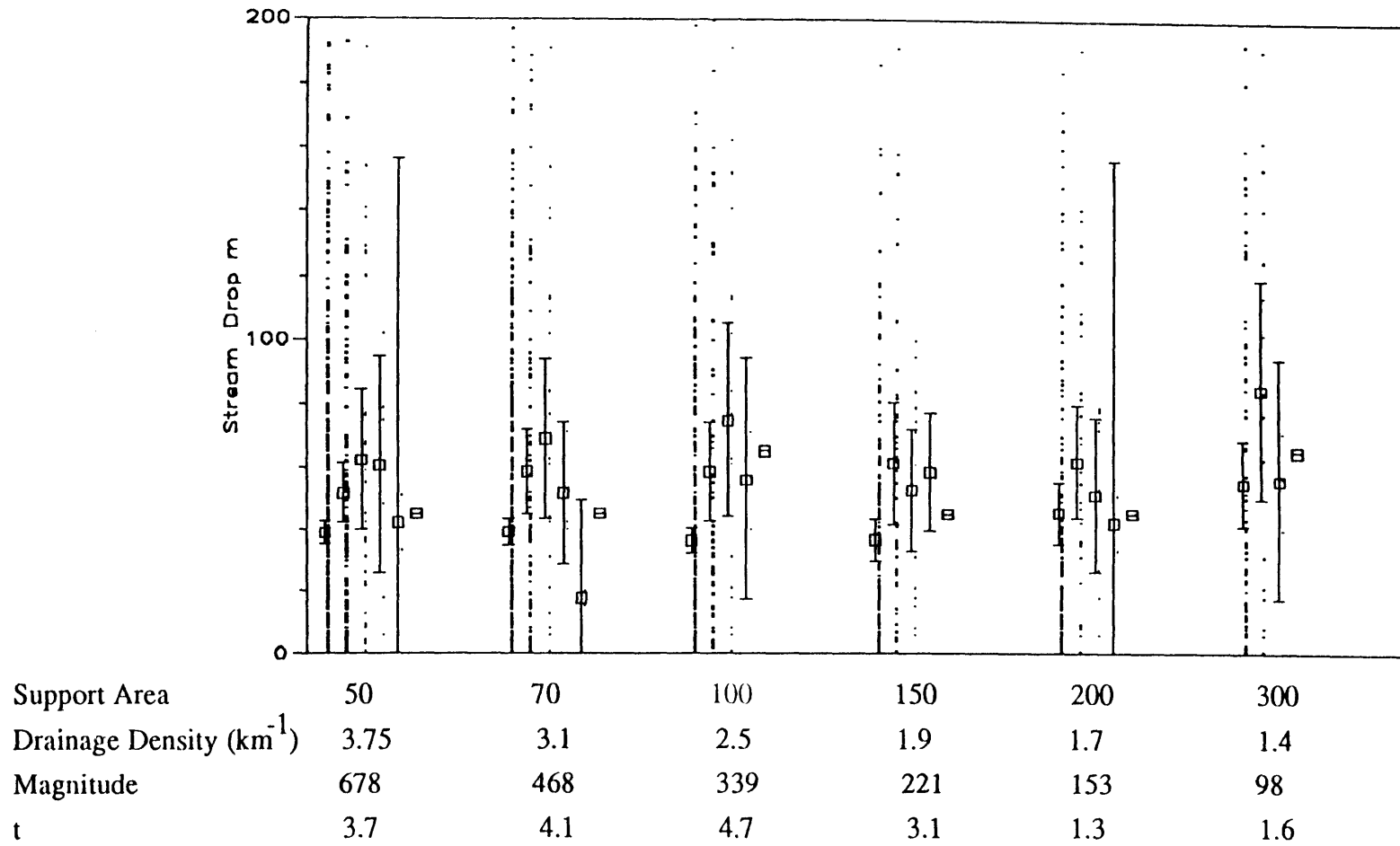


Figure 6.7(k) HAK Stream drops variation with Order and support area.

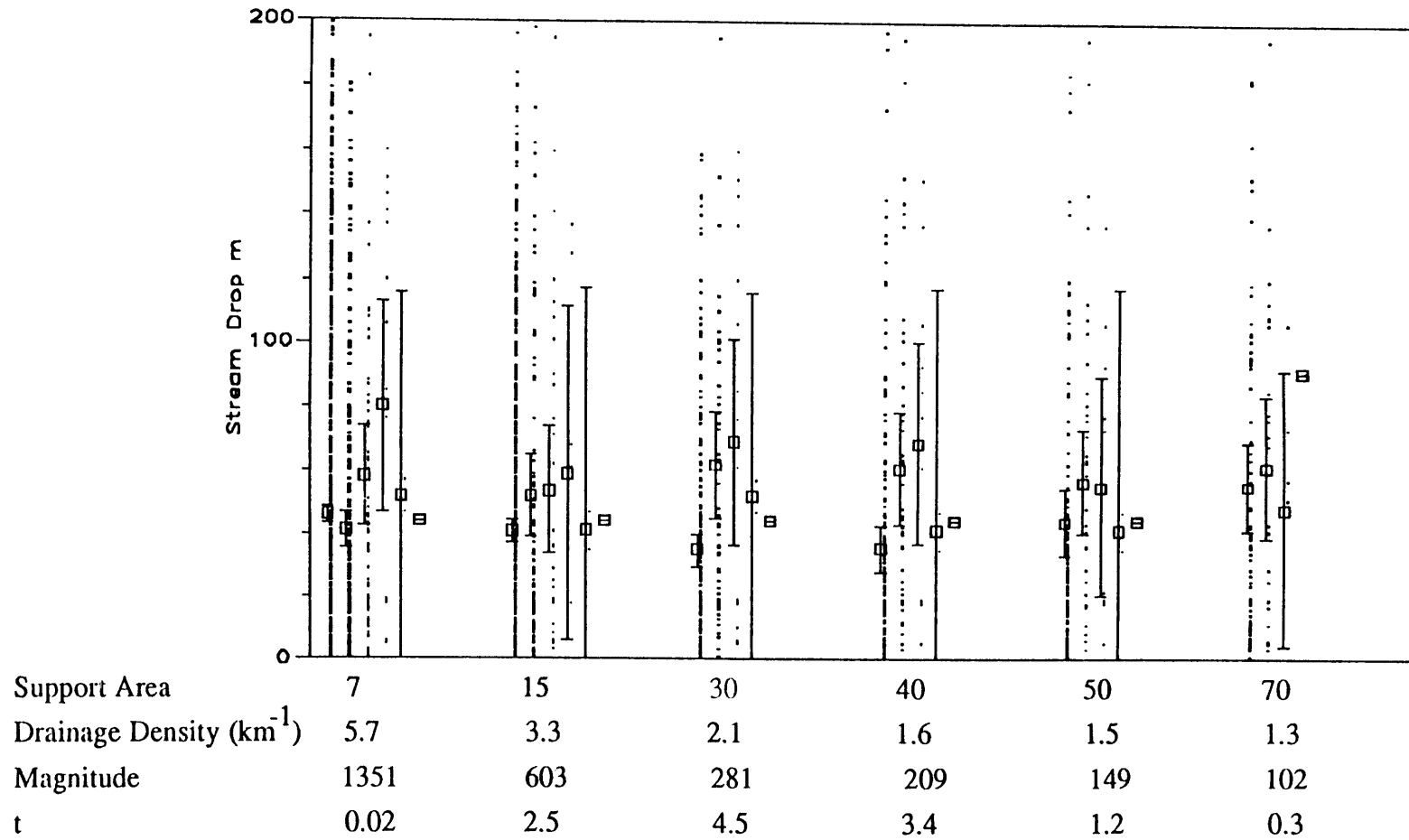
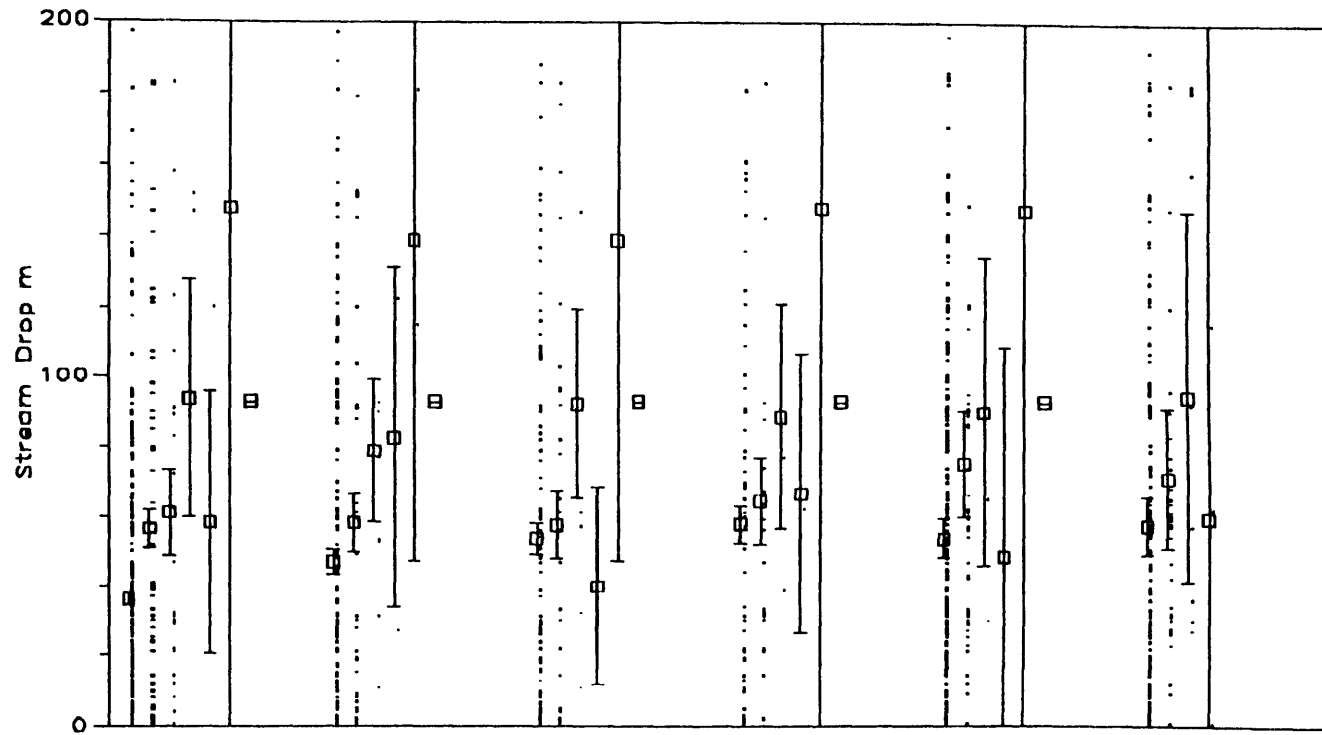


Figure 6.7(l) HAKA2S Stream drops variation with Order and support area.



Support Area	50	100	150	200	300	500
Drainage Density (km^{-1})	1.3	0.84	0.68	0.58	0.48	0.38
Magnitude	2331	1050	681	506	356	213
t	10.1	4.2	2.2	2.1	3.8	2.2

Figure 6.7(m) SCHO Stream drops variation with Order and support area.
(Points have been omitted for clarity of plot)

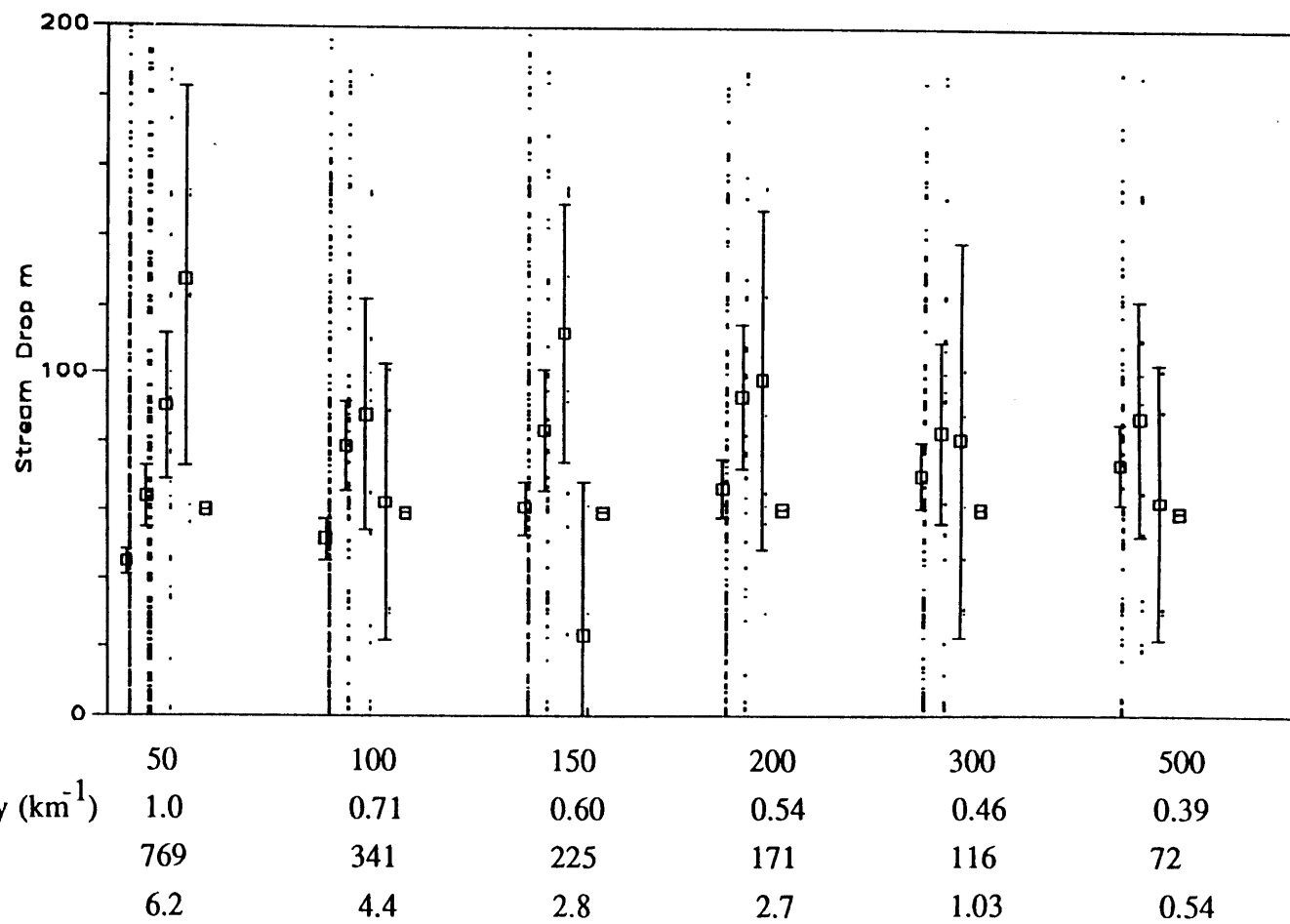


Figure 6.7(n) EDEL Stream drops variation with Order and support area.

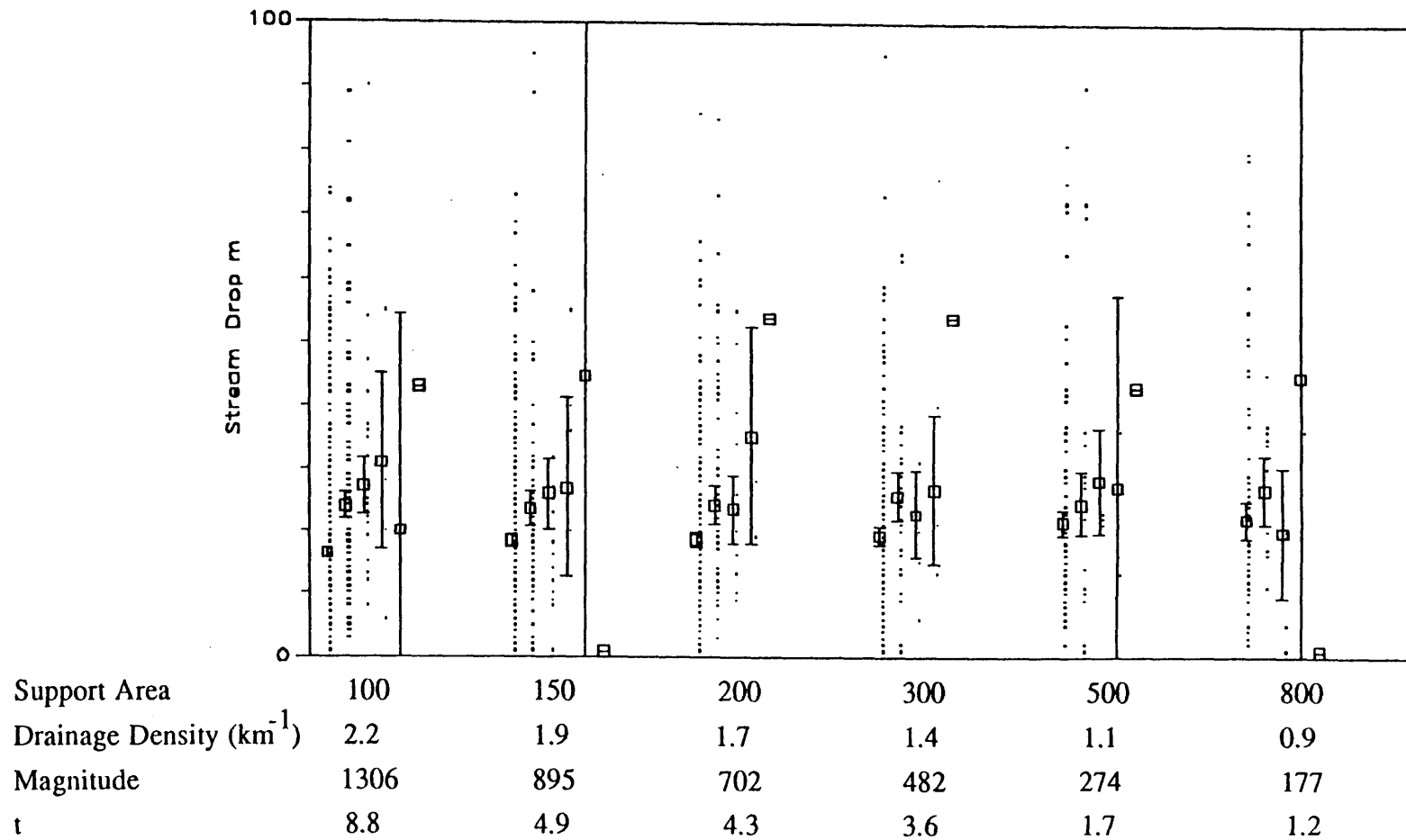


Figure 6.7(o) RACOON Stream drops variation with Order and support area.
(Points have been omitted for clarity of plot)

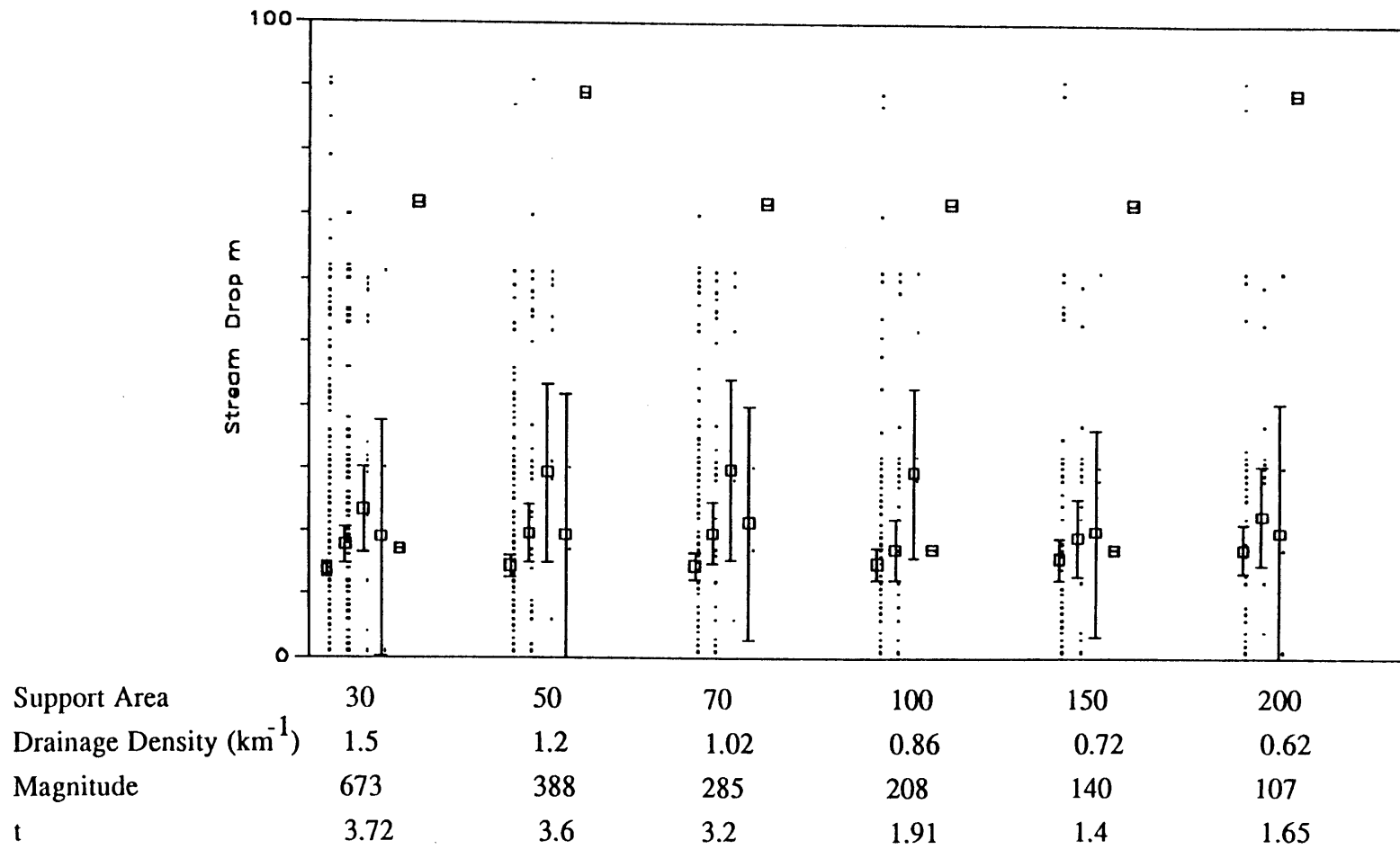


Figure 6.7(p) RACOONDMA Stream drops variation with Order and support area.

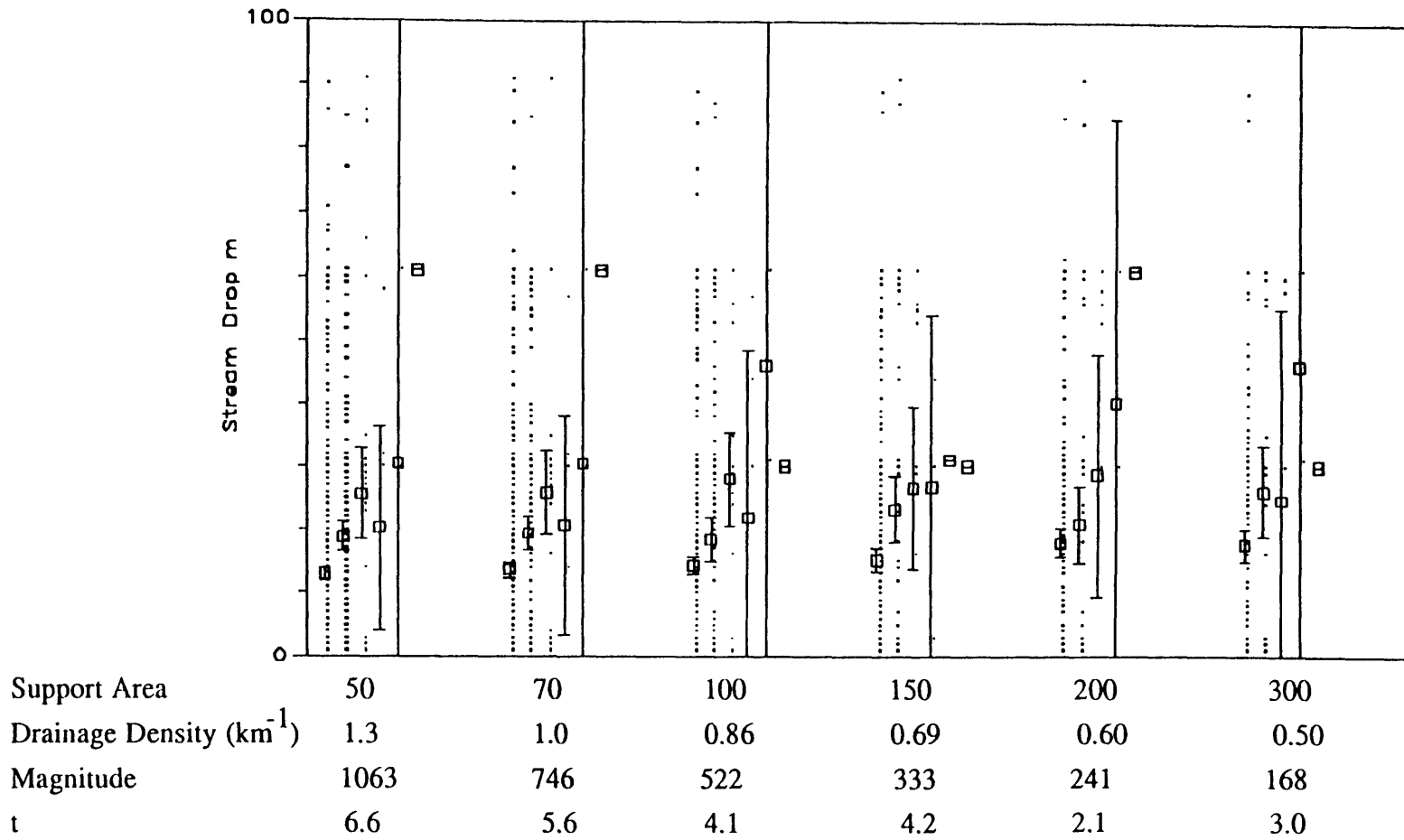


Figure 6.7(q) BEAVER Stream drops variation with Order and support area.

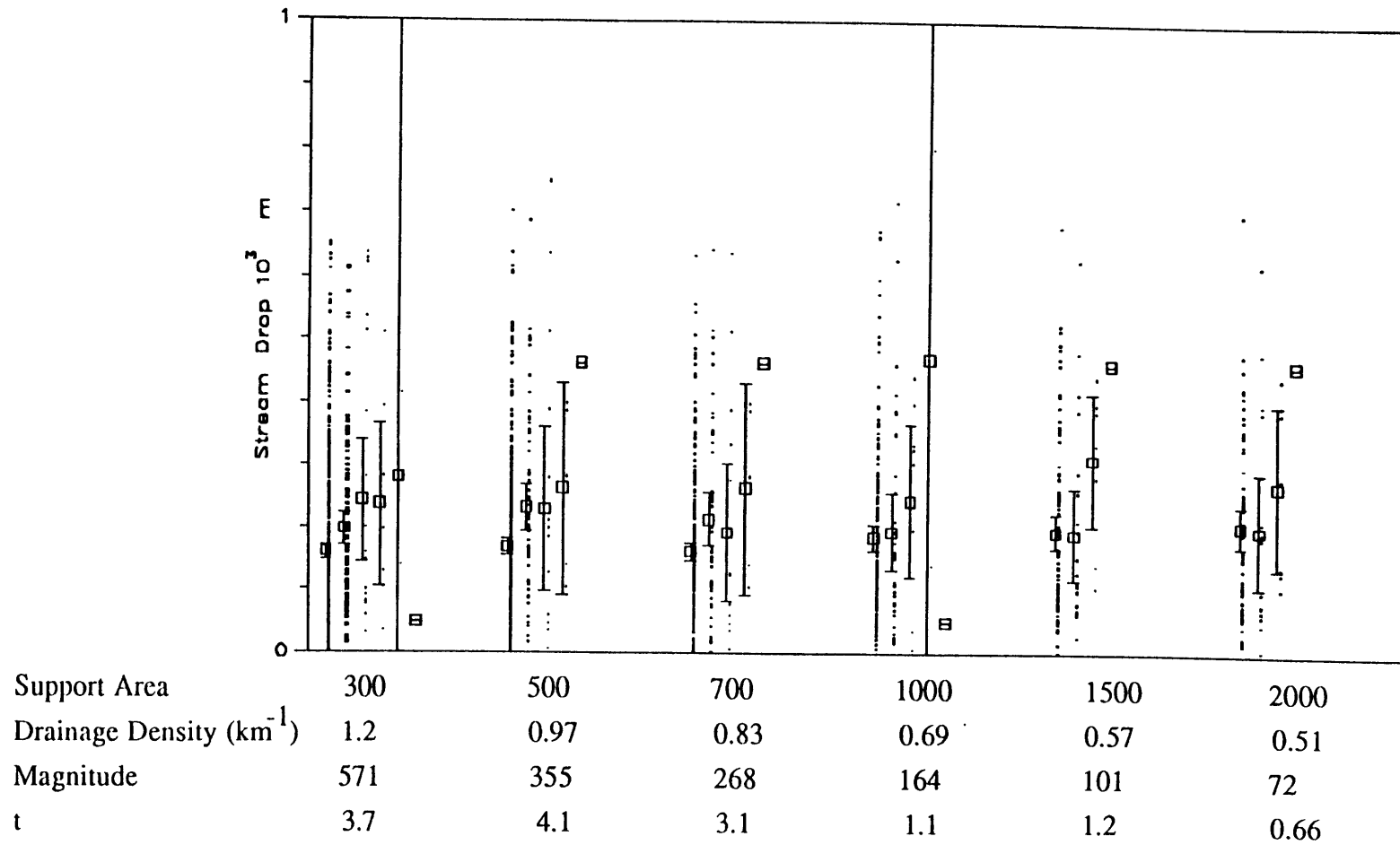


Figure 6.7(r) BUCK Stream drops variation with Order and support area.

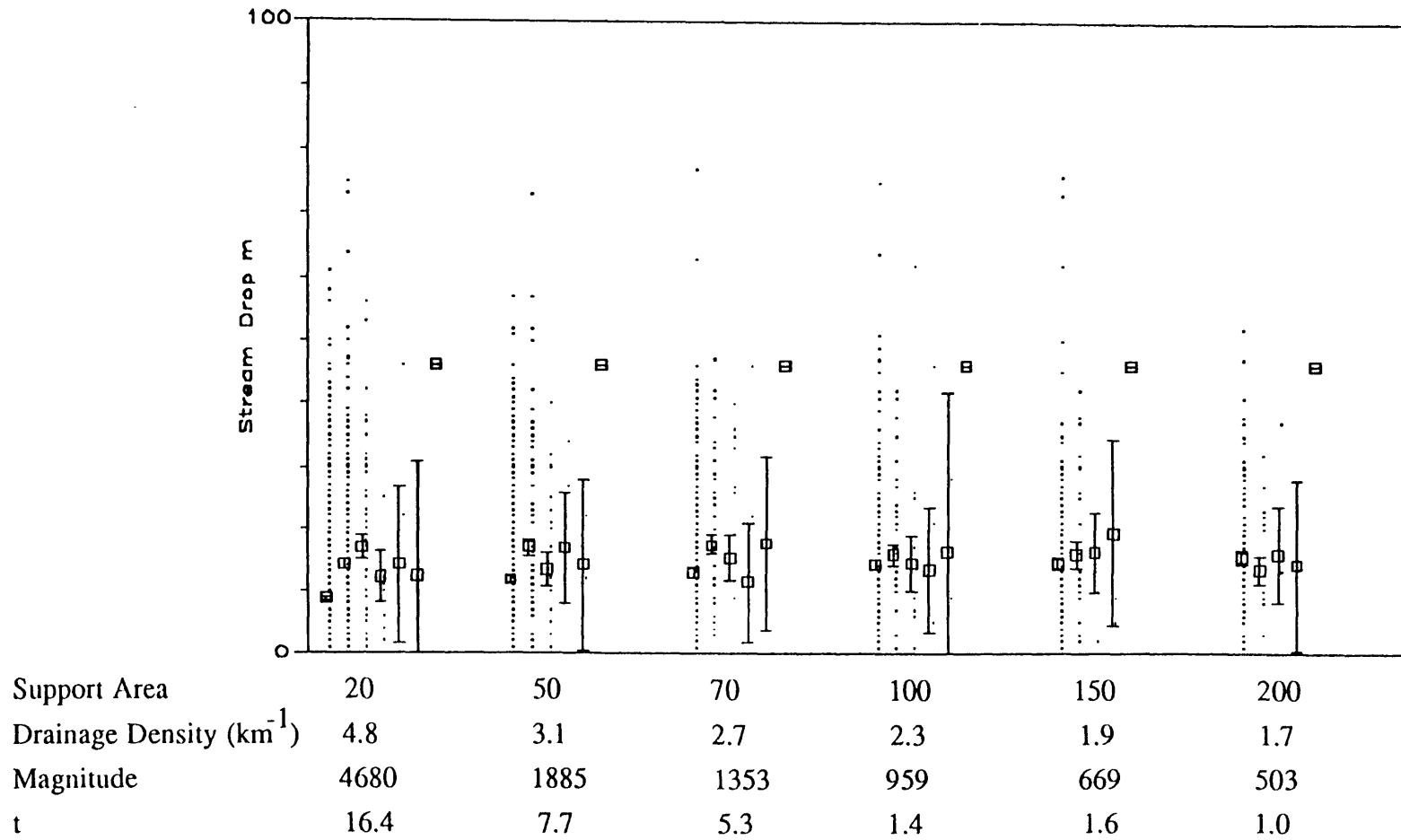


Figure 6.7(s) BRUSHY Stream drops variation with Order and support area.
(Points have been omitted for clarity of plot)

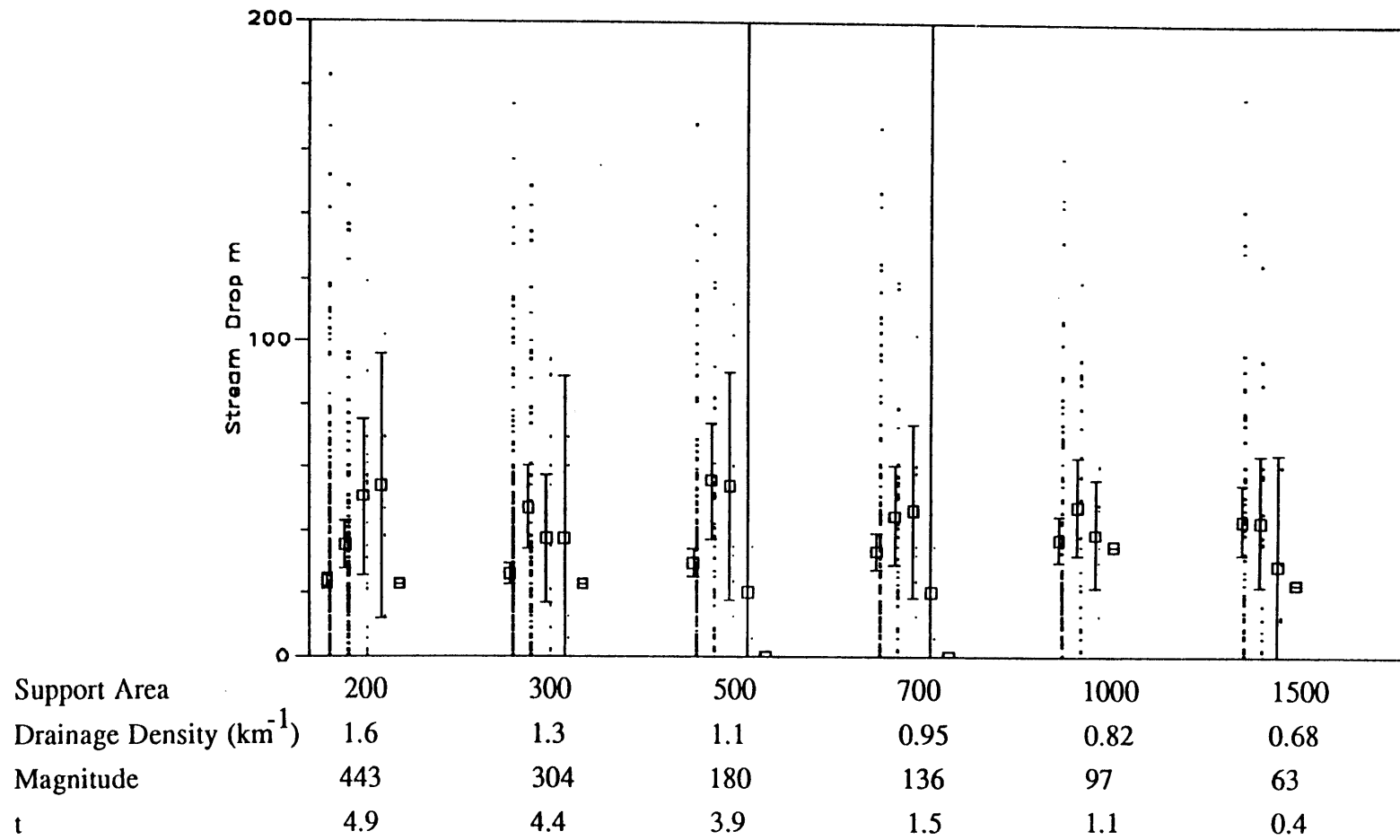


Figure 6.7(t) MOSHANNON Stream drops variation with Order and support area.

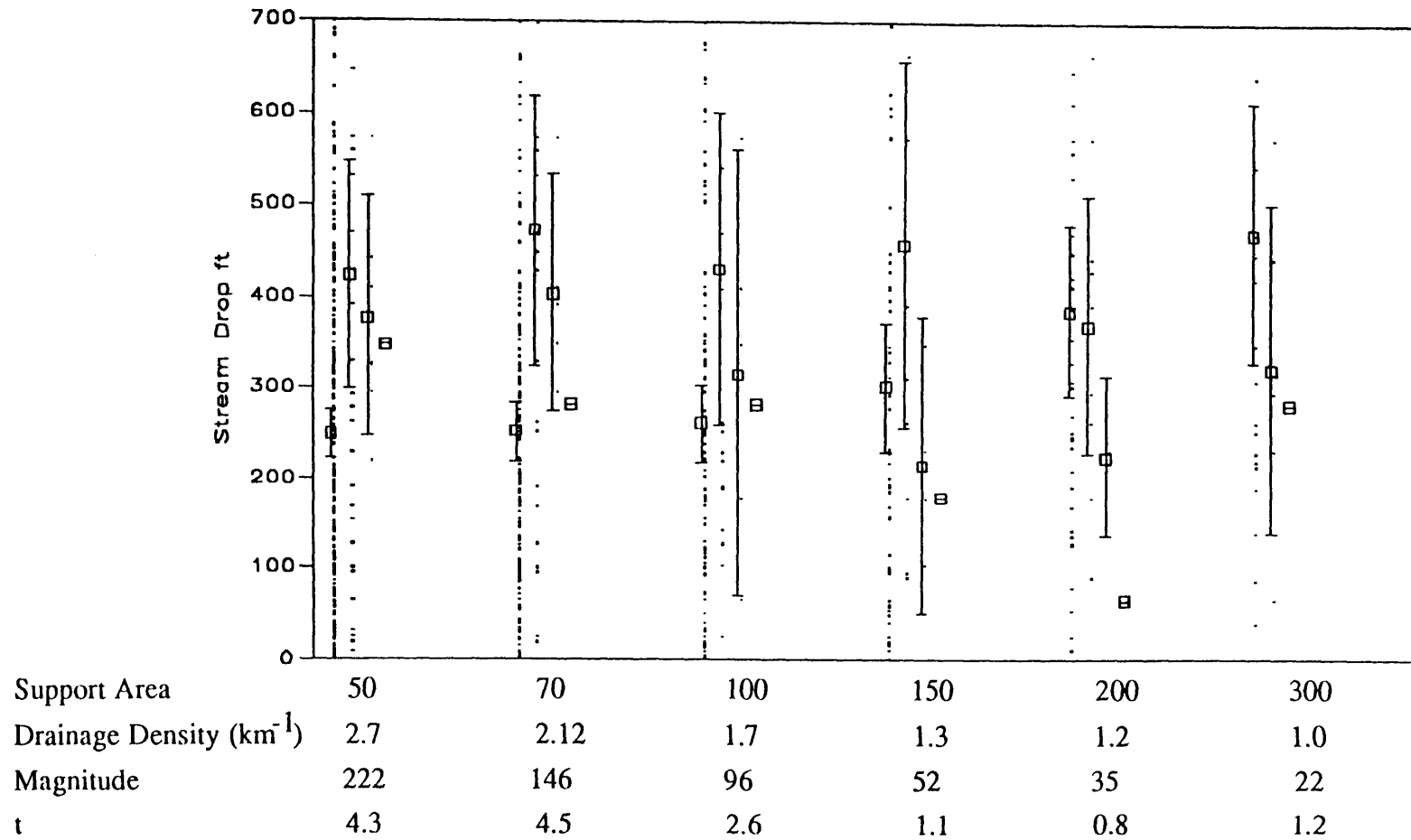


Figure 6.7(u) TVA Stream drops variation with Order and support area.

6.4 Localized DEM Procedures

The above procedures have used a support area threshold to extract channel networks from DEM's. Intrinsic process-related scaling and breaks in that scaling were used to identify what we believe is the correct support area threshold. This section will investigate more direct procedures for identifying valleys within DEM's.

Band (1986, reviewed in Chapter 3) discusses the Peuker and Douglas (1975) algorithm for identifying concave pixels, to extract channel networks from DEM's. Figure 6.8 gives an example of pixels identified by such a procedure for the CALD data set. The main drainage paths are apparent, but the problem is that they are not connected, i.e., there are gaps. Band (1986) suggests procedures to connect these to form network. These are not discussed here.

We should point out that in obtaining Figure 6.8 a moving average smoothing of the data was used. We used the simple smoothing kernel

0.05	0.1	0.05
0.1	0.4	0.1
0.05	0.1	0.05

Without smoothing the Peuker-Douglas algorithm performs poorly, identifying pixels that hardly resembled a network at all, presumably due to many adjacent pixels of the same elevation since elevations are given in integer meters.

The density of points in Figure 6.8 can be used to give an idea of the drainage density. A length ($\frac{1}{2}$ the length of a side + $\frac{1}{2}$ the length of a diagonal) is associated with each pixel so drainage density is estimated from number of identified pixels x length divided by area.

Mark (1974) describes the line intersection method for estimating drainage density. This consists of counting the number (N) of intersections with the drainage net per length (L) of a traverse line. Drainage density is then

$$D_d = \pi/2 \times N/L \quad (6.11)$$

A variant of this idea is to count local minima along a traverse line over a DEM, with the assumption that local minima are usually on the drainage network. Local minima can be identified along each grid line in both orthogonal directions and if these are marked, we get a plot such as Figure 6.9. This again resembles the channel network and is very similar to results from the Peuker–Douglas algorithm. The same moving average smoothing was used to qualitatively improve the results. The density of points in Figure (6.9) can also be used to estimate drainage density. We find that the drainage density from this procedure and the Peuker–Douglas algorithm are practically identical in most cases, so have used the Peuker–Douglas drainage density as a representative drainage density from local procedures for comparison with other results. For comparison with Figures 6.8 and 6.9, Figure 6.10 gives all pixels with accumulation area greater than 200 pixels for the CALD data set.



Figure 6.8. Pixels identified by the Peuker and Douglas Algorithm applied to the CALD dataset.

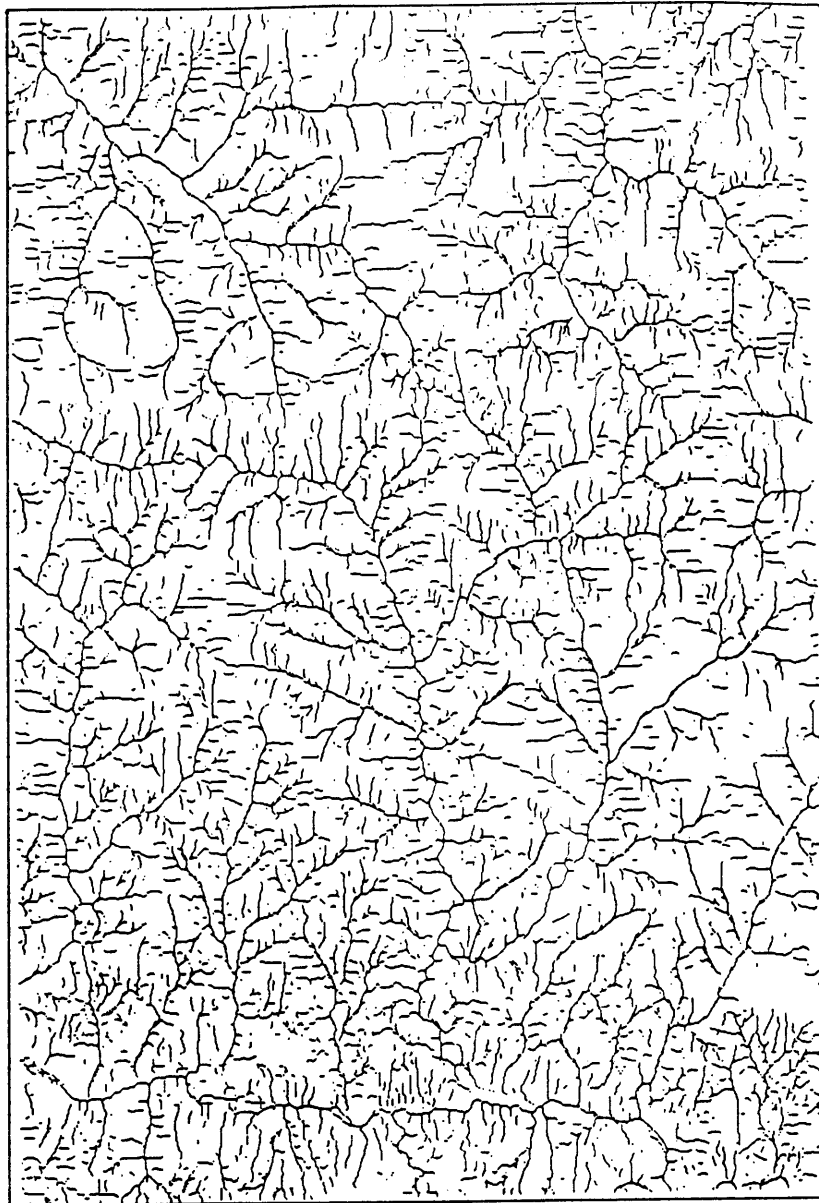


Figure 6.9. Pixels identified as one way local minima in the CALD dataset.

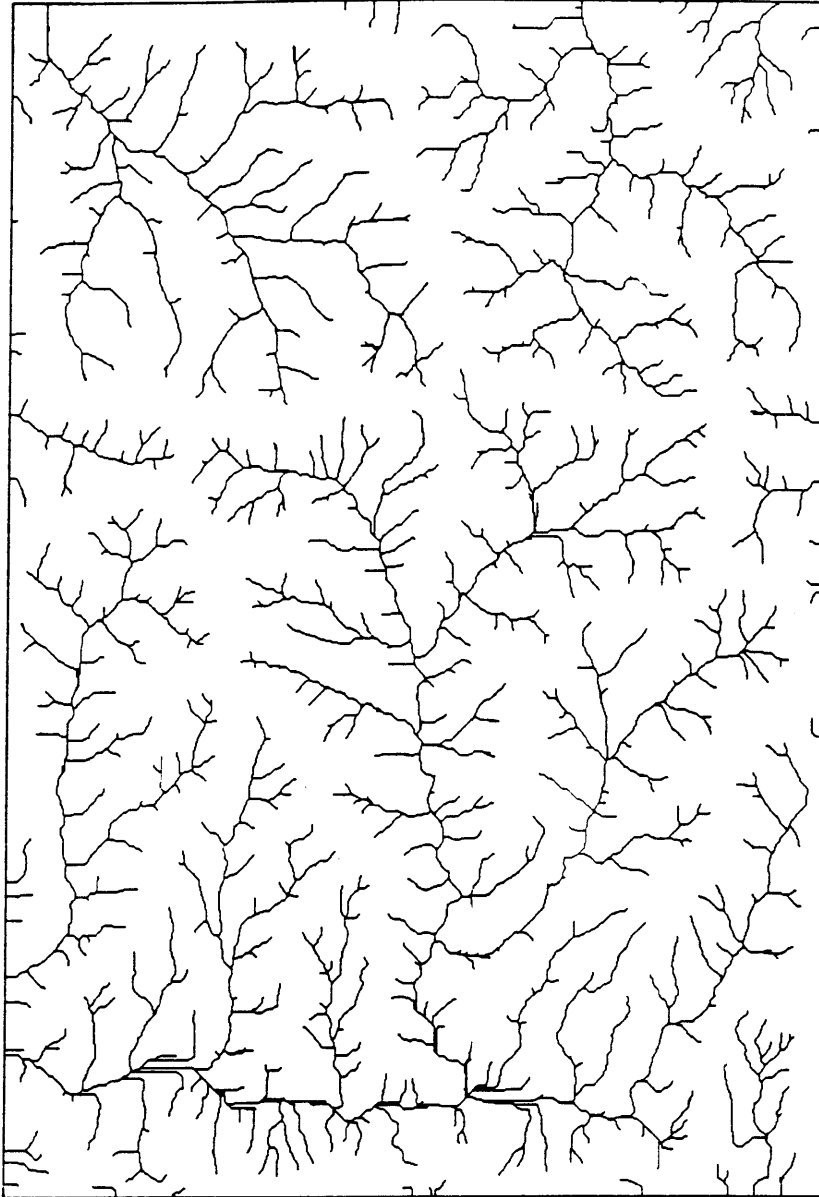


Figure 6.10. Pixels that exceed accumulation area threshold of 200 pixels in the CALD dataset.

6.5 Detailed Results

Table 6.2 summarizes all the landform scale results, comparing drainage density estimated from the three techniques described above. The drainage densities from the different techniques are also compared in Figure 6.11. The scatter about a straight line at 45° measures the degree of agreement between the different estimates of drainage density. Within the scatter there appears to be reasonable agreement between drainage densities obtained from slope scaling and the constant drop analysis. The agreement with the Peuker–Douglas D_d is not as good and there appears to be a bias with the Peuker–Douglas procedure consistently over estimating drainage density relative to the other two procedures. Perhaps this is due to the Peuker–Douglas procedure being more sensitive to local differences and errors in the data.

Evaluation of these results raises the following concerns:

- Are the scales (drainage density) obtained dependent on data resolution and data set size?
- What is the effect of data errors?
- The slope–area scaling two phase regression [Figures 6.4(a)–(u)] more often than not does not break into a negative slope at small area as required by the analysis in Section 6.2 for the stability and smooth hillslopes interpretation.

To address the first concern, five pairs of data sets are actually the same river basin with DEM's of different pixel size. These are (W15, W15A2S), (HAK, HAKA2S), (CALD, SPOKBC), (STREGIS, STREGISDMA) and (RACOON, RACOONDMA). In the first two of these the low resolution DEM was formed from the high resolution DEM by averaging together the elevations of four adjacent pixels. In the other three the low resolution data set is a DMA data set on three arc second grid while the high resolution data set is a USGS data set on

Table 6.2 Summary of Landform Scale Results.

Basin	Area (km ²)	Constant Drop Analysis				Slope Scaling Analysis					Peuker Douglas
		A (km ²)	D _d (km ⁻¹)	H (m)	H D _d	A _l (km ²)	A _b (km ²)	A _u (km ²)	D _d (km ⁻¹)	θ	D _d (km ⁻¹)
W7	12.8	0.09	2.5	18	0.045	0.0018 ¹	0.0018 ¹	0.0024	26.3	0.30	5.5
W15	22.7	0.045	3.4	15	0.051	0.0018 ¹	0.0024	0.0045	19.4	0.29	4.7
W15A2S	22.7	0.072	2.7	15	0.039	*	*	*	*	0.25	3.3
CALD	146.9	0.27	1.2	130	0.16	0.16	0.19	0.24	1.3	0.51	3.19
SPOKBC	146.9	0.41	0.93	128	0.12	0.32	0.45	0.68	0.9	0.48	1.5
NELK	440.2	0.41	0.98	89	0.087	0.21	0.30	0.42	1.1	0.47	1.7
STJOE	2834	1.16	0.59	140	0.082	0.75	0.96	1.18	0.65	0.47	1.45
STJOEUP	384.6	0.27	1.1	114	0.13	0.30	0.34	0.40	1.0	0.56	3.03
STREGIS	786.6	0.63	0.81	148	0.12	0.45	0.53	0.61	0.88	0.55	3.01
STREGISDMA	796.2	0.89	0.71	139	0.098	0.98	1.52	2.65	0.56	0.55	1.45
HAK	98.2	0.18	1.6	48	0.077	0.044	0.076	0.12	2.76	0.48	5.19
HAKA2S	98.75	0.18	1.5	47	0.070	0.018	0.027	0.041	5.6	0.42	2.27
SCHO	2408	0.95	0.68	56	0.038	1.51	2.08	3.12	0.46	0.43	1.21
EDEL	933.0	1.9	0.47	73	0.034	0.98	1.43	2.07	0.51	0.55	1.24
RACONN	448.0	0.45	1.1	22	0.024	0.31	0.43	0.63	1.1	0.51	7.2
RACONDMA	480.1	0.65	0.86	16	0.014	*	*	*	*	0.34	2.14
BEAVER	1223	0.18	0.6	19	0.011	0.077	0.29	0.89	1.37	0.34	2.14
BUCK	606.2	0.9	0.69	191	0.013	0.32	0.37	0.41	1.1	0.48	4.47
BRUSHY	321.8	0.09	2.3	14.5	0.033	0.12	0.18	0.26	1.7	0.53	5.73
MOSHANNON	325.4	0.63	0.95	35.5	0.034	1.6	2.1	2.7	0.57	0.58	7.2
TVA	36.5	0.14	1.3	97.5	0.13	0.57	0.68	0.99	0.79	0.85	4.5

Key:

- A. Lowest Support Area for which constant drop property cannot be rejected.
- D_d. Drainage density.
- H. Mean stream drop.
- A_l. Switch point lower 95% confidence bound.
- A_b. Switch point with minimum residual sum of squares.
- A_u. Switch point upper 95% confidence bound.
- θ. Log(slope)-Log(area) scaling exponent above switch point.

Notes:

- 1. At lower limit of range of possible switch points.
- *. Could not be obtained or was not significant.

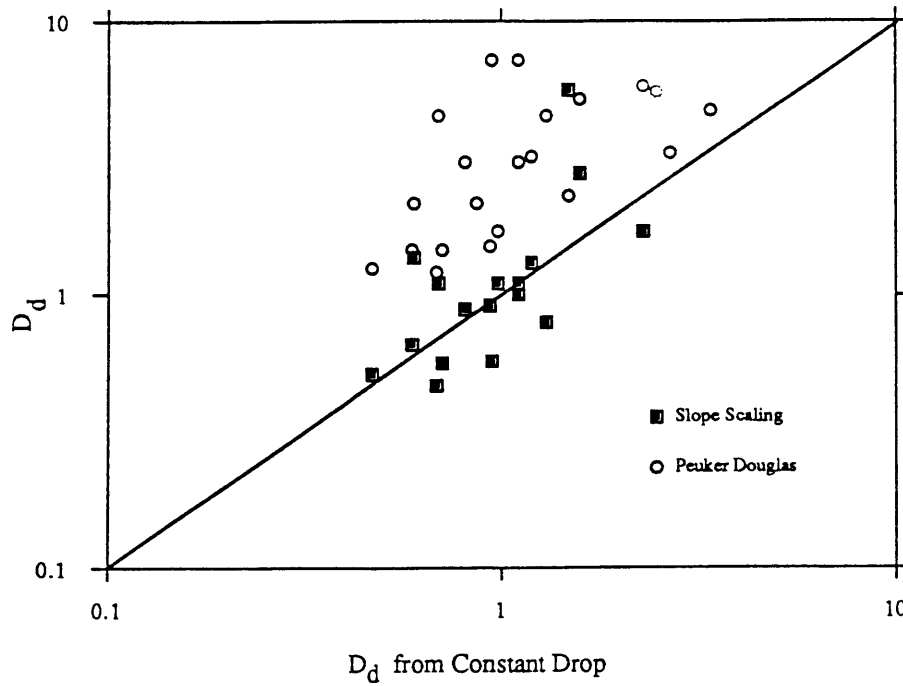
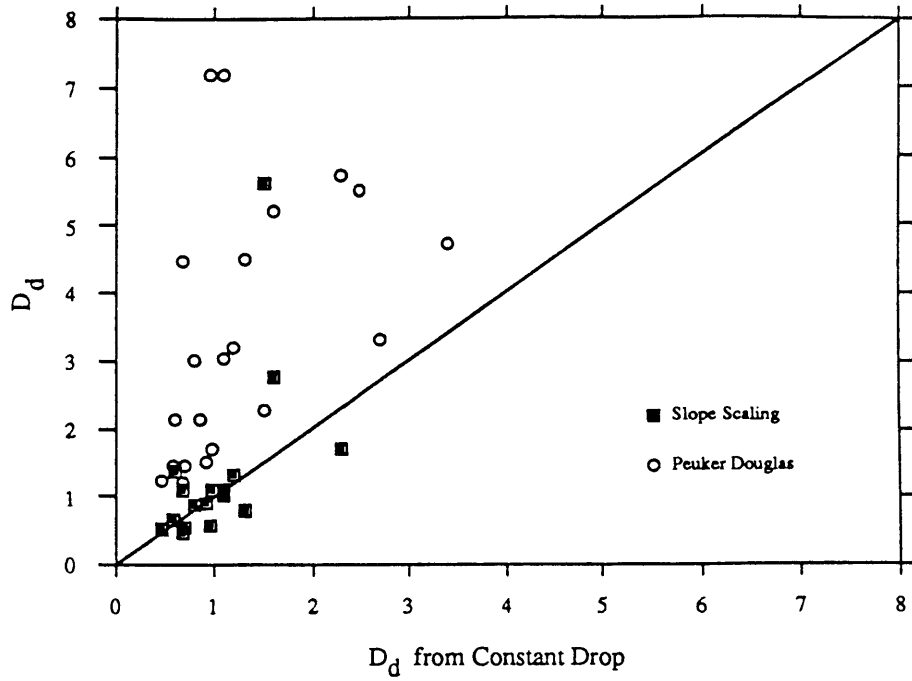


Figure 6.11. Comparison of Drainage density from different techniques.

30m grid. We see that the drainage densities obtained from the constant drop analysis agree fairly well for all five of these data sets. The comparison of slope scaling drainage densities for the (CALD, SPOKBC) and (STREGIS, STREGISDMA) pairs is also good. For the (HAK, HAKA2S) pair the slope scaling drainage density comparison is not good and also differs from the constant drop drainage density. For the RACOONDMA and W15A2S data sets the slope scaling does not give a detectable break so the comparison cannot be made.

Some of the data sets are also nested. CALD and STJOEUP are sub-basins within STJOE and HAK is a sub-basin within SCHO. Analysis of these suggests a higher drainage density for the sub-basin, possibly some indication of a data set size or scale effect. In principle if the drainage density was uniform, D_d of the sub-basins should be the same as the D_d of the larger enclosing basin. This is not the case. STJOE has $D_d \approx 0.5 \text{ km}^{-1}$ while CALD and STJOEUP have $D_d \approx 1 \text{ km}^{-1}$. SCHO has $D_d \approx 0.7 \text{ km}^{-1}$ while the sub-basin HAK has $D_d \approx 1.7 \text{ km}^{-1}$. The sub-basins are from higher resolution data, but the comparisons in the previous paragraph suggest this should not have an effect. A possible explanation is that larger basins imply more streams and a larger sample size for detection of trends or breaks in scaling, so for larger basins our scale detection threshold may be lower, an undesirable basin size effect in the results. There is also the possibility of variations in drainage density within the large basins being responsible for this. The large basins (SCHO and STJOE) have lengths of the order of 50 – 100 km, in which it is entirely plausible that D_d could vary considerably. It is not possible with the information at hand to resolve this issue and further research on this point may be warranted.

The second and third concerns and the whole issue of interpretation of the slope–area scaling plots [Figures 6.4(a)–(u)] appear to be related. The estimation of local slopes from DEM data is erratic because data is reported in integer meters

and random errors have large effects on measured slope. At the scale of a single (30m) pixel the integer data does not allow us to resolve slopes between $1/30 = 0.033$ and 0. We attempt to avoid this effect by averaging over larger lengths (see Table 6.2) using higher support areas. This has the effect of smoothing slope estimates at the expense of some resolution of areas. Areas smaller than the support area threshold used cannot be resolved. This results in a scale effect apparent in some of the Figures 6.4(a)–(u). This is most apparent in the STJOE basin, Figure 6.4(g) where the break in slope is much more marked for the higher support areas and also appears to occur at a higher area for higher support areas. The two phase regression on all the data is a form of compromise between wanting accurate slope estimates and good area resolution.

To understand the effect of data errors on slope–area scaling we constructed some data sets of hillslopes with known theoretical slope–area functions and applied random noise to them. The hillslope profiles used were one–dimensional governed by

$$\text{A. } z = 250 - x^2/9000 \quad (6.12)$$

and

$$\text{B. } z = 150 - 0.1x \quad (6.13)$$

For one–dimensional profiles $x = a$, hence

$$\text{A. } S = \left| \frac{dz}{dx} \right| = \frac{a}{4500} \quad (6.14)$$

$$\text{B. } S = \left| \frac{dz}{dx} \right| = 0.1 \quad (6.15)$$

Equations (6.12) and (6.13) were used to compute elevations on a 51 x 102 grid with spacing 30m schematically shown in Figure 6.12. A random measurement error simulated from a zero mean Gaussian distribution with variance σ^2 was added to each elevation which was then rounded to the nearest meter for storage as an integer value as with real DEM data. Slope–area profiles were then computed using the same procedures as for digital elevation models. The results are given in Figures 6.13 and 6.14 and show even for the relatively small errors simulated a large effect on the slope–area profile. The theoretical lines are obtained from Equations (6.14) and (6.15). The good data is with no added measurement noise and has scatter due to the rounding of elevations to the nearest meter. In the noisy data the errors introduce a negative correlation between slope and area which tends to reduce the positive slope or increase the negative slope of slope–area curves and may be responsible for the negative slopes in the slope–area data [Figures 6.4(a)–(u)] to the left of the break in scaling at scales or areas we interpret as hillslopes.

To understand this effect consider an error in the elevation of a single pixel. If the error reduces the apparent elevation of a pixel, the apparent slope is reduced. This is because the slope of a pixel is measured as the difference in elevation between the pixel in consideration and its downslope neighbor, divided by the distance between pixels. Also adjacent pixels are more likely to drain towards the pixel in consideration due to its reduced elevation, thus increasing the apparent area that it drains. Similarly an error that increases the apparent elevation increases slope and reduces area so the net effect is that errors result in a negative correlation between slope and area or negative slope in slope–area plots.

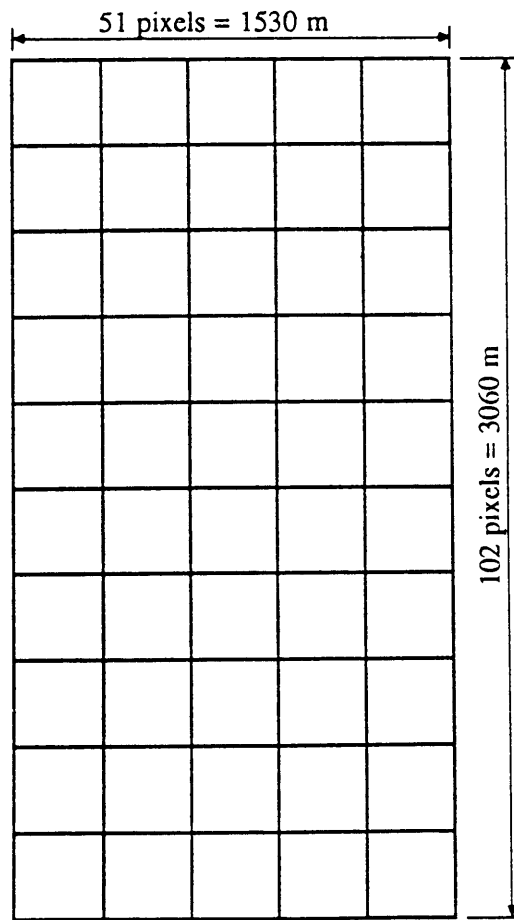
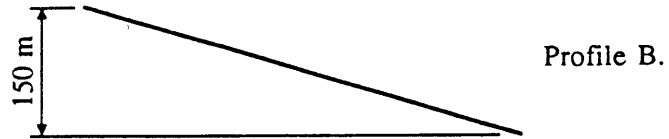
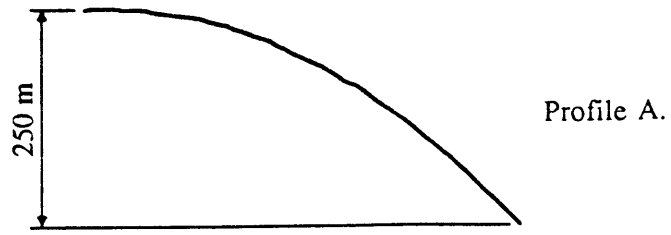


Figure 6.12 Schematic diagram of simulated slope profiles.

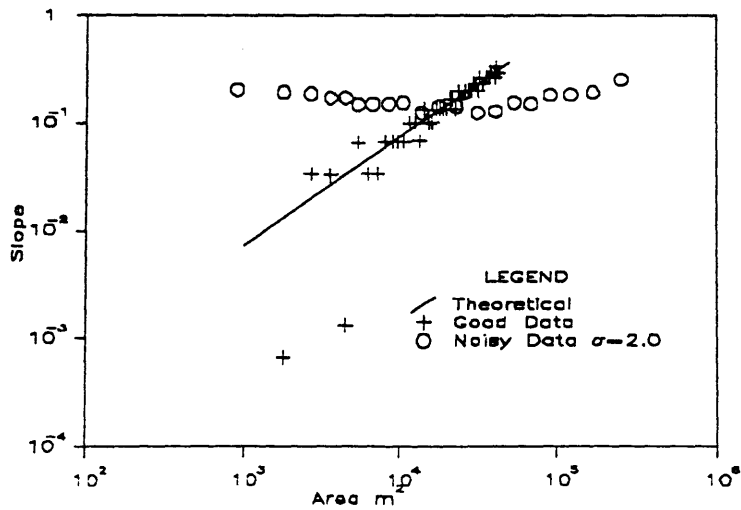
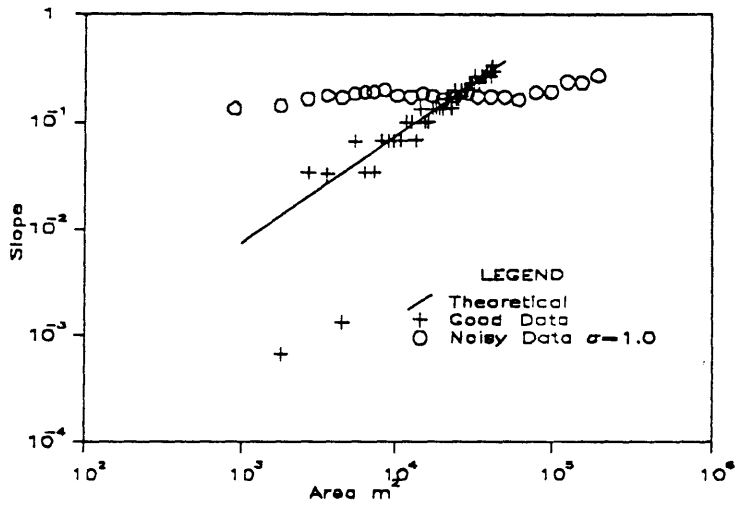
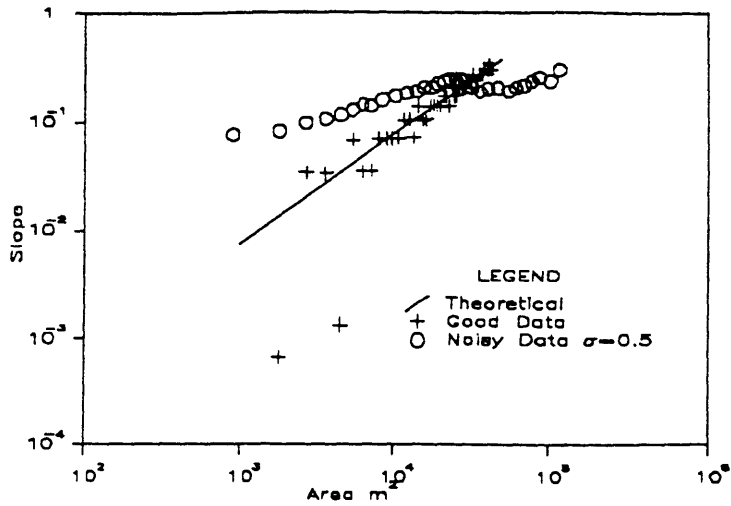


Figure 6.13. Slope-Area plots for Simulated Hillslope Profile A.

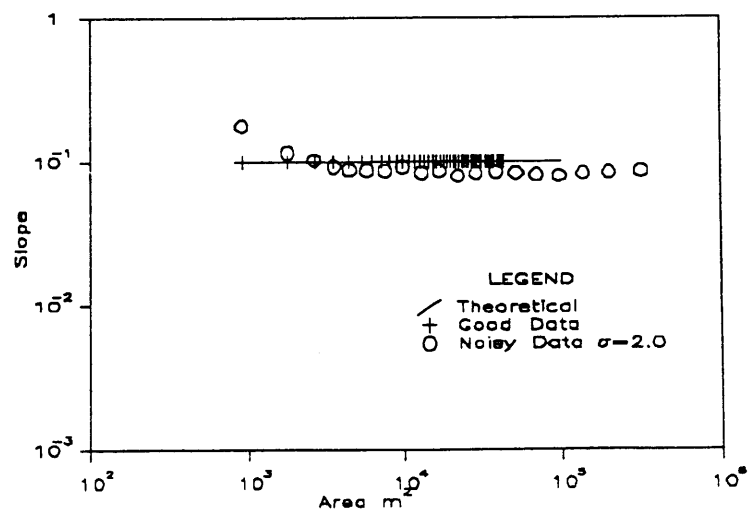
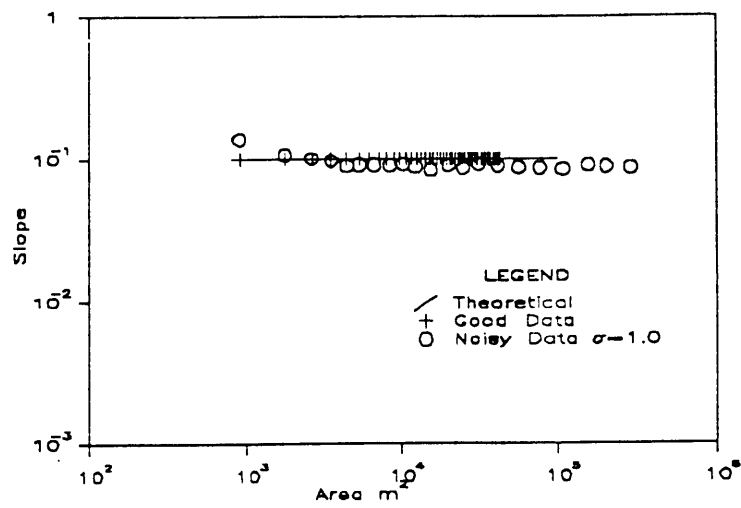
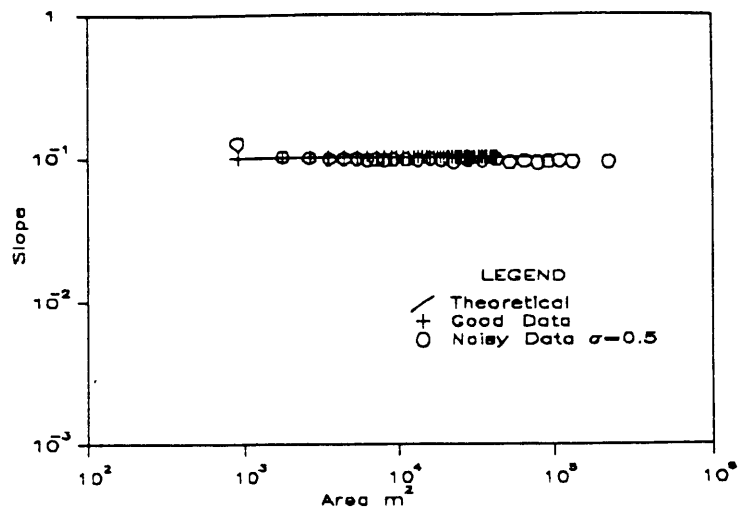


Figure 6.14. Slope-Area plots for Simulated Hillslope Profile A.

It is clear from the above analysis that the slope—area analysis is error prone, and that these errors may result in negative gradients in slope versus area plots, where a positive gradient is expected. Also the dynamic equilibrium assumptions upon which it is based may frequently not be valid. A combination of these factors is probably responsible for some inconsistency in the drainage densities from the slope—area scaling analysis. The constant drop analysis results were more consistent, but do not have the same theoretical justification as the slope—area scaling in terms of stability analysis. However, as practically applied the slope—area scaling break was usually just a steepening of a negative slope and not a change from positive to negative slope as required by the theoretical stability analysis. Given this, the consistency of the constant drop analysis probably makes it a more useful practical procedure.

Despite the effect of errors and concerns with the theoretical justification, the fact that there are fundamental or basic scales where the constant drop and slope—area scalings break, suggests different processes above and below the break. Here the different processes have been given the interpretation of hillslope and channel processes and the break is interpreted as drainage density. This interpretation is justified by the comparisons and at least order of magnitude agreement between the constant drop analyses, slope—area scaling, and Peuker—Douglas drainage densities.

Chapter 7

CONCLUSIONS

7.1 Introduction

Chapters 4 through 6 contain the main scientific results of this work. Here we summarize and highlight the important conclusions.

7.2 Planar Scaling

Chapter 4 discussed the planform scaling of river networks. Two distinct scaling regimes were found. At large scale, larger than the hillslope length or length scale associated with drainage density, the river network reaches everywhere and is thus space filling, characterized by a fractal dimension $D = 2$. This was observed in the data using three different techniques to measure D , as well as argued for physically. At smaller scales individual streams were found to be fractal with dimension D_ℓ just greater than 1 (1 – 1.2). This had been suggested by Mandelbrot (1983) from the relationship between slope and area (Equation 2.37). The relationship between network fractal dimension D and parameters characterizing scaling, i.e., Horton's length and bifurcation ratios and Tokunaga's parameters was given [Equations (4.17) and (4.33)]. Here it was important to recognize that the individual stream elements of which the network is composed may themselves be fractal with dimension D_ℓ , so D_ℓ enters into these relationships. With the space filling constraint ($D = 2$) and D_ℓ fixed, these relationships give bifurcation ratio R_b in terms of length ratio R_ℓ or Tokunaga parameter K in terms Q thus showing the relationship between scaling parameters. Hence only one parameter is needed to describe planform scaling in the network.

7.3 Slope Scaling

Chapter 5 discussed the scaling of slope with area as a scaling index. This was put in the context of networks using link magnitude as a surrogate measure for area. We showed (as had been seen before by Flint, 1974) the power relationship between Mean Slope and Area. This has been used by Gupta and Waymire (1989) to hypothesize that link slopes are self-similar. We showed that for our data this was not the case. The coefficient of variation of link slope increases with area or magnitude, ruling out self-similarity. The scaling of the full probability distribution of link slopes requires more general multi-scaling models to characterize it. A model that regarded links as composed of distinct steps in elevation fits the data well. The location and height of steps was taken as random and the observed scaling of the variance was reproduced when the mean density of steps (number of steps per unit length) scaled according to a power law. This model describes the nature of the multi-scaling of link slopes. The step-like behavior may be due to pools and riffles which Yang (1971a) suggests are due to a minimum energy principle. Further work is required to justify this or discover alternative physical mechanisms responsible for this scaling. We speculate that the step-like behavior may be due to intermittency and erraticism resulting from instability in the large scale sediment transport regime above the switch point discussed in Chapter 6.

7.4 Basic Scale

In Chapter 6 we point out that the scaling characterized in Chapter 5 cannot hold down to infinitely small scales and must break at some point. This break point represents a basic scale which we associate with hillslope length, or drainage density, by showing that the negative gradient of a log (slope)–log (area) plot can be associated with instability and hence channel formation while the positive slope implies stability and smooth hillslopes. The break point where gradient changes

therefore represents the transition scale or drainage density. Chapter 6 presents slope–area plots for much of our data. Many of these exhibit a break in gradient but the lower scale gradient is not positive. We show by simulation that data errors in DEM data induce a negative correlation between slope and area and suggest that this may be responsible for the lower scale gradient. We suggest that the break in gradient nevertheless represents a physical transition or basic scale that should be interpreted as drainage density.

Chapter 6 also uses the fact that the scaling of channel slopes with area is practically equivalent to the constant stream drop property. Statistical tests of the constant stream drop property for networks extracted with different support area result in the constant drop property being rejected for small support area, but accepted for large support area. The threshold support area at which this transition occurs is shown to result in drainage densities roughly equivalent to the drainage density estimated from slope scaling. The agreement of this data justifies both techniques for detecting the drainage density as a fundamental scale in the landscape. These drainage densities are also shown to correspond, although not quite as well, with drainage densities estimated from altogether different local procedures for detecting curvature in DEM's.

7.5 Concluding Remarks

This work has shown the feasibility of using DEM data for geomorphologic and hydrologic studies. Techniques have been developed that could be used in automated procedures for extracting channel networks from DEM's at a scale or drainage density that has some physical justifications in terms of land forming processes. These procedures are still fairly tentative though and need to be validated on high resolution data. The question of what resolution data is sufficiently detailed for hydrologic purposes is still not completely resolved. Where

the basic length scales are large (low drainage density) the same scale can be detected from 30m and 90m resolution data sets, suggesting that for these scales the 90m dataset is sufficient. However for smaller length scales (larger drainage densities) this is not the case. The question of resolutions will only be truly resolved by comparing to results obtained from very high resolution ($\pm 4\text{m}$ pixel) data sets. DEM's have proven to be a useful test in investigating and extending our understanding of the structures and scaling of river networks and landscapes.

7.6 Future Research

This work points to several areas where future research is required to: confirm the more tentative results; implement some of the techniques developed; and understand the scaling discovered.

Firstly it is important to test the procedures for identifying basic scales on more and higher resolution data sets. We need to more convincingly show that the results are not dependent on the resolution of the data available. Accurate, high resolution data is needed to resolve whether the negative gradient in slope–area plots at small area is due to data errors, as suggested here, or is really present in the landscape, in which case other explanations need to be sought.

Secondly, an explanation of the slope scaling characterized in Chapter 5 is needed. Yang (1971a) has suggested that pools and riffles are due to channels naturally evolving towards states that result in least time rate of energy expenditure. In the limit this results in long flat reaches of channel with practically no energy dissipation and sharp steps or discontinuities where the elevation drop occurs. We have reservations as to whether this thermodynamic principle is applicable here. In any event this thermodynamic principle does not predict the size or distribution of discrete steps. The slope scaling examined in Chapter 5 led to specific inferences about the size and distribution of steps. These need explanation.

We suggest looking to physical principles that result in scaling for an explanation. The notion of self-organized criticality (Bak, et al., 1987; Hwa and Kardar, 1989) has been used to describe the physics of fractals. The idea is that power law scaling and fractal properties arise as the minimally stable states of dynamical systems with extended spatial degrees of freedom. These minimally stable states are called critical states by the analogy with thermodynamics and the scaling behavior of substances near the thermodynamic critical point. There are indications that the landscape at scales larger than the drainage density scale may be in such a critical state. The governing equations (2.40 and 2.41) are unstable, but perturbations cannot grow without bound, due to the presence of diffusive mechanisms. The governing equations also follow conservation principles, a requirement for the renormalization procedures of Hwa and Kardar (1989) to be applied. We feel that the explanation of the slope scaling characterized in Chapter 5 may lie in understanding the governing equations in the context of self-organized criticality.

To prompt this understanding a modeling approach along the lines of Willgoose (1989) may be useful. A problematic issue is that of stability. Numerical diffusion may eliminate much of the instability present in the governing equations (2.40 and 2.41). If as we hypothesize, it is this instability that is responsible for the slope scaling variability of Chapter 5, then it may be hard to reproduce this slope scaling variability in the models. The Willgoose (1989) approach may be particularly prone to this problem as nodes are not permitted to revert back from channels to hillslopes. Once channelization has occurred, it is locked in, preventing any movement of the channel. It may be possible to circumvent this problem by using the idea due to Luke (1974) of channels as shock discontinuities. Numerical procedures using the method of characteristics to solve the governing equations in two dimensions need to be developed to explore this further. These procedures would have to include techniques to track the movement of discontinuities in two

dimensions and investigate their structure. Do they form a network? What scaling laws do "networks" of discontinuities obey?

One motivation for this work was the hope that it may lead to improved prediction of runoff from ungauged basins. It is not immediately apparent whether any progress has been made towards this goal. The measures of drainage density (basic horizontal length scale) and mean stream drop (basic vertical length scale) from DEM's are, we believe, more objective than their counterparts from topographic maps, which are subject to operator subjectivity and interpretation effects. A rainfall–runoff modeling exercise may benefit from being done at physically justifiable scales. Further work needs to be done on the relationship of these basic scales with variables describing streamflow, climate and geology. Streamflow records at several points within basins that have DEM data available should be obtained. Then the relationships between streamflow, at various time scales or recurrence intervals (e.g., annual average, annual maximum, two–year recurrence interval, etc.), and the basic scales as well as slope scaling parameters should be explored. Climatic geologic and lithologic variables should be incorporated where these are felt to be important.

Another approach to quantifying the relation between geomorphology and runoff may be a coupling of channel/landscape evolution models along the lines of Willgoose (1989) and Ahnert (1987) with more traditional rainfall–runoff models such as the SHE model (Abbot et al., 1986; Beven, 1985) or Topmodel (Beven and Kirkby, 1979; Beven and Wood, 1983). This would effectively involve the incorporation of more realistic runoff generation mechanisms, such as saturation from below and interflow, into the landscape evolution models. These mechanisms need to take account of the topography so as to correctly model enhanced runoff due to zones of convergence. The effect of spatial and temporal variability in rainfall needs to be included since it affects streamflow and may affect the landforms that

develop. Streamflow statistics at different points within river basins in these model landscapes need to be compiled so that their scaling and variability can be related to the basic scales, scaling and variability of the landscape. This modeling approach obviously suffers from the fact that it is a simplification of reality, but has the advantage that controlled experiments where single factors are varied can be conducted to try to establish causality in the relationship between independent and dependent variables.

An appealing notion is the idea that runoff production is somehow organized spatially in a way that is related to spatial organization in the network. Work to develop and check this may be worthwhile. We explored this approach in a limited way by looking at the spatial organization of pixels with large area to slope ratio. These are area's likely to generate runoff from the saturation from below mechanism according to the model of Beven and Kirkby (1979). Organization was defined using information entropy and information scaling notions from Hentchel and Procaccia (1983). The results (not given here because they were inconclusive) seemed to indicate that runoff generation area's had a basic scale associated with them that was effectively the same as the basic length scale of the network. This approach did not seem to be leading to new insights, perhaps because the physical justification for using entropy idea's was lacking. For this approach to be worthwhile physically justifiable measures of organization appropriate for runoff generation area's need to be developed.

Finally for work with digital elevation models to be implemented in a useful manner the procedures developed here need to be incorporated into computerized geographic information systems. There they can be coupled with other hydrologically relevant data, such as radar rainfall measurements and land use and cover data, perhaps from satellites, to be used for flood forecasting and land management.

REFERENCES

- Abbott, M.B., J.C. Bathurst, J.A. Cunge, P.E. O'Connell, and J. Ramussen (1986), "An introduction to the European hydrological system – Systeme Hydrologique Europeen, "SHE", 2: Structure of a physically based distributed modelling system," J. Hydrol., 87, 61–77.
- Abrahams, A. D. (1972), "Factor analysis of drainage basin properties: evidence for stream abstraction accompanying degradation of relief," Water Resources Research, 8:624–633.
- Abrahams, A. D. (1984), "Channel networks: A geomorphological perspective," Water Resources Research, 20(2):161–168.
- Abrahams, A. D. and A. J. Miller (1982), "The mixed gamma model for channel link lengths," Water Resources Research, 18:1126–1136.
- Ahnert, F. (1984), "Local relief and the height limits of mountain ranges," American Journal of Science, 284:1035–1055.
- Ahnert, F. (1987), "Process–response models of denudation at different spatial scales," in Geomorphological Models, ed. F. Ahnert, Catena supplement 10:31–50.
- Andrews, D. J. and R. C. Bucknam (1987), "Fitting degradation of shoreline scarp by a nonlinear diffusion model," Journal of Geophysical Research, 92(B12):12857–12867.
- Andrle, R. and A. D. Abrahams (1989), "Fractal techniques and the surface roughness of talus slopes," Earth Surface Processes and Landforms, 14(3):197–209.
- Bak, P., C. Tang, and K. Wiesenfeld (1987), "Self–organized criticality: an explanation of 1/f noise," Physical Review Letters, 59(4):381–384.
- Band, L. E. (1985), "Simulation of slope development and the magnitude and frequency of overland flow erosion in an abandoned hydraulic gold mine," in

- Models in Geomorphology, ed. M. J. Woldenburg, Proceedings of the 14th Annual Geomorphology Symposium, held at Binghamton, NY, 1983. Symposium No. 14.
- Band, L. E. (1986) "Topographic partition of watersheds with digital elevation models," Water Resources Research, 22(1):15–24.
- Beven, K.J. (1985), "Distributed models," in Anderson, M.G. and T.P. Burt (eds.), Hydrological Forecasting, John Wiley and Sons, Chichester, 604 pp.
- Beven, K. J. and Kirkby, M. J. (1979), "A physically based variable contributing area model of basin hydrology," Hydrological Sciences Bulletin, 24(1):43–69.
- Beven, K.J. and E.F. Wood (1983), "Catchment Geomorphology and the Dynamics of Runoff Contributing Areas," Journal of Hydrology, 65:139–158.
- Bras, R. L. and I. Rodriguez-Iturbe (1985), Random Functions and Hydrology, Addison Wesley, Reading, MA.
- Broscoe, A. J. (1959), "Quantitative analysis of longitudinal stream profiles of small watersheds," Office of Naval Research, Project NR 389–042, Technical Report No. 18, Department of Geology, Columbia University, New York, 73 pp.
- Carrara, A. (1988), "Drainage and divide networks derived from high fidelity digital terrain models," in C. F. Chuna, et al. (eds.), Quantitative Analysis of Mineral and Energy Resources, NATO ASI Series C, Mathematical and Physical Sciences, Vol. 223, Proceedings of the NATO Advanced Study Institute, Italy, June 22–July 4, 1986, D. Reidel Publishing Company.
- Carson, M. A. and M. J. Kirkby (1972), Hillslope Form and Process," Cambridge University Press, 475 p.
- Chorley, R. J. (1957), "Illustrating the laws of morphometry," Geological Magazine, 94:140–150.

- Church, M. and D. M. Mark (1980), "On size and scale in geomorphology," Progress in Physical Geography, 4:342–390.
- Cox, D. R. and Isham, V., (1980), Point Processes, Chapman and Hall, London and New York, 182 pp.
- Culling, W. E. H. (1960) "Analytical theory of erosion," Jour. Geol., 68:336–344.
- Culling, W. E. H. (1963), "Soil creep and the development of hillside slopes," Jour. Geol., 71:127–161.
- Culling, W. E. H. (1965), "Theory of erosion on soil covered slopes," Journal of Geology, 73:230–254.
- Culling, W. E. H. (1986), "On Hurst phenomenon in the landscape," Trans. Japanese Geomorphological Union, 7(4):221–243.
- Culling, W. E. H. and M. Datko (1987), "The fractal geometry of the soil-covered landscape," Earth Surfaces Processes and Landforms, 12:369–385.
- Davis, W. M. (1899), "The geographical cycle," Geogr. J., 14:481–504 (reproduced in Geographical Essays, edited by W. M. Davis, Ginn, Boston, MA, 1909).
- Davison, C. (1889), "On the creeping of the soil-cap through the action of frost", Geol. Mag. 6:255.
- Dunne, T. (1980), "Formation and controls of channel networks," Progress in Physical Geography, 4:211–239.
- Eagleson, P. (1970), Dynamic Hydrology, McGraw-Hill, New York.
- Eyles, R. J. (1968), "Stream net ratios in west Malaysia," Bull. of the Geol. Soc. of Amer., 79:701–712.
- Feller, W. (1971), An Introduction to Probability Theory and Its Applications, Volume II, John Wiley and Company, 2nd edition, 669 pages.
- Flint, J. J. (1974), "Stream gradient as a function of order, magnitude and discharge," Water Resources Research, 10(5):969–973.

- Goodchild, M. F. (1988), "Lakes on fractal surfaces: a null hypothesis for lake-rich landscapes," Math. Geology, 20(6).
- Goodchild, M. F., B. Klinbenger, M. Glioca and M. Hasan (1985), "Statistics of hydrologic networks on fractional brownian surfaces," Modeling and Simulation, V. 16 (Proceedings of the 16th Annual Pittsburgh Conference), pp. 317–23.
- Goodchild, M. F. and D. M. Mark (1987), "The fractal nature of geographic phenomena," Annals Assoc. Amer. Geog., 77(2):265–278.
- Gupta, V. K. and Mesa, O. J. (1988), "Runoff generation and hydrologic response via channel network geomorphology — recent progress and open problems," Journal of Hydrology, 102:3–28.
- Gupta, V. K., I. Rodriguez-Iturbe, and E. F. Wood (eds.) (1986), Scale Problems in Hydrology Runoff Generation and Basin Response, D. Reidel Publishing Company, Dordrecht.
- Gupta, V. K. and E. Waymire (1983), "On the formation of an analytical approach to hydrologic response and similarity at the basin scale," Journal of Hydrology, 65:95–123.
- Gupta, V. K. and E. Waymire (1989), "Statistical self-similarity in river networks parameterized by elevation," Water Resources Research, 25(3):463–476.
- Gupta, V. K., E. Waymire, and C. T. Wang (1980), "A representation of an instantaneous unit hydrograph from geomorphology," Water Resources Research, 16(5):855–862.
- Gupta, V. K., E. Waymire, and I. Rodriguez-Iturbe (1986), "On scales, gravity and network structure in basin runoff," In: Scale Problems in Hydrology, V. K. Gupta, et al., (editors), D. Reidel, Dordrecht, Holland.

- Hack, J. T. (1957), "Studies of longitudinal stream profiles in Virginia and Maryland," U.S.G.S. Professional Paper 294-B, pp. 45-97.
- Hentschel, H. G. E. and I. Procaccia (1983), "The infinite number of generalized dimensions of fractals and strange attractors," Physica, 8D:435-444.
- Hinkley, D. V. (1969), "Influence about the intersection in two phase regression," Biometrika, 56(3):495-504.
- Hirano, M. (1975), "Simulation of developmental process of interfluvial slopes with reference to graded form," Jour. of Geology, 83:113-123.
- Hjelmfelt, A. T. (1988), "Fractals and the river-length catchment area ratio," Water Resources Bulletin, 24(2):455-459.
- Horton, R. E. (1932), "Drainage basin characteristics," Transactions American Geophysical Union, 13:350-361.
- Horton, R. E. (1945), "Erosional development of streams and their drainage basins: hydrophysical approach to quantitative morphology," Geol. Soc. Amer. Bull., 56:275-370.
- Huang, K. (1963), Statistical Mechanics, John Wiley and Sons, New York, 470 p.
- Hugget, R. J. (1988), "Dissipative systems: Implications for geomorphology," Earth Surface Processes and Landforms, 13:45-49.
- Hurst, H.E. (1951), "Long-term Storage Capacity of Reservoirs," Transactions American Society of Civil Engineers, 116:770-799.
- Hwa, T. and M. Kardar (1989), "Dissipative transport in open systems: an investigations of self-organized criticality," Physical Review Letters, 62:1813-1816.
- James, W. R. and W. C. Krumbein (1969), "Frequency distribution of stream link lengths," Journal of Geology, 77:544-565.
- Jarvis, R. S. and M. J. Woldenberg (1984), River Networks, Hutchinson Ross

Publishing Company, Stroudsburg.

- Karlinger, M. R. and B. M. Troutman (1989), "A random spatial network model based on elementary postulates," Water Resources Research, 25(5):793–798.
- Kirkby, M. J. (1969), "Erosion by water on hillslopes," in Water, Earth and Man, ed. R. J. Chorley, pp. 229–38.
- Kirkby, M. J. (1971), "Hillslope process–response models based on the continuity equation," in Slopes Form and Processes, Institute of British Geographers, Special Publication No. 3.
- Kirkby, M. J. (1976), "Tests of the random model and its applications to basin hydrology," Earth Surface Processes, 1:197–212.
- Kirkby, M. J. (1980), "The stream head as a significant geomorphic threshold," in Thresholds in Geomorphology, ed. D. R. Coates and J. D. Vitek.
- Kirkby, M. J. (1986), "Modelling some influences of soil erosion, landslides and valley gradient on drainage density and hollow development," in Geomorphological Models, ed. F. Ahnert, Catena, Supplement 10:1–14.
- La Barbera, P. and R. Rosso (1987), "The fractal geometry of river networks," EOS Transactions American Geophysical Union, 68(44):1276.
- La Barbera, P. and R. Rosso (1989), "On the fractal dimension of stream networks," Water Resources Research, 25(4):735–741.
- Leopold, L. B. and W. B. Langbein (1962), "The concept of entropy in landscape evolution," U.S.G.S., Prof. Paper 500–A.
- Leopold, L. B. and T. Maddock (1953), "The hydraulic geometry of stream channels and some physiographic implications," U. S. Geol. Surv. Prof. Paper 252.
- Leopold, L. B. and J. P. Miller (1956), "Ephemeral streams – Hydraulic factors and their relation to the drainage net," U. S. Geol. Survey Prof. Paper 282–A.
- Leopold, L. B., M. G. Wolman and J. P. Miller (1964), Fluvial Processes in Geomorphology, W. H. Freeman, San Francisco.

- Lovejoy, S., D. Schertzer, and A. A. Tsonis (1987), "Functional box counting and multiple elliptical dimensions in rain," Science, 235:1036–1038.
- Luke, J. C. (1972), "Mathematical models for landform evolution," Journal of Geophysical Research, 77(14):2460–2464.
- Luke, J. C. (1974), "Special solutions for nonlinear erosion problems," Journal of Geophysical Research, 79(26):4035–4040.
- Mandelbrot, B. B. (1977), Fractals, Form, Chance and Dimension, W. W. Freeman and Company, San Francisco.
- Mandelbrot, B. B. (1983), The Fractal Geometry of Nature, W. H. Freeman and Company, New York.
- Mark, D. M. (1983), "Relation between field surveyed channel networks and map based geomorphic measures, Inez, Kentucky," Annals of the Association of American Geographers, 73(3):358–372.
- Mark, D. M. (1988), "Network models in geomorphology," Chapter 4 in Modelling in Geomorphological Systems, ed. M. G. Anderson, John Wiley.
- Mark, D. M. and P. B. Aronson (1984), "Scale-dependent fractal dimensions of topographic surfaces: An empirical investigation with applications in geomorphology and computer mapping," Math. Geol. 16(7):671–683.
- Melton, M. A. (1958), "Geometric properties of mature drainage systems and their representation in an E_4 phase space," Journal of Geology, 66:35–66.
- Mesa, O. J. (1986), "Analysis of channel networks parameterized by elevation," Ph.D. dissertation, Department of Civil Engineering, University of Mississippi.
- Moore, I., E. M. O'Loughlin and G. J. Burch (1988), "A contour based topographic model for hydrological and ecological applications," Earth Surface Processes and Landforms, 13:305–320.
- Morisawa, M. E. (1962), "Quantitative geomorphology of some watersheds in the

- Appalachian plateau," Geol. Soc. Am. Bull., 73:1025–1046.
- Morris, D. G. and R. G. Heerdegen (1988), "Automatically derived catchment boundaries and channel networks and their hydrological applications," Geomorphology, 1:131–141.
- Musgrave, G. W. (1947), "The quantitative evaluation of factors in water erosion: a first approximation," J. Soil Wat. Conserv., 2, 133–38.
- Negele, J. W. and H. Orland (1987), Quantum many-particle systems, Frontiers in Physics:68, Addison Wesley, Redwood City, CA, 459 pp.
- O'Callaghan, J. F. and D. M. Mark, (1984), "The extraction of drainage networks from digital elevation data," Computer Vision, Graphics and Image Processing, 28:323–344.
- O'Loughlin, E. M. (1986), "Prediction of surface saturation zones in natural catchments by topographic analysis," Water Resources Research, 22(5):794–804.
- Palacios-Velez, O. L., and B. Cuevas-Renaud (1986), "Automated river-course, ridge and basin delineation from digital elevation data," Journal of Hydrology, 86:299–314.
- Peucker, T. K. and D. H. Douglas (1975), "Detection of surface-specific points by local parallel processing of discrete terrain elevation data," Comput. Graphics Image Process., 4:375–387.
- Priest, R.F., J.M. Bradford, and R.G. Spomer (1975), "Mechanisms of erosion and sediment movement from gullies," Proceedings of the Sediment Yield Workshop, USDA, Sedimentation Laboratory, Oxford, Mississippi, November 1972.
- Rodriguez-Iturbe, I., M. Gonzalez-Sanabria, and R. L. Bras (1982), "A geomorphoclimatic theory of the instantaneous unit hydrograph," Water Resources Research, 18(4):877–886.

- Rodriguez-Iturbe, I. and V. K. Gupta (eds.) (1983), "Scale problems in hydrology," Journal of Hydrology, Special Issue, 65.
- Rodriguez-Iturbe, I. and J. B. Valdes (1979), "The geomorphologic structure of hydrologic response," Water Resources Research, 15(5):1409-1420.
- Scheidegger, A.E. (1970), Theoretical Geomorphology, Berlin: Springer Verlag.
- Schumm, S.A. (1956), "Evolution of drainage systems and slopes in Badlands at Perth Amboy, New Jersey," Geological Society of America Bulletin, 67:597-646.
- Schumm, S. A. (1964), "Seasonal variations of erosion rates on hillslopes in Western Colorado," Z. Geomorph., Suppl. 5, 215-38.
- Shreve, R. L. (1966), "Statistical law of stream numbers," Journal of Geology, 74:17-37.
- Shreve, R. L. (1967), "Infinite topologically random channel networks," Journal of Geology, 75:178-186.
- Shreve, R. L. (1969), "Stream lengths and basin areas in topologically random channel networks," Journal of Geology, 77:397-414.
- Smart, J. S. (1968), "Statistical properties of stream lengths," Water Resources Research, 4(5):1001-1014.
- Smart J. S. (1978), "The analysis of drainage network composition," Earth Surface Processes, 3:129-170.
- Smart, J. S. (1981), "The random model in fluvial geomorphology," in Fluvial Geomorphology, ed. M. Morisawa, a Proceedings volume of the 4th annual Geomorphology Symposia series held at Binghamton, NY, 1973.
- Smith, K. G. (1950), "Standards for grading texture of erosional topography," Amer. Jour. of Sci., 248:655-668.
- Smith, T. R. (1974), "A derivation of the hydraulic geometry of steady-state channels from conservation principles and sediment transport laws," Journal

- of Geology, 82:98–104.
- Smith, T. R. and F. P. Bretherton (1972), "Stability and the conservation of mass in drainage basin evolution," Water Resources Research, 8(6):1506–1529.
- Solow, A. R. (1987) "Testing for climate change: an application of the two phase regression model," Journal of Climate and Applied Meteorology, 26:1401–1405.
- Strahler, A. N. (1952), "Hypometric (area altitude) analysis of erosional topography," Geol. Soc. Amer. Bull., 63:1117–1142.
- Strahler, A. N. (1957), "Quantitative analysis of watershed geomorphology," Transactions American Geophysical Union, 38:913–920.
- Tarboton, D. G., R. L. Bras, and I. Rodriguez-Iturbe (1988), "The fractal nature of river networks," Water Resources Research, 24(8):1317–1322.
- Thornes, J. B. (1980), "Structural instability and ephemeral channel behavior," Zeitschrift für Geomorphologie, Supplement 36:233–244.
- Thornes, J.B. (1983), "Evolutionary geomorphology," Geography, pp. 225–235.
- Tokunaga, E. (1978), "Consideration on the composition of drainage networks and their evolution," Geographical Report No. 13, Tokyo Metropolitan University.
- Troutman, B. M. and M. R. Karlinger (1984), "On the expected width function for topologically random channel networks," Journal Appl. Prob., 21:836–849.
- Troutman, B. M. and M. R. Karlinger (1985), "Unit hydrograph approximations assuming linear flow through topologically random channel networks," Water Resources Research, 21(5):743–754.
- U. S. Agricultural Research Service (1961), "A universal equation for predicting rainfall–erosion losses," Spec. Rep., 22–26.
- U. S. Geological Survey (1987), "Digital elevation models, data users guide 5," U.S. Department of the Interior, Reston, VA, 38 pp.

- van der Tak, L. and R. L. Bras (1989), "Stream length distributions and hillslopes stream effects in the geomorphologic IUH," submitted to Water Resources Research.
- Voss, R. F. (1986), "Random fractals: characterization and measurement," Phys. Sci., T13:27–32.
- Willgoose, G. R. (1989), "A physically based channel network and catchment evolution model," Ph.D. Thesis, M.I.T., Cambridge, MA.
- Wolman, M. G. (1955), "The natural channel of Brandywine Creek, Pennsylvania," U. S. Geological Survey Prof. Paper 271, 56pp.
- Wood, E. F., M. Sivaplan, K. Beven, and L. Band (1988), "Effects of spatial variability and scale with implications to hydrologic modeling," Journal of Hydrology, 102:29–47.
- Wood, W. F. and J. B. Snell (1957), "The dispersion of geomorphic data around measures of central tendency and its applications, Natick, MA," U. S. Army Quartermaster Research and Development Center, Research study report GA–8, 204 pp.
- Woodruff, J. F. (1964), "A comparative analysis of selected drainage basins," The Professional Geographer, 16(4):15–19.
- Yang, C. T. (1971a), "Formation of riffles and pools," Water Resources Research, 7(6):1567–1574.
- Yang, C. T. (1971b), "Potential energy and stream morphology," Water Resources Research, 7(2):311–322.
- Zhang, Y. (1982), "Plotting positions of annual flood extremes considering extraordinary values," Water Resources Research, 18(4):859–864.
- Zingg, A. W. (1940), "Degree and length of land slope as it affects soil loss in runoff," Agric. Engng 21, 59–64.

APPENDIX

Computer Codes.

DEMSETUP.FOR

```

C
C   Program to set up digital elevation model.
C
C   BY DAVID G TARBOTON
C
C   This code reads a dem file in standard format as supplied by the
C   U.S.G.S. described in U.S. Geological survey (1987), "Digital elevation
C   models, data users guide 5," U.S. Department of the Interior, Reston,
C   VA, 38 pp, and outputs the data in a binary matrix file.
C
C   Input is read from file DEMSETUP.IN which consists of 2 up to 80
C   character records. The first record is the name of the input file and
C   the second record the name of the binary matrix file which must end with
C   .BIN for the data to be written unformatted (i.e. binary) which is most
C   efficient from a storage point of view. A file DEMINFO.DAT is also
C   output. This gives information about the size and location of the data
C   set read from the U.S.G.S. input file header record.
C
C   This program uses subroutines from DEMUTIL.FOR, the set of subroutines
C   for I/O of binary matrix files.
C
C   PARAMETER (IGX=1201, IGY=1201)
C   INTEGER*2 ELEV (IGY, IGX), INELEV (IGY)
C   DIMENSION DCORNS (4, 2)
C   DOUBLE PRECISION CORNS (4, 2), XMIN, XMAX, YMIN, YMAX, X, Y, DATUM
C   CHARACTER*80 DEMIN, DEMOUT
C   CHARACTER*1024 RECORD
C   CHARACTER*144 HEADER
C   CHARACTER*6 VUNITS (2), HUNITS (0:3)
C   DATA ARCSEC, RAD/30.89, 57.2957795131/
C   DATA VUNITS/'FEET ', 'METRES'/
C   DATA HUNITS/'RADIAN', ' FEET ', 'METRES', 'ARCSEC'/
C   OPEN (UNIT=7, FILE='DEMSETUP.IN', STATUS='OLD')
C   READ (7, 50) DEMIN, DEMOUT
50  FORMAT (A80/A80)
C
C   OPEN (UNIT=8, FILE=DEMIN, STATUS='OLD', READONLY)
C   OPEN (UNIT=11, FILE='DEMINFO.DAT', STATUS='NEW')
C
C   READ FIRST RECORD U.S.G.S. A FORMAT
C
C   READ (8, 100) HEADER, IUNITH, IUNITV, (CORNS (I, 1), CORNS (I, 2), I=1, 4),
& DX, DY, DZ, NP
C   IUNITH GIVES PLANAR COORDS (0=RADIAN, 1=FEET, 2=METRES, 3=ARCSEC)
C   IUNITV GIVES VERT COORDS (1=FEET, 2=METRES)
C   CORNS IS ARRAY THAT CONTAINS CORNER CO-ORDS
C   DX, DY AND DZ ARE SPATIAL RESOLUTIONS IN THREE DIRECTIONS
C   NP = NUMBER OF PROFILES
100  FORMAT (A144, 384X, I6, I6, 6X, 4 (2D24.15), 78X, 3E12.6, 6X, I6)
C   WRITE (11, 60) HEADER (1:80)
C   WRITE (11, 62) NP, HUNITS (IUNITH), VUNITS (IUNITV)
60  FORMAT (1X, A80)
62  FORMAT (1X, I5, ' PROFILES'/1X, 'PLANAR UNITS', 1X, A6
& /1X, 'ELEVATION UNITS ', A6//1X, 'CORNERS AT'/
& 1X, ' X Y')
C   DO 1 I=1, 4
1   WRITE (11, 65) CORNS (I, 1), CORNS (I, 2)
65  FORMAT (1X, 2E24.15)
C   IF (IUNITH.EQ.3) THEN ! TRANSLATE ARC SECONDS TO DEGREES
C   WRITE (11, *) 'CORNERS IN DEGREES'
C   DSUM=0.
C   DO 2 I=1, 4
C   DCORNS (I, 1) =CORNS (I, 1) /3600.
C   DCORNS (I, 2) =CORNS (I, 2) /3600.
C   WRITE (11, 71) DCORNS (I, 1), DCORNS (I, 2)
71  FORMAT (1X, 2F24.6)
C   DSUM=DSUM+DCORNS (I, 2)
2   CONTINUE
C   DSUM=DSUM/4.
C   DXM=ARCSEC*DX*COS (DSUM/RAD)
C   DYM=ARCSEC*DY
C   ELSE

```

```

DXM=DX
DYM=DY
ENDIF
WRITE (11, 72) DXM, DYM
72  FORMAT (1X, 'DXM=', F10.3, ' DYM=', F10.3)
C---FIND MIN AND MAX COORDS
XMIN=CORNS (1, 1)
YMIN=CORNS (1, 2)
XMAX=CORNS (1, 1)
YMAX=CORNS (1, 2)
DO 3 I=2, 4
XMIN=MIN (XMIN, CORNS (I, 1))
YMIN=MIN (YMIN, CORNS (I, 2))
XMAX=MAX (XMAX, CORNS (I, 1))
3  YMAX=MAX (YMAX, CORNS (I, 2))
C----BOUNDS OF GRID
MINX=INT (XMIN/DX)
MAXX=INT (XMAX/DX)
MINY=INT (YMIN/DY)
MAXY=INT (YMAX/DY)
IF (XMAX/DX.GT.FLOAT (MAXX)) MAXX=MAXX+1
IF (YMAX/DY.GT.FLOAT (MAXY)) MAXY=MAXY+1
NX=MAXX-MINX+1
NY=MAXY-MINY+1
XGMIN=DX*FLOAT (MINX)
XGMAX=DX*FLOAT (MAXX)
YGMIN=DY*FLOAT (MINY)
YGMAX=DY*FLOAT (MAXY)
WRITE (11, 61) NX, NY
61  FORMAT (1X, 'DEM GRID ', I5, ' BY', I5)
WRITE (11, 70) XGMIN, XGMAX, YGMIN, YGMAX
70  FORMAT (1X, 'GRID BOUNDARIES'/1X, 'XMIN=', F15.1/
& 1X, 'XMAX=', F15.1/1X, 'YMIN=', F15.1/1X, 'YMAX=', F15.1)
C---INITIALISE MATRIX
DO 4 I=1, NY
DO 4 J=1, NX
4  ELEV (I, J) = 0
C---READ IN PROFILES
DO 5 IP=1, NP
200 READ (8, 200) RECORD
FORMAT (A1024)
READ (RECORD, 205) NN, X, Y, DATUM
C  WRITE (11, *) 'ROW', IP, NN, ' ELEVS WITH DATUM', DATUM
C  WRITE (11, *) X, Y
205  FORMAT (12X, I6, 6X, 3D24.15)
READ (RECORD, 206) (INELEV (I), I=1, MIN (NN, 146))
206  FORMAT (144X, 146I6)
IF (NN.GT.146) THEN ! RECORD OVERFLOWS
NTOGO=NN-146
NRECS=(NTOGO-1)/170+1
DO 6 IREC=1, NRECS
IST=147+(IREC-1)*170
IEND=MIN (NN, IST+169)
6  READ (8, 207) (INELEV (I), I=IST, IEND)
207  FORMAT (170I6)
ENDIF
C----STORE ELEVS READ IN IN ARRAY
ICOL=NINT ((X-XGMIN)/DX)+1
IROFF=NINT ((YGMAX-Y)/DY)+2
DO 7 I=1, NN
7  ELEV (IROFF-I, ICOL) = INELEV (I) + NINT (DATUM)
5  CONTINUE
CALL IWR2 (ELEV, DEMOUT, NX, NY, IGY, DXM, DYM)
STOP 'WHAT A PLEASURE TO FINISH THAT ONE'
END

```

DEMSETUP.IN

```

dem tomb.dat
tomb.BIN

```

DEMCOMB.M.FOR

```
C
C   Program to combine digital elevation models.
C
C   CREATED BY DAVID G TARBOTON
C
C   This program reads and combines two or more adjacent binary matrix files
C   into one binary matrix file. It is used for setting up data sets that
C   span several DEM quadrangles.
C
C   Input is read from file DEMCOMB.IN which has the following structure.
C   First Record: Name of final combined output matrix file.
C   2nd Record:   Name of first input matrix file.
C   3rd Record:   Row then column of element (1,1) of the input file in the
C                 combined output file.
C   Subsequent pairs of records: Same as the second and third records for
C   the remainder of input files.
C
C   No data is recorded as zero elevation so the program checks that where
C   files overlap the non zero elevations correspond and does not overwrite
C   a non zero elevation with a zero elevation.
C
PROGRAM DEMCOMB
PARAMETER (IGX=2401, IGY=1201)
INTEGER*2 ELEV (IGY, IGX), TROW (IGX)
CHARACTER*80 DEM, NEWFILE
CHARACTER*4 BIN
CHARACTER*11 FMAT
DATA BIN / '.BIN' /
OPEN (UNIT=11, FILE='DEMCOMB.IN', STATUS='OLD', READONLY)
READ (11, 22) NEWFILE
NXM=0
NYM=0
C---INITIALIZE ELEV
DO 2 I=1, NY
  DO 2 J=1, NX
    ELEV (I, J) =0
2  CONTINUE
1  READ (11, 22, END=99) DEM
22  FORMAT (A80)
    READ (11, *) IROW, ICOL
C
C   SEARCH DEM FILE NAME FOR .BIN - IF IT IS PRESENT IT IS A BINARY FILE
C
    FMAT='FORMATTED '
    DO 21 I=1, 77
      IF (DEM (I: I+3) .EQ. BIN) THEN
        FMAT='UNFORMATTED'
        GO TO 3
      ENDIF
21  CONTINUE
3   OPEN (UNIT=10, FILE=DEM, STATUS='OLD', FORM=FMAT)
C
C   READ OLD DEM
C
    IF (FMAT .EQ. 'UNFORMATTED') THEN
      READ (10) NX, NY, DX, DY
      NXM=MAX (NXM, ICOL+NX-1)
      NYM=MAX (NYM, IROW+NY-1)
      WRITE (6, *) NXM, NYM, DEM
      IF (NXM.GT. IGX. OR. NYM.GT. IGY) THEN
        STOP 'DIMENSIONS TOO SMALL'
      ENDIF
      DO 18 I=1, NY
        READ (10) (TROW (J), J=1, NX)
        DO 18 J=1, NX
          IF (TROW (J) .GT. 0) THEN
            IF (ELEV (I+IROW-1, J+ICOL-1) .EQ. 0) THEN
              ELEV (I+IROW-1, J+ICOL-1) =TROW (J)
            ELSE IF (TROW (J) .NE. ELEV (I+IROW-1, J+ICOL-1)) THEN
              WRITE (6, 30) I, J, DEM
30             FORMAT (1X, 'NON ZERO ELEV THAT DOES NO MATCH AT', 2I5 /
                & 'FROM FILE ', A80)
            ENDIF
          ENDIF
        ENDIF
18  CONTINUE
    CLOSE (10)
```



```

ELSE
READ (10,*)NX,NY,DX,DY
NXM=MAX(NXM,ICOL+NX-1)
NYM=MAX(NYM,IROW+NY-1)
WRITE(6,*)NXM,NYM,DEM
IF(NXM.GT.IGX.OR.NYM.GT.IGY)THEN
STOP'DIMENSIONS TOO SMALL'
ENDIF
DO 8 I=1,NY
READ(10,*)(TROW(J),J=1,NX)
DO 8 J=1,NX
IF(TROW(J).GT.0)THEN
IF(ELEV(I+IROW-1,J+ICOL-1).EQ.0)THEN
ELEV(I+IROW-1,J+ICOL-1)=TROW(J)
ELSE IF(TROW(J).NE.ELEV(I+IROW-1,J+ICOL-1))THEN
WRITE(6,30)I,J,DEM
ENDIF
ENDIF
8 CONTINUE
CLOSE(10)
ENDIF
GO TO 1

C
C WRITE NEWFILE
C
C SEARCH DEM FILE NAME FOR .BIN - IF IT IS PRESENT IT IS A BINARY FILE
C
99 FMT='FORMATTED '
DO 23 I=1,77
IF(NEWFILE(I:I+3).EQ.BIN)THEN
FMT='UNFORMATTED'
GO TO 31
ENDIF
23 CONTINUE
31 OPEN(UNIT=12,FILE=NEWFILE,STATUS='NEW',FORM=FMT)
IF(FMT.EQ.'UNFORMATTED')THEN
WRITE(12)NXM,NYM,DX,DY
DO 9 I=1,NYM
9 WRITE(12)(ELEV(I,J),J=1,NXM)
ELSE
WRITE(12,*)NXM,NYM,DX,DY
DO 10 I=1,NYM
10 WRITE(12,100)(ELEV(I,J),J=1,NXM)
100 FORMAT(1X,21I6)
ENDIF
END

```

DEMCOMBM.IN

```

stregis.BIN
wallacenet.BIN
33 1 ROW, COL
saltesenw.BIN
28 115
saltesene.BIN
22 429
haugannw.BIN
15 743
hauganne.BIN
9 1057
stregisnw.BIN
1 1371
saltesese.BIN
485 437
haugansw.BIN
479 752
hauganse.BIN
472 1066
stregissw.BIN
464 1381
simmonsnet.BIN
935 1076
illinoisnwt.BIN
927 1391

```

DEMEX.FOR

```
C      Program to extract portion of DEM matrix file.
C
C      CREATED BY DAVID G TARBOTON
C
C      Input is read form file DEMEX.In in the following format:
C      Record 1: Number of bits in binary (unformatted files to be read/written)
C                (2= 2 bit integer, 4= 4 bit integer, anything else= real)
C      Record 2: File name of input file
C      Record 3: File name for writing extracted file
C      Record 4: First column, Last column, First row, Last row of portion to be
C                extracted from input file and written to extracted file.
C
C      This program uses subroutines from DEMUTIL.FOR, the set of subroutines
C      for I/O of binary matrix files.
C
C      PROGRAM DEMEX
C      parameter(igx=1201,igy=1201)
C      INTEGER*2 ia2(igy,igx)
C      integer ia(igy,igx)
C      DIMENSION A(IGY,IGX)
C      EQUIVALENCE(a(1,1),Ia(1,1),Ia2(1,1))
C      CHARACTER*80 DEM,NEWFILE
C      OPEN(UNIT=11,FILE='DEMEX.IN',STATUS='OLD')
C      read(11,*)ibits
C      READ(11,22)DEM,NEWFILE
22  FORMAT(A80/A80)
C      READ(11,*)IXMIN,IXMAX,IYMIN,IYMAX
C---read old file
C      if(ibits.eq.2)then
C          call iread2(ia2,dem,nx,ny,igy,dx,dy)
C
C      create NEWFILE
C
C          nnx=ixmax-ixmin+1
C          nny=ymax-iymin+1
C          DO 9 I=1,nny
C              do 9 j=1,nnx
C                  ia2(i,j)=ia2(i+iymin-1,j+ixmin-1)
9          continue
C          call iwr2(ia2,newfile,nnx,nny,igy,DX,DY)
C          else if(ibits.eq.4)then
C              call iread(ia,dem,nx,ny,igy,dx,dy)
C
C      create NEWFILE
C
C          nnx=ixmax-ixmin+1
C          nny=ymax-iymin+1
C          DO 19 I=1,nny
C              do 19 j=1,nnx
C                  ia(i,j)=ia(i+iymin-1,j+ixmin-1)
19          continue
C          call iwr(ia,newfile,nnx,nny,igy,dx,dy)
C          else
C              call rread(a,dem,nx,ny,igy,dx,dy)
C
C      create NEWFILE
C
C          nnx=ixmax-ixmin+1
C          nny=ymax-iymin+1
C          DO 29 I=1,nny
C              do 29 j=1,nnx
C                  a(i,j)=a(i+iymin-1,j+ixmin-1)
29          continue
C          call rwr(a,newfile,nnx,nny,igy,dx,dy)
C      ENDIF
C      END
```

DEMEX.IN

```
2
tomb.BIN
w7elev.BIN
40 210 47 227
```

DEMUTIL.FOR

```
C   This is a set of subroutines to do Input/Output of DEM matrix files
C
C       CREATED BY DAVID G TARBOTON
C
C   The format of Matrix files is:
C
C   First record: No. of columns(NX), No. of Rows(NY),
C                   Column Spacing(DX) (meters), Row Spacing(DY)
C   Remaining records: Matrix of elements in order read/written using
C   DO 9 I=1,NY
C 9   READ/WRITE( ) (ARRAY(I,J),J=1,NX)
C
C   The file is unformatted, i.e. Binary if extension is .BIN (must be Upper
C   Case), Otherwise Free format.
C
C   The following Routines are included.
C   IWR: To write Integer*4 matrix.
C   RWR: To write Real*4 matrix.
C   IWR2: To write Integer*2 matrix.
C   IREAD: To read Integer*4 matrix.
C   RREAD: To read Real*4 matrix.
C   IREAD2: To read Integer*2 matrix.
C
C   ROUTINE TO WRITE INTEGER FILE
C
C       SUBROUTINE IWR(ARRAY,FILE,NX,NY,IGRID,DX,DY)
C           INTEGER ARRAY(IGRID,1)
C           CHARACTER*80 FILEN
C           CHARACTER*4 BIN
C           CHARACTER*11 FMAT
C           PARAMETER (BIN='.BIN')
C
C   SEARCH FILE NAME FOR .BIN - IF IT IS PRESENT IT IS A BINARY FILE
C
C       FMAT='FORMATTED '
C       DO 2 I=1,77
C           IF (FILEN(I:I+3).EQ.BIN) THEN
C               FMAT='UNFORMATTED'
C               GO TO 3
C           ENDIF
C 2   CONTINUE
C 3   OPEN(UNIT=10,FILE=FILEN,STATUS='new',FORM=FMAT)
C
C   write FILE
C
C       IF (FMAT.EQ.'UNFORMATTED') THEN
C           WRITE(10)NX,NY,DX,DY
C           DO 9 I=1,NY
C 9           WRITE(10) (ARRAY(I,J),J=1,NX)
C           ELSE
C           WRITE(10,*)NX,NY,DX,DY
C           DO 8 I=1,NY
C 8           WRITE(10,*) (ARRAY(I,J),J=1,NX)
C           ENDIF
C           CLOSE(10)
C           RETURN
C           END
C
C
C
C   ROUTINE TO WRITE REAL FILE
C
C       SUBROUTINE RWR(ARRAY,FILE,NX,NY,IGRID,DX,DY)
C           DIMENSION ARRAY(IGRID,1)
C           CHARACTER*80 FILEN
C           CHARACTER*4 BIN
C           CHARACTER*11 FMAT
C           PARAMETER (BIN='.BIN')
C
C   SEARCH FILE NAME FOR .BIN - IF IT IS PRESENT IT IS A BINARY FILE
C
C       FMAT='FORMATTED '
C       DO 2 I=1,77
C           IF (FILEN(I:I+3).EQ.BIN) THEN
C               FMAT='UNFORMATTED'
C               GO TO 3
```

```

        ENDIF
2   . CONTINUE
3   OPEN(UNIT=10,FILE=FILEN,STATUS='new',FORM=FMAT)
C
C   write FILE
C
        IF (FMAT.EQ.'UNFORMATTED') THEN
        write(10)NX,NY,DX,DY
        DO 9 I=1,NY
9         write(10) (ARRAY(I,J),J=1,NX)
        ELSE
        write(10,*)NX,NY,DX,DY
        DO 8 I=1,NY
8         write(10,*) (ARRAY(I,J),J=1,NX)
        ENDIF
        CLOSE(10)
        RETURN
        END
C
C
        SUBROUTINE IWR2 (ARRAY, FILEN, NX, NY, IGRID, DX, DY)
        INTEGER*2 ARRAY (IGRID,1)
        CHARACTER*80 FILEN
        CHARACTER*4 BIN
        CHARACTER*11 FMAT
        PARAMETER (BIN='.BIN')
C
C   SEARCH FILE NAME FOR .BIN - IF IT IS PRESENT IT IS A BINARY FILE
C
        FMAT='FORMATTED '
        DO 2 I=1,77
        IF (FILEN(I:I+3).EQ.BIN) THEN
        FMAT='UNFORMATTED'
        GO TO 3
        ENDIF
2   CONTINUE
3   OPEN(UNIT=10,FILE=FILEN,STATUS='new',FORM=FMAT)
C
C   write FILE
C
        IF (FMAT.EQ.'UNFORMATTED') THEN
        WRITE(10)NX,NY,DX,DY
        DO 9 I=1,NY
9         WRITE(10) (ARRAY(I,J),J=1,NX)
        ELSE
        WRITE(10,*)NX,NY,DX,DY
        DO 8 I=1,NY
8         WRITE(10,*) (ARRAY(I,J),J=1,NX)
        ENDIF
        CLOSE(10)
        RETURN
        END
C
C   ROUTINE TO READ IN FILE
C
        SUBROUTINE IREAD (ARRAY, FILEN, NX, NY, IGRID, DX, DY)
        INTEGER ARRAY (IGRID,1)
        CHARACTER*80 FILEN
        CHARACTER*4 BIN
        CHARACTER*11 FMAT
        PARAMETER (BIN='.BIN')
C
C   SEARCH FILE NAME FOR .BIN - IF IT IS PRESENT IT IS A BINARY FILE
C
        FMAT='FORMATTED '
        DO 2 I=1,77
        IF (FILEN(I:I+3).EQ.BIN) THEN
        FMAT='UNFORMATTED'
        GO TO 3
        ENDIF
2   CONTINUE
3   OPEN(UNIT=10,FILE=FILEN,STATUS='OLD',FORM=FMAT,readonly)
C
C   READ FILE
C
        IF (FMAT.EQ.'UNFORMATTED') THEN
        READ(10,err=20)NX,NY,DX,DY
        go to 21
c---use default spacing if not in file

```

```

20  dx=30.
    dy=30.
21  continue
    DO 9 I=1,NY
9    READ(10) (ARRAY(I,J),J=1,NX)
    ELSE
    READ(10,*)NX,NY,DX,DY
    DO 8 I=1,NY
8    READ(10,*) (ARRAY(I,J),J=1,NX)
    ENDIF
    CLOSE(10)
    RETURN
    END

C
C
C  ROUTINE TO READ IN FILE
C
    SUBROUTINE RREAD (ARRAY, FILEN, NX, NY, IGRID, DX, DY)
    DIMENSION ARRAY(IGRID,1)
    CHARACTER*80 FILEN
    CHARACTER*4 BIN
    CHARACTER*11 FMAT
    PARAMETER (BIN='.BIN')

C
C  SEARCH FILE NAME FOR .BIN - IF IT IS PRESENT IT IS A BINARY FILE
C
    FMAT='FORMATTED '
    DO 2 I=1,77
        IF (FILEN(I:I+3) .EQ. BIN) THEN
            FMAT='UNFORMATTED'
            GO TO 3
        ENDIF
2    CONTINUE
3    OPEN(UNIT=10, FILE=FILEN, STATUS='OLD', FORM=FMAT, readonly)

C
C  READ FILE
C
    IF (FMAT.EQ. 'UNFORMATTED') THEN
    READ(10,err=20)NX,NY,DX,DY
    go to 21
c---use default spacing if not in file
20  dx=30.
    dy=30.
21  continue
    DO 9 I=1,NY
9    READ(10) (ARRAY(I,J),J=1,NX)
    ELSE
    READ(10,*)NX,NY,DX,DY
    DO 8 I=1,NY
8    READ(10,*) (ARRAY(I,J),J=1,NX)
    ENDIF
    CLOSE(10)
    RETURN
    END

C
C
C  SUBROUTINE IREAD2 (ARRAY, FILEN, NX, NY, IGRID, DX, DY)
    INTEGER*2 ARRAY(IGRID,1)
    CHARACTER*80 FILEN
    CHARACTER*4 BIN
    CHARACTER*11 FMAT
    PARAMETER (BIN='.BIN')

C
C  SEARCH FILE NAME FOR .BIN - IF IT IS PRESENT IT IS A BINARY FILE
C
    FMAT='FORMATTED '
    DO 2 I=1,77
        IF (FILEN(I:I+3) .EQ. BIN) THEN
            FMAT='UNFORMATTED'
            GO TO 3
        ENDIF
2    CONTINUE
3    OPEN(UNIT=10, FILE=FILEN, STATUS='OLD', FORM=FMAT, readonly)

C
C  READ FILE
C
    IF (FMAT.EQ. 'UNFORMATTED') THEN
    READ(10,err=20)NX,NY,DX,DY

```

```
      go to 21
c---use default spacing if not in file
20  dx=30.
    dy=30.
21  continue
    DO 9 I=1,NY
9    READ(10) (ARRAY(I,J),J=1,NX)
    ELSE
    READ(10,*) NX,NY,DX,DY
    DO 8 I=1,NY
8    READ(10,*) (ARRAY(I,J),J=1,NX)
    ENDIF
    CLOSE(10)
    RETURN
    END
```

SETUP.FOR

C This is Two subroutines to open and close GKS and interactively request
C the Plot device/workstation being used for the programs that use
C graphics.

C CREATED BY DAVID G TARBOTON

```
C
SUBROUTINE SETUP(FNAME, IDEV, IUNIT, ITYPE)
CHARACTER*50 FNAME
INCLUDE 'SYSS$LIBRARY:GKSDEFS.BND'
IF (IUNIT.EQ.5) THEN
  WRITE(6,*) 'DEVICE TYPE'
  WRITE(6,100)
100  format(1x, '1=SCREEN'/1x, '2=LASERWRITER'/1x, '3=tek4010'
&      /1x, '4=default'/1x,
&      '5=NARROW SCREEN FOR SCREEN DUMP'/1x, '6=decwindows')
ENDIF
READ(IUNIT,*) IDEV
CALL GOPKS(99)          ! OPEN GKS  ERRORS TO UNIT 99
IF (IDEV.EQ.1.OR.IDEV.EQ.5) THEN
  ITYPE=GVSII
  CALL GOPWK(1,GWCONID,ITYPE)      ! OPEN WORKSTATION
ELSE IF (IDEV.EQ.3) THEN
  ITYPE=GT4014
  CALL GOPWK(1,GWCONID,ITYPE)      ! OPEN WORKSTATION
ELSE IF (IDEV.EQ.4) THEN
  ITYPE=GWSDEF
  CALL GOPWK(1,GWCONID,ITYPE)      ! OPEN WORKSTATION
ELSE IF (IDEV.EQ.6) THEN
  ITYPE=GDECW
  CALL GOPWK(1,GWCONID,ITYPE)      ! OPEN WORKSTATION
ELSE
  if(fname.eq.' ')then
    write(6,*) 'input laserwriter file name'
    write(6,*) 'return for direct routing'
    read(iunit,50) fname
50    format(a80)
  endif
  ITYPE=GPTSC
  if(fname.eq.' ')then
    call gks$open_ws(1,'txa2:',itype)
  else
    ICONID=20
    OPEN(UNIT=ICONID,FILE=FNAME,STATUS='NEW')
    CALL GOPWK(1,ICONID,itype)      ! OPEN WORKSTATION
  endif
ENDIF
CALL GACWK(1)          ! ACTIVATE WORKSTATION
RETURN
END

C
SUBROUTINE TIDYUP(IDEV)
INCLUDE 'SYSS$LIBRARY:GKSDEFS.BND'
IF (IDEV.ne.2) THEN
  CALL GUWK(1,GPERFO)
  write(6,*) 'Return when finished viewing plot'
  READ(5,*)
ENDIF
CALL GDAWK(1)          ! DEACTIVATE WORKSTATION
CALL GCLWK(1)          ! CLEAR WORKSTATION
CALL GCLKS             ! CLOSE GKS
RETURN
END
```

CUTIL.C

```
/* This is a C implementation of some of the Input/Output routines for */
/* matrix files for use with AREAC.C and ZAREAC.C */

/* Created by David G Tarboton */

/* The following routines are included. */
/* IREAD2: To read Short integer (Integer*2) matrix. */
/* IWR: To write Integer(*4) matrix. */

/* function to read binary file */
#include <stdio.h>
#define MAXREC 2044
/* routine to read 2 bit matrix file */
iread2(pfile,dir,nxr,nyr,dxr,dyr,igx)
char pfile[];
short int dir[];
int *nxr,*nyr;
float *dxr,*dyr;
int igx;
/* test if binary file for read */
{
    FILE *fp;
    int cc1,cc2,cc3,cc4,i,j,nx,ny,sz,nr,nin;
    float dx,dy;
    float row[2];
    int *sl;
    if(binary(pfile)==0)
    {
        fp=fopen(pfile,"r","rfm-var");
        cc1=getc(fp);
        cc2=getc(fp);
        nx=getw(fp);
        ny=getw(fp);
        sz = 2*sizeof(float);
        nr=1;
        fread(row, sz, nr, fp);
        dx=row[0];
        dy=row[1];
        for(i=0; i< ny; i++)
        { cc3=getc(fp); /* carriage control characters */
          cc4=getc(fp);
          sl = &dir[i*igx];
          if(cc3==3) /* only record */
              fread(sl, sizeof(short int) , nx, fp);
          else
          {
              nr=MAXREC-2;
              nin=0;
              sz=1;
              while(cc3 != 2) /* 2 indicates last block */
              {
                  fread(sl, sz , nr, fp);
                  nin=nin+nr;
                  cc3=getc(fp);
                  cc4=getc(fp);
                  sl= &dir[i*igx+nin/2];
              }
              nr=nx*2-nin;
              fread(sl, sz , nr, fp);
          }
        }
    }
    else
    {
        fp=fopen(pfile,"r");
        fscanf(fp,"%d %d %f %f\n",&nx,&ny,&dx,&dy);
        for(i=0; i< ny; i++)
        { for(j=0; j< nx; j++)
          fscanf(fp,"%d",&dir[i*igx+j]);
        }
    }
    fclose(fp);
    /* return values */
    *nxr=nx;
    *nyr=ny;
}
```



```

    *dxr=dx;
    *dyr=dy;
}

/* function to write binary file */
iwr(file,area,nx,ny,dx,dy,igx)
char file[];
int area[];
int nx,ny;
float dx,dy;
int igx;
{
    FILE *fa;
    int cc0,cc1,cc2,cc3,i,j,nr,sz,sz1,nseg,ncount,iseg;
    char *sl; /* make sl a character pointer so can add single bytes */
    float row2[2];
/* test if binary file for write */
if(binary(file)==0)
    {
        fa=fopen(file,"w","rfm=var","mrs=2044");
/* this gives files the same as fortran unformatted */
/* MAXREC=2044 seems to be the same size that fortran max records are */
        cc3=3; /* only record */
        cc1=1; /* first record */
        cc2=2; /* last record */
        cc0=0; /* another record to come */
        putc(cc3,fa); /* replace fortran line start characters */
        putc(cc0,fa);
        putw(nx,fa);
        putw(ny,fa);
        nr=1; /* use fwrite to finish of first record so area */
        row2[0]=dx; /* data starts writing on a new record */
        row2[1]=dy;
        sz=2*sizeof(float);
        fwrite(row2, sz, nr, fa);
        sz=nx*sizeof(int);
        for(i=0; i<ny; i++)
            {
                if(sz>MAXREC-2)
                    {
                        nseg=sz/(MAXREC-2); /* actually no of segments -1 */
/* first seg */
                        sl = &area[i*igx];
                        putc(cc1,fa); /* replace fortran line start characters */
                        putc(cc0,fa);
                        sz1=MAXREC-2;
                        ncount=sz1;
                        fwrite(sl, sz1, nr, fa);
/* remaining segments */
                        for(iseg=1; iseg<nseg; iseg++)
                            {
                                putc(cc0,fa); /* replace fortran line start characters */
                                putc(cc0,fa);
                                sl = sl+sz1;
                                ncount=ncount+sz1;
                                fwrite(sl, sz1, nr, fa);
                            }
/* Last segment */
                                putc(cc2,fa); /* 2 indicates last segment */
                                putc(cc0,fa);
                                sl = sl+sz1;
                                sz1=sz-ncount;
                                fwrite(sl, sz1, nr, fa);
                            }
                        else /* single record */
                            {
                                sl = &area[i*igx];
                                putc(cc3,fa); /* only record */
                                putc(cc0,fa);
                                fwrite(sl, sz, nr, fa);
                            }
                    }
            }
        }
    else
    {
        fa=fopen(file,"w");
        fprintf(fa,"%7d %7d %9.5f %9.5f\n",nx,ny,dx,dy);
        for(i=0; i<ny; i++)
            { for(j=0; j<nx-1; j++)

```

```

        ( fprintf(fa,"%5d",area[i*lgx+j]);
        }
        fprintf(fa,"%5d\n",area[i*lgx+nx-1]);
    }
}
fclose(fa);
}
/* function to test if file name has .bin in it */
binary(file)
char *file;
{
    char test[5];
    char *bin;
    int ret,i,j,maxln;
    bin = ".bin";
    ret=1;
    maxln=strlen(file);
    /* convert to lower case */
    for(i=0; i<maxln; i++) file[i] =tolower(file[i]);
    for(j=0; (j<maxln-3 && ret==1); j++)
    {
        for(i=0; i<4; i++)test[i]= file[i+j];
        if(test[0]==bin[0] && test[1]==bin[1] && test[2]==bin[2]
            && test[3]==bin[3])ret=0;
    }
    /* if(strcmp(test,bin)==0)ret=0; */
    return(ret);
}

```

SETDIR.FOR

```

C   Program to set up pointers from DEM elevation matrix file and adjust
C   elevations of pits by increasing their elevation till they drain,
C   i.e. pointers can be assigned consistently.
C
C   CREATED BY DAVID G TARBOTON
C
C   Input is read from file BRANCH.IN which has the following structure.
C   Record 1: File name of raw elevation data file.
C   Record 2: File name of pointer file to be output.
C   Record 3: File name of area file (Not used).
C   Record 4: File name of adjusted elevation data file to be output.
C   Subsequent records: Number of subdivisions in X and Y directions for
C   matrix to be divided into in first sweeps to speed up adjustment of
C   elevations.
C
C   MEANING OF POINTERS IS -----
C
C       0 = POINTS TO SELF           I 4 I 3 I 2 I
C         I.E. UNRESOLVED           -----
C       -1= BOUNDARY PIXEL           I 5 I 0 I 1 I
C                                     -----
C                                     I 6 I 7 I 8 I
C                                     -----
C
C   This program uses subroutines from DEMUTIL.FOR, the set of subroutines
C   for I/O of binary matrix files.
C
C
C   Program SETDIR
C   PARAMETER(IGRIDY=1201, IGRIDX=1201)
C   PARAMETER(IGY=IGRIDY/2+1, IGX=IGRIDX/2+1)
C   INTEGER*2 ELEV(IGRIDY, IGRIDX), DIR(IGRIDY, IGRIDX)
C   INTEGER*2 ELEVP(IGY, IGX)
C   CHARACTER*80 DEMFILE, POINTFILE, AREAFILE, NEWFILE
C   CHARACTER*4 BIN
C   CHARACTER*11 FMAT
C   DATA BIN/' .BIN'/
C   LOGICAL IZERO
C
C   READ INPUT
C
C   OPEN(UNIT=11, FILE='BRANCH.IN', STATUS='OLD', readonly)
C   READ(11, 22) DEMFILE, POINTFILE, AREAFILE, NEWFILE
22  FORMAT(A80/A80/A80/A80)
C   CALL IREAD2(ELEV, DEMFILE, NX, NY, IGRIDY, DX, DY)
C   if (nx.gt.igridx.or.ny.gt.igridy) then
C     write(6, 38) nx, igridx, ny, igridy
38  format(1x, 'array dimensions too small'/
& 1x, 'x', 218, '    y', 218)
C     stop
C   endif
C
C---LOOP HERE FOR NESTED PARTITIONS
C
1  READ(11, *, END=99) NPX, NPY
C   DO 2 IP=1, NPY
C     DO 2 JP=1, NPX
C       I1=MAX(((IP-1)*NPY)/NPY, 1)
C       I2=(IP*NPY)/NPY
C       J1=MAX(((JP-1)*NPX)/NPX, 1)
C       J2=(JP*NPX)/NPX
C       NXP=J2-J1+1
C       NYP=I2-I1+1
C       IF (NXP.LE.IGX.AND.NYP.LE.IGY) THEN
C
C-----LOAD ELEVATIONS INTO PARTITION ARRAY
C
C       DO 3 I=I1, I2
C         DO 3 J=J1, J2
C           ELEVP(I-I1+1, J-J1+1)=ELEV(I, J)
3       CONTINUE
C       WRITE(6, 100) IP, JP
100  FORMAT(1X, 'PARTITION', 2I5)
C       CALL SETDF(ELEVP, DIR, IGX, IGY, NXP, NYP, DX, DY)
C

```

```

C---WRITE ELEVATIONS BACK INTO MAIN ARRAY
C
      DO 4 I=I1,I2
        DO 4 J=J1,J2
          ELEV(I,J)=ELEV(I-I1+1,J-J1+1)
4      CONTINUE
      ELSE
        WRITE(6,*) 'PARTITION TOO BIG',IP,JP,NXP,NYP
      ENDIF
2      CONTINUE
      GO TO 1
C
C---CALL SETDF FOR WHOLE AREA TO SMOOTH OFF JOINS
C
99      CALL SETDF(ELEV,DIR,IGRIDX,IGRIDY,NX,NY,DX,DY)
      CALL IWR2(ELEV,NEWFILE,NX,NY,IGRIDY,DX,DY)
      CALL IWR2(DIR,POINTFILE,NX,NY,IGRIDY,DX,DY)
      END
C
C---SUBROUTINE TO DO THE BULK OF THE WORK
C
      SUBROUTINE SETDF(ELEV,DIR,IGRIDX,IGRIDY,NX,NY,DX,DY)
      INTEGER*2 ELEV(IGRIDY,IGRIDX),DIR(IGRIDY,IGRIDX)
      INTEGER*2 IS(500000),JS(500000)
      LOGICAL CH1,CH2,IZERO
      DIMENSION FACT(8)
      INTEGER D1(8),D2(8)
      DATA D1/0,-1,-1,-1,0,1,1,1/
      DATA D2/1,1,0,-1,-1,-1,0,1/
C
C      MEANING OF POINTERS IS -----
C      I 4 I 3 I 2 I
C      0 - POINTS TO SELF -----
C      I.E. UNRESOLVED I 5 I 0 I 1 I
C      -1- BOUNDARY PIXEL -----
C      I 6 I 7 I 8 I
C      -----
C
      INITIALISE BOUNDARY POINTERS IN MATRIX DIR
C
      DO 2 I=1,NX
        DIR(I,I)=-1
        DIR(NY,I)=-1
2      CONTINUE
      DO 3 I=1,NY
        DIR(I,1)=-1
        DIR(I,NX)=-1
3      CONTINUE
      IUP=0
C
C---initialise internal pointers (-ve elevation indicates outside domain)
C
      do 31 i=2,ny-1
        do 31 j=2,nx-1
          if(elev(i,j).le.0)then
            dir(i,j)=-1
          else
            dir(i,j)=0
          endif
31      continue
C
C      TEST ALL INTERNAL ELEVATIONS AND SET POINTERS
C
C      WRITE(6,*) 'FACTORS'
      DO 21 K=1,8
        FACT(K)=1./SQRT(D1(K)*DY*D1(K)*DY+D2(K)*D2(K)*DX*DX)
C      WRITE(6,*) K,FACT(K)
21      CONTINUE
      WRITE(6,*) 'PROBLEM PIXELS'
      WRITE(6,*) '      FLATS      UNRESOLVED'
C
C      TEST ALL INTERNAL ELEVATIONS AND SET POINTERS
C
1      DO 4 I=2,NY-1
        DO 4 J=2,NX-1
          if(elev(i,j).gt.0)CALL SET(ELEV,DIR,I,J,IGRIDY,FACT)
4      CONTINUE
C
C---FIRST FIXING PASS

```

```

C   ELIMINATE FLATS
C   STORE UNRESOLVED PIXELS IN A STACK
      N=0
      DO 7 I=2,NY-1
        DO 7 J=2,NX-1
          IF (DIR(I,J).EQ.0) THEN
            N=N+1
            IS(N)=I
            JS(N)=J
          ENDIF
          IF (N.GE.500000) THEN
            WRITE(6,*) 'ARRAYS NOT BIG ENOUGH 1'
            WRITE(6,*) I,J
            WRITE(6,*) ELEV(I-1,J-1),ELEV(I-1,J),ELEV(I-1,J+1)
            WRITE(6,*) ELEV(I,J-1),ELEV(I,J),ELEV(I,J+1)
            WRITE(6,*) ELEV(I+1,J-1),ELEV(I+1,J),ELEV(I+1,J+1)
            RETURN
          ENDIF
7      CONTINUE
      NFLAT=N
C---CALL ROUTINE TO MAKE FLATS DRAIN TO NEIGHBOUR'S
      CALL VDN(ELEV,DIR,IS,JS,IGRIDY,N)
C
C   ANY UNRESOLVED PIXELS HERE ARE POOLS SO RAISE THEM AND START
C   AGAIN
C
      IUP=IUP+1
      DO 51 II=1,N
        I=IS(II)
        J=JS(II)
C---DETERMINE ELEVATION OF LOWEST NEIGHBOUR
        ILN=MIN(ELEV(I,J+1),ELEV(I-1,J+1),ELEV(I-1,J),ELEV(I-1,J-1),
          &      ELEV(I,J-1),ELEV(I+1,J-1),ELEV(I+1,J),ELEV(I+1,J+1))
C---INCREMENT IS 1 OR DIFFERENCE BETWEEN LOWEST NEIGHBOUR
        ELEV(I,J)=ELEV(I,J)+MAX(1,ILN-ELEV(I,J))
51     CONTINUE
        WRITE(6,*)NFLAT,N
C---TEST IF COMPLETE
        IF(N.GE.1)GO TO 1 ! LOOP BACK IF SOMETHING CHANGED
        RETURN
      END
C
C   ROUTINE TO DRAIN UNRESOLVED PIXELS TOWARDS NEIGHBOURS
C
      SUBROUTINE VDN(ELEV,DIR,IS,JS,IGRIDY,N)
      INTEGER*2 IS(*),JS(*),ELEV(IGRIDY,*),DIR(IGRIDY,*),ED
      INTEGER*2 DN(500000)
      INTEGER*2 D1(8),D2(8),I1,I3,K,I2
      DATA D1/0,-1,-1,-1,0,1,1,1/
      DATA D2/1,1,0,-1,-1,-1,0,1/
C---INITIALISE NEW DIRECTIONS TO 0
1     DO 4 IP=1,N
4       DN(IP)=0
      DO 2 K=1,7,2
        DO 2 IP=1,N
          ED=ELEV(IS(IP),JS(IP))-ELEV(IS(IP)+D1(K),JS(IP)+D2(K))
          IF(ED.GE.0.AND.DIR(IS(IP)+D1(K),JS(IP)+D2(K)).NE.0.AND.
            &      DN(IP).EQ.0)DN(IP)=K ! LOGICAL EQUIVALENTS TO COND M'S BELOW
C
C           I1=CVMGP(1,0,ED)
C---I1 IS 1 IF DROP IS .GE.0
C           I3=CVMGZ(0,1,DIR(IS(IP)+D1(K),JS(IP)+D2(K)))
C---I3 IS 0 UNLESS NEIGHBOUR HAS DIRECTION SET
C           DN(IP)=CVMGZ(I1*13*K,dn(ip),DN(IP))
C---DN IS NEW DIRECTION POINTER
2     CONTINUE
      DO 12 K=2,8,2
        DO 12 IP=1,N
          ED=ELEV(IS(IP),JS(IP))-ELEV(IS(IP)+D1(K),JS(IP)+D2(K))
          IF(ED.GE.0.AND.DIR(IS(IP)+D1(K),JS(IP)+D2(K)).NE.0.AND.
            &      DN(IP).EQ.0)DN(IP)=K ! LOGICAL EQUIVALENTS TO COND M'S BELOW
C
C           I1=CVMGP(1,0,ED)
C---I1 IS 1 IF DROP IS .GE.0
C           I2=CVMGZ(K,DIR(IS(IP),JS(IP)),DIR(IS(IP),JS(IP)))
C---I3 IS 0 UNLESS NEIGHBOUR HAS DIRECTION SET
C           DN(IP)=CVMGZ(I1*13*K,dn(ip),DN(IP))
C---DN IS NEW DIRECTION POINTER
12    CONTINUE
      NI=0

```

```

DO 3 IP=1,N
  IF (DN(IP) .GT. 0) THEN
    DIR (IS (IP) , JS (IP)) =DN (IP)
  ELSE
    NI=NI+1
    IS (NI) =IS (IP)
    JS (NI) =JS (IP)
  ENDIF
3 CONTINUE
C WRITE (6,*) 'IN VDN: NI, N ',NI,N
C IF (NI.LT.N) THEN
  N=NI
  GO TO 1
ENDIF
N=NI
RETURN
END

C
C SUBROUTINE TO SET POINTERS IN DIRECTION OF STEEPEST DESCENT
C
SUBROUTINE SET (ELEV, DIR, I, J, IGRIDY, FACT)
INTEGER*2 ELEV (IGRIDY, 1) , DIR (IGRIDY, 1)
DIMENSION SLOPE (8) , FACT (8)
INTEGER D1 (8) , D2 (8)
DATA D1 /0, -1, -1, -1, 0, 1, 1, 1/
DATA D2 /1, 1, 0, -1, -1, -1, 0, 1/
DO 2 K=1, 8
  SLOPE (K) =FACT (K) *FLOAT (ELEV (I, J) -ELEV (I+D1 (K) , J+D2 (K) ))
2 CONTINUE
SMAX=0.
DIR (I, J) =0
DO 3 K=1, 8
  IF (SLOPE (K) .GT. SMAX) THEN
    SMAX=SLOPE (K)
    DIR (I, J) =K
  ENDIF
3 CONTINUE
RETURN
END

```

AREAC.C

```

/* Program to compute area contributing to each pixel from pointers using */
/* recursive algorithm */

/* Created by David G Tarboton */

/* Input is read from file BRANCH.IN which has the following structure. */
/* Record 1: File name of raw elevation data file (not used). */
/* Record 2: File name of pointer file input. */
/* Record 3: File name of area file output. */
/* Record 4: File name of adjusted elevation data file (not used). */
/* Subsequent records: (not used) */

/* This program uses Input/Output routines from CUTIL.C */

#include <stdio.h>
#define IGX 1201
#define IGY 1201
#define MAXLN 80
main()
{
    extern int nx,ny;
    extern float dx,dy;
    char efile[MAXLN],pfile[MAXLN],afile[MAXLN];
    extern short int dir[IGY][IGX];
    extern int area[IGY][IGX],d1[9],d2[9];
    FILE *fin;
    int i,j;
/* define directions */
d1[1]=0; d1[2]= -1; d1[3]= -1; d1[4]= -1; d1[5]=0; d1[6]=1; d1[7]=1; d1[8]=1;
d2[1]=-1; d2[2]=1; d2[3]=0; d2[4]= -1; d2[5]= -1; d2[6]= -1; d2[7]=0; d2[8]=1;
/* read in data */
    fin=fopen("branch.in","r");
    fscanf(fin, "%s", efile);
    fscanf(fin, "%s", pfile);
    fscanf(fin, "%s", afile);
/* read pointers */
    irect2(pfile,dir,&nx,&ny,&dx,&dy,IGX);
/* initialize area array to 0 */
    for(i=0; i<ny; i++)
    { for(j=0; j<nx; j++)
        area[i][j]=0;
    }
/* call drainage area subroutine for each area */
/* work from middle outwards to avoid deep recursions */
    for(i=ny/2; i<ny-1; i++)
    { for(j=nx/2; j<nx-1; j++)
        darea(i,j);
        for(j=nx/2-1; j>=1; j--)
            darea(i,j);
    }
    for(i=ny/2-1; i>=1; i--)
    { for(j=nx/2; j<nx-1; j++)
        darea(i,j);
        for(j=nx/2-1; j>=1; j--)
            darea(i,j);
    }
/* write out areas */
    1wr(afile,area,nx,ny,dx,dy,IGX);
}

/* function to compute area recursively */
darea(i,j)
int i,j;
{
    extern int area[IGY][IGX],d1[9],d2[9],nx,ny;
    extern short int dir[IGY][IGX];
    int in,jn,k;
    if(area[i][j]==0)
    {
        if(i!=0 && i!=ny-1 && j!=0 && j!=nx-1 && dir[i][j]!= -1)
            /* not on boundary */
            {
                area[i][j]=1;
                for(k=1; k<=8; k++)
                    in=i+d1[k];
            }
    }
}

```

```

        jn=j+d2[k];
/* test if neighbor drains towards cell excluding boundaries */
        if(dir[in][jn]>=0 && (dir[in][jn]-k==4|dir[in][jn]-k==4))
        {
            darea(in,jn);
            area[i][j]=area[i][j]+area[in][jn];
        }
    }
}

```

BRANCH.IN

```

W7ELEV.BIN
W7P.BIN
W7AREA.BIN
W7ADJ.BIN
5 5
3 3
2 2

```


PIXMAP.FOR

```

C   Program to plot a cell array of pixels that exceed a specified threshold
C   from a DEM matrix file. This is used to identify river networks in DEM
C   data sets and determine the outlet pixel to be used to isolate the basin.
C
C   CREATED BY DAVID G TARBOTON
C
C   Input is read from file PIXMAP.IN which has the following structure:
C   Record 1: Number of bits per data item in input file
C             (1= real, 2= 2 bit integer, 4= 4 bit integer).
C   Record 2: Threshold for real data (used only if record 1 = 1).
C   Record 3: File name of matrix file to be mapped.
C   Record 4: Device unit number for remainder of input.
C             This should be 11 for continued input from the same file of 5
C             for interactive input.
C   Remainder: The rest of the file is only read if record 4 is 11 and is the
C   response to interactive questions regarding the plot to be produced.
C
C   This program uses subroutines from DEMUTIL.FOR, the set of subroutines
C   for I/O of binary matrix files.
C
PROGRAM PIXMAP
PARAMETER (IGPX=1201,IGPY=1201)
INTEGER COLP (IGPX,IGPY),col (igpy)
DIMENSION XL(5),YL(5)
CHARACTER*50 FNAME
CHARACTER*80 HEADER
character*5 reply
logical yes
OPEN (UNIT=11,FILE='PIXMAP.IN',STATUS='OLD')
READ (11,*) IBITS
read(11,*)tresh      ! tresh only used for real data files
CALL INPUT (COLP,NX1,NY1,tresh,IGPX,IBITS,dx,dy)
READ (11,*) IUNIT
1  FNAME=' '
   CALL SETUP (FNAME,IDEV,IUNIT,ITYPE)
   CALL QDQSP (ITYPE,IER,IUNITS,PX,PY,LX,LY)
C---DEFINE WORKSTATION TRANSFORMATION
   PM=MAX (PX,PY)
   P1=PX/PM          ! COORDS OF VIEWPORT ON NDC
   IF (IDEV.EQ.1) THEN
     P2=PY/PM*.9
     PYM=0.1*PY
   ELSE
     P2=PY/PM
     PYM=0.
   ENDIF
   CALL GSWKWN (1,0.,P1,0.,P2)      ! SET WORKSTATION WINDOW
   CALL GSWKVP (1,0.,PX,PYM,PY)    ! SET WORKSTATION VIEWPORT
   NWIND=1
   RAT=P1/P2
   XWMIN=0
   XWMAX=RAT
   YWMIN=0
   YWMAX=1.
   CALL GSWN (NWIND,XWMIN,XWMAX,YWMIN,YWMAX) ! SET WINDOW
   CALL GSVP (NWIND,0.,P1,0.,P2)      ! SET VIEWPORT
   CALL GSELNT (NWIND)                ! SELECT NORM. TRANS.
   call gsvpip (nwind,0,0)           ! sets this transformation
c                                     to be higher priority than default transformation no 0.
   XR=XWMAX-.1 ! PLOTTING RANGES
   YR=YWMAX-.2
   RRAT=XR/YR
22  write(6,*) 'input threshold'
   read(iunit,*) ltresh
13  WRITE (6,*) 'number of columns ',NX1
   WRITE (6,*) 'number of rows   ',NY1
   WRITE (6,*) 'INPUT SUBARRAY TO PLOT'
   WRITE (6,*) 'COLMIN, COLMAX, ROWMIN, ROWMAX'
   READ (IUNIT,*) ICB, ICT, IRB, IRT
   if (icb.gt.0.and.icb.lt.ict.and.ict.le.nx1) then
     if (irb.gt.0.and.irb.lt.irt.and.irt.le.ny1) then
       go to 15
     endif
   endif
   write(6,*) 'row and col out of range'

```

```

go to 13
15 . NX=ICT-ICB+1
    NY=IRT-IRB+1
    DRAT=FLOAT(NX)*dx/(FLOAT(NY)*dy)
    IF (RRAT.LT.DRAT) THEN      ! WIDTH (X) LIMITED
        PX=YMIN+.05
        QX=YMAX-.05
        YMID=0.55
        PY=YMID+(QX-PX)/(DRAT*2.)
        QY=YMID-(QX-PX)/(DRAT*2.)
    ELSE      ! HEIGHT (Y) LIMITED
        PY=.95
        QY=.15
        XMID=RAT/2.
        PX=XMID-(PY-QY)*DRAT/2.
        QX=XMID+(PY-QY)*DRAT/2.
    ENDIF
    XL(1)=PX
    XL(2)=QX
    XL(3)=QX
    XL(4)=PX
    XL(5)=PX
    YL(1)=QY
    YL(2)=QY
    YL(3)=PY
    YL(4)=PY
    YL(5)=QY
    do 2 i=1,nx
        do 3 j=1,ny
            col(j)=0
3            if(colp(icb+i-1,j+irb-1).ge.itresh)col(j)=1
            pxp=px+(qx-px)*float(i-1)/float(nx)
            qxp=px+(qx-px)*float(i)/float(nx)
            CALL GCA(PXp,PY,QXp,QY,1,IGPY,1,1,1,NY,COL)
2        continue
C---BOUNDARIES
    CALL GPL(5,XL,YL)
    WRITE(HEADER,71)ITRESH
71  FORMAT(1X,'Pixels that exceed or equal threshold',I5)
C---TEXT
    X=0.25
    Y=0.05
    CALL GSTXFP(1,2)
    CALL GSCHH((YMAX-YMIN)/50.)
    CALL GTX(X,Y,HEADER)
    write(6,*)'do you want to locate a pixel'
    read(iunit,144)reply
    yes=.false.
    do 146 i=1,5
        if(reply(i:i).eq.'y'.OR.REPLY(I:I).EQ.'Y')yes=.true.
146    continue
    if(yes)then      ! locate pixel
        CALL GSTXFP(1,2)
        CALL GSCHH((YMAX-YMIN)/100.)
73    call grqlc(1,1,instatus,ixform,posx,posy)
        ix=(posx-px)/(qx-px)*nx
        iy=(posy-qy)/(py-qy)*ny
        j=icb+ix
        i=irt-iy
        IF (Ix.Ge.0) THEN
            X=PX+FLOAT(J-ICB)*(QX-PX)/FLOAT(NX)
            Y=PY+FLOAT(I-IRB+1)*(QY-PY)/FLOAT(NY)
            CALL GTX(X,Y,'X')
c            CALL GUWK(1,GPERFO)
            WRITE(6,*)i,j,COLP(J,I)
            GO TO 73
        ENDIF
    endif
    write(6,*)'do you want another plot on same workstation'
    read(iunit,144)reply
144  format(a5)
    do 145 i=1,5
        if(reply(i:i).eq.'y'.or.reply(I:I).eq.'Y')then
            call gclrwk(1,1)
            go to 22
        endif
    endif
145  continue
    CALL TIDYUP(IDEV)
    write(6,*)'do you want another plot'

```

```

    read(iunit,144)reply
    do 147 i=1,5
      if(reply(i:i).eq.'y'.or.reply(I:I).eq.'Y')go to 1
147  continue
      STOP
      END
C
C
C
      SUBROUTINE INPUT(COL,NX,NY,tresh,IGPX,IBITS,dx,dy)
      INTEGER COL(IGPX,1),IROW(1201)
      integer*2 irow2(1201)
      DIMENSION ROW(1201)
      CHARACTER*80 FILEN
      CHARACTER*4 BIN
      CHARACTER*11 FMAT
      DATA BIN/'.BIN'/
      READ(11,22)FILEN
      FORMAT(A80)
22
C
C SEARCH FILE NAME FOR .BIN - IF IT IS PRESENT IT IS A BINARY FILE
C
      FMAT='FORMATTED '
      DO 2 I=1,77
        IF(FILEN(I:I+3).EQ.BIN)THEN
          FMAT='UNFORMATTED'
          GO TO 3
        ENDIF
2  CONTINUE
3  OPEN(UNIT=10,FILE=FILEN,STATUS='OLD',FORM=FMAT)
C
C READ FILE
C
      IF(IBITS.EQ.4)THEN ! INTEGER
      IF(FMAT.EQ.'UNFORMATTED')THEN
      READ(10,err=33)NX,NY,dx,dy
      go to 34
33  dx=30.
      dy=30.
34  continue
      DO 9 I=1,NY
        READ(10)(IROW(J),J=1,NX)
        DO 9 J=1,NX
          COL(J,I)=irow(j)
9  CONTINUE
      ELSE
      READ(10,*)NX,NY,dx,dy
      DO 8 I=1,NY
        READ(10,*)(IROW(J),J=1,NX)
C---SET COL ACCORDING TO THRESHOLD
        DO 8 J=1,NX
          COL(J,I)=irow(j)
8  CONTINUE
      ENDIF
      else IF(IBITS.EQ.2)THEN ! INTEGER*2
      IF(FMAT.EQ.'UNFORMATTED')THEN
      READ(10,err=43)NX,NY,dx,dy
      go to 44
43  dx=30.
      dy=30.
44  continue
      DO 29 I=1,NY
        READ(10)(IROW2(J),J=1,NX)
        DO 29 J=1,NX
          COL(J,I)=irow2(j)
29  CONTINUE
      ELSE
      READ(10,*)NX,NY,dx,dy
      DO 28 I=1,NY
        READ(10,*)(IROW2(J),J=1,NX)
C---SET COL ACCORDING TO THRESHOLD
        DO 28 J=1,NX
          COL(J,I)=irow2(j)
28  CONTINUE
      ENDIF
      ELSE ! REAL
      IF(FMAT.EQ.'UNFORMATTED')THEN
      READ(10,err=53)NX,NY,dx,dy

```

```

53   go to 54
     dx=30.
     dy=30.
54   continue
     DO 19 I=1,NY
       READ(10) (ROW(J),J=1,NX)
       DO 19 J=1,NX
         IF (ROW(J) .GE. TRESH) COL (J, I)=1
19   CONTINUE
     ELSE
       READ(10,*)NX,NY,dx,dy
       DO 18 I=1,NY
         READ(10,*) (ROW(J),J=1,NX)
C---SET COL ACCORDING TO THRESHOLD
         DO 18 J=1,NX
           IF (ROW(J) .GE. TRESH) COL (J, I)=1
18   CONTINUE
     ENDIF
     ENDIF
     CLOSE(10)
     RETURN
     END

```

PIXMAP.IN

```

4     NO OF BITS PER INTEGER IN UNFORMATTED FILE
1     THRESHOLD for real data
w7area.BIN
5     INPUT DEVICE NO FOR INTERACTION (11 FOR THIS FILE, 5 OTHERWISE)
2     DEVICE TYPE 1-SCREEN, 2-LASERWRITER, 3-tektronix
pixmap.las
1     threshold      (must be <= 1 for real data)
1,1201,1,1201      COL MIN AND MAX, ROW MIN AND MAX
n     Locate pixel
n     another plot same workstation
n     another plot

```

ZAREAC.C

```
/* Program to zero area of pixels that dont drain to a designated outlet */
/* pixel by calculating areas of pixels draining to the outlet pixel */
/* using a recursive algorithm starting from the outlet pixel */

/* Created by David G Tarboton */

/* Input is read from file ZAREA.IN which has the following structure. */
/* Record 1: File name of pointer file input. */
/* Record 2: File name of area file input (not used). */
/* Record 3: File name of isolated area file output. */
/* Subsequent Records: Row and Column of the outlet pixels isolate on. */
/* More than one is possible to allow subnetworks to be computed */
/* first to prevent recursion depth or storage of two networks */
/* in the same file. */

/* This program uses Input/Output routines from CUTIL.C */

#include <stdio.h>
#define IGX 1720
#define IGY 1170
#define MAXLN 80
main()
{
    int nx,ny,sz,nr;
    float dx,dy;
    char efile[MAXLN],pfile[MAXLN],afile[MAXLN],cc1,cc2,cc3,cc4;
    short int dir[IGY][IGX],row[IGX];
    int area[IGY][IGX],d1[9],d2[9],row2[IGX];
    FILE *fp,*fa,*fin;
    int i,j,irz,icz;
    /* define directions */
    d1[1]=0; d1[2]=-1; d1[3]=-1; d1[4]=-1; d1[5]=0; d1[6]=1; d1[7]=1; d1[8]=1;
    d2[1]=1; d2[2]=1; d2[3]=0; d2[4]=-1; d2[5]=-1; d2[6]=-1; d2[7]=0; d2[8]=1;
    /* read in data */
    fin=fopen("zarea.in","r");
    fscanf(fin,"%s",pfile);
    fscanf(fin,"%s",efile); /* this file name not used */
    fscanf(fin,"%s",afile);
    /* read pointers */
    fread2(pfile,dir,&nx,&ny,&dx,&dy,IGX);
    /* initialize area array to 0 */
    for(i=0; i<ny; i++)
    { for(j=0; j<nx; j++)
        area[i][j]=0;
    }
    /* get pixels to zero on */
    /* There may be several with the first few judiciously chosen to */
    /* restrict recursion depth */
    i=fscanf(fin,"%d %d",&irz,&icz);
    while(i != 0)
    {
        /* call drainage area subroutine for pixel to zero on */
        irz=irz-1; /* decrease index for c indexing starting from 0 */
        icz=icz-1;
        area[irz][icz]=darea(irz,icz,dir,area,d1,d2,nx,ny);
        i=fscanf(fin,"%d %d",&irz,&icz);
    }
    /* write out areas */
    iwr(afile,area,nx,ny,dx,dy,IGX);
}

/* function to compute area recursively */
darea(i,j,dir,area,d1,d2,nx,ny)
int i,j,area[IGY][IGX],d1[9],d2[9],nx,ny;
short int dir[IGY][IGX];
{
    int a,in,jn,k;
    if(area[i][j]==0)
    {
        if(i!=0 && i!=ny-1 && j!=0 && j!=nx-1) /* not on boundary */
        {
            a=1;
            for(k=1; k<=8; k++)
            { in=i+d1[k];
                jn=j+d2[k];
            }
        }
    }
}
```

```
/* test if neighbor drains towards cell excluding boundaryies */
    if(dir[in][jn]>=0 && (dir[in][jn]-k==4||dir[in][jn]-k==4))
        a=a+darea(in,jn,dir,area,d1,d2,nx,ny);
    }
    area[i][j]-a;
}
else
    a=area[i][j];
return(a);
}
```

ZAREA.IN

```
w7p.BIN
w7area.BIN
w7AREAI.BIN
20,45
```

NETEX.FOR

```

C
C   Program to extract channel network from DEM area and pointer files
C   based on a support area threshold.
C
C       CREATED BY DAVID G TARBOTON
C
C   Input is read from file NETEX.IN in the following format.
C   Record 1: Pointer matrix file name for input.
C   Record 2: Isolated area matrix file name for input.
C   Record 3: Tree file name for output.
C   Record 4: IJ file name for output of temporary pixel coordinates
C   Record 5: Elevation matrix file name (Not Used).
C   Record 6: Coordinate file name (Not used)
C   Record 7: Support area threshold (Number of pixels)
C
C   Based on the support area threshold this program identifies each link in
C   the channel network and sets up the tree file defining its topological
C   structure. The (I,J) row and column numbers of each pixel along each link
C   are output in the temporary IJ file for later reading by NETPROP.FOR.
C
C   This program uses subroutines from DEMUTIL.FOR, the set of subroutines
C   for I/O of binary matrix files.
C
C       PROGRAM NETEX
C       PARAMETER(IGX=1201,IGY=1401,MNL=50000)
C       CHARACTER*80 TREEFILE,COORDFILE
C---with MNL = 50000 the number of links can exceed 32767 the max two
C   bit integer value so link pointers have to be 4 bit integers
C       (NEXTL,PREVL1,PREVL2,IPOINT)
C       INTEGER AREA(IGY,IGX),NEXTL(MNL),PREVL1(MNL),PREVL2(MNL),IPOINT(7)
C       INTEGER*2 DIR(IGY,IGX),D1(8),D2(8),IST((MNL+1)/2),JST((MNL+1)/2),
C       &IORD(MNL),
C       &ISTART(MNL),JSTART(MNL),IEND(MNL),JEND(MNL),MAG(MNL),IORDUP(7)
C       DATA D1/0,-1,-1,-1,0,1,1,1/
C       DATA D2/1,1,0,-1,-1,-1,0,1/
C       LOGICAL START
C
C   READ INPUT
C
C       CALL INPUT(AREA,DIR,NX,NY,IGX,IGY,TREEFILE,COORDFILE,ITRESH)
C
C       MEANING OF POINTERS IS -----
C
C           0 = POINTS TO SELF           I 4 I 3 I 2 I
C           I.E. UNRESOLVED             I 5 I 0 I 1 I
C           -1= BOUNDARY PIXEL          I 6 I 7 I 8 I
C           -----
C
C---FIRST FIND ALL START PIXELS
C
C       N=0
C       nmax=(mnl+1)/2
C       DO 2 I=1,NY
C         DO 2 J=1,NX
C           IF (START(I,J,AREA,DIR,NX,NY,IGX,IGY,ITRESH)) THEN
C             N=N+1
C             if(n.le.nmax)then
C               IST(N)=I
C               JST(N)=J
C             endif
C           ENDIF
C         2 CONTINUE
C       WRITE(6,*) 'MAGNITUDE',N
C       if(n.gt.nmax)stop 'too big'
C
C---ZERO AREA ARRAY
C
C       DO 12 I=1,NY
C         DO 12 J=1,NX
C           12 AREA(I,J)=0
C
C---TRACE STREAMS DOWNWARDS ADDING 1 TO MAGNITUDE OF EACH PIXEL
C       (MAGNITUDE STORED IN AREA ARRAY)
C       DO 3 IS=1,N

```

```

      I=IST(IS)
      J=JST(IS)
4     IF (DIR (I, J) .GT.0) THEN
          AREA (I, J) =AREA (I, J) +1
          INEXT=I+D1 (DIR (I, J))
          JNEXT=J+D2 (DIR (I, J))
          I=INEXT
          J=JNEXT
          GO TO 4
      ENDIF
3     CONTINUE
C
C----IDENTIFY LINKS BY DIFFERENT MAGNITUDES
C
      ILINK=1
      DO 5 IS=1,N
          ISTART (ILINK) =IST (IS)
          JSTART (ILINK) =JST (IS)
C----INITIALISE POINTERS
          PREVL1 (ILINK) =0
          PREVL2 (ILINK) =0
          I=IST (IS)
          J=JST (IS)
          MAG (ILINK) =AREA (I, J)
          IORD (ILINK) =1
6         INEXT=I+D1 (ABS (DIR (I, J)))
          JNEXT=J+D2 (ABS (DIR (I, J)))
C----CHECK FOR END
          IF (DIR (INEXT, JNEXT) .EQ.0) GO TO 90 ! END
          MNEXT=AREA (INEXT, JNEXT)
          I=INEXT
          J=JNEXT
          IEND (ILINK) =I
          JEND (ILINK) =J
          IF (MNEXT .EQ. MAG (ILINK)) GO TO 6
C----CONTINUE HERE FOR NEW LINK
C----CHECK IF JUNCTION ALREADY REACHED (FLAGGED BY NEGATIVE DIRECTION)
          IF (DIR (I, J) .LT.0) THEN
C----CHECK IF ALL LINKS CONVERGING HERE HAVE BEEN DONE BY SUMMING
C          MAGNITUDE
          MSUM=0
          IORDM=0
          ICONV=0
          DO 7 IL=1, ILINK
              IF (IEND (IL) .EQ. I .AND. JEND (IL) .EQ. J) THEN
                  ICONV=ICONV+1 ! COUNTER OF NUMBER OF LINKS THAT CONVERGE
                  IPOINT (ICONV) =IL
                  IORDUP (ICONV) =IORD (IL)
                  MSUM=MSUM+MAG (IL)
              ENDIF
7          CONTINUE
          IF (MSUM .EQ. MNEXT) THEN ! YES ALL LINKS HAVE BEEN PROCESSED
C----SORT IORDUP, IPOINT INTO DECENDING STREAM ORDER
          DO 11 IC=1, ICONV-1
              DO 11 IIC=IC+1, ICONV
                  IF (IORDUP (IIC) .GT. IORDUP (IC)) THEN ! SWITCH THESE
                      ITEMP=IORDUP (IIC)
                      IORDUP (IIC) =IORDUP (IC)
                      IORDUP (IC) =ITEMP
                      ITEMP=IPOINT (IIC)
                      IPOINT (IIC) =IPOINT (IC)
                      IPOINT (IC) =ITEMP
                  ENDIF
11         CONTINUE
          DO 17 IC=1, ICONV-1
              ILINK=ILINK+1
              ISTART (ILINK) =I
              JSTART (ILINK) =J
              PREVL1 (ILINK) =IPOINT (IC)
              PREVL2 (ILINK) =IPOINT (IC+1)
              NEXTL (IPOINT (IC)) =ILINK
              NEXTL (IPOINT (IC+1)) =ILINK
              MAG (ILINK) =MAG (PREVL1 (ILINK)) +MAG (PREVL2 (ILINK))
              IORD (ILINK) =MAX (IORDUP (1), IORDUP (2)) +1
              IPOINT (IC+1) =ILINK
              IEND (ILINK) =I
              JEND (ILINK) =J
17         CONTINUE
          GO TO 6 ! CONTINUE TRACING DOWN

```



```

        ELSE
            ILINK=ILINK+1
        ENDIF
    ELSE
        DIR(I,J)--DIR(I,J)
        ILINK=ILINK+1
    ENDIF
5    CONTINUE
    WRITE(6,*)'LOGIC ERROR LINK LOOP ENDED'
    STOP
C
C----WRITE TREE FILE
C
90    OPEN(UNIT=10,FILE=COORDFILE,STATUS='NEW')
    OPEN(UNIT=12,FILE=TREEFILE,STATUS='NEW')
    ICORD=0
C----WRITE ROOT LINK FIRST
    DO 10 IL=ILINK,ILINK
        I=ISTART(IL)
        J=JSTART(IL)
        ICS=ICORD
20    WRITE(10,*)I,J
        ICEND=ICORD
        ICORD=ICORD+1
        IF(.NOT.(I.EQ.IEND(IL).AND.J.EQ.JEND(IL)))THEN
            INEXT=I+D1(ABS(DIR(I,J)))
            JNEXT=J+D2(ABS(DIR(I,J)))
            I=INEXT
            J=JNEXT
            GO TO 20
        ENDIF
        WRITE(12,*)0,ICS,ICEND,-1,PREVL1(IL)
        & ,PREVL2(IL),IORD(IL)
10    CONTINUE
    WRITE(6,*)'ROOT AT COORD. NUMBER ',ICORD
    WRITE(11,*)ICORD
C----WRITE REMAINDER OF LINKS
    DO 110 IL=1,ILINK-1
        I=ISTART(IL)
        J=JSTART(IL)
        ICS=ICORD
120    WRITE(10,*)I,J
        ICEND=ICORD
        ICORD=ICORD+1
        IF(.NOT.(I.EQ.IEND(IL).AND.J.EQ.JEND(IL)))THEN
            INEXT=I+D1(ABS(DIR(I,J)))
            JNEXT=J+D2(ABS(DIR(I,J)))
            I=INEXT
            J=JNEXT
            GO TO 120
        ENDIF
        IF(NEXTL(IL).EQ.ILINK)NEXTL(IL)=0
        WRITE(12,*)IL,ICS,ICEND,NEXTL(IL),PREVL1(IL)
        & ,PREVL2(IL),IORD(IL)
110    CONTINUE
    END
C
C    THIS FUNCTION RETURNS TRUE IF THE PIXEL IS A STREAM SOURCE
C    ACCORDING TO THE THRESHOLD
C
LOGICAL FUNCTION START(I,J,AREA,DIR,NX,NY,IGX,IGY,ITRESH)
INTEGER*2 DIR(IGY,IGX)
INTEGER AREA(IGY,IGX),D1(8),D2(8)
DATA D1/0,-1,-1,-1,0,1,1,1/
DATA D2/1,1,0,-1,-1,-1,0,1/
START=.TRUE.
IF (AREA(I,J).LT.ITRESH) THEN
    START=.FALSE.
    IF (AREA(I,J).EQ.0)DIR(I,J)=0 ! ZERO DIRECTIONS OUTSIDE AREA
ELSE ! CHECK UPSTREAM PIXELS
    DO 2 K=1,8
        IN=I+D1(K) ! NEIGHBOUR PIXEL
        JN=J+D2(K)
        IF (DIR(IN,JN).GT.0) THEN
            IND=IN+D1(DIR(IN,JN)) ! PIXEL DOWNSTREAM FROM NEIGHBOUR
            JND=JN+D2(DIR(IN,JN))
            IF (IND.EQ.I.AND.JND.EQ.J) THEN !NEIGHBOUR DRAINS INTO (I,J)
                IF (AREA(IN,JN).GE.ITRESH) START=.FALSE.
            ENDIF
        ENDIF
    END DO
END IF

```

```

        ENDIF
        ENDIF
2      CONTINUE
        ENDIF
        RETURN
        END
C
C
        SUBROUTINE INPUT (AREA, DIR, NX, NY, IGX, IGY, TREEFILE, COORDFILE, ITR)
        INTEGER*2 DIR (IGY, IGX)
        INTEGER AREA (IGY, IGX)
        CHARACTER*80 POINTFILE, AREAFILE, TREEFILE, COORDFILE, JFILE
        OPEN (UNIT=11, FILE='NETEX.IN', STATUS='OLD')
        READ (11, 22) POINTFILE, AREAFILE, TREEFILE, COORDFILE
22      FORMAT (A80/A80/A80/A80)
        READ (11, 32) JFILE
        READ (11, 32) JFILE
32      FORMAT (A80)
        READ (11, *) ITR
        CALL IREAD2 (DIR, POINTFILE, NX, NY, IGY, DX, DY)
        CALL IREAD (AREA, AREAFILE, NXN, NYN, IGY, DX, DY)
        IF (NXN.NE.NX.OR.NYN.NE.NY) WRITE (6, *) 'AREAFILE INCOMPATIBLE SIZES'
        RETURN
        END

```

NETEX.IN

```

W7P.BIN
W7AREAI.BIN
TREE.DAT
NETIJ.DAT
W7adj.BIN
COORD.DAT

```

50

9

NETPROP.FOR

```

C   Program to compute channel network properties for each pixel on the channel
C   network
C
C       CREATED BY DAVID G TARBOTON
C
C   Input is read from file NETEX.IN in the following format.
C   Record 1: Pointer matrix file name for input.
C   Record 2: Isolated area matrix file name for input.
C   Record 3: Tree file name for input (Created by NETEX.FOR).
C   Record 4: IJ file name for input of pixel row and column coordinates
C             (Created by NETEX.FOR)
C   Record 5: Elevation matrix file name for input.
C   Record 6: Coordinate file name for output.
C   Record 7: Support area threshold (Number of pixels)
C   Record 8: Number in coord file of outlet pixel (Input not required. This
C             is written into this file by NETEX.FOR)
C
C   This program follows after NETEX.FOR and computes the X and Y coordinates
C   of pixels on the channel network from row and column numbers using the SW
C   (Lower left) corner as an origin. It also writes elevations, distances to
C   the outlet along the streams and contributing area for each pixel to the
C   coordinate file.
C
C   This program uses subroutines from DEMUTIL.FOR, the set of subroutines
C   for I/O of binary matrix files.
C
C   PROGRAM NETPROP
C   PARAMETER (IGX=1201, IGY=1201, MC=100000)
C   CHARACTER*80 IJFILE, COORDFILE, ELEVFILE, AREAFILE, POINTFILE
C   INTEGER AREA(IGY, IGX)
C   REAL RAREA(MC), LENGTH(MC)
C   INTEGER*2 DIR(IGY, IGX), D1(8), D2(8), ELV(MC), IA(MC), JA(MC)
C   DATA D1/0, -1, -1, -1, 0, 1, 1, 1/
C   DATA D2/1, 1, 0, -1, -1, -1, 0, 1/
C
C   READ INPUT
C
C   OPEN(UNIT=11, FILE='NETEX.IN', STATUS='OLD')
C   READ(11, 22) POINTFILE, AREAFILE, IJFILE, ELEVFILE, COORDFILE
22  FORMAT(A80/A80//A80/A80/A80)
C   OPEN(UNIT=10, FILE=IJFILE, STATUS='OLD')
C   DO 5 N=1, MC
C   READ(10, *, END=110) IA(N), JA(N)
5   CONTINUE
C   WRITE(6, *) 'TOO MANY COORDS'
110  CLOSE(10)
C   N=N-1
C
C---COMPUTE AREAS
C
C   CALL IREAD (AREA, AREAFILE, NX, NY, IGY, dx, dy)
C   DO 6 IC=1, N
6   RAREA(IC) = FLOAT (AREA (IA (IC), JA (IC))) * dx * dy
C
C---READ ELEVATIONS
C
C   CALL IREAD2 (DIR, ELEVFILE, NX, NY, IGY, dx, dy)
C   DO 7 IC=1, N
C   ELV (IC) = DIR (IA (IC), JA (IC))
7   CONTINUE
C---READ ROOT COORDS
C   READ (11, *) ISUP      ! ISUP IS SUPPORT AREA
C   READ (11, *) ICR      ! ICR IS COORD OF ROOT
C   IROOT = IA (ICR)
C   JROOT = JA (ICR)
C
C---READ POINTERS AND COMPUTE LENGTHS
C
C   CALL IREAD2 (DIR, POINTFILE, NX, NY, IGY, dx, dy)
C
C   MEANING OF POINTERS IS -----
C                               I 4 I 3 I 2 I
C   0 = POINTS TO SELF         -----
C                               I 5 I 0 I 1 I
C   I.E. UNRESOLVED           -----
C  -1= BOUNDARY PIXEL         -----

```

```

C                                     I 6 I 7 I 8 I
C                                     -----
C
C----TRACE STREAMS DOWNWARDS
      DO 3 IC=1,N
        LENGTH(IC)=0.
        I=IA(IC)
        J=JA(IC)
        IF (.NOT. (I.EQ.IROOT.AND.J.EQ.JROOT)) THEN      ! LOOP
4          INEXT=I+D1(DIR(I,J))
            JNEXT=J+D2(DIR(I,J))
            DXx=dx*FLOAT(J-JNEXT)
            DYy=dy*FLOAT(I-INEXT)
            LENGTH(IC)=LENGTH(IC)+SQRT(DXx*DXx+DYy*DYy)
            IF (.NOT. (INEXT.EQ.IROOT.AND.JNEXT.EQ.JROOT)) THEN
              I=INEXT
              J=JNEXT
              GO TO 4
            ENDIF
          ENDIF
        3 CONTINUE
C--WRITE OUTPUT
      OPEN(UNIT=10,FILE=COORDFILE,STATUS='NEW')
      DO 10 IC=1,N
        X=JA(IC)*dx
        Y=dy*(NY-IA(IC))
        WRITE(10,*)X,Y,LENGTH(IC),ELV(IC),RAREA(IC)
10     CONTINUE
      END

```